HYDROPHILIC ACRYLICS: POLYMERISATION KINETICS, ADSORPTION/ DESORPTION ISOTHERMS

A THESIS SUBMITTED TO THE

UNIVERSITY OF PUNE

FOR THE DEGREE OF

DOCTOR OF PHILOSOPHY

(IN CHEMICAL ENGINEERING)

BY

RAJIV KUMAR TAYAL

RESEARCH GUIDE

Dr. B. D. Kulkarni

CHEMICAL ENGINEERING AND PROCESS DEVELOPMENT DIVISION
NATIONAL CHEMICAL LABORATORY
PUNE 411 008, INDIA

April 2013

राष्ट्रीय रासायनिक प्रयोगशाला
(वैज्ञानिक तथा औद्योगिक अनुसंधान परिषद)
डॉ. होमी भाभा रोड, पुणे - 411 008. भारत
NATIONAL CHEMICAL LABORATORY
(Council of Scientific & Industrial Research)
Dr. Homi Bhabha Road, Pune - 411008. India

CERTIFICATE

Certified that the work incorporated in the thesis entitled **"Hydrophilic Acrylics: Polymerisation Kinetics, Adsorption/Desorption Isotherms"** submitted by **Rajiv Kumar Tayal** was carried out by the candidate at National Chemical Laboratory, Pune – 411008, under my supervision. Such material as obtained from other sources has been duly acknowledged in this thesis.

April 2013

Pune

Dr. B. D. Kulkarni

(Research guide)

Dr. S. Ponrathnam

(Co-Guide)

Communications Channels ☎ +91 20 25902000 +91 20 25893300 +91 20 25893400 Fax +91 20 25902601 (Director) +91 20 25902660 (Admin.) +91 20 25902639 (Business Development) URL : www.ncl-india.org

DECLARATION

I hereby declare that the thesis entitled **"Hydrophilic Acrylics: Polymerisation Kinetics, Adsorption/Desorption Isotherms"** submitted for Ph. D. degree to the University of Pune has been carried out at National Chemical Laboratory, Pune, India, under the supervision of **Dr. B. D. Kulkarni,** Chemical Engineering & Process Development Division, National Chemical Laboratory, Pune - 411008. The work is original and has not been submitted in part or full by me for any degree or diploma to this or any other University.

April 2013 (**Rajiv Kumar Tayal)**

Pune

ACKNOWLEDGEMENT

It is my immense pleasure to express my gratitude towards many people who have helped me in various stages of this research. First of all, I express my deep sense of reverence and gratitude to my mentor and research guide, ***Dr. B. D. Kulkarni****, Chemical Engineering & Process Development Division, NCL, Pune for his inspiring guidance, never diminishing encouragement, sincere advice, unstinted support and complete dedication during the progress of my Ph.D work. I absolutely admire his desire to do high quality science and instilling the thirst for science in not only his students but in all whom he comes across. I wish I could imbibe some of those qualities and practice them myself, for the rest of my life.*

I am deeply indebted to my co-guide, ***Dr. S. Ponrathnam,*** *for valuable research discussions, guidance and his time and efforts in systematically designing my experiments. His suggestions and criticisms had helped me to develop myself to carry out scientific research with optimal usage of personal and organizational resources.*

I would like to thank ***Dr. C. R. Rajan*** *for his helpful suggestions and support, provided during my entire research career. My special and sincere thanks also go to* ***Dr. N. N. Chavan,*** *whose presence helped me significantly in speeding up my work.*

I express my sincerity to ***Dr. Sourav Pal*** *(Director-N.C.L.) for allowing me an opportunity to carry out my research at N.C.L. and providing all infrastructural facilities. I am also grateful to* ***Dr. V. V. Ranade*** *(Head-Chemical Engineering & Process Development Division) for allowing me to use necessary resources and facilities in the division.*

I would like to extend my sincere thanks to my colleagues ***K. S. Rajdeo, S. S. Bhongale, R. V. Ghorpade, S. Daniels, S. B. Deokar, S. M. Bhosale*** *and* ***S. A. Mule*** *for their constant support and help provided at crucial junctures. An individual thanks goes to* ***A. A. Shaikh*** *and* ***R. Harikrishna*** *who have helped me in all possible ways during the tenure of my work.*

As always, it is impossible to mention everybody who helped me to complete this work. Indeed, there would be several others to have made this journey worthwhile. I find no words to express my feelings for my parents whose support, love and encouragement was always there in all my endeavors. I also wish to thank my family for their unfailing support and affection.

Rajiv Kumar Tayal

TABLE OF CONTENTS

CHAPTER I

INTRODUCTION

CHAPTER II

KINETIC PARAMETERS AND REACTIVITY RATIOS

CHAPTER III

SYNTHESIS AND CHARACTERISATION METHODOLOGIES

CHAPTER IV

RESULTS AND DISCUSSION

Part A: Reactivity Ratio

LIST OF FIGURES

Chapter I: INTRODUCTION

Chapter III: SYNTHESIS AND CHARACTERISATION METHODOLOGIES

Chapter IV: RESULTS AND DISCUSSION

LIST OF TABLES

Chapter I: INTRODUCTION

Chapter II: KINETIC PARAMETERS AND REACTIVITY RATIOS

Chapter III: SYNTHESIS AND CHARACTERISATION METHODOLOGIES

Chapter IV: RESULTS AND DISCUSSION

Chapter VII: SUMMARY, CONCLUSION AND FUTURE DIRECTIONS

LIST OF SCHEMES

Chapter III: SYNTHESIS AND CHARACTERISATION METHODOLOGIES

LIST OF ABBREVIATIONS

AIBN	2,2'-Azoisobutyronitrile
BA	Butyl acrylate
BMA	Butyl methacrylate
DSC	Differential scanning calorimetry
EGDMA	Ethylene glycol dimethacrylate
EHA	2-Ethylhexyl acrylate
EHMA	2-Ethylhexyl methacrylate
EWC	Equilibrium water content
Ext. KT	Extended Kelen-Tudos
FR	Fineman-Ross
GC-FID	Gas chromatography-Flame ionization detector
HEA	2-Hydroxyethyl acrylate
HEMA	2-Hydroxyethyl methacrylate
HPA	2-Hydroxypropyl acrylate
HPMA	2-Hydroxypropyl methacrylate
IOL	Intraocular lens
IR	Infra red
KT	Kelen-Tudos
MA	Methyl acrylate
MEHQ	Monomethyl ether of hydroquinone
MH	Mao-Huglin
MIBK	Methyl isobutyl ketone
MMA	Methyl methacrylate
NMR	Nuclear magnetic resonance
PCO	Posterior capsule opacification
PMMA	Poly(methyl methacrylate)
PVA	Poly(vinyl alcohol)
RI	Refractive index
R_f	Response factor
R_t	Retention time
RSD	Relative standard deviation
SR	Swelling ratio
Tg	Glass transition temperature
TGA	Thermogravimetric analysis
UV	Ultraviolet-visible

Hydrophilic Acrylics: Polymerisation Kinetics, Adsorption/ Desorption Isotherms

Abstract of Thesis

Hydrogels are polymeric materials with a large number of hydrophilic groups that are capable of absorbing and retaining water in their three dimensional networks. They swell by absorbing water and shrink on drying but are prevented from dissolving due to their chemically or physically crosslinked network. They can retain large amounts of water even under different physiological conditions and fluid containing electrolytes. This water holding and biocompatibility property of these hydrogels able to used these materials in different biomedical applications.

Soft and flexible ocular implants offer several possible advantages over traditional hard acrylic (PMMA) IOLs. Hydrogels among the best candidate materials for this application. For the application of hydrophilic copolymer in ophthalmic lens, water swelling-deswelling profile against isotonic salt solution, glass transition temperature (T_g), thermal stability and biocompatibility are the key parameters. Relationship between monomer compositions of hydrogels with physical properties were studied. A major objective was to find suitable composition with improved properties.

Cataract is the opacification of the lens due to age, ocular trauma or inflammation that decreases the transparency of the eye. Surgical procedure is the replacement of natural crystalline lens with a hydrophilic/hydrophobic polymer (intraocular) lens (IOL). Co- and terpolymerisation of several combinations of hydrophilic acrylic monomers is extensively investigated with the objective to find out suitable combination of monomers with desired properties. Co- and terpolymerisation are used effectively to increase the amorphous character of the polymer which increases the transparency and the flexibility of the polymer chains. Copolymers tend to have a set of properties uniquely their own, setting them apart from that of their parent homopolymers. In copolymers the sequence distribution of the different monomers is a key parameter to ensure homogeneity. Thus, investigation of copolymerisation kinetics is of paramount importance.

In human contact applications it is an intrinsic requirement that the level of residual monomers be extremely low. One way to ensure this is to follow polymerisation kinetics till the very end so as to ensure sufficient time is given for all the monomers to

have converted into polymers. However, since both monomers in a copolymerisation will have differing relative rate of addition to the copolymer chain, one of the monomers will be depleted ahead of the other and the final several percentage of the copolymerisation will be essentially homopolymerisation of the less reactive monomer. In such a case the copolymer and homopolymer may phase-separate leading to in-homogeneity, thereby affecting transparency.

It is, thus, highly essential that a very careful study of the copolymerisation be made so as to establish chemical kinetically an unique (azeotropic) composition for each two component copolymer system wherein the copolymer has an exact identical composition. Such a copolymer will have best chance for complete homogeneity as well as very low levels of residual monomers.

The present investigation is a detailed kinetic study of several hydrophilic-hydrophobic, hydrophilic-hydrophilic copolymerisation systems which have a very high potential for suitability for use as intraocular lens materials. In industrially relevant systems, azeotropic composition is established by studying each copolymerisation for reactivity ratio kinetics using differing mole ratios of the two monomers. We have investigated all our systems using a much larger set to establish greater accuracy.

Chapter I deals with the genesis to the present state of knowledge regarding hydrogels and applications thereof in intraocular lenses.

Chapter II deals with the different copolymerisation kinetic methodologies established since its origin in 1944. All the methods are reviewed in depth.

Chapter III discusses about synthesis characterisation methodology of these amphiphilic polymers. This includes the extraction method of unreacted monomers, method development for analytical protocol which separates unreacted monomer peaks from each other by gas chromatography, determination of unreacted concentration of monomers to establish data for reactivity ratio analysis. The chapter also deals with characterisation techniques such as differential scanning calorimetry and thermo-gravimetric analysis for glass transition temperature (T_g) and thermal stability of the synthesised copolymers.

Chapter IV divided into two parts. The first part consists of synthesis of binary copolymers, their reactivity ratio estimation.

In copolymerisation kinetic studies, the estimation of reactivity ratios is of a great significance. Copolymerisation reactivity ratios were originally measured for the purpose of describing the relative reactivities of various monomers towards various radicals. Nowadays they are being treated as a quantitative data and so the need to accurately measure it arises. The calculation of the monomer reactivity ratios requires the mathematical treatment of experimental data on the composition of copolymers and monomer in feed mixtures. Copolymerisation is the most successful and powerful method for effecting systematic changes in polymer properties. The incorporation of two different monomers, having diverse physical and/or chemical properties, in the same polymer molecule in varying proportions leads to the formation of new materials with great scientific and commercial importance.

Several hydrophilic-hydrophobic, hydrophilic-hydrophilic copolymerisation systems are studied which are listed below. (1) 2-ethylhexyl acrylate with 2-hydroxyethyl methacrylate; (2) 2-ethylhexyl acrylate with 2-hydroxypropyl methacrylate; (3) 2-ethylhexyl methacrylate with 2-hydroxyethyl methacrylate; (4) 2-ethylhexyl methacrylate with 2-hydroxypropyl methacrylate; (5) 2-ethylhexyl acrylate with 2-hydroxyethyl acrylate; (6) 2-ethylhexyl acrylate with 2-hydroxypropyl acrylate; (7) 2-ethylhexyl methacrylate with 2-hydroxyethyl acrylate; (8) 2-ethylhexyl methacrylate with 2-hydroxypropyl acrylate; (9) methyl methacrylate with 2-hydroxyethyl methacrylate; (10) methyl methacrylate with 2-hydroxyethyl acrylate; (11) methyl methacrylate with 2-hydroxypropyl methacrylate; (12) methyl methacrylate with 2-hydroxypropyl acrylate; (13) methyl acrylate with 2-hydroxyethyl methacrylate; (14) methyl acrylate with 2-hydroxyethyl acrylate; (15) methyl acrylate with 2-hydroxypropyl methacrylate; (16) methyl acrylate with 2-hydroxypropyl acrylate; (17) butyl acrylate with 2-hydroxyethyl methacrylate; (18) butyl acrylate with 2-hydroxyethyl acrylate; (19) butyl acrylate with 2-hydroxypropyl methacrylate; (20) butyl acrylate with 2-hydroxypropyl acrylate; (21) 2-hydroxypropyl methacrylate with 2-hydroxyethyl methacrylate; (22) 2-hydroxyethyl methacrylate with 2-hydroxyethyl acrylate; (23) 2-hydroxyethyl acrylate with 2-

hydroxypropyl methacrylate; (24) 2-hydroxypropyl acrylate with 2-hydroxypropyl methacrylate and (25) 2-hydroxyethyl acrylate with 2-hydroxypropyl acrylate.

Copolymers were prepared by free radical solution polymerisation in methyl isobutyl ketone using azobisisobutyronitrile (AIBN) as initiator. Copolymer compositions are determined from gas chromatographic (GC) analysis. The reactivity ratios are estimated using the Fineman-Ross, Kelen-Tudos, extended Kelen-Tudos and Mao-Huglin graphical methods. The samples were also characterised by DSC for thermal transitions, glass transition temperature (T_g) and amorphous character.

In second part, swelling-deswelling studies azeotropic compositions of monomer combinations obtained from estimated reactivity ratio values were carried out. Terpolymers were synthsised by bulk polymerisation method using Cumene hydroperoxide-ethanolamine as redox initiator with varying cross-link density of EGDMA. Prepared cross-linked polymers were characterised to evaluate thermal properties (DSC and TGA).

In chapter V deals with the overall conclusions of the work reported in this thesis. This is followed by suggestions related to possible future research work related to these systems.

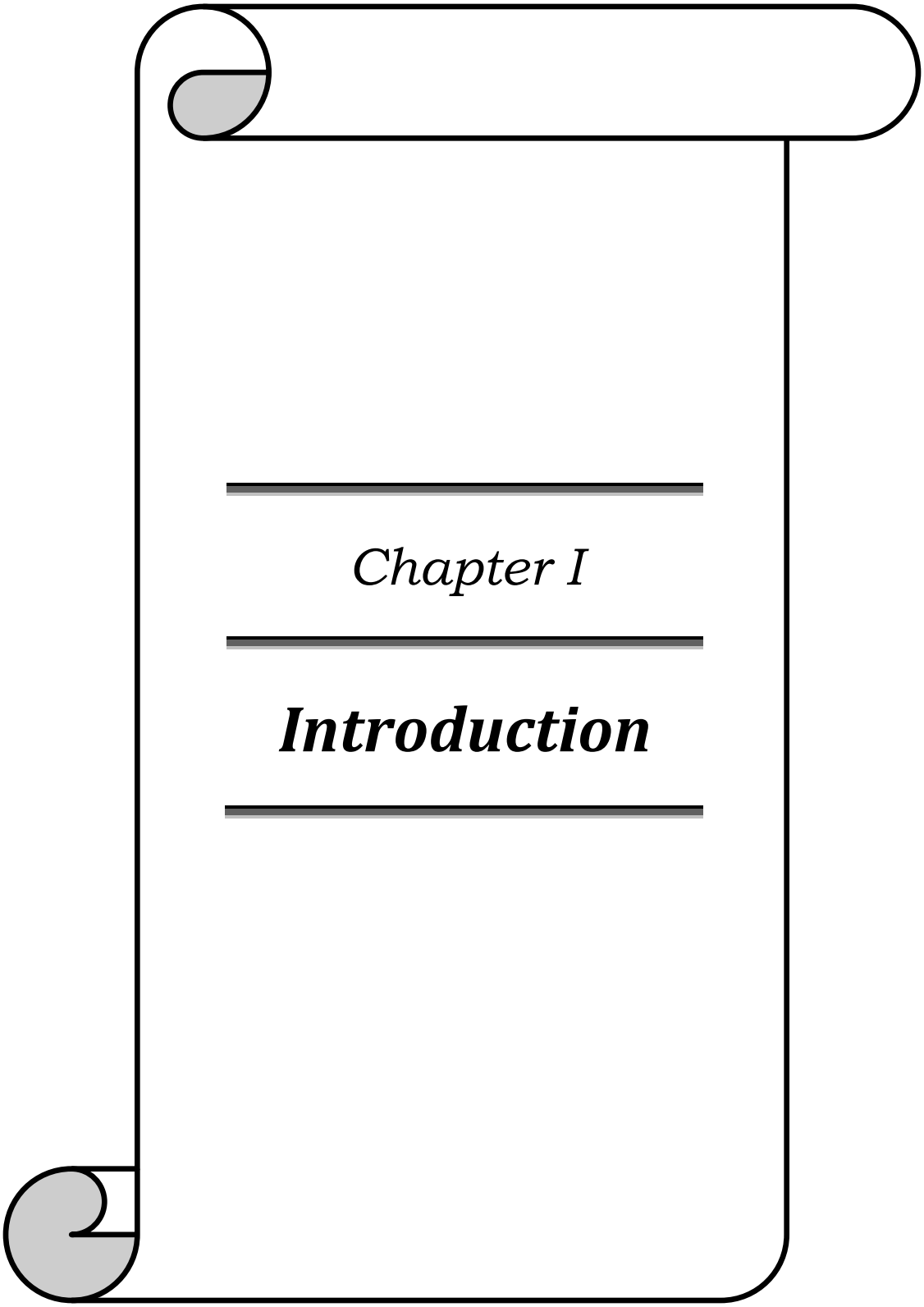

Chapter I

Introduction

1.1 Introduction

Hydrogels are an unique class of polymeric materials that impact numerous areas of biotechnology, medicine as well as personal care products such as sanitary pads, contact and intraocular lenses. Theses are materials that can retain considerable amounts of water by swelling, but do not dissolve.[1] Synthetic polymers or linear molecules based on nearly infinite series of carbon atoms, can be used to produce hydrogels. Water absorption in polymeric hydrogels results from hydrophilic functional side-groups attached to the main carbon-atom chain: these include hydroxyl, carboxylic acid or amide moieties. Hydrogels are insoluble due to the presence of cross-links or chemical bonds between side-groups of adjacent polymer chains that result in an anisotropic, three-dimensional network.[2] Although necessary for insolubility, cross-link junctions render hydrogels inhomogeneous affecting physical properties and water-polymer interactions.[3] The water in a hydrogel provides a medium for the transport of water-soluble species: this property of hydrogels differentiates them from other polymers.[4] Generally, water comprises at least 20 wt.% of the total weight of a hydrogel, and if greater than 95 wt% water is absorbed, the hydrogel is referred to as super absorbent. In addition to synthetic polymers, hydrogels include numerous natural products of animal origin, for example cartilage (a fiber reinforced hydrogel), tendons and some proteins,[5] and also of plant origin, for example, lignin (the second major component of wood pulp) and cellulose.[6] Swelling of a gel results in a build-up of a network pressure due to an elastic extension of the polymeric matrix.[7] However, the physical behaviour of the hydrogel's swollen-state is mainly affected by the thermodynamic interactions of polymer-solvent pairs.[8]

1.2 Swelling of Hydrogels

The equilibrium water content (EWC) is important for bio-molecule separations because it allows for the transport of water-soluble species through the hydrogel matrix. Water-polymer interactions are governed by an equilibrium between the swelling, that results from the osmotic pressure produced by polymer-solvent interaction, and the counteracting elastic restorative or refractive force of the deformed network.[9] The extent of swelling in a hydrogel depends on the solvent and the structure of the polymer. In a

hydrogel the network structure is permanent and the solvent expands the structure without disrupting the essential skeleton, as depicted in Figure 1.1.

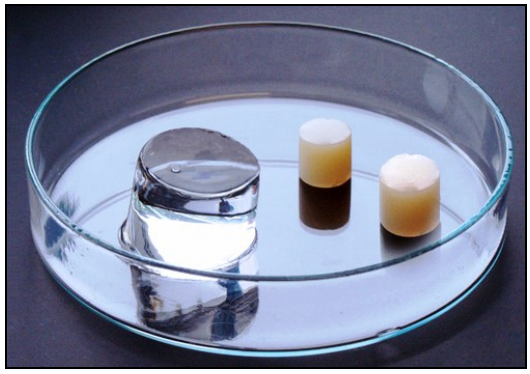

Figure 1.1: Swelling of hydrogel

During swelling, the interconnected polymeric chains comprising the network assume less probable configurations during the necessary elongation. The result is a decrease in chain configuration entropy. In opposition is the increase in mixing entropy of the solvent with the polymer that accompanies swelling. Therefore, neglecting heat of mixing, equilibrium is attained when these two entropy changes are equal in magnitude: the entropy of chain configuration equals the entropy of the osmotic, or the mixing entropy.[10,11] Investigations of the swelling behaviour of hydrogels have been reported repeatedly; however, theories are still unable to predict physical properties from synthesis-design.[12] Therefore, it is necessary to establish new copolymers and predict course of polymerisation as well as the physical properties and absorption characteristics of a hydrogel in order to prepare materials for suitable end use.

1.3 Applications of Hydrogels

The numerous technological and biomedical applications of hydrogels result from the high water content of these materials.[13] The biocompatibility of hydrogels can be attributed to low interfacial tension with biological fluids, high gas permeation, high diffusion of low molecular weight compounds, reduced mechanical and frictional irritation to tissue, and to the existence of a certain balance between hydrophobic micro domains at the surface of the hydrogel.[14] Currently, hydrogels are used as separation

media, soft contact lenses, artificial organs, dental materials, optical lens implants, artificial skin, materials for encapsulated cells, carriers for controlled drug delivery, optical sensors, and dialysis media.[15-20] The suitability of hydrogels as biomaterials is due to their similarities to living tissue, including high water content, soft and rubbery consistency, and low interfacial tension. Specifically, the hydrogels used for this dissertation, which contains pendent hydroxyl alkyl or alkyl groups, are resilient, pliable, chemically stable, biocompatible, relatively inert, capable of swelling to a predetermined volume, and have the ability to modify elastic mechanical behaviour by varying the amount of cross-linking agent.[21]

The deficiency of hydrogels are poor mechanical properties, especially strength, due to the high water content. However, short side chains on the main polymer chain that are hydrophobic, such as alkyl side groups, can enhance the rigidity and strength of the swollen hydrogel; for example, pHEMA is much more rigid compared to poly(hydroxyethyl acrylate) due to the presence of an α–CH_3 group on the pHEMA carbon chain.[22] Composites also can improve mechanical performance of hydrogels such as additions of hydrophobic polycaprolactone.[23] Specifically, the mechanical properties of HEMA can be improved for some applications by forming composites with polypropylene fibrillated films and poly(ethylene terephthalate) (PET) reinforcing fibres and tricot PET net.[24] Copolymerisation of hydrogels with polyolefins is another useful method for upgrading properties of both polyolefins and hydrogels.[25] HEMA containing copolymers are used in ultra-filtration membranes for purification of air and water for important separations in the chemical and biotechnology industries.[26] Specifically, hydrogels can be used for the removal of toxic metals in the semiconductor industry.[27] In fact, some hydrogels closely mimic the behaviour of the renal glomerular basement membrane (GBM), which serves to ultra-filter blood in the kidneys.[28]

Since hydrogels contain such high water content, these materials mimic the structure of natural tissues, and many hydrogels are therefore biocompatible.[29] Successful applications of HEMA have included uses as burn dressing, for breast augmentation, in reconstructive facial surgery, for suture coatings,[30] and dental applications, such as lining

materials for acrylic dentures.[31] However, HEMA-based implants are prone to calcification; the calcification of bioprosthetic materials is one of the perennial problems in using hydrogels as implants.[21]

1.3.1 Hydrogels for drug delivery systems

The controlled release of solutes, particularly for drug delivery, is an important application for hydrogels. Currently, conventional methods for drug delivery are based on single or successive doses, administered directly or indirectly to a target area, for example by injection or oral dispensation.[32] One disadvantage to this conventional approach is short drug-activity duration. Also, the drug quantity actually delivered may differ from the optimum, desired quantity at the target area. Polymeric systems offer several advantages over this traditional approach.[33] Hydrogels could reduce or eliminate harmful side effects that result from systematic local administration by delivering a drug from a polymer-supported reservoir, particularly drugs with short lifetimes in the body. Also, hydrogels could maintain drug delivery at a desirable concentration over long periods of time in order to avoid a high dose.[34] Hydrogels used for pharmaceutical controlled-release systems are based on swelling characteristics.[35] When a bioactive agent is dissolved or dispersed in a dry, glassy polymer matrix, transport is minimal.

In the presence of a suitable solvent, generally water, matrix penetration occurs, resulting in considerable volume expansion or swelling, and the diffusion of the bioactive agent is dramatically amplified as the drug diffuses through the hydrogel quickly into the surroundings.[36] Therefore, the rate-determining step for release is the swelling of the polymer. Predicting the rate of swelling is essential for determining the rate of drug delivery for pharmaceutical applications. Similar systems could be used in agriculture to release pesticides or fertilizers from a polymer into the surrounding soil.[34] Drug release from hydrogels can be affected by several parameters such as pore size degradability of hydrogel, size, hydrophobicity, concentration of a drug, and the presence of specific interactions between hydrogels and the incorporated drug.[37]

1.3.2 Hydrogelas in separation media

Many bio-analytical techniques utilise hydrogels as a separation media, including; GPC, LC, CGE, and gel electrophoresis.[38] These separation techniques rely on the differential migration of molecules through hydrogel networks based on their various physical and chemical characteristics, such as charge, size, shape, affinity, hydrophobicity, and hydrophilicity. Gel permeation chromatography, GPC, and gel electrophoresis both utilise hydrogel polymer matrices of various pore size distributions for separations based on size and shape, and charge for electrophoresis. Hydrogels for use as a separation medium must meet specific material requirements. The distribution of pore sizes within a hydrogel is controlled by the concentrations of monomer and cross-linker in solution before polymerisation. Firstly, hydrogels have conflicting requirements. Good mechanical integrity requires high concentrations of monomer and high degrees of cross-linking, and thus creating small effective pore sizes; whereas large pores needed for larger biomolecule separations require low polymer concentrations and low cross-link densities, leading to poor mechanical strength. The mechanical integrity of hydrogel media directly affects maximum flow rates and speed of separations.[38] Secondly, hydrogels contain broad distributions of pore sizes. The random cross-linking between propagating polymer chains during polymerisation leads to an uncontrolled distribution of pore sizes. The lack of an internally organised pore structure within a hydrogel diminishes the separation potential between similarly sized molecules. Thirdly, all hydrogel separation media have limiting maximum pore size distributions due to inherently poor material characteristics at minimum polymer and cross-linker concentrations.[39]

1.3.3 Hydrogels for contact lenses

A contact lens is an ophthalmologic device that covers the cornea of the eye throughout blinking (Figure 1.2). Contact lenses are generally used to correct vision problems associated with corneal surface defects, but contact lenses impregnated with pharmaceuticals can be used to medically treat certain diseases associated with the eye.[40] Hydrogels for use as contact lenses must also meet several very strict material

requirements. To allow for extended wearing times, a soft contact lens must achieve a high level of oxygen transmissibility from the atmosphere to the cornea while remaining optically clear, bio-compatible and mechanically sound.[38]

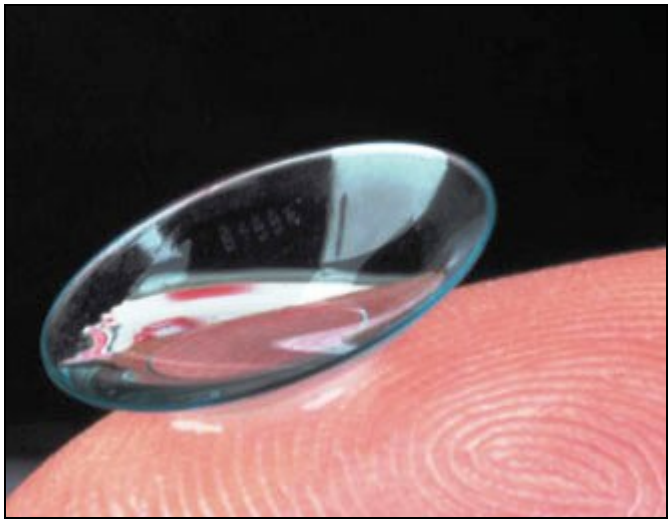

Figure 1.2: Contact lens

The materials used to fabricate contact lenses range from hard to soft. Hard lenses are generally based on poly(methyl methacrylate) (PMMA). Single wear, daily lenses, or soft contacts are based on hydrogels, such as poly(2-hydroxyethyl methacrylate) p(HEMA) and poly(N-vinyl pyrrolidone) (pNVP), poly(2,3-dihydroxypropyl methacrylate) (pDHPMA) and poly(methacrylic acid) (pMA).[41] Generally, DHPMA is copolymerised with HEMA, or hydroxyethyl methacrylate, and cross-linked with ethylene glycol dimethacrylate, to produce a hydrogel suitable for soft contact lens use.[42] The absorption of water by these hydrogels is the exclusive result of the hydroxyl content (-OH) whereas water absorption in N-vinyl pyrrolidone, another soft contact lens material, results from the amide (-N-C=O) content. Since the hydroxyl group binds water stronger than the amide group, hydroxyl-based hydrogel materials are more comfortable to wear as contact lenses.[42] Oxygen permeability is the major criterion that governs the selection of materials used for contact lenses.[43] The cornea is an avascular tissue with active aerobic metabolism.

Oxygen is normally supplied to the epithelium of the cornea through the tear film.[44] If the eyelids are closed, then oxygen is supplied to the cornea by blood capillaries of the palpebral conjunctiva (the posterior part of the eyelids).[45] In the event that the supply of oxygen to the cornea is restricted, epithelium glycogen decreases and lactic acid production increases due to anaerobic glycolysis. The result is that the cornea swells and hazes impairing vision. Therefore, it is imperative that any material considered for contact lens applications must not disrupt oxygen supply to the cornea. This can be accomplished by oxygen-rich tear exchange under the lens, and oxygen permeation through the lens.[41] Although optical glasses were the first materials used for contact lenses, acrylic plastics were introduced in 1937 for contact lens applications. The excellent optical properties of poly(methyl methacrylate) or PMMA, as well as its resistance to discolouration, good machining and polishing qualities, low incidence of irritation and allergic response in patients, and light weight are the qualities that made this material dominate the contact lens industry during the early stages of its development. However, the main problem with hard contact lenses made from PMMA is that this material is virtually impermeable to oxygen. Therefore, contact lenses made with PMMA copolymerised with comonomers such as fluoro alkyl methacrylates and butyl methacrylates have been used to increase oxygen permeability.[46]

Soft contact lenses made from hydrogel materials offer numerous advantages over hard contact lenses, even hard contacts that are permeable to oxygen. Hydrogel-based contact lenses are relatively rich in water, between 30 and 80% by weight. This aqueous phase in a hydrogel is exceptionally permeable to oxygen. Soft contact lenses adhere closely to the cornea so there is a thin tear film of capillary thickness between the posterior surface of the lens and the corneal surface that facilitates oxygen exchange. Hydrogel lenses are less irritating and can be worn for a longer time, compared to hard contact lenses. However, since hydrogel lenses are composed of at least one-third water by weight, the mechanical properties are poor and handling can be difficult.[47] Hydrogels based on polymerised 2-hydroxyethyl methacrylate or pHEMA were first introduced as materials for biomedical applications in 1951. The water soluble monomer can be easily polymerised, and since the material posses hydrophilic pendant groups, it forms a

hydrogel when cross-linked.[48] The overall properties of HEMA hydrogels for contact lens applications are unsurpassed, so pHEMA serves as the benchmark for comparison of the performance of new hydrogel materials for contact lens applications.[49] This commercially available chemical is prepared in a single step from methyl methacrylate or methacrylic acid, and can be easily polymerised to produce a biocompatible hydrogel.

The first review of the applications of HEMA polymers appeared in 1960.[48] The first synthesis of HEMA along with its polymerisation, was described in 1936. Two schemes can be utilised to produce HEMA, either a transesterification reaction with ethylene glycol and methyl methacrylate, or a reaction between ethylene oxide and methacrylic acid. Both methods result in the formation of ethylene glycol dimethacrylate (EGDMA). The presence of EGDMA cart be removed using ion-exchange resins or extraction with various solvents. However, the presence of EGDMA may be adventitious for certain applications of HEMA, since it is a cross-linking agent, and cross-linking is necessary to produce an insoluble hydrogel. Polymerised HEMA can be produced using free-radical initiators, y-irradiation or UV exposure in the presence of photo-stabilisers.[48]

1.3.4 Hydrogels in intraocular lenses (IOLs)

One of the objectives of the present thesis is to establish copolymer compositions that will be suitable for the synthesis of hydrogel materials for Intraocular Lens (IOL) application. We will quickly review various aspects related to IOLs.

1.3.4.1 The eye

The structure of the eye (Figure 1.3) is remarkable being able to receive light and to transmit it as pulses recognised as images by the brain. The eye is housed in an eye socket (or orbit) within the skull. The size of the orbit largely exceeds that one of the soft tissue eyeball. The space between the eyeball and the orbit is filled with fat and lined with a sheet of connective tissue, which allows the free motion of the globe.

The eye is a nearly spherical hollow globe with an average diameter of about 2.5 cm filled with fluids. The three layer wall consists of (i) a peripheric fibrous protective envelope, known as the sclerocorneal layer, whose posterior part, i.e. the sclera, is white

and covers approximately five sixths of the eye surface, (ii) the anterior sclerocorneal layer, known as the cornea, and (iii) the middle vascular layer, that contains the choroid and the iris.

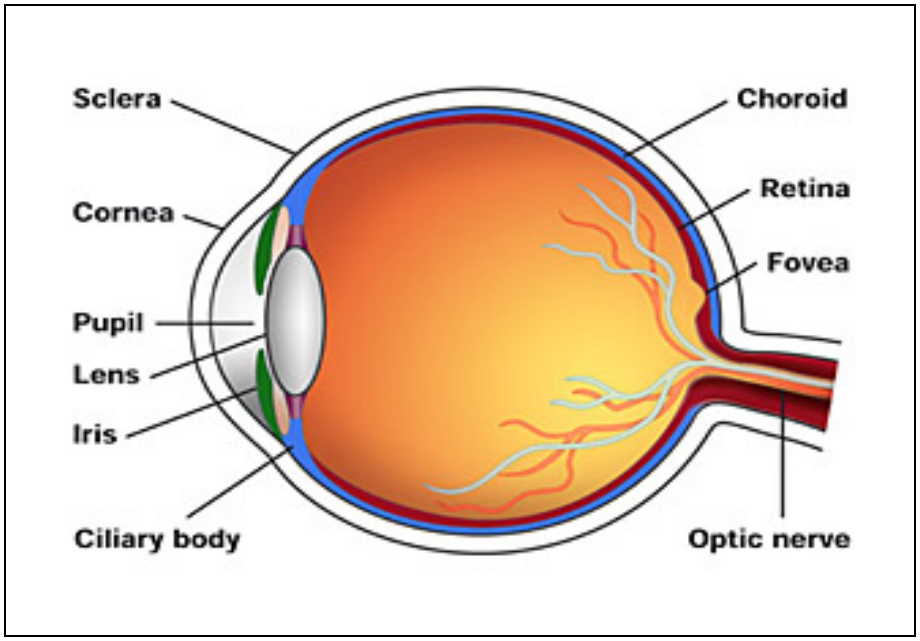

Figure 1.3: Eye anatomy

The lens is a 4 mm thick transparent biconvex body, with an average diameter of 9 mm. It is attached to the ciliary body via a network of elastic fibres, the zonules. No cell loss and long lived proteins in a light-saturated environment are key features of the lens. However, the lens core proteins are exposed to environmental damage, such as age related environmental issues, sudden physical trauma, radiation pulse or poor nutrition, which often results in the opacification of the lens, known as 'Cataract'.[50-52]

1.3.4.2 Cataract

Cataract is a clouding of the lens of the eye which impedes the passage of light (Figure 1.4). Most cases of cataract are related to the aging process. However, children can be born with a cataract or develop it in their teenage years. Furthermore, a cataract may develop after eye injuries, inflammation, and some other eye diseases. According to studies of the World Health Organisation (WHO), more than 50 million people suffer

from cataract worldwide which makes cataract the cause for about half of all worldwide cases of blindness.[53] Although cataracts can be surgically removed, in many countries surgical services are inadequate, and cataract remains the leading cause of blindness. With an increase in average life expectancy, the number of people suffering from cataract is growing.

Cataract is thus an important cause of bad vision in both developed and developing countries. Comprehensive prevention of cataract development is not known yet. The treatment of cataract through an operation is very successful in restoring sight. The opaque lens is removed and replaced by an artificial intraocular lens (IOL).[54] Even though the first successful implantation of an IOL was accomplished, yet some significant drawbacks related to IOL surgery still exist today. A typical post-operative complication is posterior capsule opacification (PCO), the so-called secondary cataract. PCO is caused by proliferation and migration of retained lens epithelial cells into the optical axis, and leads to a progressive deterioration and disturbances in visual activity.[55-61]

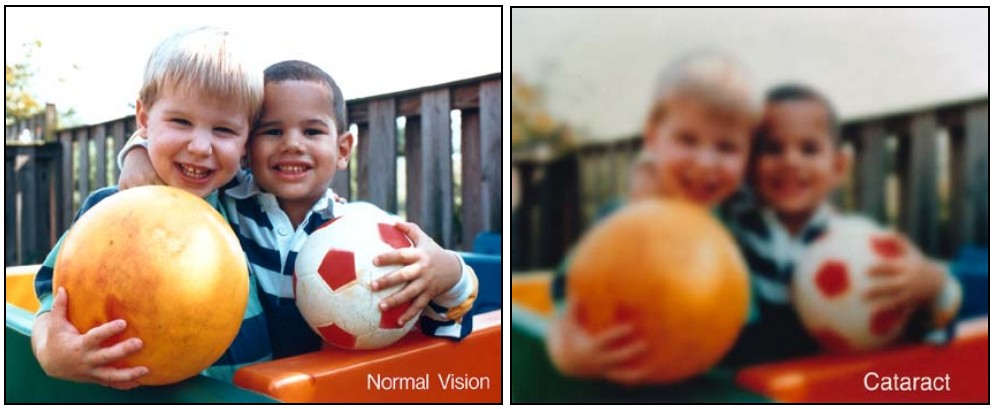

Figure 1.4: Comparison of normal and cataractous eye lenses

Intraocular lens (IOL) is a classic example of the improvement of biomaterial with the active cooperation of science and industry. It involves a reciprocating but overlapping evolutionary relationship of cataract removal technology with IOL design. Cataract surgery evolved through extracapsular cataract extraction (ECCE), intracapsular extraction (ICCE), machine-assisted ECCE, phacoemulsification by external nuclear

attack, and phacoemulsification-assisted internal nuclear disassembly.[62] For IOL fixation, the evolution has been posterior chamber, anterior chamber (AC), pupil and iris, iridocapsular, ciliary sulcus, asymmetric placement, and capsular bag. As with any evolutionary process, this has been and still is a leapfrogging phenomenon, so that at any one point in time several cataract surgery strategies and IOL implantation techniques can be considered good science and good medicine. The process continues as microincision phacoemulsification procedures gain sophistication in search of an IOL to be inserted through a ~2.0 mm incision.[62]

Polymeric materials still provide some of the most important avenues for research, primarily because of their ease of processing and the ability of researchers to readily control their chemical and physical properties via molecular synthesis. An important advance in the field of ophthalmology has been the intraocular lens (IOL). Operating microscope facilitated the establishment of microsurgical techniques, sophisticated cataract procedure and intraocular lens implants.

Thus, two of the most significant achievements in ophthalmology have been improvement of cataract surgery and development of the IOL. Cataract is the most prevalent ophthalmic disease. As indicated earlier, more than 50 million people worldwide suffer from cataracts resulting in visual impairment.[63]

Phakia is the presence of the natural crystalline lens. Aphakia is the absence of the natural crystalline lens, either from natural causes or because it has been removed. Pseudophakia is the substitution of the natural crystalline lens with a synthetic lens. Pseudophakic IOLs are used in cataract surgery. Prior to the IOL, the aphakic spectacles, prescribed for patients after removal of natural lens, were unsatisfactory due to the visual distortions in such high powered lens. Aphakic spectacles magnified vision, thereby drastically altering depth perception.[64] In addition, if only one eye needed cataract removal, stereopsis, or three-dimensional vision, was virtually impossible.

Cataracts develop for a variety of reasons, including long-term exposure to ultraviolet light, exposure to radiation, secondary effects of diseases such as diabetes,

hypertension and advanced age, or trauma (possibly much earlier); they are usually a result of denaturation of lens protein. Genetic factors are often a cause of congenital cataracts and positive family history may also play a role in predisposing someone to cataracts at an earlier age, a phenomenon of "anticipation" in pre-senile cataracts. Cataracts may also be produced by eye injury or physical trauma.

Cataract treatment has been practiced for many centuries using a wide variety of techniques. The major complication before the invention of the IOL was attaining high quality post-operative visual rehabilitation because removal of the natural lens resulted in a significant visual disability.[65] IOL implantation is performed after cataract removal to replace the optical function of the natural lens. Surgical removal combined with IOL implantation has become one of the most widespread and highly successful medical procedures with almost 5 million surgeries per year worldwide.[66]

The invention of the contact lens overcomes many of the complications.[67] However, not everyone can wear contact lenses. Poor tolerances of contact lenses are caused by problems such as dry eyes, a low blink rate, or problems with hygiene.[68] The invention in late 1940s of the IOL changed forever the aphakic visual rehabilitation.[69]

In 1949, Dr. Ridley performed the first intraocular lens implantation.[63] Since then, design, manufacturing, and haptic material developments for lOLs, as well as surgical procedure improvements, have advanced, but PMMA (Figure 1.5) is still the primary material for IOL optics.

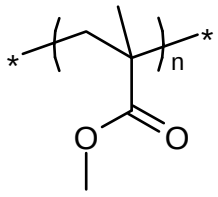

Figure 1.5: Poly(methyl methacrylate) (PMMA)

From the first implantation to present day, IOL has evolved through six generations.

● Generation I: IOLs were made and implanted from 1949-1954.[70] These lenses were designed to be similar in size and shape to the human crystalline lens which is anatomically in the posterior chamber of the eye.

● Generation II: IOLs were implanted between 1952 and 1962.[71] The anterior chamber of the eye was chosen due to its narrow confines and surgically it was an easier procedure to perform with PMMA.

● Generation III: Lenses were developed and implanted during 1953-1973.[70] Iris support IOLs were designed in an attempt to overcome the problems with Ridley's posterior chamber lens as well as the anterior chamber lenses developed in the 1950s.

● Generation IV: Later Model Anterior Chamber, PMMA IOLs were implanted between 1963 and mid 1980s, but were withdrawn due to manufacturing defects and design flaws.

● Generation V: Modern PMMA Posterior Chamber IOLs were designed and implanted from 1975 to 1990's. During this period, the evolution of extracapsular cataract extraction was marked by four major milestones: Microscopic surgery, phacoemulsification for cataract removal, iridocapsular fixation, and use of flexible haptics.[70]

● Generation VI: This generation of IOLs began in the mid 1980s and is the most common type of IOL implanted today. The major advantage of foldable IOLs is the ability to insert the lens through a 2.5 mm corneal incision.[72]

1.3.4.3 Types of IOL

These are several types of IOLs.[73] The following subsections are devoted to specific cases.

a. Monofocal IOL

Monofocal, or single vision lenses, are the standard lenses that have been implanted at the time of routine cataract surgery for many years. These lenses take the

place of cataract and can help one to see distant objects. However, these lenses will not correct astigmatism and will not correct near vision, so it is likely that one will need to wear glasses at least part-time for distance visions and full-time for near work.

b. Toric IOL

In addition to correcting nearsightedness or farsightedness, toric lenses have the ability to correct astigmatism. If one has significant astigmatism before surgery, then this lens option will provide you with a better opportunity to have clear distance vision without glasses. Toric lenses still correct primarily distance vision and will not correct near vision.

c. Multi-focal IOL

Multi-focal lenses are appropriate for some patients who have a strong desire to see distant and near objects without glasses and are willing to potentially somewhat compromise the quality of their vision to obtain freedom from glasses. In appropriate candidates, multi-focal lenses can improve distance, intermediate (computer distance), and near vision and can reduce their dependency on spectacles at all of these distances. However, neither lens restores the natural vision at all distances one had as a youth, and the person may experience some problems with these lenses. These include, but are not limited to: poor night vision, including glare and halos, less sharpness of vision than may be obtained with a mono-focal IOL and spectacles, and inadequate near and intermediate vision that still may require the use of glasses. Multi-focal lenses may require some time for adaptation, and in very rare cases, the vision obtained with multi-focal lenses may be so poor that replacement of the lens with a mono-focal lens may be necessary. This is a separate procedure, and it carries additional surgical risks.

d. Pseudo-accommodative IOL

These IOLs are designed to provide good distance acuity and a moderate amount of intermediate and near correction. Most patients would find that they still require reading glasses for most near tasks.

1.3.4.4 Manufacture of IOL

Polymerisation techniques to make materials for IOLs

The process for the production of IOLs consists of the following steps:

(a) Copolymerisation of monomers

(b) Casting into lenses

(c) Machining, cutting and grinding

(d) Fixing of the haptic to the optic.

a. Copolymerisation: The polymers for foldable intraocular lenses and rigid intraocular lenses are made by the conventional polymerisation. Mixtures of the liquid monomers in the desired proportion, and a conventional thermal free radical initiator are injected into a suitable mold consisting of the optic and haptic portions.

b. Cast polymerisation: The mixture is then subjected to a heating cycle to activate the initiator. Free radical initiator such as peroxides, peroxydicarbonates and azonitriles are used. To facilitate the polymerisation, conventional photo initiator compounds are also used.

Optional additives such as UV absorbing materials are used so that the lenses may have an ultraviolet absorbance imitating that of the natural lens of the eye. The ultraviolet absorbing material can be any compound that absorbs ultraviolet light but does not absorb substantial amounts of visible light. The ultraviolet absorbing compound is incorporated into the monomer mixture and entrapped in the polymer matrix when the monomer mixture is polymerised.[74] To prevent leaching out of the ultraviolet absorbing compound, compounds that can covalently bond to the polymer matrix are chosen.

IOLs can also be cast into sheet form by a conventional two step procedure.[75] In the first step, the casting mixture is prepared by heating the mixture of monomers, cross-linking agent and initiator at 80°C. In the second step, the mixture is transferred to a cell suitable for casting sheets and polymerised by subjecting the cell to suitable heating. IOLs are lathe cut from sheets while holding the temperature of sheets below 0°C.[76]

c. Cutting, grinding and machining: After the polymerisation cycle, molding and drilling operations are carried out. The mold containing the optical material is placed on a

lathe and the desired optic chamber is lathe cut. The lathing and drilling operation is carried out by cooling the mold/optic in a freezer to less than 10 °C and preferably less than 0 °C.[77]

d. Attachment of the haptics: The next step involves the attachment of the haptic to the optic in the case of a multipiece IOL. Two holes are drilled into the side of the lens. The haptic is then inserted into the optic with the help of a laser source. Suitable haptic materials are polypropylene and PMMA.

e. Techniques of making IOLs from base materials: Rigid intraocular lens made of PMMA and soft intraocular lens made of modified acrylates or silicones can be manufactured by:

1. Cast molding: - A method of injecting a monomer into a casting mold designed to produce lenses of a desired shape. Cast molding is also used to cast optical blanks, which are further processed into lenses.

2. Lathe cutting: - A method of cutting a sheet obtained by polymerising and curing of a monomer into an intraocular lens of a desired shape. Another alternative is to use the optical blanks and subjecting it to the lathe machine to cut lenses out.

Sometimes in the IOLs manufactured by the methods indicated above, formation of voids was observed. These voids get filled up with the vitreous humor of the eye and results in the formation of luminescent spots which do not affect the visual activity, but influence the contrast sensitivity of the IOL.[78]

Ichikawa, et al.[79] developed a multi-step process to overcome the void formation as detailed below:

- ✓ Step 1: The monomer mixed solution is polymerised to produce a base material.
- ✓ Step 2: One part of the base material produced in the first step is heated in an oven to complete the polymerisation.

- ✓ Step 3: The completely polymerised material is immersed into the second portion of the base material produced during step 1. In case any voids formed in the polymerised material can be filled by the base material during this step.
- ✓ Step 4: The impregnated material from the above step is taken out and excess of unpolymerised base material is removed from the surface.
- ✓ Step 5: The setting of a protective coating is done after removing excess of unpolymerised material from the surface of the base material as in step 4.

Basically, this method was earlier tried for preparation of other polymeric materials such as Poly(vinyl chloride) to eliminate the voids, also termed as fish eye. The multistep process of making IOLs is useful in that respect. By adopting suitable methodology for preparation of IOLs, certain biocompatibility problems could be resolved. For example, according to Hung et al., a bicomposite IOL optic comprising an anterior surface material consisting of an ophthalmically acceptable lens-forming material and a posterior surface material, different from the anterior surface material, for reducing the risk of posterior capsule opacification is prepared.[80] The posterior surface material consisted essentially of two or more aryl acrylic hydrophobic functional monomers. The method of preparation of IOLs involves the following steps:

(a) Forming a posterior surface layer of material by polymerising a posterior surface material composition consisting essentially of two or more aryl acrylic hydrophobic monomers and a cross-linking agent in a mold having the desired IOL posterior surface shape and by

(b) Forming an anterior surface layer by adding a liquid anterior composition consisting of an ophthalmically acceptable IOL material to the top of the posterior surface layer and polymerising the liquid anterior composition.

Another method for producing IOLs include a combination of steps which helped to increase the pull strength between the fixation member of the IOL and the optic of the IOL without requiring sophisticated high frequency corona discharge activation or plasma activation of the fixation member or primer coating of the fixation member.

It may appear simple, but achieving the complete polymerisation to obtain a material of desired characteristics, without any optical flaws, remains a subject of research and development, in spite of the existing experience of so many years and for several types of materials.

Attempts to resolve the biocompatibility related issues by developing novel methods of preparation of IOLs are a welcome trend. As far as the concept of providing a single material with completely different surfaces is concerned, it presents several opportunities if one looks at the challenges.

1.3.4.5 Hydrophilic IOL's Literature

Despite good biocompatibility and optical properties, several problems still exist for PMMA lOLs. Some problems are listed below:

1) The corneal endothelium adheres to the hydrophobic PMMA and may be damaged in the event of contact intra-operatively or post-operatively.
2) PMMA lenses cannot be autoclaved. Ethylene oxide sterilisation requires caution to exclude toxic derivatives of ethylene oxide.
3) The hardness of PMMA may introduce hazards of pressure trauma to implanted eyes Several solutions for the above problems have been studied.

The use of sodium hyaluronate solutions (e.g. Healon) or hydrophilic surface modification of PMMA lOLs[80-87] is reported to reduce the endothelium damage. Polycarbonate was studied as a tougher, stronger IOL material, which is also autoclavable.[80] A number of soft flexible materials are being investigated for use in lOLs.[87-91] Silicone and poly(hydroxyethyl methacrylate) (pHEMA) hydrogels are two of the most promising soft materials. Both can be autoclaved, and surgical trauma may be reduced for the hydrogels due to surface properties. An added advantage of soft lOLs is that they may be folded and implanted through smaller incisions and then unfolded to the normal shape. Hydrogels have been used in various biomedical applications for many years because they are soft, highly hydrated, and begin to simulate living tissue in their physical properties. Successful biomedical applications include soft contact lenses,[94-96] drug release devices,[97-99] soft lining of dentures,[100] etc.

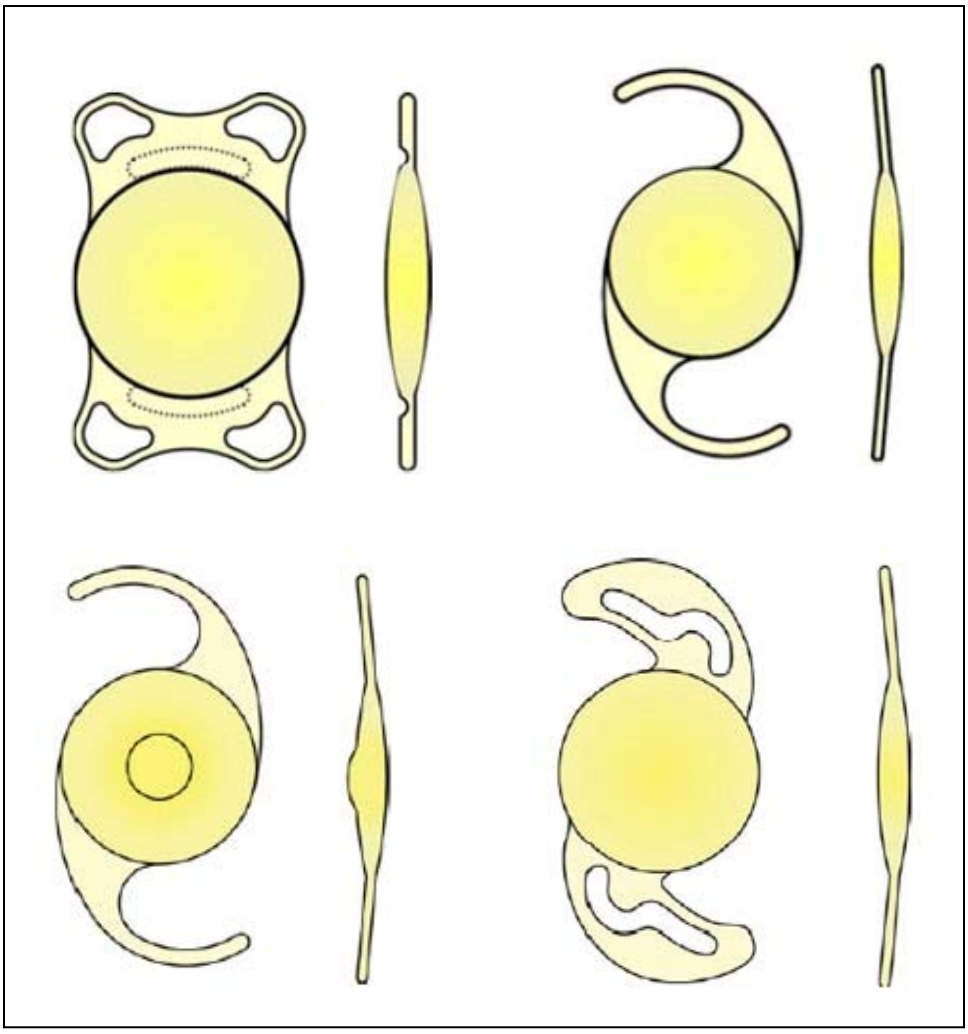

Figure 1.6: Hydrophilic intraocular lenses

The feasibility of hydrogels as IOL materials has been considered in 1970s.[91,101] Since then, several studies on the biocompatibility of hydrogel lOLs have been reported.[88-92] Yalon et al. studied the biocompatibility and endothelium contact damage of several hydrogel lOLs.[88] Soft IOLs made of an aminopolyamide and a poly(hydroxyethyl methacrylate) (pHEMA) hydrogel were implanted in cats. Results indicated that these lenses were better tolerated than the PMMA lOLs in reducing endothelium damage. Blumenthal studied the use of high water content hydrogels as lOLs.[91] He reported that the tensile strength of his hydrogels could reach a level of 220 psi, but the composition and the water content of the hydrogels were not reported.

Clinical data suggested that these hydrogel lOLs were well tolerated by the human eyes. Siepser has studied "expansile" hydrogel IOLs using a rabbit implant model.[92] In one study, dehydrated hydrogel lOLs with 3.2 mm diameter optics were implanted through a 3.5 mm incision and hydrated to 5.8 mm. These lenses were also reported to be biocompatible.

In contrast with their reported biocompatibility, hydrogels generally display very poor mechanical properties. For example, the tensile strength of PHEMA or NVP-MMA hydrogel contact lenses is in the range of 50 to 150 psi.[102-104] Hydrogel implants are therefore readily torn or damaged during surgical manipulation. The strength of hydrogels therefore has to be improved if they are to be used for foldable lOLs and become accepted for general clinical use. Several methods have been found to improve the mechanical strength of hydrogels. These include incorporation of powders or fibers in the hydrogel matrix,[100,103,105] increasing chemical or physical cross-linking,[103,106,108] and copolymerisation with hydrophobic monomers.[102,104,109,110] The use of fibre-reinforced hydrogels for synthetic tendons was studied by Kolarik et al.[105-110] and Migliaresi and Nioolais.[112] Model synthetic tendons were prepared by reinforcing a pHEMA matrix using texturised poly(ethylene terephthalate) fibres (a bundle of 38 fibres, 1.22 x 10.2 mm^2 in cross section).[105] The tensile strength of the resulting hydrogel composites are in the range of 7000 to 12000 psi.

Their mechanical properties approximate that of natural tendons, which are composite structures consisting of collagen fibres embedded in a gel-like mucopolysaccharide. The application of such fibre-reinforced hydrogels for lOLs is limited by the opacity of the resulting compositions due to the dimensions of the fibers in use. However, the corneal stroma itself is a composite material composed of 20 wt.% collagen fibrils, 5 wt.% protein, and 75 wt.% water.[133] Therefore, fibre-reinforced hydrogel lOLs might be possible if the refractive index of the fibre can approximate the hydrogel matrix or if very fine fibres are used. Fiaab and Janacek prepared reinforced PHEMA networks by crosslinking and copolymerisation in the presence of different concentrations of silica powder and studied the mechanical properties.[134] The volume fraction of filler was in the range of 0 to 0.194. The tensile strength increased almost four

times for the samples containing the highest volume concentration of the filler. The strain at break remained approximately constant. The optical properties of the resulting gels depended on the powder size and the volume fraction of the powder incorporated. The tensile strength of hydrogels generally increased with increasing crosslinking density. Raab and Janacek[135] studied the effect of crosslinker concentration upon tensile strength and strain at break for pHEMA. The concentration of crosslinker, ethylene dimethacrylate, was in the range of 0.1 to 10%. The tensile strength increased from 50 psi for the lowest crosslinker concentration (0.1%) to 270 psi for the highest (10%). The strain at break fell from 480 to 50%.

Even though the strength can be improved by increasing chemical crosslink density, rigidity also increases and hydration decreases. Wichterle[116] suggested that the strength of hydrogels may be improved by physical rather than chemical crosslinking with avoidance of embrittlement caused by chemical crosslinks. Physical crosslinking in hydrophilic networks can be achieved in two ways:

1) Formation of crystalline domains
2) Formation of hydrophobic microphases

Ordering of network segments into crystalline domains occurs rarely. Peppas and Merrill[106-108] studied the mechanical properties of poly(vinyl alcohol) hydrogel with 30 to 65% crystallinity. To prepare these hydrogels, aqueous poly(vinyl alcohol) solutions were crosslinked via electron beam irradiation. Partial crystallisation of these hydrogels was then induced by a two-stage dehydration-annealing process. The resulting materials showed greatly improved mechanical properties including higher modulus (200 to 1500 psi), tensile strength (500 to 1500 psi), and elongation at break (120 to 500%) as compared to the uncrystallised hydrogels (up to 70 psi tensile modulus, less than 10 psi tensile strength, less than 90% elongation at break).The tensile strengths varied between 500 and 1500 psi, and moduli between 200 and 1500 psi, depending on the annealing conditions and the crosslinking density. However, a major limitation of these hydrogels for flexible lOLs is that the strength is low when amorphous and the optical properties are poor when they become stronger and semicrystalline.[117]

Nakashima et al. prepared graft-type copolymers composed of hydrophilic PHEMA as a backbone and hydrophobic PMMA as a long branch.[110] Films of this copolymer cast from solution in dimethyl formamide were found to form hydrophobic domains dispersed in the hydrophilic matrix. The dimension of PMMA domains was about 200 to 300 A, and the hydrogels were therefore transparent. The tensile strength was in the range of 50 to 250 psi depending on polymer composition.

Another route to improved mechanical properties of hydrogels is copolymerisation with hydrophobic monomers. Randomly crosslinked copolymers of HEMA and MMA were prepared and their mechanical properties studied by Migliaresi et al.[104] The tensile strength of the hydrogels increased from 50 to 4000 psi with increasing MMA concentration (from 0 to 80%), as did the tensile modulus (from 100 psi at 0% MMA to 70000 psi at 80% MMA). However, hydrogels with high moduli lost their flexibility and become too rigid to be useful for flexible ocular implants despite their high mechanical strength. Hosaka et al.[102] studied the mechanical properties of the hydrogels of poly(methyl methacrylate-co-N-vinyl pyrrolidone). Properties included tensile strength, tensile fracture energy, flexibility, and recovery from deformation.

The STAAR Surgical *Collamer IOL* (CC4204BF) is a plate haptic, single-piece foldable lens manufactured from a "collamer material".[66] The overall length of the IOL is 10.8 mm (11.2 mm corner to diagonal corner) with an optic diameter of 6.0 mm. The haptic design has two 0.9-mm fenestrations to facilitate capsular fixation. These fenestrations are smaller than those of 1.15 mm incorporated into STARR's silicone plate haptic IOL. This acrylic IOL is composed of a hydrophilic collagen polymer (copolymer of 63% hydroxylethyl methacrylate, 0.3% porcine collagen, and 3.4% of a benzophenone for UV absorption), with a water content of 34%, a light transmission of 99%, and a refractive index of 1.45 at 35 °C.

A newly designed hydrophilic acrylic IOL has escaped the stigma associated with some of the previous IOLs. The Rayner *C-flex*, formerly Centerflex (Rayner Intraocular Lenses Ltd.), is a newly developed one-piece, hydrophilic acrylic IOL in use today. The lens is made of a copolymer of hydrophilic and hydrophobic methacrylates with a water

content of 26%, namely, HEMA and methyl methacrylate. Its material incorporates a benzophenone UV-absorbing agent, and it is inserted into the eye by means of a disposable cartridge-injector system.[66]

1.3.4.6 IOLs from hydrophilic-hydrophobic monomer combinations

Hydrogel IOLs varying in composition and differing in water content, refractive index, folding behaviour, and biocompatibility have been developed.[118-119]

In general, hydrogel materials have a relatively low refractive index, making them less desirable than other materials because of the thicker lens optic necessary to achieve a given refractive power.[120]

An increase of the refractive index is always desirable because it permits the IOL manufacture of lower thickness and the subsequent reduction in the size of the incision. In this sense, hydrogel materials based on hydrophilic monomers of high refractive index were developed. Silicone materials generally have a higher refractive index than hydrogels, but tend to unfold explosively after being placed in the eye in a folded position.[120]

Explosive unfolding can potentially damage the corneal endothelium and/or rupture the natural lens capsule. Acrylic materials are desirable because they typically have a higher refractive index than silicone materials and unfold more slowly or controllably than silicone materials. Thus, hydrogels were obtained from copolymerisation of N-vinyl pyrrolidone and 3-hydroxypropyl methacrylate[121] which showed good *in vivo* bio-tolerance. HEMA was copolymerised with N-vinyl pyrrolidone and diacetone acrylamide to get materials particularly useful for use in the posterior chamber of the eye.[122] The production of hydrogels with long-term stability has been attempted by copolymerisation with N-benzyl-N-methyl acrylamides.[123] Also the copolymerisation reaction with vinyl comonomers and different cross-linking agents formed optically transparent, high water content, and high refractive index hydrogels, suitable for intraocular lenses manufacture and as super-absorbents materials.[124]

Post-operative endophthalmitis following intraocular lens implantation is still one of the most feared complications of cataract surgery. Once it is triggered, the only way to end the infection is to remove the infected IOL. One strategy to avoid or prevent endophthalmitis has been the modification of the biomaterial's surface. Thus, heparin-surface modified PMMA IOLs (Pharmacia Production B.V.) provided a significantly lower number of attached bacteria with respect to untreated ones,[125] reducing the risk of endophthalmitis post-implantation.[126] The coating of acrylic IOLs with poly(2-methacryloyloxyethyl phosphoryl-choline-co-n-butyl methacrylate) also resulted in effective inhibition of both bacterial and fibroblast adhesion.[127] Other surface-modified hydrogels have been prepared by electrostatic binding of porphyrins to copolymers of HEMA with methacrylic acid (MAA) that displayed required properties for clinical application.[128]

Hydrophilic, aromatic monomer that has an aromatic group substituted with at least one hydrophilic substituent and a reactive functional group has been reported.[129] Polymers comprising such a hydrophilic, aromatic monomers avoid or reduce the risk of forming vacuoles of absorbed water. These polymers have high refractive index and, thus, are useful for making intraocular lenses. Transparent, high refractive index hydrogels were synthesised by copolymerisation of hydrophilic monomers with high refractive index monomers like phenylethyl acrylate for IOL applications having a refractive index of 1.45 or above and a water content of approximately 5 to 30 percent by weight.[130]

Thus copolymerisation of two or more monomers to achieve desired prosperities of material suitable for IOL applications is a necessity. Co- and terpolymerisation are used effectively to increase the amorphous character of the polymer which increases the transparency and the flexibility of the polymer chains. Copolymers tend to have a set of properties uniquely their own, setting them apart from that of their parent homopolymers. In copolymers sequence distribution of two monomers is key to ensure homogeneity. Thus, investigation of copolymerisation kinetics is of paramount importance.

It is quite obvious that the IOLs are designed to remain inserted in the eye as an integral part of eye playing the role of a naturally existing crystalline lens of the eye.

Thus, it is essential that the material to be used for making IOLs must meet the following basic criteria mentioned in Table 1.1.[131]

Table 1.1: Essential properties of material for IOL application

Property	**Description**
Transparent	The polymer may not be opaque. Otherwise scattering will be caused by the polymer or embedded particles generating glare.
Colourless	The material should be without colour. Only a slight yellowish tone caused by absorption of blue light can be tolerated. Coloured materials are not suitable.
Elastomeric	The material should have elastomeric properties to obtain a foldable IOL and avoid plastic deformation.
Cross-linked	To afford elastomeric properties the polymer must be a cross-linked network. A cross-linking procedure that does not involve a photochemical process is favorable to avoid undesired changes in refractive index.
Bulk polymerisable	The corresponding monomer should be polymerisable to a plate by bulk polymerisation. Bulk polymerisation is the conversion of monomer into a polymer without the aid of a solvent.
Suitable for turning	The mechanical properties of the polymer must allow the fabrication of IOLs by diamond turning.
Biocompatible	The polymer must not have any toxic or injurious effects on the eye.
Non-degradable	Despite being biocompatible the polymer should not be biodegradable. Otherwise, the IOL would degrade over the long time it needs to stay in the eye.
Thermally stable	Polymeric material should be thermally stable.
Immune to sunlight	The overall IOL must be designed in such a way that light from the sun or other common light sources cannot change the refractive power even after extended periods of time.

In view of the foregoing, the purpose of this study was to obtain a better understanding of the relationships between the physical properties of hydrogels and their compositions to provide a basis for developing new and more rubbery hydrgels for flexible ocular implants.

The present study aims at synthesis and chemical kinetic estimation of copolymerisation of a hydrophilic monomer with a hydrophobic monomer which would yield new soft, hydrophilic acrylic copolymers which would suitable for foldable IOLs.[131]

Table 1.2: Characteristics of some currently available hydrophobic IOLs

IOL/manufacturer (country)	Material composition*	Refractive index	T_g
Three-piece and one-piece AcrySof/Alcon Laboratories, Inc. (US)	Copolymer of phenylethyl acrylate and phenylethyl methacrylate, cross-linked with butanediol diacrylate	1.555	14.0
Sensar AR40 and AR40e one-piece Tecnis/Abbott Medical Optics Inc. (US)	Copolymer of ethyl acrylate, ethyl methacrylate, and 2,2,2-trifluoroethyl methacrylate, cross-linked with ethylene glycol dimethacrylate	1.470	12.21
AF-1 series iMics 1/Hoya Surgical Optics (Japan)	Cross-linked copolymer of phenylethyl methacrylate and n-butyl acrylate, fluoroalkyl methacrylate	1.520	11
XACT/Advanced Vision Science, Inc. (US)	Copolymer of hydroxyethyl methacrylate, polyethylene glycol phenyl ether acrylate, and styrene, cross-linked with ethylene glycol dimethacrylate	1.540	15–20
HP 757SQ/Aurolab (India)	Copolymer of ethylacrylate and ethylmethacrylate, cross-linked with a difunctional acrylate/methacrylate	1.470	11 ±2
Acrylmex/Ophthalmic Innovations International (now Aaren Scientific) (US)	Terpolymer of butyl acrylate, ethyl methacrylate, and N-benzyl-N-isopropylpropenamide, cross-linked with ethylene glycol dimethacrylate	1.490	NP
Matrix Acrylic Aurium/Medennium (US)	Poly(2-phenyloxyethyl acrylate), cross-linked with phenyl-containing dimethacrylate (IOL has a photochromic chromophore)	1.560	NP
Hydromax/Carl Zeiss Meditec (Germany)	Homopolymer of 2-phenoxy ethyl acrylate, cross-linked with ethoxylated (2) bisphenol A dimethacrylate	1.560	16
SeeLens HP/Hanita (Israel)	Ethoxyethyl methacrylate and methyl methacrylate with incorporated violet-filtering chromophore	1.480	10
Mediflex/Mediphacos (Brazil)	Copolymer of acrylate/methacrylate with blue-light filtering chromophore nonaromatic acrylic rubber	1.480	5
* All models have ultraviolet light blockers, NP = not provided			

1.4 References

[1] A. P. Kyritsis, J. Pissis, R. Gomez and M. Monleon Pradas, *Calorimetric and Sorption Isotherm Measurements,* **1995**, 3, 445.

[2] N. A. Peppas and R. S. Langer, Biopolymers in *Adv.Poly. Sci.*, **1995**, 122, 126.

[3] Y. Cohen, O. Ramon, Kopelrnan and S. Mizrahi, *J. Poly. Sci.: Part B: Poly. Phys.*, **1992**, 30, 1055.

[4] S. M. Murphy, C. J. Hamilton, M. L. Davies and B. J. Tighe, *Biomaterials,* **1992**, 13, 979.

[5] L. Ambrosio, R. DeSantis and L. Nicolais, *J. Eng. Medicine*, **1998**, 212, 93.

[6] T. Hatakeyama, S. Hirose and H. Hatakeyama, *Makromol. Chemie*, **1993**, 184, 1265.

[7] S. Eichler, O. Ramon, I. Ladyzhinski, Y. Cohen and S. Mizrahi, *Food Research International*, **1997**, 30, 719.

[8] D. Hu and M. Lin, *Polymer*, **1994**, 35, 4416.

[9] Y. Cohen, O. Ramon, I. Kopelrnan and S. Mizrahi, *J. Poly. Sci.: Part B: Poly. Phys.*, **1992**, 30, 1055.

[10] J. Ferry, *Polymer*, **1979**, 20, 1343.

[11] P.J. Flory, *J. Chem. Phys.*, **1993**, 11, 521.

[12] S. Durmaz. and O. Okay, *Polymer*, **2000**, 41, 5729.

[13] J. Rosiak and F. Yoshii, *Nuclear Instruments and Methods in Physics Research B,* **1999**, 151, 56.

[14] J. Gomez Rbelles, M. Monleon Pradas, G. Gallego Ferret, N. Peidro Torres, V. Perez Gimenez, P. Pissis and A. Kyritsis, *J. Poly. Sci.: Part B: Poly. Phys.*, **1999,** 37, 1587.

[15] W. Timmer, *Chem. Technol*., **1979**, 79, 175.

[16] B. D. Ratner, *Comprehensive Poly. Sci.*, **1989**, 7, 201.

[17] N. A. Peppas, H. J. Moyniham, *Hydrogels in Medicine and Pharmacy*, Vol. 2, Peppas, N. A., Boca Raton, FL, CRC Press, **1987**.

[18] M. V. Sefton and W. T. K. Stevenson, *Adv. Polym. Sci*., **1996**, 107, 143.

[19] T. Tsurauta, *Adv. Poly. Sci.*, **1992**, 126, l.

[20] M. L. Davies, S. M. Murphy, C. J. Hamilton and B. J. Tighe, *Biomaterials*, **1992**, 13, 991.

[21] J. D. Rao, V. Ramesh and K. Panduranga Rao, *Biomaterials,* **1994**, 15, 383.

[22] N. A. Peppas and R. S. Langer, Biopolymers, *Adv.Poly. Sci.*, **1995**, 122, 126.

[23] L. Ambrosio, R. DeSantis and L. Nicolais, *J. Eng. Medicine*, **1998**, 212, 93.

[24] C. Migliaresi, L. Nicodemo, P. Nicolais, P. Passerini, *Polymer*, **1982**, 25, 686.

[25] Y. Zhihui, Z. Yajie, Z. Xiaomin and Y. Jinghua, *Polymer*, **1998**, 39, 547.

[26] J. R. Fried, *Polymer Science and Technology,* Prentice Hall, New York, **1995**.

[27] K. Sunaga, M. Kim, K Saito, K. Sugita, T. Sugo, *Chemical Materials II*, **1999**, ll, 1986.

[28] B. Leung and G. Robinson, *J. Appl. Poly. Sci.,* **1993**, 47, 1207.

[29] C. Peniche, M. E. Cohen, B. Vazquez and J. San Roman, *Polymer,* **1997**, 38, 5977.

[30] H. Dorrington, N. McCrum and W. Watson, *Polymer,* **1977**, 18, 712.

[31] M. Braden and P. Wright, *Journal of Dental Research*, **1982**, 62, 764.

[32] C. Brazel and N. Peppas, *Polymer*, **1999**, 40, 3383.

[33] S. Mallapragada and N. Peppas, *J. Controlled Release*, **1977**, 45, 87.

[34] S. Lustig and N. Peppas, *J. Appl. Poly. Sci.*, **1987**, 33, 533.

[35] Z. Sedlakova, K. Bouchal and M. Iiavsky, *Poly. Bulletin*, **2000,** 44, 585.

[36] L. Masaro and X. Zhu, *Prog.Poly. Sci.*, **1999**, 24, 731.

[37] B. Jeong, H. Bae and S. W. Kim, *J. Controlled Release*, **2000**, 63, 155.

[38] B. C. Patterson, The Florida State University, *Ph. D. Thesis*, **2000.**

[39] G. Paradossi, F. Cavalieri, E. Chiessi, C. Mondelli and M. F. Telling, *Chem. Phys.*, **2004**, 302, 143.

[40] V. Michailova, St. Titeva, R. Kotsilkova and E. Krusteva, *Colloids and Surfaces A: Physiochemical and Engineering Aspects*, **1999**, 149, 515.

[41] J. Singh, and K Agrawal, *J. Macromol. Sci.- Revs. Macromol. Chem. Phys.*, **1992**, C(32), no. 3 & 4, 521-534.

[42] M. J. Refojo, *J. Appl. Poly. Sci.*, **1965**, 9, 3161.

[43] J. Guzman, M. lglesias, E. Riande and V. Compan, .*Polymers*, 1997, 46.

[44] D. Mirejovsky, A. Patel and G. Young, *Biomaterials*, **1993**, 14, 1080.

[45] D. Harvitt and J. A. Bonanno, *Investigative Ophthalmololgv and Visual Science*, **1998**, 39, 2778.

[46] R. B. Mandell, *Contact Lens Practice 3rd Ed*. Charles C. Thomas: Springfield III, **1981.**

[47] A. Phillips and L. Speedwell, *Contact Lenses 4th Edition*. Reed Educational and Professional Publishing Ltd., Oxford, **1997**.

[48] J. Montheard, M. Chatzopoulos and D. Chappard, *J. Macromol. Sci.-Revs. Macromol. Chem. Phys.*, **1992**, C32, 1.

[49] Y. C. Lai and L. J. Baccei, *Journal of Applied Polymer Science*, **1991**, 42, 3173.

[50] R. A. Weale, *J. Physiol.,* **1988**, 395, 577.

[51] S. Zigman, in: H. Maisel (Ed.), *The Ocular Lens: Structure, Function and Pathology*, Academic Press, London, **198**5, pp. 117–150.

[52] K. R. Hightower, *Curr. Eye Res.*, **1994**, 14, 71.

[53] www.who.int/mediacentre/factsheets/fs282/en/, cited on May **2012.**

[54] G. Brian, H. Taylor, *Cataract blindness - challenges for the 21st century*, *Bull. World Health Organ.*, **2001**, 79(3), 249.

[55] D. Apple, N. Mamalis, K. Loftfield, J. M. Googe, L. C. Novak, D. Kavka-Van Norman, S. E. Brandy and R. *J. Olson, Surv. Ophthalmol*., **1984**, 29, 1.

[56] D. J. Apple, K. D. Solomon, M. R. Tetz, E. I. Assia, E. Y. Holland, U. F. Legler, J. C. Tsai, V. E. Casteneda, J. P. Hoggatt and A. M. Kosick, *Surv. Ophthalmol.*, **1992**, 37, 73.

[57] D. A. Schaumberg, M. R. Dana, W. G. Christen and R. J. Glynn, *Ophthalmol.*, **1998**, 105, 1213.

[58] M. E. Wilson, *Ophthalmol.*, **1996**, 103, 1719.

[59] S. K. Pandey, M. E. Wilson, R. H. Trivedi, A. M. Izak, T. A. Macky, L. Werner, D. J. Apple, *Int. Ophthalmol. Clin*., **2001**, 41, 175.

[60] T. Kohnen, R. Pena-Cuesta and D. D. Koch, *Ger. J. Ophthalmol.*, **1996**, 5, 171.

[61] J. Zwaan, P. B. Mullaney, A. Awad, S. al Mefser, D. T. Wheeler, *Ophthalmol.*, **1998**, 105, 112.

[62] *http://www.oculist.net/downaton502/prof/ebook/duanes/pages/v6/v6c011.html* cited on April **2013.**

[63] D. T. Azar, *Intraocular Lenses in Cataract and Refractive Surgery*, Saunders, Philadelphia, **2001**.

[64] H. Gernt, *Annual Ophthalmology*, **1979**, 11, 617.

[65] S. Duke-Elder and D. Abrams; *System of Ophthalmology Ophthalmic Optics and Refraction*, Vol. 5, The C.V. Mosby Company, St. Louis, Missouri, **1970**.

[66] R. Reboul, *Synthesis and Properties of Acrylic Copolymers for Ocular Implantation.* (Univ. Florida), Ph. D. thesis, **2006**.

[67] P. B. Petersen and T. Sorensen.; *Acta Ophthalmol*., **1983**, 61, 382.

[68] E. Gruber, T. *Ophthalmol. Soc.,* UK, **1980**, 100, 231.

[69] D. J. Apple, G. U. Auffarth, G. Peng and N. Visessook, *Solution of Intraocular Lenses*, University of Utah Printing Service, Salt Lake City, Utah, **1985**.

[70] D. J. Apple, *Complications of intraocular lenses: A historical and histopathological review. Survey of Ophthalmology*, **1984**, 29, 1.

[71] D. J. Apple, R. J. Olson, M. C. Kincaid, *Intraocular Lenses: Evolution, Designs Complications, and Pathology, ed. Brown*, Williams and Wilkins, Baltimore, Maryland, **1989**.

[72] S. P. Shearing, *Journal of American Intra-Ocular Implant Society*, **1984**, 10, 343.

[73] *www.eyecenter.emory.edu*, on May **2012.**

[74] K. Inomata, K. Nakazato, N. Nakabayashi and K. Ishihara, JP 169526, **2000**.

[75] F. Oener, S. Hakan, A. Osman, S. D. Sarioglu, K. Ismet and C. Sueleyman, *Ophthalmologica* , **2003** , 217(2), 124.

[76] A. R. Leboeuf and M. Karakelle, *WO9907756*, **1999**.

[77] K. Mentak, *WO0061646*, **2000.**

[78] N. Ichikawa, Y. Akahata and T. Sunada, *US 7160488*, **2007**.

[79] A. T. Milauskas, *Archives of Ophthalmology*, **1991**, 109, 913.

[80] X. D Hung, K. Yao, Z. Zhang, Y. Zhang, Y. Wang, *J. Cataract and Refractive Surgery,* **2010**, 36, 290.

[81] D. C. Osborn, *Ph. D. Thesis*, University of Florida, **1985.**

[82] J. W. Sheets, *Ph. D. Thesis*, University of Florida, **1983.**

[83] M. Yalon, J. W. Sheets, Jr., S. Reich, and E. P. Goldberg, *Int. Congr. Opthalmol.*, **1982**, 25, 273.

[84] S. Reich, M. Levy, A. Meshorer, M. Blumental, M. Yalon, J. W. Sheets, and E. P. Goldberg, *J. Biomed. Mat. Res.,* **1984**, 18, 737.

[85] S. Kirk, R. M. Burde, and S. R. Waltman, *Investigative Ophthalmology and Visual Science,* **1997**, 16, 1053.

[86] D. Miller, P. O'Connor and J. Williams, *Ophthalmic Surgery*, **1977**, 8, 58.

[87] L. G. Pape and E. A. Balazs, *Ophthalmology,* **1980**, B1, 699.

[88] M. Yalon, M. Blumenthal and E. P. Goldberg, *J. Am. lntraocul. Implant Soc*., **1984**, 10, 115.

[89] K. R. Mehta, S. N. Sathe and S. D. Karyekar, *J. Am. lntraocul. Implant Soc.,* **1978**, 4, 200.

[90] M. Blumenthal, *Opthalmology Times*, **1985**, 19, 1.

[91] M. Blumental. In T. R. Mazzocco, G. M. Rajacich, and E. Epstein, (Eds.), *Intraocular lens*, Slack lnc., Thorotare, New Jersey, **1986**.

[92] J. Siepser, T. R. Mazzocco, G. M. Rajacich, and E. Epstein, (Eds.), *Soft Implant Lenses in Cataract Surgery*, Slack lnc., Thorofare, New Jersey, **1986**, p.107.

[93] E. Epstein, T. R. Mazzocco, G. M. Rajacich, and E. Epstein, (Eds.), Slack lnc., Thorofare, New Jersey, **1986**, p.83.

[94] D. G. Pedlev, P. J. Skelly, and B. J. Tighe, *Brit. Poly. J.*, **1980**, 12, 99.

[95] M. F. Rafejo, *International Ophthalmology Clinics*, **1980**, 1, 13.

[96] J.F. Kunzler, Hydrogels, *Encyclopedia Poly. Sci. Tech.,* Vol. 2, lnterscience

Publishers, New York, **2002**, p. 691.

[97] D. R. Cowasar, O. R. Tarwater, and A. C. Tanquary, *Am. Chem. Soc., Symp. Ser*., **1976**, 31, 180.

[98] M. Stol, M. Tolar, and K. Kliment, *J. Biomed. Mat. Res.*, **1969**, 3, 333.

[99] R. Prans and L. Krejii, *Ophthalmic Research*, **1977**, 9, 213.

[100] K. Kliment, M. Stol, M. Raab, and J. Stokr, *J. Biomed. Mat. Res.*, **1968**, 2, 473.

[101] J. J. Alpar and P. U. Fechner, *Intraocular lenses*, Thieme lnc., New York, **1986**, p. 23.

[102] S. Hosaka, A. Yamada, H. Tanzawa, T. Momose, H. Magatani, and A. Nakajima, *J. Biomed. Mat. Res.*, **1980**, 14, 557.

[103] J. Janacek, *J. Macromol. Sci.-Revs. Macromol. Chem*., **1973**, C9 (1), 1.

[104] C. Migliaresi, L. Nicodemo, L. Nicolais, P. Passerini, M. Stol, J. Hrouz and P. Cefelin, *J. Biomed. Mat. Res.*, **1984**, 18, 137.

[105] J. Kolarik, C. Migliaresi, M. Stol and L. Nicolais, *J. Biomed. Mat. Res.*, **1981**, 15, 147.

[106] N. A. Peppas and E. W. Merrill, *J. Poly. Sci.: Poly. Chem. Ed.*, **1976**, 14, 441.

[107] J. C. Bray and E. W. Merrill, *J. Appl. Poly. Sci.*, **1973**, 12, 3779.

[108] N. A. Peppas and E. W. Merrill, *J. Poly. Sci.: Poly. Chem. Ed.*, **1976**, 14, 459.

[109] K. Ulbrich and J. Kopecek, *J. Poly. Sci.: Polym. Symp*., **1979**, 56, 209.

[110] T. Nakashima, K. Takakura and Y. Komoto, *J. Biomed. Mat. Res.*, **1977**, 11, 787.

[111] J. Kolarik, J. Vanicek and C. Migliaresi, *J. Biomed. Mat. Res.*, **1984**, 18, 115.

[112] C. Migliaresi and L. Nicolais, *lntl. J. Artificial Organs*, **1980**, 8, 114.

[113] S. D. Bruck, *J. Biomed. Mat. Res.*, **1973**, 7, 387.

[114] M. Raab and J. Janacek, *Proc. Conf. "Polymer 71",* Bulgaria, **1971.**

[115] M. Raab and J. Janacek, *lntl. J. Poly. Mat.,* **1972**, 1, 147.

[116] O. Wichterle, *2nd World Congress on Biomaterials, Washington D.C.*, **1984**, p.20.

[117] N. A. Peppas, (Ed.), *Hydrogels in Medicine and Pharmacy, Vol. ll,* CRC Press, lnc., Boca Raton, Florida, **1987**, p.1.

[118] M. Tehrani, H. B. Dick, B. Wolters and T. Pakula, T. *Ophthalmologica,* **2004**, 218, 57.

[119] S. Saika, T. Miyamoto and Y. Ohnishi, *J. Cat. Refract. Surg.,* **2003**, 29, 1198.

[120] A. E. Akinay and W. R. Laredo, *US 2012/0309899 A1*, Novartis AG, Basel(CH), **2012.**

[121] J. Singh, K. Agrawal, A. R. Ray, J. P. Singhal, H. Singh, V. K. Dada and M. R. Mehta, *J. Biomed. Mater. Res.,* **1992**, *26*, 1253.

[122] G. D. Barret, *Patent No. WO/85/000965*, Mar. 3, **1985.**

[123] X. Liao, Y. Wang and S. Q. Zhou, *U.S. Patent No. 5,717,049,* Feb. 10, **1998.**

[124] X. Liao, Y. Wang, S. Q. Zhou and T. Richards, *U.S. Patent No. 5,439,950*, Aug. 8, **1995.**

[125] A. M. A. El-Asrar, A. M. Shibl, K. F. Tabbara and S. A. Al-Kharashi, *Intern. Ophthalmol.,* **1997**, *21*, 71.

[126] P. G. Montan, G. Koranyi, H. E. Setterquist, A. Stridh, B. T. Philipson and K. Wiklund, *Ophthalmology,* **1998**, *105*, 2171.

[127] M. Shigeta, T. Tanaka, N. Koike, N. Yamakawa and M. Usui, *J. Cat. Refract. Surg.,* **2006**, *32*, 859.

[128] C. Brady, S. E. J. Bell, C. Parsons, S. P. Gorman, D. S. Jones and C. P. McCoy, *J. Phys. Chem., B,* **2007**, 111, 527.

[129] J. C. Salamone, J. F. Kunzler, R. M. Ozark, *U.S. Pat. Appl. Publ. US 2006270749 A1*, Bausch & Lomb Inc., Rochester, New York, USA, Nov., **2006.**

[130] P. V. Davi, St. Louis, Missouri, *US 6,657,030 B2*, Bausch & Lomb Inc., Rochester, New York, USA, Dec., **2003.**

[131] R. V. Ghorpade, *Ph. D. Thesis*, University of Pune, Sept., **2012.**

Chapter II

Kinetic Parameters and Reactivity Ratios

2.1 Introduction

Copolymer is a polymer derived from two (or more) monomeric species. Copolymerisation reactions involve the simultaneous incorporation of two or more monomers in the same chain during polymerisation. Monomers differ in their tendencies to be incorporated into a copolymer chain. This is because each of the two monomers present in a copolymerisation reaction reacts at different rate with the two differing free radical species present in the system.

Staudinger,[1] noted that the copolymer formed had almost no characteristics similar to those of the homopolymers derived from each of the monomers. Furthermore, the relative reactivities of monomers in a copolymerisation were also quite different from their reactivities in homopolymerisation. Thus, some monomers were more while some were less reactive during copolymerisation than during their homopolymerisation. Even more interesting was that some monomers that would not homopolymerise at all would copolymerise relatively well with a second monomer to form copolymers. It was concluded that the homopolymerisation features do not directly relate to those of copolymerisation. Thus, it is quite difficult to identify the properties of a copolymer from it's architecture.

Several classes of copolymers are known and the process of copolymerisation can often be changed in order to obtain these structures. A statistical or random copolymer may obey some form of statistical law which relates to the distribution of each type of comonomer, incorporated into the copolymer. Thus, for example, it may follow zero or first or second order Markov statistics.[2] Copolymer chains that are formed via a zero order Markov process, or Bernoullian, compose of a random distribution of two monomer structures from monomers A and B. These are termed random copolymers:[2]

–A-A-B-B-B-A-B-A-B-B-A-A-B-A-

Alternating, block and graft copolymers are the other three types of copolymer structures. Equimolar compositions with a regularly alternating distribution of monomer units are alternating copolymers:[3-7]

–A-B-A-B-A-B-A-B-A-B-A-B-A-B-A-

A linear copolymer that contains one or more long uninterrupted sequences of each of the comonomer species is a block copolymer:[8-9]

-A-A-A-A-A-A-A-A–B-B-B-B-B-B-B-B-B-

Where A and B represent two different monomers that turn into repeating units. Different block copolymers are distinguished by the number of blocks per molecule, for example

A_xB_y	$A_xB_yA_x$	$A_xB_yA_xB_y$	$(A_xB_y)_n$
Diblock	Triblock	Tetrablock	Multiblock

which are referred as AB diblock, ABA triblock, ABAB tetrablock, and AB multiblock copolymers, respectively.

A graft copolymer[10-11] is made up of a linear chain from one monomer (homopolymer) and one or more side chains that consist of linear chains arising from homopolymer of the other monomer.

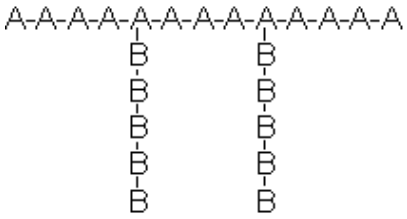

This thesis deals with the synthesis, kinetic estimation of randomly distributed or statistical copolymers, with the objective of establishing copolymer systems that can form azeotropic compositions which result in copolymer chains with the same composition through out the entire copolymerisation.

Copolymer composition is usually different from the molar composition of the starting materials charged into the polymerisation system. Therefore, monomers have different tendencies to be incorporated into the copolymer, which also means that each comonomer adds at different rate to the growing copolymer chain.

The first attempt at a quantitative, comprehensive theory of copolymerisation was made by Dostal,[12] later established quantitatively by Mayo and Lewis.[13] They demonstrated that the copolymer composition can be estimated from chemical reactivity of free radical propagating chain terminal units during copolymerisation. First order Markov statistics was applied and the terminal model of copolymerisation was proposed.

In copolymerisation kinetics the two monomers are termed as M_1 and M_2. During copolymerisation two types of propagating species exist transiently. The first of these species is a propagating chain that ends with a monomer of structure M_1 and the second species is a propagating chain that ends with a monomer of structure M_2.

For radically initiated copolymerisations, the two structures can be represented by -$M_1\cdot$ and -$M_2\cdot$, where the dash (-) represent the chain and the $M\cdot$ represents the radical at the growing end of the chain. The assumption that the reactivity of these propagating species only depends on the monomer unit at the end of the chain is called the terminal unit model.[14] If this is so, only four propagation reactions are possible for a two monomers system. The propagating chain that ends in $M_1\cdot$ can either add a monomer of type M_1 or of type M_2. Also, the propagating chain that ends in $M_2\cdot$ can add a monomer unit of type M_2 or of type M_1. Therefore, these equations can be written with the rate constants of reactions:[15]

$$-M_1\cdot + M_1 \xrightarrow{k_{11}} -M_1\cdot \qquad 2.1$$

$$-M_1\cdot + M_2 \xrightarrow{k_{12}} -M_2\cdot \qquad 2.2$$

$$-M_2\cdot + M_1 \xrightarrow{k_{21}} -M_1\cdot \qquad 2.3$$

$$-M_2\cdot + M_2 \xrightarrow{k_{22}} -M_2\cdot \qquad 2.4$$

The rate constant for the reaction of the propagating chain that ends in M_1 and adds another M_1 to the end of the chain is k_{11}, and the rate constant for the reaction of the propagating chain that ends in M_2 and adds M_1 to the end of the chain is k_{21}, and so on. The rate of disappearance of two monomers is given by:

$$-\frac{d[M_1]}{dt} = k_{11}[-M_1\cdot][M_1] + k_{21}[-M_2\cdot][M_1] \qquad 2.5$$

$$-\frac{d[M_2]}{dt} = k_{12}[-M_1\cdot][M_2] + k_{22}[-M_2\cdot][M_2] \qquad 2.6$$

In order to find the rate at which the two monomers enter into the copolymer, equation 2.5 is divided by equation 2.6 to give the copolymer composition equation:

$$\frac{d[M_1]}{d[M_2]} = \frac{k_{11}[-M_1\cdot][M_1] + k_{21}[-M_2\cdot][M_1]}{k_{12}[-M_1\cdot][M_2] + k_{22}[-M_2\cdot][M_2]} \qquad 2.7$$

A steady state concentration is assumed for both of the species -$M_1\cdot$ and -$M_2\cdot$ separately. The interconversion between the two species must be equal in order for the

concentrations of each to remain constant and hence the rates of reactions given in equations 2.2 and 2.3 must be equal:

$$k_{21}[-M_2\cdot][M_1] = k_{12}[-M_1\cdot][M_2] \qquad 2.8$$

Rearrangement of equation 2.8 and combination with equation 2.7 gives:

$$\frac{d[M_1]}{d[M_2]} = \frac{\frac{k_{11}k_{21}[-M_1\cdot][M_1]^2}{K_{12}[M_2]} + k_{21}[-M_2\cdot][M_1]}{k_{22}[-M_2\cdot][M_2] + k_{21}[-M_2\cdot][M_1]} \qquad 2.9$$

This equation 2.9 can be further simplified by dividing the right side, numerator and denominator by $k_{21}\,[-M_2\cdot]\,[M_1]$. The results are then combined with the parameters r_1 and r_2, which are defined as the reactivity ratios:

$$r_1 = \frac{k_{11}}{k_{12}} \quad , \quad r_2 = \frac{k_{22}}{k_{21}} \qquad 2.10$$

The most familiar form of copolymerisation composition equation is then obtained as:

$$\frac{d[M_1]}{d[M_2]} = \frac{r_1[M_1]^2 + [M_1][M_2]}{r_2[M_2]^2 + [M_1][M_2]} \qquad 2.11$$

The ratio of rates of addition of each monomer can also be considered as the ratio of molar concentrations of the two monomers incorporated in the copolymer, which is denoted by (m_1/m_2). The copolymer composition equation can then be written as:

$$\frac{m_1}{m_2} = \frac{r_1[M_1]^2 + [M_1][M_2]}{r_2[M_2]^2 + [M_1][M_2]} \qquad 2.12$$

Where, the monomer reactivity ratios $r_1 = k_{11}/k_{12}$ and $r_2 = k_{22}/k_{21}$ are kinetic parameters which measure the relative rate of addition of a radical to its own monomer and the addition of the same radical to the comonomer. $[M_1]$ and $[M_2]$ are molar concentrations of monomers in the feed and $d[M_1]/d[M_2]$ is the relative rate of addition of the two monomers to the chain. For low conversions, quantity in the later half may be approximated to the mole ratio of the respective monomer in the copolymer. The differential form of the copolymer composition equation has also been derived on the basis of probability of monomer addition.[16] This is suggestive of the correctness of the four basic competitive reactions assumed in the kinetic treatment of binary copolymerisations.

The probability of addition of monomer M_1 to a chain radical -$M_1^{\bullet}$ is:

$$P_{11} = \frac{k_{11}[M^{\bullet}_1][M_1]}{k_{11}[M^{\bullet}_1][M_1] + k_{12}[M^{\bullet}_1][M_2]} = \frac{r_1[M_1]}{r_1[M_1] + [M_2]} = [1 - P_{12}] \qquad 2.13$$

Similarly,

$$P_{12} = \frac{[M_2]}{r_1[M_1] + [M_2]} = [1 - P_{11}] \qquad 2.14$$

$$P_{21} = \frac{[M_1]}{[M_1] + r_2[M_2]} = [1 - P_{22}] \qquad 2.15$$

$$P_{22} = \frac{r_2[M_1]}{[M_1] + r_2[M_2]} = [1 - P_{21}] \qquad 2.16$$

The probability of occurrence of a sequence of 'n' molecules of species M_1 in a copolymer chain is:

$$P_{MI} = P_{11}^{\,n-1} P_{12} \qquad 2.17$$

The weight fraction of all M_1 sequences is:

$$W_1 = \frac{[P_{12}]}{[P_{11}]n\Sigma 1} = [P^n{}_{11}] = \frac{1}{P_{12}} \qquad 2.18$$

Likewise, the weight fraction of all M_2 sequences is :

$$W_2 = \frac{1}{P_{21}} \qquad 2.19$$

The composition of the copolymer is given by:

$$\frac{d[M_1]}{d[M_2]} = \frac{W_1}{W_2} = \frac{P_{12}}{P_{21}} \qquad 2.20$$

$$= \frac{r_1[M_1] + [M_2]}{[M_2]} / \frac{r_2[M_2] + [M_1]}{[M_1]} = [1 - P_{21}] \qquad 2.21$$

$$\frac{[M_1]}{[M_2]} = \frac{r_1[M_1] + [M_2]}{r_2[M_2] + [M_1]} \qquad 2.22$$

The copolymer composition equation can also be expressed in mole fractions instead of concentrations, which helps to make the equation more useful for experimental studies. Thus, F_1 and F_2 are the mole fractions of M_1 and M_2 in the copolymer, and f_1 and f_2 are the mole fractions of monomers M_1 and M_2 in the feed. Therefore:

$$f_1 = 1 - f_2 = \frac{[M_1]}{[M_1]+[M_2]} \qquad 2.23$$

and

$$F_1 = 1 - F_2 = \frac{d[M_1]}{d[M_1]+d[M_2]} \qquad 2.24$$

then combining equations 2.23, 2.24 and 2.11 gives

$$F_1 = \frac{r_1 f_1^2 + f_1 f_2}{r_1 f_1^2 + 2 f_1 f_2 + r_2 f_2^2} \qquad 2.25$$

This form of the copolymer equation gives the mole fraction of monomer M_1 introduced into the copolymer.[17]

2.2 Methods to Determine of Reactivity Ratios

Since the development of Mayo-Lewis equation for binary copolymerisation based on the terminal kinetic model, a large volume of literature has been devoted to it. This large quantity of experimental data has mainly been used to determine reactivity ratio, resonance stabilisation (Q) and electronegativity (e) parameters.[18] The kinetics and mechanisms involved in the free-radical binary copolymerisation of vinyl monomers have been a research topic of interest for many years. The composition and sequence distribution of a copolymer chain are dependent on the relative proportion of applied monomers as well as the monomer and radical reactivities.[19] Different models have been put forth to visualise the mechanism of addition of growing chains and the factors influencing them.

Estimation of reactivity ratios is important because of the following reasons. Primarily to predict copolymer composition and microstructure for any starting mixture, secondly to classify the relative reactivities of different monomers toward free macro-radicals and finally to understand issues related to the rate of copolymerisation and molecular weight distribution.

Copolymerisation reactivity ratios were originally measured for the purpose of describing the relative reactivities of various monomers towards various radicals. Now-a-days it is treated as quantitative data and hence the necessity of accurate measurement arises. Several methods have been developed to estimate reactivity

ratios. Some of these methods require labourious calculation procedures and so computer is put to use in an efficient manner to estimate reactivity ratios.

The estimation methods developed to determine reactivity ratio are based on the binary copolymer composition equations 2.12 and 2.26:[19-23]

$$\frac{dM_1}{dM_2} = \frac{r_1 M_1^2 + M_1 M_2}{r_2 M_2^2 + M_1 M_2} \qquad 2.26$$

where r_1 and r_2 are the monomer reactivity ratios and dM_1/dM_2 is the relative rate of addition of the two monomers to the chain. The copolymer composition may not be independent of conversion. This means the disappearance of monomer one may be faster than the disappearance of monomer two, if monomer one is being incorporated into the copolymer at a faster rate and therefore has a larger reactivity ratio than monomer two.

Depending on the reactivity ratios of the monomers, the copolymer can incorporate the comonomers in different ways. The three main types of behaviour that copolymerisations tend to follow correspond to the conditions when both r_1 and r_2 are equal to one, $r_1.r_2 < 1$ and $r_1.r_2 > 1$.

A perfectly random copolymerisation is achieved when both r_1 and r_2 values are equal to one. This type of copolymerisation will occur when the two different types of propagating species, $-M_1\cdot$ and $-M_2\cdot$ show the exact same preference for addition of each type of monomer.

An alternating copolymerisation is defined as $r_1 = r_2 = 0$. The polymer product in this type of copolymerisation shows a non-random equimolar amount of each comonomer that is incorporated into the copolymer. This may occur because the growing radical chains will not add to its own monomer. Therefore, the opposite monomer will have to be added to produce a growing chain and a perfectly alternating chain is obtained.

When $r_1 > 1$ and $r_2 > 1$, both of the monomers will add to themselves and in theory could produce block copolymers. But due to short lifetime of propagating radical, such copolymerisation produces undesirable heterogeneous products that include homopolymers. Therefore, macroscopic phase separation could occur and desirable physical properties such as transparency would not be obtained.

In order to determine the amount of comonomer that has been incorporated into the copolymer, various analytical methods must be used. Proton Nuclear Magnetic Resonance, Carbon 13 NMR, Chromatographic techniques such as Gas chromatography / HPLC and Fourier Transform Infrared Spectroscopy etc. are the sensitive instrumental techniques which are helpful in determining copolymer composition.

The copolymer composition equation is mostly employed to determine monomer reactivity ratios for low conversion copolymerisations. The copolymerisation systems are characterised by their monomer reactivity ratios under particular set of conditions (solvent, temperature etc.). Different methods, weighing in accuracy and ease of operation, have come into existence for their determination,[24-33] and excellent reviews[34,35] have also appeared.

Methods to estimate reactivity ratios are classified as differential of integral depending on whether they started from the differential or integral form of the Mayo-Lewis equation. Many methods have been used to estimate reactivity ratios of a large number of comonomers.[36] Tidwell and Mortimer distinguished four different procedures for the calculation of monomer reactivity ratios in copolymerisation, via. linearisation, approximation, intersection, and curve fitting. We will quickly review few of them which still have importance in today's context.

2.2.1 Linear Methods

2.2.1.1 The Intersection method

So as to determine the reactivity ratio of binary copolymerisations, a mathematical solution can be reached by performing two experiments.[37] Equation 2.11 is expressed into the following linear equation 2.27 given below:

$$r_2 = \frac{[M_1]}{[M_2]}\left[\frac{m_1}{m_2} - 1\right] + \frac{m_2[M_1]^2}{m_1[M_2]^2} r_1 \qquad 2.27$$

Where $[M_1]$, $[M_2]$ are the molar concentrations in the feed and m_1 and m_2 in the copolymer. A graphic representation of equation 2.27 gives a set of straight lines in r_1, r_2 coordinate, each line representing one experiment. The point whose coordinates are located at the intersection of two different experiments represents r_1 and r_2 values.

2.2.1.2 Joshi-Kapur (JK) method

As seen that points resulting from the intersection of lines at very small angles are further away from the hypothetically correct value, a weighting of the intersection points has been attempted using a function of the intersection angles [28, 38,39] where θ is the angle of intersection of the two lines.

$$r_i = \frac{\sum r_i [tg\theta]}{\sum [tg\theta]} \qquad 2.28$$

$$r_i = \frac{\sum r_i [\sin\theta]}{\sum [\sin\theta]} \qquad 2.29$$

The Joshi-Kapur method considers all *n(n-1)/2* intersections of pair combinations of all *'n'* experimental lines. So by this way the intersection points are also evaluated. These average values of r_i, estimated according to empirical criteria, do not assume that one of the points as best but expresses a possibility that another point may be a better fit to the experimental data than any of the intersection points.

2.2.1.3 Joshi and Joshi (JJ) method

Another method was put forwarded by Joshi and Joshi[40] which eliminates the subjective element in selection of the best point of intersection by statistically finding the closest point to all experimental lines.[41] This method[40,41] is an improvement of the Mayo Lewis intersection method resulting ideally in an unique intersection point. A condition was set up to make the sum of the squares of the perpendicular distances from all the lines to the best point of intersection to a minimum. This method does not suffer from the errors of reindexing the monomers.

2.2.1.4 Fineman-Ross (FR) method

The first method to balance successfully the entire set of experiments and to estimate the experimental error was developed by Fineman and Ross[42] in 1950. They reformulated the Mayo-Lewis equation so that the data points result in a single straight line. This method offers a simple graphical evaluation of reactivity ratios. A simpler method of estimation would involve carrying out the copolymerisations to low conversions and using the approximate form of differential copolymerisation equation to estimate the reactivity ratios. However, a simpler technique, which permits the use of data in the intermediate concentration regions and reduces the

uncertainties in the r values, is possible. If $f = (m_1/m_2)$ and $F = (M_1/M_2)$, then the differential equation 2.26 can be rewritten as:

$$\frac{F(1-f)}{f} = r_2 - \frac{F^2}{f} r_1 \qquad 2.30$$

Equation 2.30 can be represented as:

$$G = r_1 H - r_2 \qquad 2.31$$

where $G = (f-1)/F$ and $H = f/F^2$. A plot of G as ordinate and H as abscissa is a straight line whose slope is $-r_1$ and intercept is r_2. The method of least squares can be employed to find the line of best fit. The slope of the line of best fit is influenced to a great extent by the points which are nearer to the origin, thus giving a non-uniform weightage to the points and hence suffering from errors of reindexing the monomers. The validity is only qualitative and the estimates of r_1 and r_2 can change with each experiment by weighing the data in different ways. Furthermore, the high and low experimental composition data are unequally weighed, which produces large effects on the calculated values of r_1 and r_2.

2.2.1.5 Yezrielev- Brokhina -Roskin (YBR) method

As in the intersection method there exists a lack of symmetry, Fineman-Ross equation leads to different values of reactivity ratios even though the same equation and the same experimental data are used. To overcome this lack of symmetry Yezrielev et al.[43] derived the symmetric equation 2.32:

$$\left[1 - \frac{m_2}{m_1}\right]\sqrt{\frac{m_1}{m_2}} = \frac{M_1}{M_2}\sqrt{\frac{m_1}{m_2}} r_1 - \frac{M_1}{M_2}\sqrt{\frac{m_1}{m_2}} r_2 \qquad 2.32$$

The values of reactivity ratios can be determined by least square method. The results obtained by the symmetric equation are not spectacular, but they result in less ambiguous solution than that provided by FR method.

2.2.1.6 Kelen-Tudos (KT) method

Kelen and Tudos underlined once again the importance of placing the Fineman-Ross equation into symmetric form. A refinement of the linearisation method was introduced by Kelen and Tudos[33,34] by adding an arbitrary positive constant 'α' into the Fineman and Ross equation. This technique spreads the data

more evenly over the entire composition range to produce equal weightage to all the data. The Kelen and Tudos refined form of the copolymer equation 2.33 is as follows:

$$\eta = \left[r_1 + r_2/\alpha\right]\ \xi - r_2/\alpha \qquad 2.33$$

where $$\eta = G/(\alpha + H) \quad and \quad \xi = H/(\alpha + H) \qquad 2.34$$

By plotting η versus ξ, a straight line is produced that gives $-r_2/\alpha$ and r_1 as the intercepts on extrapolation to $\xi=0$ and $\xi=1$, respectively. Distribution of the experimental data symmetrically on the plot is performed by choosing the α value to be $(H_m \cdot H_M)^{1/2}$ where H_m and H_M are the lowest and highest H values, respectively. The KT method has been widely used not only for free-radical copolymerisation but also for ionic copolymerisation.[47-49]

2.2.2 Nonlinear methods

In order to use the Mayo-Lewis equation, one must avoid the linearisation which can leads to incorrect parameter estimation. This shortcoming can lead to its "pseudo-quantitative" character.[50]

2.2.2.1 Curve – Fitting method

The curve-fitting[51] method has a nonlinear form of Mayo-Lewis equation in the form of copolymer composition equation 2.35:

$$m_1 = \frac{M_1^2(r_1 - 1) + M_1}{M_1^2(r_1 + r_2) + 2M_1(1 - r_2) + r_2} \qquad 2.35$$

This equation is based on the assumptions that the monomer concentrations do not change much throughout the reaction and the molecular weight of the resulting polymer is relatively high. In order to determine reactivity ratios from the experimental data, a graph must be generated for the comonomer amount incorporated into the copolymer, m_1, versus the feed comonomer amount, M_1, for the entire range of comonomer concentration. Then, a curve can be drawn through the points for selected r_1 and r_2 values and the validity of the chosen reactivity ratio values can be checked by changing the r_1 and r_2 values until the experimenter can demonstrate that the curve best fits the data points.

Braun, Brendlein, and Mott'o (BBM) [52] attempted to make it less subjective by determining copolymer composition by r_2 at low concentration of M_1 and r_1 at high concentrations of M_1. This method has advantage of yielding reactivity ratios without the influence of the researcher and requires no estimation of the r_{ij} values in advance.

2.2.2.2 Nonlinear Tidwell Mortimer method

Between 1964 and 1970 several fundamental papers were published[31,32,53] which mainly emphasised nonlinear methods of determining the reactivity ratios. The nonlinear method first put forward by Behenken[32] and then by Tidwell and Mortimer[53] is an improved version of the curve-fitting method. Tidwell and Mortimer[31,53] have pointed out the defects of the different linear methods and suggested the use of a nonlinear least squares (NLLS) procedure. Hill et al.[54, 55] also noted the importance of using NLLS techniques for reactivity ratios and the drawbacks of linearisation methods. A nonlinear least-squares method is the correct way to analyse copolymer composition data and to determine the reactivity ratios.[56]

The nonlinear least-squares method is most suitable if following conditions are satisfied. (1) The terminal copolymerisation model is consistent with the experimental data; (2) errors in the dependent variable m_1 are random and statistically independent from observation to observation with constant variance; and (3) the independent variable M_1 contains no measurement error.

The Tidwell and Mortimer[53,57](TM) method employs the nonlinear least squares procedure to estimate the reactivity ratios. Briefly, the method consists of the following: given the initial estimates of r_1 and r_2 a set of computations is performed which on repetition rapidly leads to a pair of values of the reactivity ratios that yields the minimum value of the sum of the squares of the differences between the observed and computed polymer composition.

The Tidwell and Mortimer nonlinear least-squares procedure is considered[58] to be the only statistically accurate means of determining reactivity ratios from data obtained at low conversion. The reactivity ratio values obtained by this procedure are most probable values of the system, and the TM joint confidence interval is the statistically correct one.

This method has a disadvantage. If the initial estimates are quite different from the actual values of r_1 and r_2, the value of the sum of square of deviations does not

reach a minimum. In order to get rid of this, Gauss Newton nonlinear least square procedure was subjected to modifications as suggested by Box. If the initial estimates are very good then the number of iterations required for the value of the sum of square of deviations to converge is less.

The minimisation of the *F* criterion is used in the PROCOP programs in order to identify the optimal reactivity ratios. The PROCOP and TM method lead to the same results as both methods started with the Mayo-Lewis equation in its differential form.

Table: 2.1 Comparison of the FR, KT, and TM methods for Several Copolymerisation systems

Monomer 1	Monomer 2	r_1	r_2	F_{FR} x 10^3	F_{KT} x 10^3	F_{TM} x 10^3	Ref.
2,5-Dichlorostyrene	Methyl methacrylate	2.3736	0.4019	29.8	47.0	27.5	79
Vinylidene chloride	Styrene	2.1406	0.1249	27.1	39.8	26.9	80
Methyl isopropenyl ketone	Vinylidene chloride	4.0281	0.1376	22.5	160.8	14.6	81
α-Phenyl vinyl acetate	Butadiene	0.3300	0.2266	60.9	40.2	39.7	82
Styrene	Acrylonitrile	0.3471	0.0472	17.6	8.3	8.2	80
α-Choloroacrolein	Styrene	0.1588	0.0245	26.5	19.7	16.0	83

Table 2.1 compares the copolymerisation results obtained from the FR, KT and TM methods with the PROCOP program. Systems showing similar reactivity ratios were chosen, together with systems with different comonomer reactivity ratios. The table shows that in some cases the KT method better accounts for the experimental data, while in other cases the FR method yields better results. In both the situations best results are obtained through the TM method.

2.2.2.4 The Kuo-Chen (KC) method

The Kuo-Chen method[59] is a simple nonlinear extrapolation method derived from Fineman-Ross Method. Equation 2.36 is as follows:

$$\frac{M_1}{m_1} = \frac{r_1 M_1^2 + 2M_1 M_2 + r_2 M_2^2}{r_1 M_1 + M_2} \qquad 2.36$$

where M_1 and M_2 are molar concentrations of the monomers in feed and m_1 and m_2 are copolymer compositions. By plotting the ratio M_1M_2/m_1m_2 against M_1, the extrapolation to $M_1=0$ and $M_1=1.0$, respectively, gives r_1 and r_2. The challenge in

using this procedure is extrapolating a nonlinear curve from a limited number of experimental points.

The KC method leads to deviation in the results, which are calculated with the TM method (PROCOP) particularly in the case where there is significant difference in values of comonomer reactivity ratio. The reactivity ratios values estimated by the KC method are within the confidence region of copolymerisation of comonomers with similar reactivities, e.g. methyl methacrylate (M_1) and isoprene (M_2) r_1=0.2320 and r_2=0.8161.

2.2.2.5 Error in Variable Method (EVM)

A correct statistical approach to the estimation of reactivity ratios can be achieved when a method takes into account errors involved in the values of the variables[60,61](comonomer feed composition, copolymer composition, including conversion) and assesses the experimental data. The error- in- variable method (EVM) is an extension of nonlinear TM method, which correctly accounts for the error in the variables. Using a principle of least squares, the sum of the weighted squares of the residuals is made a minimum.[62,63] To estimate reactivity ratios using the nonlinear least square error in variable method, initial estimates of reactivity ratios are necessary and these can be obtained by KT method. In the calculation of reactivity ratios, the weights that should be assigned to an experimental point are proportional to derivatives of the response, with respect to the parameters evaluated under experimental conditions used to generate experimental points.

2.2.2.6 Optimisation methods

The probability maximum through the minimisation of the sum of squares (SS) can be made via an optimisation method,[64] which leading to results obtained using the TM method. If there is a small error in the values of the monomer feed composition, then it is enough to consider an error in the copolymer compositions when determining the reactivity ratios.[54] The optimisation method developed by using PROCOP programs not only leads to results which are as good as those are obtained by TM method but also represents a more flexible method that can be used for the integral form of Mayo-Lewis equation.

As indicated earlier, to estimate the reactivity ratios with the optimisation method, initial estimates of the reactivity ratio are required. They can be determined

with methods such as Fineman-Ross (FR), or Kelen-Tudos (KT) or by the intersection[65] methods.

2.2.3 Methods to estimate reactivity ratios at higher conversions

Since composition of the copolymer changes with conversion, the copolymer should be isolated at a conversion as low as possible so as to use approximately the initial composition of the feed monomers. Such a limiting conversion is dependent on the initial feed composition and the reactivity ratios of the comonomers. However, even at low conversions a certain composition change is recorded, and what is measured is the average molar copolymer composition, not the instantaneous composition.

Montgomery and Fry[66] showed that the classical methods of determining monomer reactivity ratios from the differential copolymer composition equation are erroneous. The low molecular weight species formed by termination through side reaction and impurities and the handling of small quantities of copolymer magnify the errors. Purification by dissolution and precipitation entails the loss of low molecular weight species. Polymer conversions are also generally high, violating the low conversion requirement. The differential form of copolymer composition equation does not take into consideration the drift of the monomer feed, due to unequal reactivities of the monomers, with conversion. The copolymers obtained at high conversion are the true representatives of the reaction dictated by the monomer reactivity ratios, while the initial copolymers are governed to a large extent by the monomer feed.

The integrated copolymer composition equation is represented as:[24]

$$r_2 = \frac{\log\left[\frac{M_2}{m_2}\right] - \frac{1}{P}\log\left[\frac{1-P(M_1/M_2)}{1-P(m_1/m_2)}\right]}{\log\left[\frac{M_1}{m_1}\right] + \frac{1}{P}\log\left[\frac{1-P(M_1/M_2)}{1-P(m_1/m_2)}\right]} \qquad 2.37$$

where M_1 and M_2 are the mole fractions of monomer 1 and 2 present initially and m_1 and m_2 mole fractions of the monomer remaining unreacted when the reaction is stopped. P is the integration variable, expressed as the function of the reactivity ratios:

$$P = \frac{(1-r_1)}{(1-r_2)} \qquad 2.38$$

2.2.3.1 Extended Kelen-Tudos (Ext. KT) method

Kelen and Tudos[33,34] modified their low conversion equation for high conversion data by redefining η and ξ using partial molar conversion of the monomers.[44] This is probably the most useful and widely accepted method presently. If copolymerisations are carried to higher conversions the determination of copolymerisation parameters involves labourious calculations because the integrated equation must be applied. The extended Kelen-Tudos method is used to estimate reactivity ratios with data even at high conversions. The equation may be derived by computing the partial molar monomer conversions, ζ_1 and ζ_2 and the integral z, where:

$$\varsigma_2 = w\left[\frac{\mu + x_0}{\mu + y}\right] \quad and \quad \varsigma_1 = \varsigma_2 y / x_0 \qquad 2.39$$

$$z = \frac{\log(1-\varsigma_1)}{\log(1-\varsigma_2)} \qquad 2.40$$

where x_0 is M_1/M_2, the initial mole ratio in feed; y is m_1/m_2, the final mole ratio in the copolymer; w is weight fraction conversion; and μ = *Mol. Wt. of* M_2 */ Mol. Wt. of* M_1. The variable H and G and the plotting parameters η and ξ can be computed as:

$$H = y/z^2 \quad and \quad G = (y-1)/z \qquad 2.41$$

$$\eta = G/(\alpha + H) \quad and \quad \xi = H/(\alpha + H) \qquad 2.42$$

The final equation for extended Kelen Tudos method is represented as:

$$\eta = [r_1 + r_2/\alpha]\ \xi - r_2/\alpha \qquad 2.43$$

where, $\alpha = (H_{min} \times H_{max})^{1/2}$. By plotting η versus ξ, a straight line is produced that gives $-r_2/\alpha$ and r_1 as the intercepts on extrapolation to $\xi=0$ and $\xi=1$, respectively.
The extended Kelen-Tudos method can be applicable[67] to systems with conversions not exceeding 40%. The comparison of extended KT method with other integral methods has led to acceptable results.

2.2.3.2 The Kuo - Chen (KC) method

The reactivity ratios can be estimated by fitting the data of the overall conversion and the cumulative copolymer composition. Kuo and Chen[68] have put forward a very simple integrated form of the copolymer composition equation:

$$\frac{M_1 - M_1^R}{M_2 - M_2^R} = \frac{M_1(r_1 M_1^R + M_2^R)}{M_2(M_1^R + r_2 M_2^R)} \qquad 2.44$$

where, M_i^R refers to the residual molar concentration of the comonomer.

Kuo-Chen used the molar fractions for the instantaneous comonomer composition (M_i) and the cumulative copolymer composition equation, which is similar to the equation proposed by the Fineman and Ross.

2.2.3.3 Mao - Huglin (MH) method

Mao and Huglin[67] in 1993 proposed an iterative linear method based on KT method which can be applicable to the copolymerisation system with the conversions greater than 40%. By considering the corresponding equations, computer simulation can be used for a set of data points at low and high conversions.[69] A small number of copolymerisation systems can be placed in simplified conditions to study high conversions. This method gives a solution for simultaneous estimation of both reactivity ratios for feed composition range large enough to generate results applicable over entire range of comonomer compositions.

In this method corresponding instantaneous monomer feed composition f^c may be calculated back from the calculated value, F^c of the copolymer composition.

$$f^c = \frac{\left(F^c - 1\right) + \sqrt{\left(1 + F^c\right)^2 + 4 r_1 r_2 F^c}}{2 r_1} \qquad 2.45$$

F^c can be calculated from the assumed reactivity ratios by the integrated copolymerisation equation. The convergence criterion of iteration is that the recalculated reactivity ratios become equal to the assumed ones.

In the absence of experimental data on copolymerisation at higher conversion values, all that remains is to compare actual results with those of the MH method. Other investigators have previously employed many of the aforementioned linearisation methods, but the approach which is taken here, to estimate more reliable and statistically sound monomer reactivity ratios, is different.

In the present work reactivity ratios of all monomer combinations at any conversion as well as 95% joint confidence intervals were calculated using the terminal model computer program FORTRAN 77, kindly offered by Dr. R. Mao.

2.2.3.4 The Intersection method

Reactivity ratios at significantly higher conversion level were initially estimated by Mayo and Lewis.[24] This was done through an intersection method and the integral equation 2.36. Monomer reactivity ratios can be estimated by determining the straight lines in an r_1-r_2 diagram for each experiment.

Binary polymerisations have become increasingly important technologically and a good knowledge of polymerisation parameters, including reactivity ratios, is very essential. Our research also took into account potential enhancements in reactivity ratio estimation for binary systems. Another related issue in multicomponent polymerisations is the existence of an azeotropic point. The feed composition of such a point would result in copolymer products with a homogeneous composition. Predicting the existence and also calculating the composition of the azeotropic point can reduce the effort of running costly experiments, in that computational results can be used to narrow the experimental search space.

Improvements suggested for the intersection method in its differential form can also be applied to its integral version.[70-72] Using the *F* criterion allows for the selection of appoint and even the generation of new points via different forms of averaging. The application of this new approach to improve the intersection method has led to giving a point which is located very close to the optimum point.

2.2.3.5 The Optimisation method

The optimisation methods are also taken into consideration of the conversion values of system.[72-74] For the i^{th} experimental point, the instantaneous monomer feed composition M_i, the instantaneous copolymer composition m_i, and overall copolymer composition gc_i can be calculated.

The aim is to find out copolymer composition m_i^{cal} starting from a monomer feed composition M_i, after integration up to the experimental conversion resulting in a cumulative copolymer composition. This copolymer composition is then compared with the experimentally determined value.

The simple algorithm[64,73,75] is used to minimise the difference (m_1^{exp}-m_1^{cal})[76] for the composition of unreacted monomer. Generally an integral method (PROCOP) has been used in the optimisation method.

2.2.3.6 The Error-in-Variables method (EVM)

The computational procedures have been shown that the use of an integrated form of the terminal model equation also takes into account errors in both copolymer and comonomer feed compositions. An iterative method in the computer program takes into account the effect of conversion on the polymer composition. The error-in-variables method (EVM) correctly accounts for the error in the variables. The computer program accounts for the extent of conversion and the copolymer composition equation is expressed in the form consistent with the basic assumption of the least-squares procedure. The EVM takes into the account the errors observed in both independent (monomer feed) and dependent variables (the copolymer compositions).

2.3 Statistical Distribution of Dyad Monomer Sequences

The copolymerisation equation describes the copolymer composition on a macroscopic scale, which is the overall composition of a copolymer sample produced from the comonomer feed. This leaves the two details concerning the composition of copolymer. The first concerns the exact arrangement of the two monomers along the polymer chain and second is distribution of the monomer.

Igarashi[77] developed the relation of copolymer composition with the distribution of bonds between the same and different monomer units in a binary copolymer molecule. The statistical distribution of two monomers M_1-M_1, M_2-M_2 and M_1-M_2 can be calculated by employing following equations:

$$X = \phi_1 - \frac{2\phi_1(1-\phi_1)}{1+\left[(2\phi_1-1)^2+4r_1r_2\phi(1-\phi_1)\right]^{1/2}} \qquad 2.46$$

$$Y = (1-\phi_1) - \frac{2\phi_1(1-\phi_1)}{1+\left[(2\phi_1-1)^2+4r_1r_2\phi(1-\phi_1)\right]^{1/2}} \qquad 2.47$$

$$Z = \frac{4\phi_1(1-\phi_1)}{1+\left[(2\phi_1-1)^2+4r_1r_2\phi(1-\phi_1)\right]^{1/2}} \qquad 2.48$$

where *X, Y*, and *Z* are the mole fractions of the M_1-M_1, M_2-M_2 and M_1-M_2 dyads in the copolymer, respectively, and ϕ_1 is the mole fraction of monomer 1 in copolymer.

The microstructure of a copolymer is defined by the distributions of the lengths of the M_1 and M_2 sequences, the sequence length distributions. Mean sequence lengths μ_1 and μ_2 were also calculated using the following equations:[78]

$$\mu_1 = 1 + r_1 \frac{[M_1]}{[M_2]} \qquad 2.49$$

$$\mu_2 = 1 + r_2 \frac{[M_2]}{[M_1]} \qquad 2.50$$

To summarise, the simultaneous incorporation of two monomers into a common copolymer chain by free-radically triggered copolymerisation is of significant commercial interest. Thus, arriving at exact composition of a copolymer and the prediction of reactivity of individual monomers has generated considerable research in the past. It will continue to be evaluated and examined in the future and the primary motive would be to arrive at a more accurate description of the copolymer systems.

2.4 References:

[1] H. Staudinger and J. Schneiders, *J. Ann. Chim.,* **1939,** 541, 151.

[2] C. L. McCormick and G. S. Chen, *J.Poly. Sci.: Poly. Chem. Ed.*, **1982**, 20, 817.

[3] M. Hirooka, *Pure and Appl. Chem*., **1981**, 53, 681.

[4] Y. Shirota, M. Yoshimura, A. Matsumoto and H. Mikawa, *Macromolecules*, **1974**, 7, 1.

[5] H. Hirai, *J. Macromol.: Macromol. Revs.*, **1976**, 11, 47.

[6] E. Tsuchida and T. Tomono, *Die Makromolekulare Chemie*, **1971**, 141, 265.

[7] M. Almgren, W. Brown and S. Hvidt, *Colloid. Polym. Sci*., **1995**, 273, 2.

[8] D. J. Meier, *J. Polymer Sci.: C*, **1969**, 26, 81.

[9] D. Cohn and H. Younes, *Journal of Biomedical Materials Research*, **1988**, 22, 993-1009.

[10] G. Moad, *Prog. Polym. Sci.,* **1999**, 24, 81–142.

[11] R. Rengarajan and M. Vicic, S. Lee, *Journal of Applied Polymer Science*, **1990**, 39, 1783-1791.

[12] H. Dostal, *Monatsh. Chem.,* **1936**, 69, 424.

[13] F. R. Mayo and F. M. Lewis; *J. Amer. Chem. Soc*., **1944,** 66, 1594.

[14] G. C. Odian, *Principles of Polymerisation: 3rd Edition*; John Wiley and Sons Inc., New York, **1991**.

[15] M. Almgren, W. Brown and S. Hvidt, *Colloid. Polym. Sci*., **1995**, 273, 2.

[16] G. Goldfinger, and T. Kane, *J. Polym. Sci.,* **1948***,* 3, 462

[17] P. J. Flory, P. J. *Principles of Polymer Chemistry*; Cornell University Press: Ithaca, **1953**.

[18] T. Alfrey, Jr. and C. C. Price, *J. Poly. Sci.,* **1971**, 2, 101.

[19] H. Morawetz, *Polymer: The Origins and Growth of Science,* John Wiley and Sons. **1985**.

[20] J. P. Kennedy, *Cationic Copolymerization, High Polymers* Vol. XVIII, Interscience Publishers, New York, **1964**.

[21] C. Hagiopol, *Copolymerisation: Towards a Systematic Approach*; Kluwer Academic/ Plenum Publishers, New York, **1999.**

[22] S. Ponrathnam, *Ph. D. Thesis,* **1976**.

[23] J. M. Gadgil, *Ph. D. Thesis,* **1993.**

[24] F. R. Mayo and F. M. Lewis, *J. Am. Chem. Soc.*, **1944**, 66, 1594

[25] R. G. W. Norrish and E. F. Brookman, *Proc. Roy. Soc.,* A **1937**, 163, 205.

[26] I. Skeist*, J. Am. Chem. Soc*., **1946,** 68, 1781.

27] G. A. Shtraikhman, *Zh. Fiz. Khim*, **1958**, 32, 512.

[28] G. R. Brown and J. G. Byrne, *Polymer*, **1969**, 10, 333.

[29] T. Kelen, F. Tudos and B. Turcsanyi, *Polymer Bull.,* **1980,** *2*, 71.

[30] R. G. W. Norrish and E. F. Brookman; *Proc. Roy. Soc.,* **1939,** A 171, 147.

[31] P. W. Tidwell and G. A. Mortimer, *J. Macromol. Sci. Rev. Macromol. Sci. Chem., C,* **1970,** 4(2), 281.

[32] D. W. Behenken, *J. Polym. Sci*., **1964,** A2, 645.

[33] T. Kelen and F. Tudos, *J. Macromol. Sci. Chem.,* **1975**, A9(1), 1.

[34] J. P. Kennedy, T. Kelen and F. Tudos, *J. Macromol. Sci., Chem*., **1975**, A13, 2277.

[35] R. E. Florin, *J. Am. Chem. Soc.,* **1949**, 71, 1867.

[36] A. L. Polic, T. A. Duever and A. Penlidis, *J. Polym. Sci.: Part A,* **1998,** *36*, 813.

[37] G. B. Butier, J. T. Badgett and M. Sharabash, *J. Macromol. Sci. Chem.,* A, **1970**, 4(1), 51.

[38] R. M. Joshi and S. L. Kapur, *J. Polym. Sci.*, **1954**, 14, 508.

[39] R. M. Joshi and S. L. Kapur, *J. Polym. Sci*., **1956**, 19, 582.

[40] R. M. Joshi and S. G. Joshi, *J. Macromol. Sci. Chem*., **1971**, A5, 1329.

[41] R. M. Joshi, *J. Macromol. Sci. Chem.*, **1973**, A7, 1231.

[42] M. Fineman and S. D. Ross, J. *Polym. Sci.,* **1950**, 5, 249.

[43] A. I. Yezrielev, E. L. Brokhina and E. S. Roskin, *Vysokomol. Soedin. A,* 11(8), **1969**, 1670.

[44] T. Kelen, F. Tudos, D. Braun and W. K. Czerwinnski, *Makromol. Chem.,* **1990**, 191, 1863.

[45] F. Tudos, T. Kelen, T. F.-Berezsnich B. Turcsanyi, *J. Macromol. Sci.. Part A,* **1976,** *10*, 1513.

[46] F. Tudos and T. Kelen, *J. Macromol. Sci. Part A,* **1981,** *16*, 1283.

[47] W. M. Pasika and D. J. Chen, *J. Polym. Chem*., **1991**, 29, 1475.

[48] T. Kelen, F. Tudos, B. Turcsaanyi and J. P. Kennedy, *J. Polym. Sci. Polym. Chem. Ed*., **1977**, 15, 3047.

[49] K. B. Wood and V. T. Stannett, J Poly. Sci.: A Polym. Chem., **1992**, 30, 13.

[50] M. Kinoshita, T. Irie and M. Imoto, *Makromol. Chem*., **1967**, 110, 47.

[51] T. Alfrey, Jr. J. J. Bohrer and H. Mark, *Copolymerisation, Interscience, New York*, **1952.**

[52] D. Braun, W. Brendlein and G. Mott, *J. Eur. Poly.,* **1973**, 9, 1007.

[53] P. W. Tidwell and G. A. Mortimer, *J. Polym. Sci. Part A,* **1965,** *3*, 369.

[54] D. T. J. Hill, J. H. O'Donnell and P. W. O' Sullivan, *Macromolecules,* **1982,** *15*, 960.

[55] D. T. J. Hill, J. H. O'Donnell and P. W. O' Sullivan, *Macromolecules,* **1985,** *18*, 9.

[56] R. C. McFarlane, P. M. Reilly and K. F. O'Driscoll, *J. Polym. Sci., Poly. Chem. Ed.,* **1980**, 18, 251.

[57] D. T. J. Hill, A. P. Lang, J. H. O'Donnell, *J. Eur. Polym.,* **1991,** *27*, 765.

[58] A. O. Kress, l. J. Mathias, and G. Cei, *Macromolecules,* **1989**, 22, 537.

[59] J. F. Kuo and C. Y. Chen, *J. Appl. Polym. Sci*., **1982**, 27, 2747.

[60] R. Van Der Meer, H. N. Linssen and A. L. German, *J. Polym. Sci., Polym. Chem*. *Ed*., **1978**, 16, 2915.

[61] H. Patino-Leal, P. M. Rielly and K.F. O' Driscoll, *J. Polym. Sci., Polym. Lett. Ed*., **1980**, 18, 219.

[62] B. Yamada, M. Ytahashi and T. Otsu, *J. Polym. Sci., Polym. Chem. Ed*., **1978**, 16, 1719.

[63] W. E. Wentworth, *J. Chem. Edn*., **1965**, 42, 96 and 162.

[64] J. A. Nelder and R. Mead, *Comput. J*., **1965**, 7, 308.

[65] C. Neagu, C. Hagiopol and I. S. Fazakas, *Computational Polym. Sci.,* **1993**, 3, 125.

[66] D. R. Montgomery and C. R. Fry, *J. Polym. Sci.*, **1968**, C25, 59.

[67] R. Mao and M. B. Huglin, *Polymer,* **1993**, 34, 1709.

[68] J. F. Kuo and C. Y. Chen, *J. Appl. Polym. Sci*., **1981**, 26, 1117.

[69] F. Ziaee and M. Nekoomanesh, *Polymer,* **1998**, 39, 203.

[70] C. Popov, V. Syicbitz and G. Scwachule, *Plaste Kautschuk,* **1981**, 28, 10.

[71] C. Hagiopol, O. Frangu, M. Pop, L. Dumitru, B. Marculescu and N. Cobianu, *Rev. Roum. Chim*., **1993**, 38, 91.

[72] S. K. Karode and S.G. Joshi, *J. Macrom. Sci., Pure Appl. Chem., A.,* **1997**, 34, 1499.

[73] C. Hagiopol, O. Frangu and L. Dumitru, *J. Macromol. Sci., Chem. A*., **1989**, 26, 1363.

[74] A. Giz, *Macromol. Theory Simul*., **1998**, 7, 391.

[75] A. Kim and P. Oracz, *Macromol. Theory Simul.,* **1997**, 6, 565.

[76] W. Ring, I. Mita, A. D. Jenkins and N. M. Bikales, *Pure Appl. Chem.,* **1985**, 57, 1427.

[77] S. Igarashi, *J. Polym. Sci. Polym. Lett. Ed.,* **1963**, 1, 359.

[78] H. G. Elias, *Macromolecules; Plenum Press: New York and London*, **1971**, 2, Chapter 22, 761.

[79] P. Agron, T. Alfrey, J. Bohrer, H. Haas and H. Wechesler, *J. Polym. Sci.,* **1948** 3, 157.

[80] B. R. Thompson and R. H. Raines, *J. Polym. Sci.,* **1959**, 41, 265.

[81] E. C. Chapin, G. E. Ham and C. L. Mills, *J. Polym. Sci*., **1949**, 4, 597.

[82] H. S. Bender, *J. Polym. Sci. B*., **1966,** 4, 895.

[83] H. G. Elias and W. Lengweiler, *Makromol. Chem.,* **1968**, 113, 155.

Chapter III

Synthesis and Characterisation Methodologies

3.1 Introduction

The copolymerisation method provides us with an opportunity to produce materials with the precisely required properties. Copolymerisation is the most successful and powerful method for effecting systematic changes in polymer properties.[1] The incorporation of two different types of monomers, hydrophilic and hydrophobic which have diverse physical and/or chemical properties, in the same copolymer molecule in varying proportions leads to the formation of new materials with great scientific and commercial importance[2] as hydrogels useful in human contact applications such as contact and intraocular lenses. The elucidation of copolymer structure (copolymer composition, monomer sequence distribution) and kinetics (propagation, rate coefficients) are the major concerns for the prediction of copolymer properties and the correlation between structure and properties.[3] Among the various copolymerisation reactions, radical copolymerisation is the most important since it does not demand rigorous experimental conditions and can be applied to a large variety of monomers, leading to the formation of new materials.

Several chemical and physical methods have been used in the literature for the characterisation of copolymer microstructure. Copolymer composition has been determined by elemental analysis,[4] infrared absorption spectroscopy,[5-6] ultraviolet absorption spectrophotometry,[7] proton (^{1}H) nuclear magnetic resonance and ^{13}C NMR spectroscopy,[8,9] pyrolysis gas chromatography,[10-12] and mass spectroscopy.[13,14] To overcome the solubility problem of amphiphilic copolymers we have developed a gas chromatographic method to analyse unreacted monomer. Gas chromatography is faster and a more accurate method of analysis, with minimum error in the analysis.

Copolymerisation reactivity ratios were originally measured for the purpose of describing the relative reactivities of various monomers towards various radicals. Many methods have been used to estimate reactivity ratios of a large number of comonomers. In present work only four methods are used to determine the reactivity ratios of monomer.

The estimation methods developed to determine reactivity ratio are based on the binary copolymer composition equation 3.1.[15-17]

$$\frac{dM_1}{dM_2} = \frac{r_1 M_1^2 + M_1 M_2}{r_2 M_2^2 + M_1 M_2} \qquad 3.1$$

where, r_1 and r_2 are the monomer reactivity ratios and dM_1/dM_2 is the relative rate of addition of the two monomers to the chain.

3.2 Experimental

In order to study the copolymerisation of a monomer combination, a set of experiments with different feed ratios of monomers were employed each time (monomer molar ratios: 10/90 to 90/10), and the copolymerisation reactions were quenched at rather low or moderate conversions. The conversions were determined by gas chromatography by analysing the unreacted monomer concentration. Weight fraction conversions were calculated with respect to total weight of feed monomers. The experimental results were processed on the basis of Fineman-Ross (FR),[18] Kelen-Tudos (KT),[19] extended Kelen-Tudos (ext. KT)[20] and Mao-Huglin (MH)[21] equations. These methods were described in Chapter 2, Sections 2.3.1.3, 2.3.1.5, 2.7.1 and 2.7.3, respectively.

3.2.1 Materials

All the monomers namely methyl acrylate (MA), methyl methacrylate (MMA), butyl acrylate (BA), butyl methacrylate (BMA), 2-ethyl hexyl acrylate (EHA), 2-ethyl hexyl methacrylate (EHMA), 2-hydroxyethyl acrylate (HEA), 2-hydroxyethyl methacrylate (HEMA), 2-hydroxypropyl acrylate (HPA) 2-hydroxypropyl methacrylate (HPMA) were purchased from Aldrich Chemicals (USA). All standard solutions and samples were prepared in synthesis grade methyl isobutyl ketone (MIBK) purchased from Merck Chemicals, India. 2,2'-Azobisisobutyronitrile (AIBN) was purchased from SAS Chemicals, India and recrystallised in methanol before use.

3.3 Synthesis of Copolymers

Copolymerisation was carried out by solution polymerisation technique using MIBK as solvent with 2, 2'-azobisisobutyronitrile (AIBN) as free radical initiator. The feed compositions of the monomers are varied from 10/90 to 90/10. Appropriate quantities of the monomer, MIBK and AIBN (1 mol % of total monomer moles) were taken in polymerisation tubes and flushed with oxygen free nitrogen gas for 10 min. The tubes were tightly sealed and immersed in a thermostatic water bath at 70 °C. The reaction time was selected so as to yield moderate copolymer conversions in order to be within the realm of applicability of differential copolymerisation equation. The

conversions were controlled and determined by gas chromatography. After the reaction times, the copolymers were quenched by immersing it in liquid nitrogen, followed by the subsequent addition of monomethyl ether of hydroquinone (MEHQ) at twice the initiator concentration. Cyclohexane was used as the non-solvent. It had added butyl methacrylate (BMA), unless otherwise stated, as internal standard (IS) for gas chromatography analysis.

3.4 Characterisation Techniques

3.4.1 Determination of unreacted monomers by gas chromatography

The unreacted monomer concentrations were determined using GC-FID method. The GC method was established in such a way that monomer peak must be well separated form each other. The method is as follows.

3.4.1.1 Equipment

A GC chromatograph GC-2010 (Shimadzu Corporation, Kyoto, Japan) equipped with an auto sampler (HTA) and FID was used for the experiments. Hydrogen was purchased from Inox, Mumbai. Zero air and A-grade nitrogen were supplied from Nitrogen-Air generator (Domnik Hunter, USA). The data acquisition and processing was carried out with Toshvin "GC Solution" software. The monomer standards and reaction samples were weighed on a digital balance (Mettler Toledo AG 245) with accuracy of 0.0001 mg.

3.4.1.2 Operating conditions GC/FID

The GC separation was carried out on J&W Scientific, USA DB-1 column with a dimension of 100 m × 0.25 mm and a film thickness of 0.5 μm. A-grade nitrogen was used as the carrier gas at a constant pressure of 270.6 kPa. The carrier gas flow through column was maintained at 1.5 mL/min. The optimised GC temperature program used was as follows:

The initial oven temperature of 80°C; hold for 5 minutes, was increased to 225°C with the ramp rate of 1°C /Min. The total run time was equal to 35 min. The temperature of injector and detector (FID) were maintained at 250°C and 300°C, respectively. The carrier gas flow was maintained at 1.2 mL/minute and the nitrogen purge flow was kept at 3 mL/minute. While using FID system, hydrogen and zero air flow were set at 40 mL/minute and 400 mL/minute, respectively. All the monomer standards and reaction samples were injected with the injection volume of 1.0 μL with

a split injection mode having split ratio of 20:1. A glass injection liner with de-activated glass wool was used.

3.4.1.3 Determination of response factors (R_f)

For calculating response factor[22,23] of individual monomers, five different standard solutions of individual monomer pair were prepared. And to each mixture, an amount of internal standard, butyl methacrylate (BMA), was added. All the standard solutions were prepared in Class "A" volumetric flasks. All the monomer standards were run on GC and the area counts for individual monomers were recorded from each run. The response factors for respective monomer were calculated using following equation[28].

$$Rf = \left(\frac{Conc.}{Area}\right)_{compound} \left(\frac{Area}{Conc.}\right)_{\text{int}.std.} \qquad 3.12$$

3.4.1.4 Determination of unreacted monomer concentrations:

The concentration of unreacted monomer was calculated using following equation

$$\mathbf{C_S = [A_S/A_{IS}] * (R_f) * (C_{IS})} \qquad 3.13$$

Where, C_S is concentration of sample; A_S is area of sample; A_{IS} is area of internal standard R_f is average response factor for respective monomer; C_{IS} is concentration of internal standard. After processing the data of individual chromatograph, the concentration (ppm, w/v) of unreacted monomer was determined, the amount of monomer was calculated for total reaction volume. Further the weight fraction conversion of respective pair was calculated by following formula.

$$Weight\ \ fraction\ \ conversion = \frac{Total\ \ weight\ \ of\ \ polymer}{Total\ \ weight\ \ of\ \ feed\ \ monomers} \qquad 3.14$$

3.5 Copolymerisation of methyl acrylate (MA) and 2-hydroxyethyl acrylate (HEA)

3.5.1 Synthesis of poly(MA-*co*-HEA)

Copolymers of MA-HEA of different compositions were synthesised by solution polymerisation method by using methyl isobutyl ketone (MIBK) as solvent and 2, 2'-azobisisobutyronitrile (AIBN- 1 mol% with total monomer) as free radical initiator. The feed compositions of the monomers are presented in Table 3.1. The

polymerisation was carried out at 70°C in oxygen free conditions. After a certain time interval the reaction was terminated and cyclohexane (non-solvent) was added. This contained butyl methacrylate (BMA) as internal standard for GC analysis. Synthesis of statistical copolymers poly(MA-*co*-HEA) is depicted in Scheme 3.1.

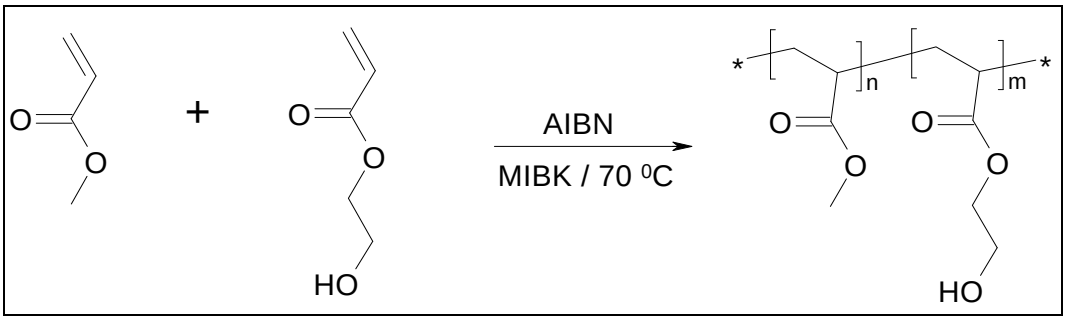

Scheme 3.1: Synthesis of poly(MA-*co*-HEA)

3.5.2 Determination of unreacted monomers by gas chromatography (GC)

The unreacted monomer concentrations were separated and determined using GC-FID methodology described in Section 3.4.1.

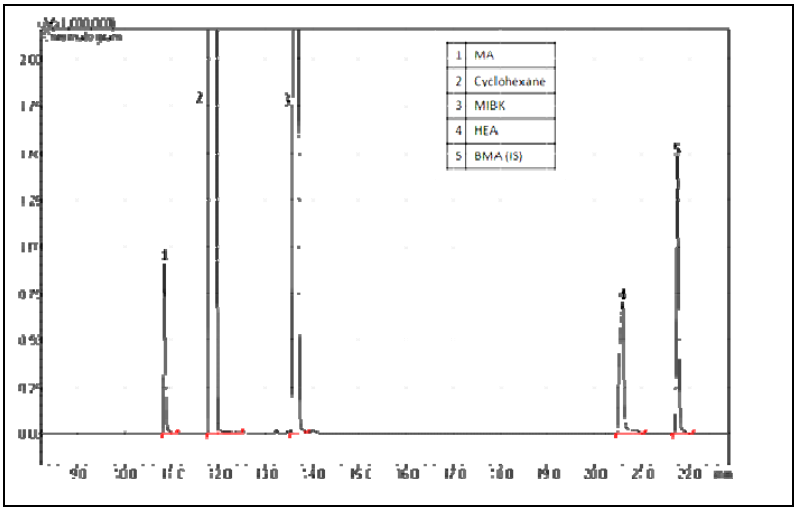

Figure 3.1: Representative GC chromatogram showing separation of MA, cyclohexane, MIBK, HEA, and BMA (IS).

Table 3.1: Response factor (R_f) of monomer MA and HEA

Sr. No.	Monomer	Retention time R_t (min.)	Mean R_f	% RSD R_f
1.	Methyl acrylate (MA)	10.89	1.10	0.62
2.	2-Hydroxyethyl acrylate (HEA)	20.80	1.74	1.74

Concentration of unreacted monomer was calculated by using above response factor for respective monomer.

Table 3.2: Composition data for copolymerisation of MA with HEA

Polymer code	Mole fraction				Weight fraction conversion
	In feed		In polymer		
	M_1	M_2	m_1	m_2	
HEA	0	1	0	1	-
MA-HEA-1	0.1000	0.9000	0.0709	0.9291	0.6072
MA-HEA-2	0.1500	0.8500	0.1135	0.8865	0.6043
MA-HEA-3	0.2000	0.8000	0.1464	0.8536	0.5119
MA-HEA-4	0.2500	0.7500	0.1957	0.8043	0.4193
MA-HEA-5	0.3500	0.6500	0.2976	0.7024	0.4268
MA-HEA-6	0.4000	0.6000	0.3401	0.6599	0.3445
MA-HEA-7	0.4501	0.5499	0.4301	0.5699	0.1538
MA-HEA-8	0.5001	0.4999	0.4973	0.5027	0.1347
MA-HEA-9	0.5501	0.4499	0.5942	0.4058	0.1563
MA-HEA-10	0.7000	0.3000	0.6872	0.3128	0.1247
MA-HEA-11	0.9000	0.1000	0.9157	0.0843	0.2900
MA	1	0	1	0	-

3.6 Copolymerisation of butyl acrylate (BA) and 2-hydroxyethyl acrylate (HEA)

3.6.1 Synthesis of poly(BA-*co*-HEA)

Copolymers of BA-HEA of different compositions were synthesised as described in Section 3.5.1. The feed compositions of the monomers are presented in Table 3.4. Synthesis of the statistical copolymers poly(BA-*co*-HEA) is depicted in Scheme 3.2.

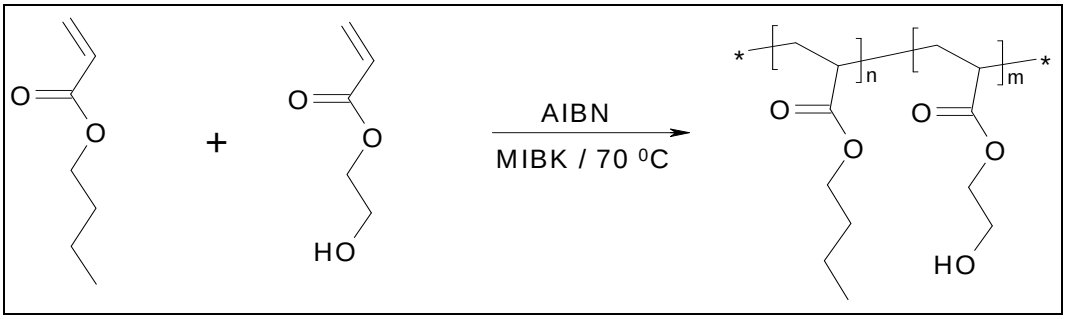

Scheme 3.2: Synthesis of poly(BA-*co*-HEA)

3.6.2 Determination of unreacted monomers by gas chromatography (GC)

The unreacted monomer concentrations were determined using GC-FID method as described in earlier Section 3.4.1.

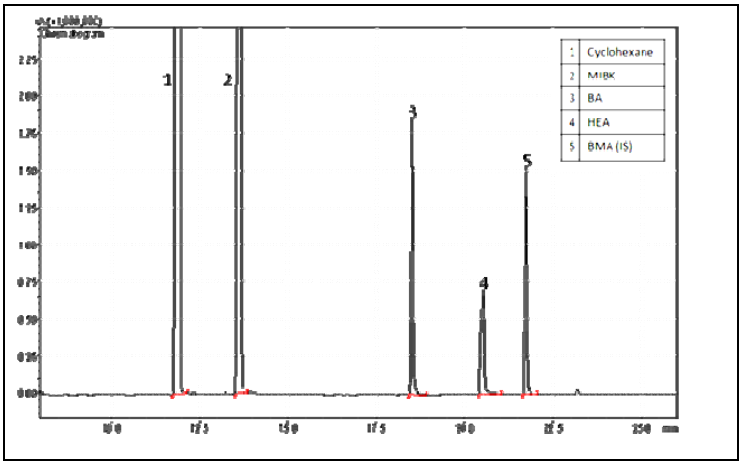

Figure 3.2: Representative GC chromatogram showing separation of cyclohexane, MIBK, BA, HEA, and BMA (IS).

Table 3.3: Response factor (R_f) of monomer BA and HEA

Sr. No.	Monomer	Retention time R_t (min.)	Mean R_f	% RSD R_f
1.	Butyl acrylate (BA)	18.61	1.10	0.59
2.	2-Hydroxy ethyl acrylate (HEA)	20.80	1.73	1.54

Concentration of unreacted monomer was calculated by using above response factors for respective monomers.

Table 3.4: Composition data for copolymerisation of BA with HEA

Polymer code	Mole fraction				Weight fraction conversion
	In feed		In polymer		
	M_1	M_2	m_1	m_2	
HEA	0	1	0	1	-
BA-HEA-1	0.1000	0.9000	0.0510	0.9490	0.5138
BA-HEA-2	0.1500	0.8500	0.0899	0.9101	0.5667
BA-HEA-3	0.2000	0.8000	0.1320	0.8680	0.4867
BA-HEA-4	0.2500	0.7500	0.1774	0.8226	0.5624
BA-HEA-5	0.3000	0.7000	0.2143	0.7857	0.5192
BA-HEA-6	0.3500	0.6500	0.2589	0.7411	0.4027
BA-HEA-7	0.4000	0.6000	0.2985	0.7015	0.3831
BA-HEA-8	0.4500	0.5500	0.3611	0.6389	0.3751
BA-HEA-9	0.5000	0.5000	0.4150	0.5850	0.1918
BA-HEA-10	0.5500	0.4500	0.4441	0.5559	0.2438
BA-HEA-11	0.6000	0.4000	0.4567	0.5433	0.1970
BA-HEA-12	0.6500	0.3500	0.5426	0.4574	0.1236
BA-HEA-13	0.7500	0.2500	0.6215	0.3785	0.1865
BA-HEA-14	0.9000	0.1000	0.8423	0.1577	0.2332
BA	1	0	1	0	-

3.7 Copolymerisation of 2-ethylhexyl acrylate (EHA) and 2-hydroxyethyl acrylate (HEA)

3.7.1 Synthesis of poly(EHA-*co*-HEA)

Copolymers of EHA-HEA of different composition were synthesised as described earlier in Section 3.5.1. The feed compositions of the monomers are presented in Table 3.6. The synthesis of the statistical copolymers poly(EHA-*co*-HEA) is depicted in Scheme 3.3.

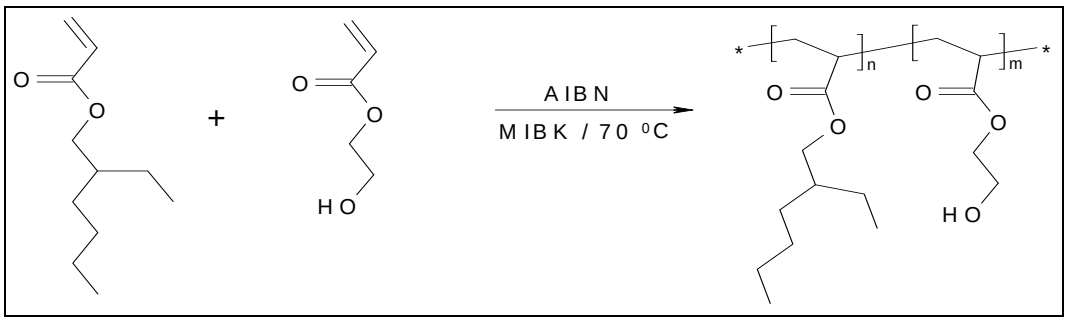

Scheme 3.3: Synthesis of poly(EHA-*co*-HEA)

3.7.2 Determination of unreacted monomers by gas chromatography (GC)

The unreacted monomer concentrations were determined using GC-FID method as described in Section 3.4.1.

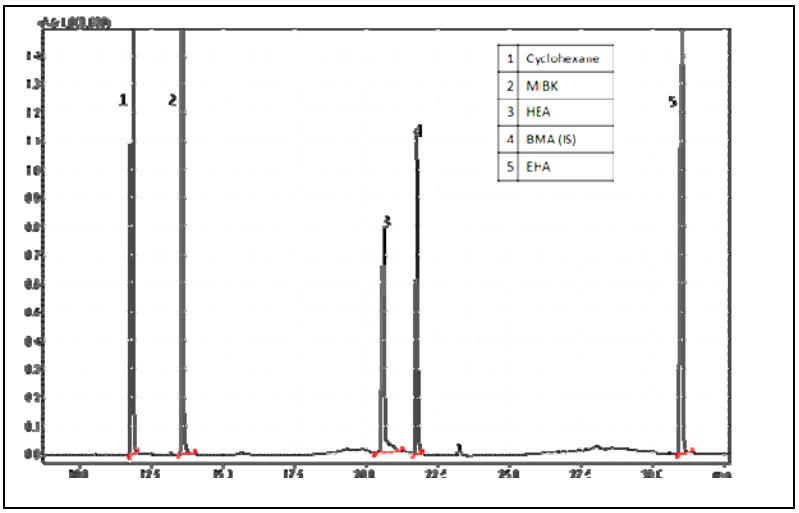

Figure 3.3: Representative GC chromatogram showing separation of cyclohexane, MIBK, HEA, BMA (IS) and EHA.

Table 3.5: Response factor (R_f) of monomer EHA and HEA

Sr. No.	Monomer	Retention time R_t (min.)	Mean R_f	% RSD R_f
1.	2-Ethyl hexyl acrylate (EHA)	31.19	0.81	1.72
2.	2-Hydroxyethyl acrylate (HEA)	20.80	1.85	1.64

Concentration of unreacted monomer was calculated by using above response factors for respective monomers.

Table 3.6: Composition data for copolymerisation of EHA with HEA

Polymer code	Mole fraction				Weight fraction conversion
	In feed		In polymer		
	M_1	M_2	m_1	m_2	
HEA	0	1	0	1	-
EHA-HEA-1	0.1500	0.8500	0.1344	0.8656	0.8610
EHA-HEA-2	0.2000	0.8000	0.1863	0.8137	0.8738
EHA-HEA-3	0.3000	0.7000	0.2843	0.7157	0.9073
EHA-HEA-4	0.3500	0.6500	0.3090	0.6910	0.8910
EHA-HEA-5	0.4000	0.6000	0.3315	0.6685	0.7764
EHA-HEA-6	0.5500	0.4500	0.4790	0.5210	0.7374
EHA-HEA-7	0.6000	0.4000	0.5337	0.4663	0.7257
EHA-HEA-8	0.6500	0.3500	0.6009	0.3991	0.7026
EHA-HEA-9	0.7500	0.2500	0.7100	0.2900	0.6661
EHA-HEA-10	0.9000	0.1000	0.8632	0.1368	0.6295
EHA	1	0	1	0	-

3.8 Copolymerisation of methyl methacrylate (MMA) and 2-hydroxyethyl acrylate (HEA)

3.8.1 Synthesis of poly(MMA-*co*-HEA)

Copolymers of MMA-HEA of different composition were synthesised as described in Section 3.5.1. The feed compositions of the monomers are presented in Table 3.8. Synthesis of statistical copolymers poly(MMA-*co*-HEA) is depicted in Scheme 3.4.

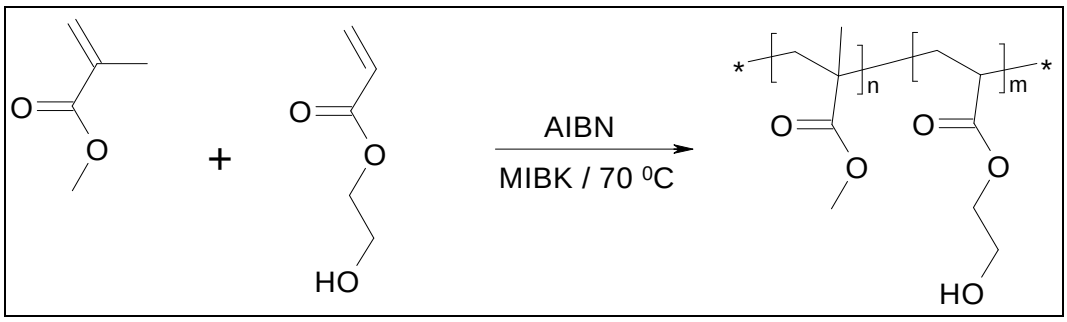

Scheme 3.4: Synthesis of poly(MMA-*co*-HEA)

3.8.2 Determination of unreacted monomers by gas chromatography (GC)

The unreacted monomer concentrations were determined using GC-FID method as described in Section 3.4.1.

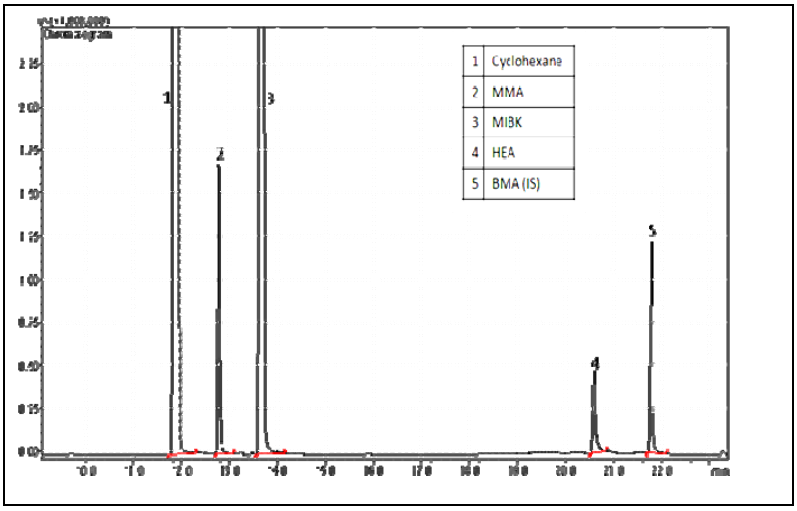

Figure 3.4: Representative GC chromatogram showing separation of cyclohexane, MMA, MIBK, HEA, and BMA (IS)

Table 3.7: Response factor (R_f) of monomer MMA and HEA

Sr. No.	Monomer	Retention time R_t (min.)	Mean R_f	% RSD R_f
1.	Methyl methacrylate (MMA)	12.74	1.75	2.5
2.	2-Hydroxy ethyl acrylate (HEA)	20.80	1.45	3.2

Concentration of unreacted monomer was calculated by using above response factors for respective monomers.

Table 3.8: Composition data for copolymerisation of MMA with HEA

Polymer code	Mole fraction				Weight fraction conversion
	In feed		In polymer		
	M_1	M_2	m_1	m_2	
HEA	0	1	0	1	-
MMA-HEA-1	0.1000	0.9000	0.1009	0.8991	0.4616
MMA-HEA-2	0.1500	0.8500	0.1255	0.8745	0.4251
MMA-HEA-3	0.2000	0.8000	0.1913	0.8087	0.5223
MMA-HEA-4	0.2500	0.7500	0.2123	0.7877	0.3465
MMA-HEA-5	0.3000	0.7000	0.2356	0.7644	0.3081
MMA-HEA-6	0.3500	0.6500	0.3134	0.6866	0.2355
MMA-HEA-7	0.4000	0.6000	0.3246	0.6754	0.3180
MMA-HEA-8	0.4500	0.5500	0.3297	0.6703	0.2567
MMA-HEA-9	0.5000	0.5000	0.3780	0.6220	0.2570
MMA-HEA-10	0.5500	0.4500	0.4235	0.5765	0.3260
MMA-HEA-11	0.6000	0.4000	0.4493	0.5507	0.3295
MMA-HEA-12	0.6500	0.3500	0.4901	0.5099	0.4201
MMA-HEA-13	0.8000	0.2000	0.6327	0.3673	0.2941
MMA	1	0	1	0	-

3.9 Copolymerisation of 2-ethylhexyl methacrylate (EHMA) and 2-hydroxyethyl acrylate (HEA)

3.9.1 Synthesis of poly(EHMA-*co*-HEA)

Copolymers of EHMA-HEA reaction of different compositions were synthesised as described in Section 3.5.1. The feed compositions of the monomers are presented in Table 3.10. Synthesis of statistical copolymers poly(EHMA-*co*-HEA) is depicted in Scheme 3.5.

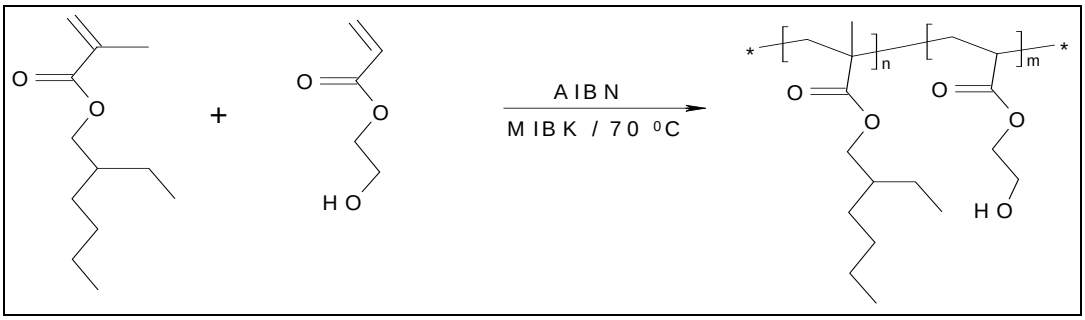

Scheme 3.5: Synthesis of poly (EHMA-*co*-HEA)

3.9.2 Determination of unreacted monomers by gas chromatography (GC)

The unreacted monomer concentrations were determined using GC-FID method as described in Section 3.4.1.

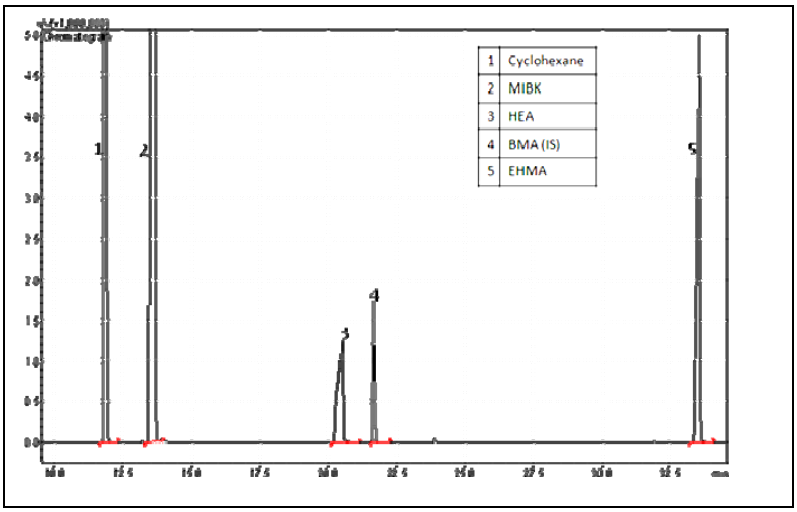

Figure 3.5: Representative GC chromatogram showing separation of cyclohexane, MIBK, HEA, BMA (IS) and EHMA.

Table 3.9: Response factor (R_f) of monomer HEA and EHMA

Sr. No.	Monomer	Retention time R_t (min.)	Mean R_f	% RSD R_f
1.	2-Hydroxyethyl acrylate (HEA)	20.80	1.86	1.31
2.	2-Ethylhexyl methacrylate (EHMA)	33.72	0.82	0.93

Concentration of unreacted monomer was calculated by using above response factors for respective monomers

Table 3.10: Composition data for copolymerisation of EHMA with HEA

Polymer code	Mole fraction				Weight fraction conversion
	In feed		In polymer		
	M_1	M_2	m_1	m_2	
HEA	0	1	0	1	-
EHMA-HEA-1	0.1000	0.9000	0.0802	0.9198	0.6111
EHMA-HEA -2	0.1500	0.8500	0.1472	0.8528	0.8789
EHMA-HEA-3	0.2000	0.8000	0.2007	0.7993	0.9247
EHMA-HEA-4	0.2500	0.7500	0.2512	0.7488	0.8942
EHMA-HEA-5	0.3000	0.7000	0.3004	0.6996	0.9272
EHMA-HEA-6	0.3500	0.6500	0.3485	0.6515	0.9569
EHMA-HEA-7	0.4000	0.6000	0.3947	0.6053	0.9516
EHMA-HEA-8	0.4500	0.5500	0.4438	0.5562	0.9119
EHMA-HEA-9	0.5000	0.5000	0.4897	0.5103	0.9020
EHMA-HEA-10	0.5500	0.4500	0.5370	0.4630	0.6704
EHMA-HEA-11	0.6000	0.4000	0.5854	0.4146	0.8439
EHMA-HEA-12	0.6500	0.3500	0.6374	0.3626	0.8790
EHMA-HEA-13	0.7000	0.3000	0.6843	0.3157	0.8388
EHMA-HEA-14	0.7500	0.2500	0.7359	0.2641	0.8272
EHMA-HEA-15	0.8000	0.2000	0.7874	0.2126	0.8716
EHMA-HEA-16	0.8500	0.1500	0.8378	0.1622	0.8406
EHMA-HEA-17	0.9000	0.1000	0.8950	0.1050	0.8726
EHMA	1	0	1	0	-

3.10 Copolymerisation of 2-hydroxyethyl methacrylate (HEMA) and 2-hydroxyethyl acrylate (HEA)

3.10.1 Synthesis of poly(HEMA-*co*-HEA)

Copolymers of HEMA-HEA of different composition were synthesised by as described earlier in Section 3.5.1. The feed compositions of the monomers are presented in Table 3.12. Synthesis of statistical copolymers poly(HEMA-*co*-HEA) is depicted in Scheme 3.6.

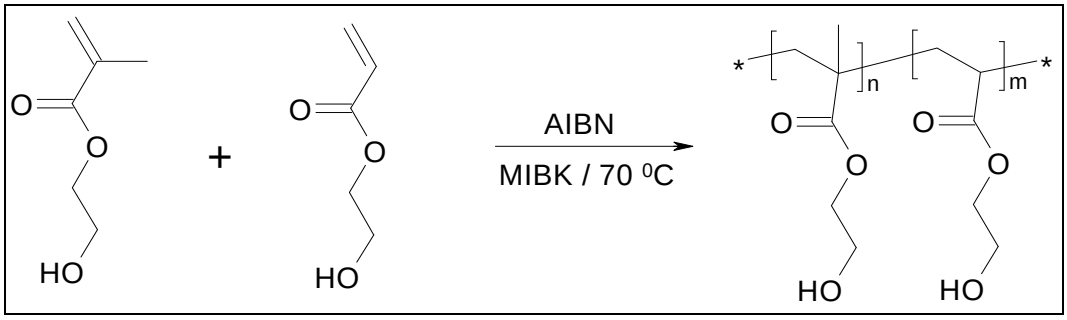

Scheme 3.6: Synthesis of poly (HEMA-*co*-HEA)

3.10.2 Determination of unreacted monomers by gas chromatography (GC)

The unreacted monomer concentrations were determined using GC-FID analysis methodologies as described in Section 3.4.1. Concentration of unreacted monomer was calculated by using response factors in Table 3.11 for respective monomers.

Table 3.11: Response factor (R_f) of monomer HEMA and HEA

No.	Monomer	R_t (min.)	Mean R_f	% RSD R_f
1.	2-Hydroxy ethyl acrylate (HEA)	20.80	1.81	1.02
2.	2-Hydroxy ethyl methacrylate (HEMA)	24.19	1.49	2.21

Table 3.12: Composition data for copolymerisation of HEMA with HEA

Polymer code	Mole fraction				Weight fraction conversion
	In feed		In polymer		
	M_1	M_2	m_1	m_2	
HEA	0	1	0	1	-
HEMA-HEA-1	0.1000	0.9000	0.1481	0.8519	0.2924
HEMA-HEA-2	0.2500	0.7500	0.2928	0.7072	0.3663
HEMA-HEA-3	0.3000	0.7000	0.3485	0.6515	0.4381
HEMA-HEA-4	0.3500	0.6500	0.4136	0.5864	0.4341
HEMA-HEA-5	0.4000	0.6000	0.4494	0.5506	0.5143
HEMA-HEA-6	0.4500	0.5500	0.4939	0.5061	0.4639
HEMA-HEA-7	0.5000	0.5000	0.5287	0.4713	0.5627
HEMA-HEA-8	0.5500	0.4500	0.5689	0.4311	0.6585
HEMA-HEA-9	0.6000	0.4000	0.6158	0.3842	0.6541
HEMA-HEA-10	0.6500	0.3500	0.6692	0.3308	0.6522
HEMA-HEA-11	0.7000	0.3000	0.7087	0.2913	0.7964
HEMA-HEA-12	0.7500	0.2500	0.7507	0.2493	0.8566
HEMA-HEA-13	0.8000	0.2000	0.7989	0.2011	0.7994
HEMA-HEA-14	0.8500	0.1500	0.8458	0.1542	0.8592
HEMA-HEA-15	0.9000	0.1000	0.8965	0.1035	0.8541
HEMA	1	0	1	0	-

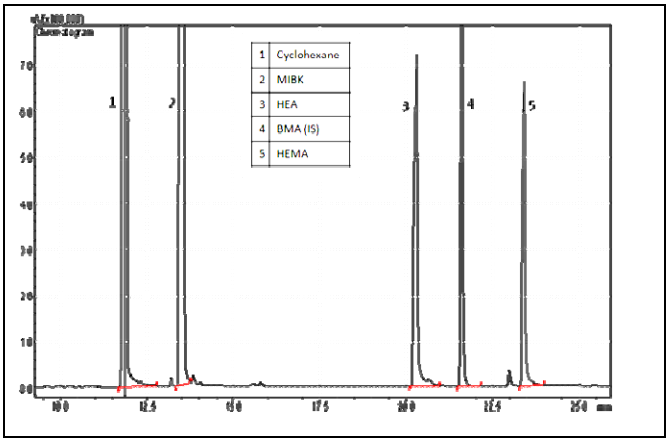

Figure 3.6: Representative GC chromatogram showing separation of cyclohexane, MIBK, HEA, BMA (IS) and HEMA.

3.11 Copolymerisation of methyl acrylate (MA) and 2-hydroxypropyl acrylate (HPA)

3.11.1 Synthesis of poly(MA-*co*-HPA)

Copolymers of MA-HPA of different composition were synthesised as described in Section 3.5.1. The feed compositions of the monomers are presented in Table 3.14. Butyl acrylate (BA) was used as internal standard for GC analysis. Synthesis of statistical copolymers poly(MA-*co*-HPA) is depicted in Scheme 3.7

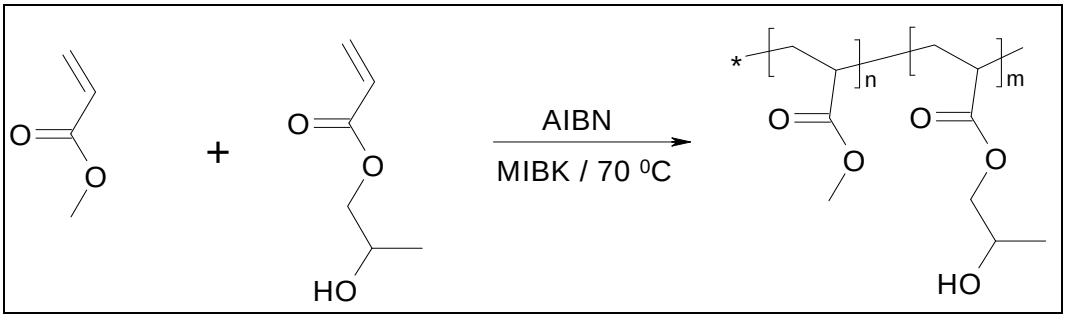

Scheme 3.7: Synthesis of poly (MA-*co*-HPA)

3.11.2 Determination of unreacted monomers by Gas Chromatography (GC)

The unreacted monomer concentrations were determined using GC-FID analysis methodologies as described in Section 3.4.1.

Table 3.13: Response factor (R_f) of monomer MA and HPA

No.	Monomer	R_t (min.)	Mean R_f	% RSD R_f
1.	Methyl acrylate (MA)	10.89	1.73	3.21
2.	2-Hydroxypropyl acrylate (HPA)	21.98	1.46	2.54

Concentration of unreacted monomer was calculated by using above response factors for respective monomers.

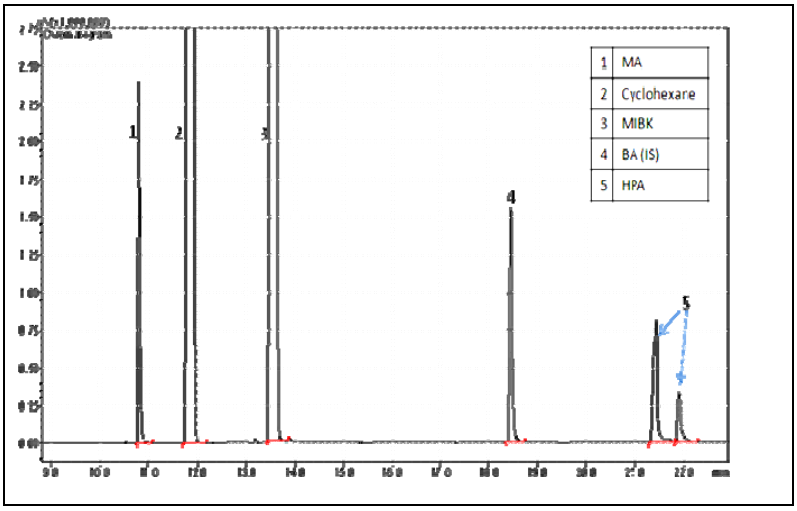

Figure 3.7: Representative GC chromatogram showing separation of MA, cyclohexane, MIBK, BA (IS), and HPA.

Table 3.14: Composition data for copolymerisation of MA with HPA

Polymer code	Mole fraction				Weight fraction conversion
	In feed		In polymer		
	M_1	M_2	m_1	m_2	
HPA	0	1	0	1	-
MA-HPA-1	0.1000	0.9000	0.1359	0.8641	0.2358
MA-HPA-2	0.2000	0.8000	0.1903	0.8097	0.4476
MA-HPA-3	0.2500	0.7500	0.2551	0.7449	0.3241
MA-HPA-4	0.3000	0.7000	0.3668	0.6332	0.2939
MA-HPA-5	0.3500	0.6500	0.3846	0.6154	0.2895
MA-HPA-6	0.4000	0.6000	0.5145	0.4855	0.1554
MA-HPA-7	0.4500	0.5500	0.5011	0.4989	0.2107
MA-HPA-8	0.8000	0.2000	0.8656	0.1344	0.2231
MA-HPA-9	0.9000	0.1000	0.9251	0.0749	0.1404
MA	1	0	1	0	-

3.12 Copolymerisation of butyl acrylate (BA) and 2-hydroxypropyl acrylate (HPA)

3.12.1 Synthesis of poly(BA-*co*-HPA)

Copolymers of BA-HPA of different composition were synthesised with method as described in Section 3.5.1. The feed compositions of the monomers are presented in Table 3.15. Methyl acrylate (MA) was used as internal standard for GC analysis. Synthesis of statistical copolymers poly(BA-*co*-HPA) is depicted in Scheme 3.8.

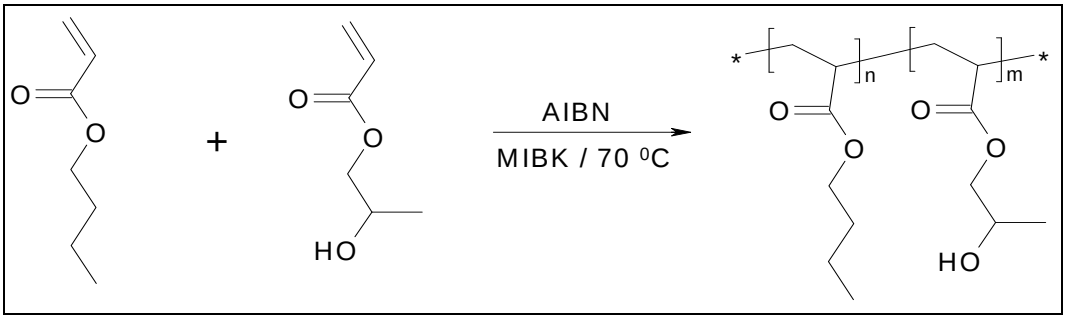

Scheme 3.8: Synthesis of poly (BA-*co*-HPA)

3.12.2 Determination of unreacted monomers by gas chromatography (GC)

The unreacted monomer concentrations were determined using GC-FID method as described in Section 3.4.1.

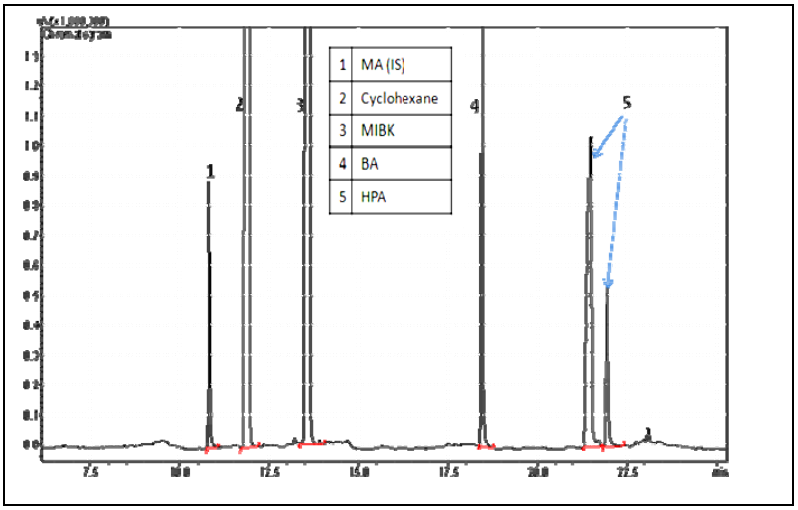

Figure 3.8: Representative GC chromatogram showing separation of MA (IS), cyclohexane, MIBK, BA, and HPA.

Table 3.16: Response factor (R_f) of monomer BA and HPA

Sr. No.	Monomer	Retention time R_t(min.)	Mean R_f	% RSD R_f
1.	Butyl acrylate (BA)	18.60	0.53	2.52
2.	2-Hydroxypropyl acrylate (HPA)	21.96	0.79	2.41

Concentration of unreacted monomer was calculated by using above response factors for respective monomers.

Table 3.15: Composition data for copolymerisation of BA with HPA

Polymer code	Mole fraction				Weight fraction conversion
	In feed		In polymer		
	M_1	M_2	m_1	m_2	
HPA	0	1	0	1	-
BA-HPA -1	0.2000	0.8000	0.1998	0.8002	0.0711
BA-HPA -2	0.2500	0.7500	0.2830	0.7170	0.0158
BA-HPA-3	0.3000	0.7000	0.2174	0.7826	0.0945
BA-HPA-4	0.3500	0.6500	0.2949	0.7051	0.1679
BA-HPA-5	0.4500	0.5500	0.2962	0.7038	0.0209
BA-HPA-6	0.5000	0.5000	0.3742	0.6258	0.1743
BA-HPA-7	0.5500	0.4500	0.4336	0.5664	0.1696
BA-HPA-8	0.7000	0.3000	0.4551	0.5449	0.0738
BA-HPA-9	0.8000	0.2000	0.5928	0.4072	0.0732
BA-HPA-10	0.9000	0.1000	0.6444	0.3556	0.0721
BA	1	0	1	0	-

3.13 Copolymerisation of 2-ethylhexyl acrylate (2-EHA) and 2-hydroxypropyl acrylate (HPA)

3.13.1 Synthesis of poly(EHA-*co*-HPA)

Copolymers of EHA-HPA of different composition were synthesised by methodology as described earlier in Section 3.5.1. The feed compositions of the monomers are presented in Table 3.18. Butyl acrylate (BA) is used as internal standard for GC analysis. Synthesis of statistical copolymers poly(EHA-*co*-HPA) is depicted in Scheme 3.9.

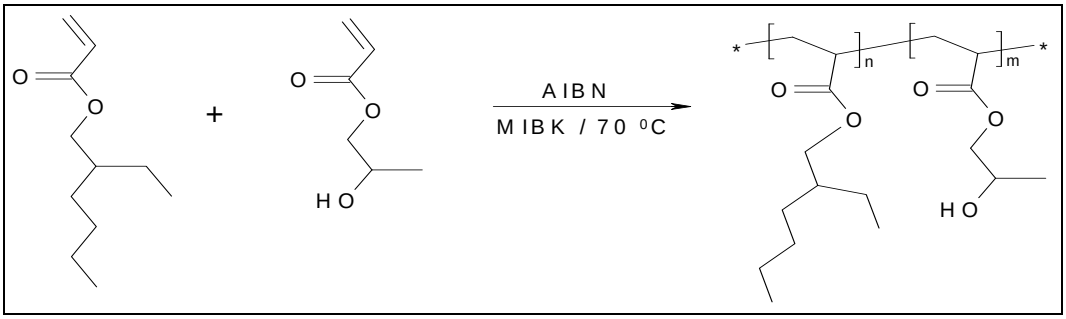

Scheme 3.9: Synthesis of poly (EHA-*co*-HPA)

3.13.2 Determination of unreacted monomers by Gas Chromatography (GC)

The unreacted monomer concentrations were determined using analysis methodologies as described in Section 3.4.1.

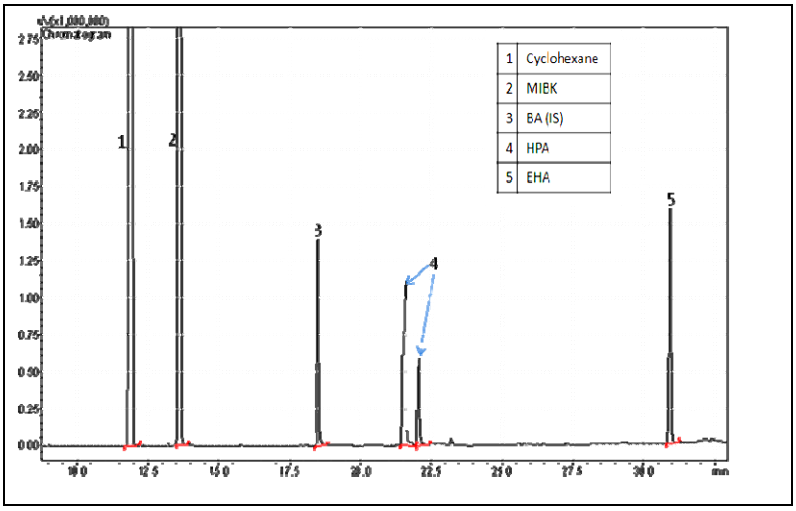

Figure 3.9: Representative GC chromatogram showing separation of cyclohexane, MIBK, BA (IS), HPA, and EHA

Table 3.17: Response factor (R_f) of monomer EHA and HPA

Sr. No.	Monomer	Retention time R_t (min.)	Mean R_f	% RSD R_f
1.	2-Hydroxypropyl acrylate (HPA)	21.96	1.37	1.92
2.	2-Ethyl hexyl acrylate (EHA)	31.19	0.67	1.74

Concentration of unreacted monomer was calculated by using above response factors for respective monomers.

Table 3.18: Composition data for copolymerisation of EHA with HPA

Polymer code	Mole fraction				Weight fraction conversion
	In feed		In polymer		
	M_1	M_2	m_1	m_2	
EHA	0	1	0	1	-
EHA-HPA -1	0.1000	0.9000	0.0794	0.9206	0.8276
EHA-HPA -2	0.2000	0.8000	0.1930	0.8070	0.8975
EHA-HPA-3	0.2500	0.7500	0.2188	0.7812	0.6838
EHA-HPA-4	0.3000	0.7000	0.2758	0.7242	0.9306
EHA-HPA-5	0.3500	0.6500	0.2751	0.7249	0.4625
EHA-HPA-6	0.4000	0.6000	0.3347	0.6653	0.2383
EHA-HPA-7	0.5500	0.4500	0.5262	0.4738	0.1828
EHA-HPA-8	0.6000	0.4000	0.5332	0.4668	0.1342
EHA-HPA-9	0.7000	0.3000	0.6688	0.3312	0.5259
EHA-HPA-10	0.8000	0.2000	0.7594	0.2406	0.4416
EHA-HPA-11	0.8500	0.1500	0.8164	0.1836	0.6707
HPA	1	0	1	0	-

3.14 Copolymerisation of methyl methacrylate (MMA) and 2-hydroxypropyl acrylate (HPA)

3.14.1 Synthesis of poly(MMA-*co*-HPA)

Copolymers of MMA-HPA of different composition were synthesised as described in Section 3.5.1. The feed compositions of the monomers are presented in Table 3.20. Butyl acrylate (BA) is used as internal standard for GC analysis. Synthesis of statistical copolymers poly(MMA-*co*-HPA) is depicted in Scheme 3.10.

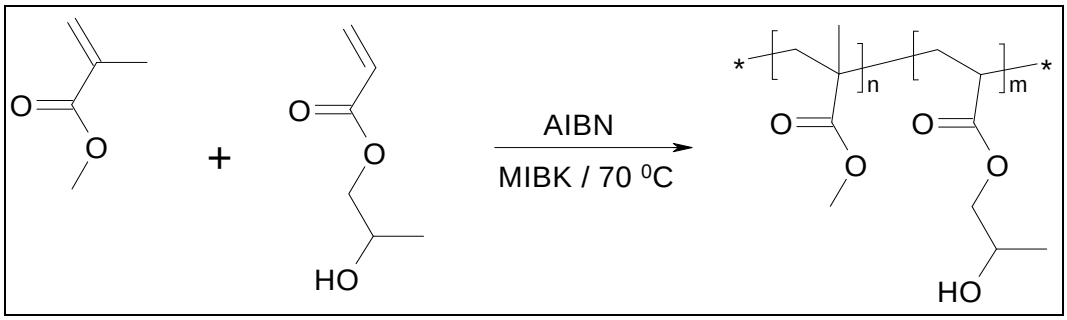

Scheme 3.10: Synthesis of poly (MMA-*co*-HPA)

3.14.2 Determination of unreacted monomers by Gas Chromatography (GC)

The unreacted monomers were determined as described in Section 3.4.1.

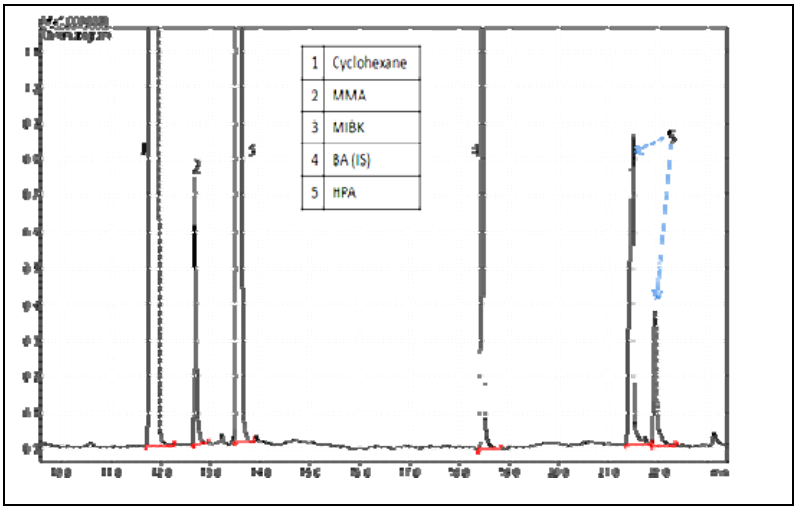

Figure 3.10: Representative GC chromatogram showing separation of MMA, cyclohexane, MIBK, HEA, and BMA (IS)

Table 3.19: Response factor (R_f) of monomer MMA and HPA

Sr. No.	Monomer	Retention time R_t (min.)	Mean R_f	% RSD R_f
1.	Methyl methacrylate (MMA)	12.73	1.29	0.25
2.	2-Hydroxypropyl acrylate (HPA)	21.96	1.43	0.91

Concentration of unreacted monomer was calculated by using above response factors for respective monomers.

Table 3.20: Composition data for copolymerisation of MMA with HPA

Polymer code	Mole fraction				Weight fraction conversion
	In feed		In polymer		
	M_1	M_2	m_1	m_2	
HPA	0	1	0	1	-
MMA-HPA -1	0.1000	0.9000	0.1304	0.8696	0.3987
MMA-HPA -2	0.1500	0.8500	0.1969	0.8031	0.4201
MMA-HPA-3	0.2000	0.8000	0.2412	0.7588	0.4465
MMA-HPA-4	0.2500	0.7500	0.2580	0.7420	0.6736
MMA-HPA-5	0.3000	0.7000	0.3369	0.6631	0.5007
MMA-HPA-6	0.3500	0.6500	0.3747	0.6253	0.5127
MMA-HPA-7	0.4000	0.6000	0.4245	0.5755	0.6091
MMA-HPA-8	0.4500	0.5500	0.5113	0.4887	0.4109
MMA-HPA-9	0.5000	0.5000	0.5452	0.4548	0.4121
MMA-HPA-10	0.5500	0.4500	0.5965	0.4035	0.3725
MMA-HPA-11	0.6000	0.4000	0.6208	0.3792	0.4153
MMA-HPA-12	0.6500	0.3500	0.6881	0.3119	0.3702
MMA-HPA-13	0.7000	0.3000	0.7167	0.2833	0.3778
MMA-HPA-14	0.7500	0.2500	0.7551	0.2449	0.2573
MMA-HPA-15	0.8000	0.2000	0.7964	0.2036	0.4219
MMA-HPA-16	0.8500	0.1500	0.8562	0.1438	0.4074
MMA-HPA-17	0.9000	0.1000	0.8966	0.1034	0.3957
MMA	1	0	1	0	-

3.15 Copolymerisation of 2-ethylhexyl methacrylate (2-EHMA) and 2-hydroxypropyl acrylate (HPA)

3.15.1 Synthesis of poly(EHMA-*co*-HPA)

Copolymers of EHMA-HPA of different composition were synthesised as described in Section 3.5.1. The feed compositions of the monomers are presented in Table 3.22. Butyl acrylate (BA) is used as internal standard for GC analysis. Synthesis of statistical copolymers poly(EHMA-*co*-HPA) is depicted in Scheme 3.11.

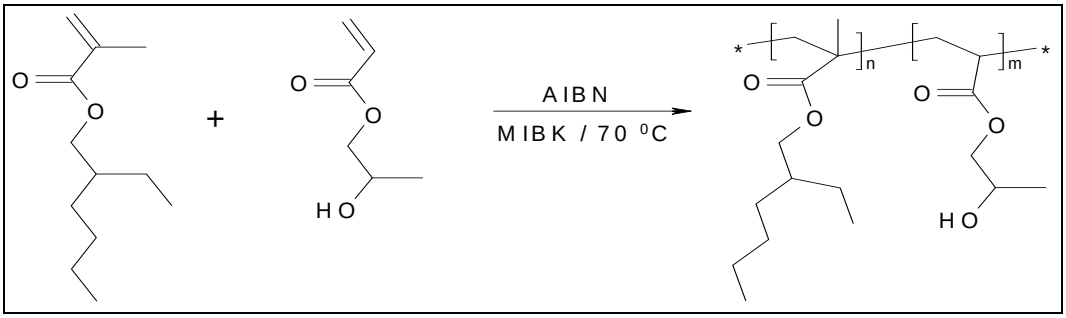

Scheme 3.11: Synthesis of poly (EHMA-*co*-HPA)

3.15.2 Determination of unreacted monomers by gas chromatography (GC)

The unreacted monomers were determined as described in Section 3.4.1.

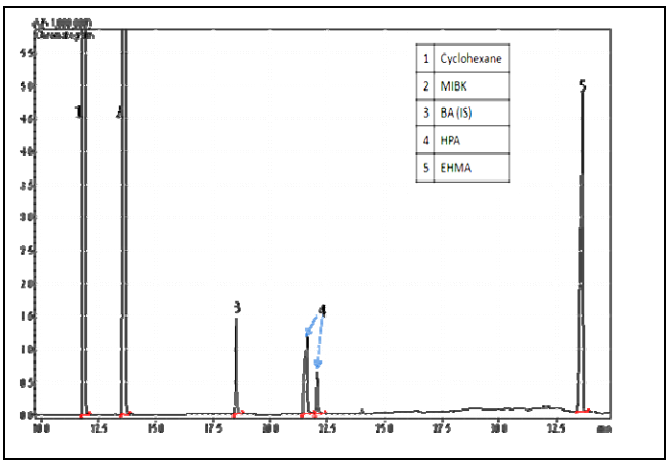

Figure 3.11: Representative GC chromatogram showing separation of cyclohexane, MIBK, BA (IS), HPA, and EHMA.

Table 3.21: Response factor (R_f) of monomer EHMA and HPA

No.	Monomer	R_t (min.)	Mean R_f	% RSD R_f
1.	2-Hydroxypropyl acrylate (HPA)	21.96	1.38	0.94
2.	2-Ethyl hexyl methacrylate (EHMA)	33.72	0.67	2.13

Concentration of unreacted monomer was calculated by using above response factors.

Table 3.22: Composition data for copolymerisation of EHMA with HPA

Polymer code	Mole fraction				Weight fraction conversion
	In feed		In polymer		
	M_1	M_2	m_1	m_2	
HPA	0	1	0	1	-
EHMA-HPA-1	0.1000	0.9000	0.1008	0.8992	0.8855
EHMA-HPA-2	0.1500	0.8500	0.1556	0.8444	0.9140
EHMA-HPA-3	0.2000	0.8000	0.1956	0.8044	0.8767
EHMA-HPA-4	0.2500	0.7500	0.2470	0.7530	0.9554
EHMA-HPA-5	0.3000	0.7000	0.2967	0.7033	0.9449
EHMA-HPA-6	0.3500	0.6500	0.3433	0.6567	0.8962
EHMA-HPA-7	0.4000	0.6000	0.3944	0.6056	0.8932
EHMA-HPA-8	0.4500	0.5500	0.4351	0.5649	0.8476
EHMA-HPA-9	0.5000	0.5000	0.4954	0.5046	0.8570
EHMA-HPA-10	0.5500	0.4500	0.5377	0.4623	0.8581
EHMA-HPA-11	0.6000	0.4000	0.5937	0.4063	0.7934
EHMA-HPA-12	0.6500	0.3500	0.6364	0.3636	0.8414
EHMA-HPA-13	0.7000	0.3000	0.6888	0.3112	0.8090
EHMA-HPA-14	0.7500	0.2500	0.7312	0.2688	0.8159
EHMA-HPA-15	0.8000	0.2000	0.7824	0.2176	0.8505
EHMA-HPA-16	0.8500	0.1500	0.8425	0.1575	0.8569
EHMA-HPA-17	0.9000	0.1000	0.8938	0.1062	0.8469
EHMA	1	0	1	0	-

3.16 Copolymerisation of 2-hydroxyethyl acrylate (HEA) and 2-hydroxypropyl acrylate (HPA)

3.16.1 Synthesis of poly(HEA-*co*-HPA)

Copolymers of HEA-HPA of different composition were synthesised as described in Section 3.5.1. The feed compositions of the monomers are presented in Table 3.24. Butyl acrylate (BA) is used as internal standard for GC analysis. Synthesis of statistical copolymers poly(HEA-*co*-HPA) is depicted in Scheme 3.12.

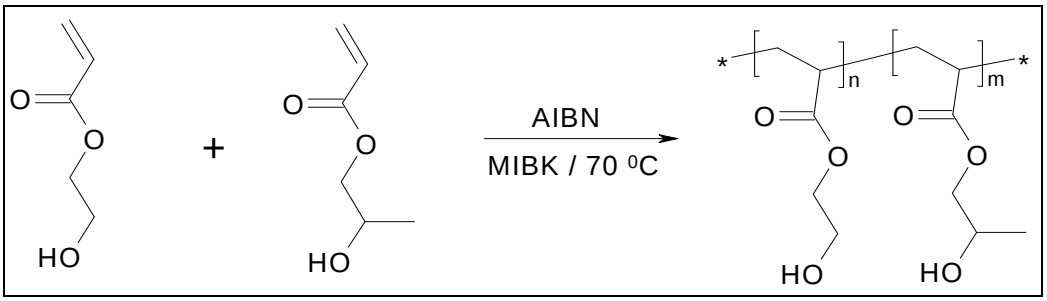

Scheme 3.12: Synthesis of poly (HEA-*co*-HPA)

3.16.2 Determination of unreacted monomers by gas chromatography (GC)

The unreacted monomer concentrations were determined using GC-FID analysis methodologies as described earlier in Section 3.4.1.

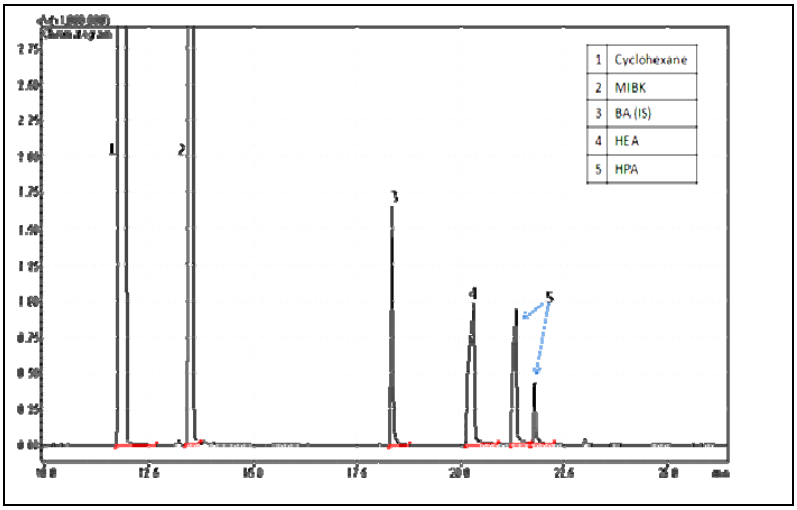

Figure 3.12: Representative GC chromatogram showing separation of cyclohexane, MIBK, BA (IS), HEA, and HPA.

Table 3.23: Response factor (R_f) of monomer HEA and HPA

No.	Monomer	R_t (min.)	Mean R_f	% RSD R_f
1.	2-Hydroxyethyl acrylate (HEA)	20.80	1.62	1.11
2.	2-Hydroxypropyl acrylate (HPA)	21.96	1.36	1.03

Concentration of unreacted monomer was calculated by using above response factors.

Table 3.24: Composition data for copolymerisation of HEA with HPA

Polymer code	Mole fraction				Weight fraction conversion
	In feed		In polymer		
	M_1	M_2	m_1	m_2	
HPA	0	1	0	1	-
HEA-HPA-1	0.1500	0.8500	0.1761	0.8239	0.4328
HEA-HPA-2	0.2000	0.8000	0.2128	0.7872	0.6508
HEA-HPA-3	0.2500	0.7500	0.2950	0.7050	0.2079
HEA-HPA-4	0.3500	0.6500	0.3575	0.6425	0.2753
HEA-HPA-5	0.4000	0.6000	0.4204	0.5796	0.0677
HEA-HPA-6	0.4500	0.5500	0.4517	0.5483	0.0523
HEA-HPA-7	0.6000	0.4000	0.4790	0.5210	0.0389
HEA-HPA-8	0.6500	0.3500	0.4898	0.5102	0.0584
HEA-HPA-9	0.8500	0.1500	0.5528	0.4472	0.0360
HEA-HPA-10	0.9000	0.1000	0.6423	0.3577	0.0297
HEA	1	0	1	0	-

3.17 Copolymerisation of methyl acrylate (MA) and 2-Hydroxyethyl methacrylate (HEMA)

3.17.1 Synthesis of poly(MA-*co*-HEMA)

Copolymers of MA-HEMA of different composition were synthesised as described in earlier Section 3.5.1. The feed compositions of the monomers are presented in Table 3.26. Synthesis of statistical copolymers poly(MA-*co*-HEMA) is depicted in Scheme 3.13.

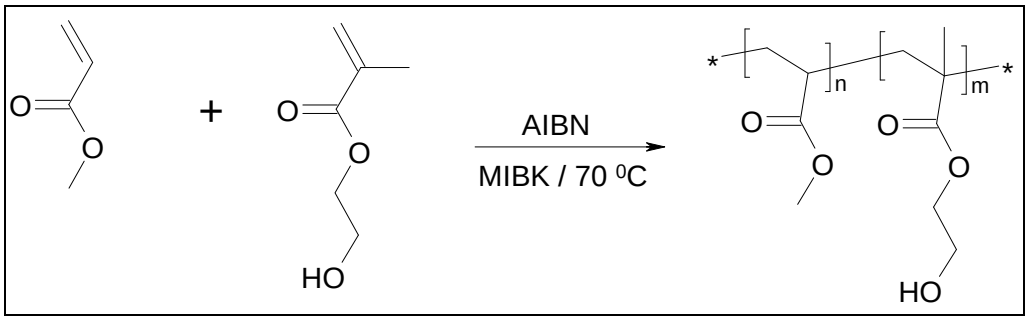

Scheme 3.13: Synthesis of poly (MA-*co*-HEMA)

3.17.2 Determination of unreacted monomers by Gas Chromatography (GC)

The unreacted monomer concentrations were determined using GC-FID analysis methodologies as described earlier in Section 3.4.1.

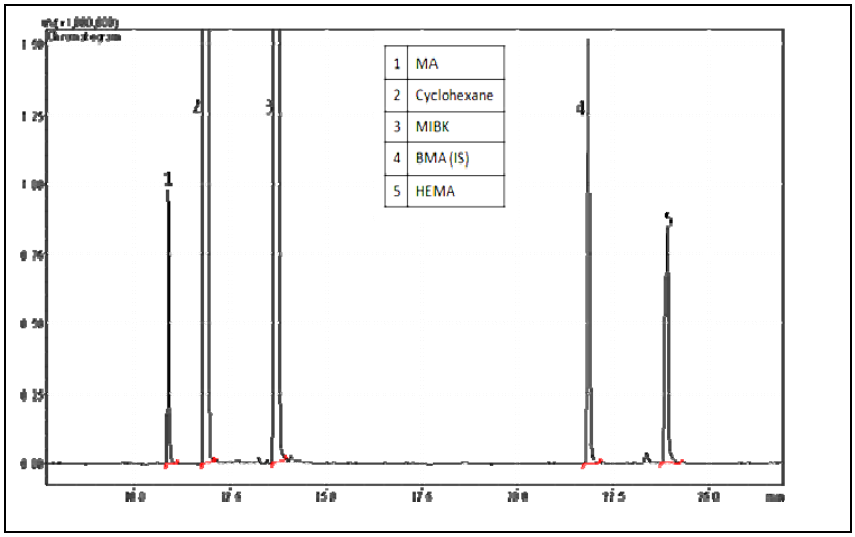

Figure 3.13: Representative GC chromatogram showing separation of MA, cyclohexane, MIBK, BMA (IS), and HEMA.

Table 3.25: Response factor (R_f) of monomer MA and HEMA

No.	Monomer	R_t (min.)	Mean R_f	% RSD R_f
1.	Methyl acrylate (MA)	10.89	2.34	1.9
2.	2-Hydroxyethyl methacrylate (HEMA)	24.19	1.48	2.1

Concentration of unreacted monomer was calculated by using above response factors for respective monomers.

Table 3.26: Composition data for copolymerisation of MA with HEMA

Polymer code	Mole fraction				Weight fraction conversion
	In feed		In polymer		
	M_1	M_2	m_1	m_2	
MA	0	1	0	1	-
MA-HEMA-1	0.1000	0.9000	0.0404	0.9596	0.6657
MA-HEMA-2	0.1500	0.8500	0.0776	0.9224	0.6797
MA-HEMA-3	0.2001	0.7999	0.1002	0.8998	0.6558
MA-HEMA-4	0.2500	0.7500	0.1139	0.8861	0.5648
MA-HEMA-5	0.3500	0.6500	0.1452	0.8548	0.4503
MA-HEMA-6	0.5501	0.4499	0.3262	0.6738	0.2388
MA-HEMA-7	0.6500	0.3500	0.4870	0.5130	0.1748
MA-HEMA-8	0.8000	0.2000	0.6302	0.3698	0.2035
MA-HEMA-9	0.8500	0.1500	0.7085	0.2915	0.1543
MA-HEMA-10	0.9000	0.1000	0.7967	0.2033	0.1316
HEMA	1	0	1	0	-

3.18 Copolymerisation of butyl acrylate (BA) and 2-hydroxyethyl methacrylate (HEMA)

3.18.1 Synthesis of poly(BA-*co*-HEMA)

Copolymers of BA-HEMA of different composition were synthesised as described in Section 3.5.1. The feed compositions of the monomers are presented in Table 3.28. Synthesis of statistical copolymers poly(BA-*co*-HEMA) is depicted in Scheme 3.14.

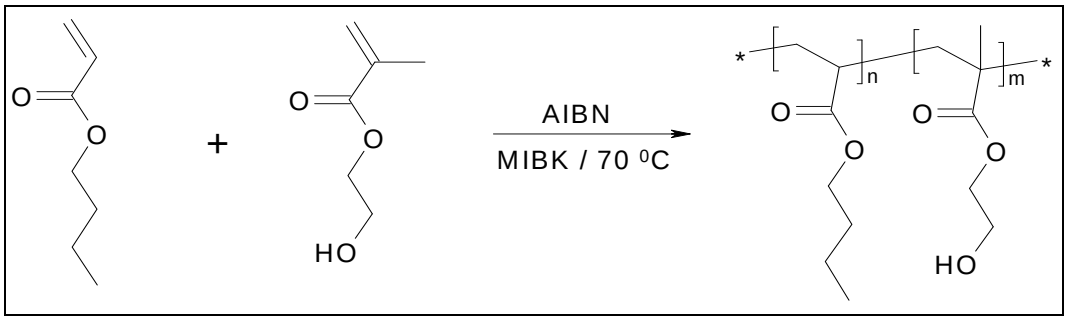

Scheme 3.14: Synthesis of poly (BA-*co*-HEMA)

3.18.2 Determination of unreacted monomers by gas chromatography (GC)

The unreacted monomer concentrations were determined using GC-FID analysis methodologies as described in Section 3.4.1.

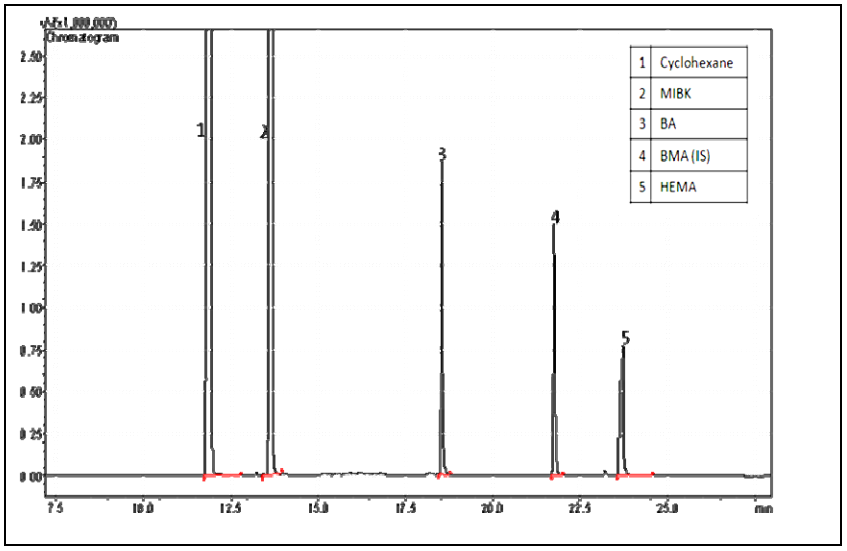

Figure 3.14: Representative GC chromatogram showing separation of cyclohexane, MIBK, BA, BMA (IS), and HEMA.

Table 3.27: Response factor (R_f) of monomer BA and HEMA

No.	Monomer	R_t (min.)	Mean R_f	% RSD R_f
1.	Butyl acrylate (BA)	18.60	0.75	0.95
2.	2-Hydroxyethyl methacrylate (HEMA)	24.19	0.87	1.12

Concentration of unreacted monomers was calculated using above response factors.

Table 3.28: Composition data for copolymerisation of BA with HEMA

Polymer code	Mole fraction				Weight fraction conversion
	In feed		In polymer		
	M_1	M_2	m_1	m_2	
BA	0	1	0	1	-
BA-HEMA-1	0.1000	0.9000	0.0412	0.9588	0.6669
BA-HEMA-2	0.1500	0.8500	0.0870	0.9130	0.6604
BA-HEMA-3	0.2000	0.8000	0.0870	0.9130	0.6078
BA-HEMA-4	0.2500	0.7500	0.1439	0.8561	0.6096
BA-HEMA-5	0.3000	0.7000	0.1857	0.8143	0.6119
BA-HEMA-6	0.3500	0.6500	0.2023	0.7977	0.4887
BA-HEMA-7	0.4000	0.6000	0.1993	0.8007	0.4049
BA-HEMA-8	0.4500	0.5500	0.1943	0.8057	0.2678
BA-HEMA-9	0.5000	0.5000	0.2327	0.7673	0.2790
BA-HEMA-10	0.5500	0.4500	0.2896	0.7104	0.2170
BA-HEMA-11	0.6500	0.3500	0.4435	0.5565	0.1489
BA-HEMA-11	0.7000	0.3000	0.4916	0.5084	0.1139
BA-HEMA-12	0.8000	0.2000	0.6792	0.3208	0.0738
BA-HEMA-13	0.9000	0.1000	0.8413	0.1587	0.1033
BA-HEMA-14	0.1000	0.9000	0.0412	0.9588	0.6669
HEMA	1	0	1	0	-

3.19 Copolymerisation of 2-ethyl hexyl acrylate (EHA) and 2-Hydroxyethyl methacrylate (HEMA)

3.19.1 Synthesis of poly(EHA-*co*-HEMA)

Copolymers of EHA-HEMA of different composition were synthesised as mentioned in Section 3.5.1. The feed compositions of the monomers are presented in Table 3.30. Synthesis of statistical copolymers poly(EHA-*co*-HEMA) is depicted in Scheme 3.15.

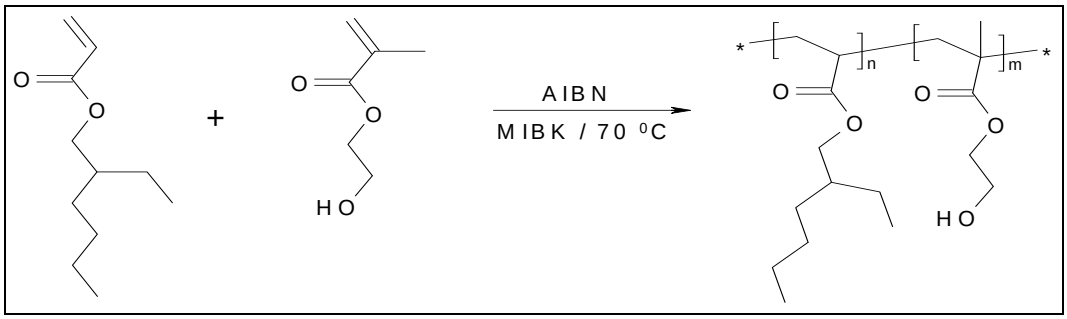

Scheme 3.15: Synthesis of poly (EHA-*co*-HEMA)

3.19.2 Determination of unreacted monomers by gas chromatography (GC)

The unreacted monomer concentrations were determined using GC-FID methodologies as described in Section 3.4.1.

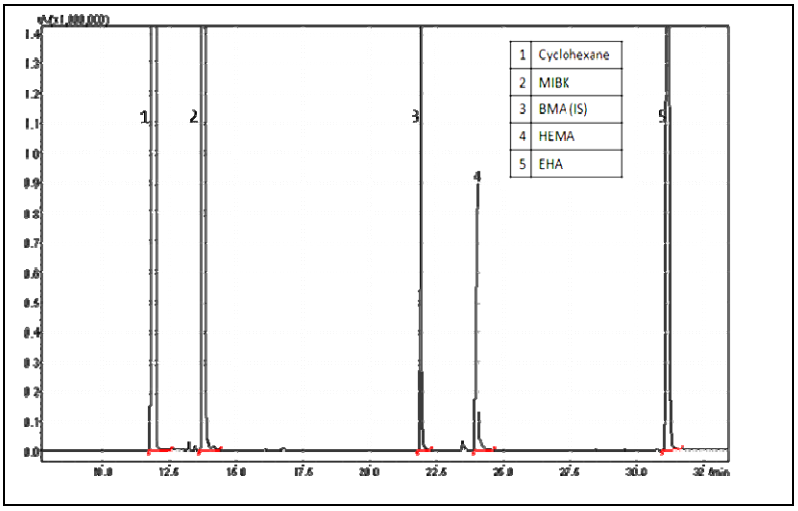

Figure 3.15: Representative GC chromatogram showing separation of cyclohexane (solvent), MIBK, BMA (IS), HEMA and EHA

Table 3.29: Response factor (R_f) of monomer EHA and HEMA

No.	Monomer	R_t (min.)	Mean R_f	% RSD R_f
1.	2-Hydroxyethyl methacrylate (HEMA)	24.19	0.81	1.24
2.	2-Ethyl hexyl acrylate (EHA)	31.19	1.52	0.94

Concentration of unreacted monomer was calculated by using above response factors.

Table 3.30: Composition data for copolymerisation of EHA with HEMA

Polymer code	Mole fraction				Weight fraction conversion
	In feed		In polymer		
	M_1	M_2	m_1	m_2	
EHA	0	1	0	1	-
EHA-HEMA-1	0.1000	0.9000	0.0439	0.9561	0.7317
EHA-HEMA-2	0.1500	0.8500	0.0608	0.9392	0.7238
EHA-HEMA-3	0.2000	0.8000	0.0836	0.9164	0.6285
EHA-HEMA-4	0.2500	0.7500	0.1117	0.8883	0.6193
EHA-HEMA-5	0.3000	0.7000	0.1632	0.8368	0.5889
EHA-HEMA-6	0.4000	0.6000	0.2151	0.7849	0.4107
EHA-HEMA-7	0.4500	0.5500	0.2970	0.7030	0.3863
EHA-HEMA-8	0.5000	0.5000	0.3268	0.6732	0.3381
EHA-HEMA-9	0.5500	0.4500	0.3774	0.6226	0.2680
EHA-HEMA-10	0.6000	0.4000	0.4734	0.5266	0.3583
EHA-HEMA-11	0.6500	0.3500	0.5108	0.4892	0.4007
EHA-HEMA-12	0.7000	0.3000	0.6323	0.3677	0.4835
EHA-HEMA-13	0.7500	0.2500	0.6542	0.3458	0.2808
EHA-HEMA-14	0.8000	0.2000	0.6988	0.3012	0.1807
EHA-HEMA-15	0.8500	0.1500	0.7961	0.2039	0.1668
HEMA	1	0	1	0	-

3.20 Copolymerisation of methyl methacrylate (MMA) and 2-Hydroxyethyl methacrylate (HEMA)

3.20.1 Synthesis of poly(MMA-*co*-HEMA)

Copolymers of MMA-HEMA of different composition were synthesised as described in earlier Section 3.5.1. The feed compositions of the monomers are presented in Table 3.32. Synthesis of statistical copolymers poly(MMA-*co*-HEMA) is depicted Scheme 3.16.

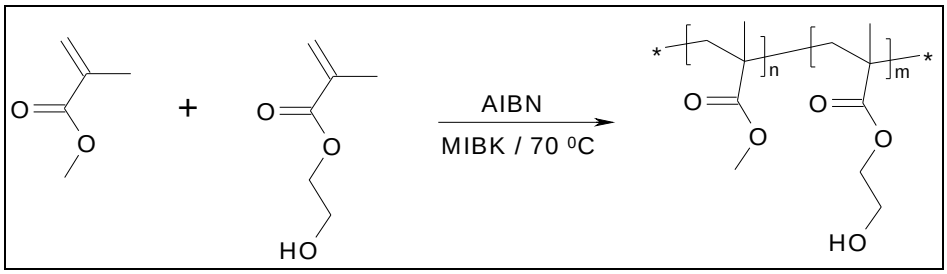

Scheme 3.16: Synthesis of poly (MMA-*co*-HEMA)

3.20.2 Determination of unreacted monomers by gas chromatography (GC)

The unreacted monomer concentrations were determined using GC-FID method as described in Section 3.4.1.

Table 3.31: Response factor (R_f) of monomer MMA and HEMA

No.	Monomer	R_t (min.)	Mean R_f	% RSD R_f
1.	Methyl methacrylate (MMA)	12.73	1.83	2.42
2.	2-Hydroxyethyl methacrylate (HEMA)	24.19	1.08	1.34

Concentration of unreacted monomer was calculated by using above response factors.

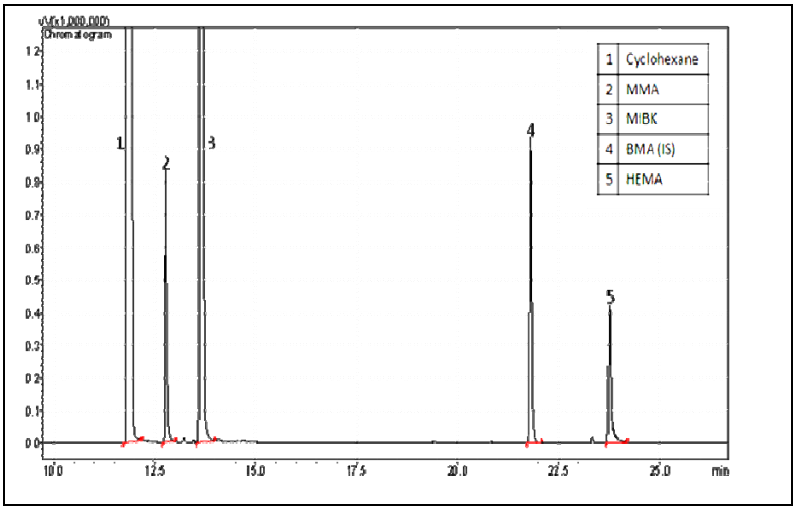

Figure 3.16: Representative GC chromatogram showing separation of MMA, cyclohexane, MIBK, BMA (IS), and HEMA.

Table 3.32: Composition data for copolymerisation of MMA with HEMA

Polymer code	Mole fraction				Weight fraction conversion
	In feed		In polymer		
	M_1	M_2	m_1	m_2	
MMA	0	1	0	1	-
MMA-HEMA-1	0.1000	0.9000	0.0543	0.9457	0.7113
MMA-HEMA-2	0.2000	0.8000	0.1110	0.8890	0.7269
MMA-HEMA-3	0.2500	0.7500	0.1275	0.8725	0.6458
MMA-HEMA-4	0.3000	0.7000	0.1563	0.8437	0.5927
MMA-HEMA-5	0.4000	0.6000	0.2388	0.7612	0.5935
MMA-HEMA-6	0.5000	0.5000	0.3786	0.6214	0.6803
MMA-HEMA-7	0.5500	0.4500	0.3986	0.6014	0.5843
MMA-HEMA-8	0.6500	0.3500	0.4923	0.5077	0.5277
MMA-HEMA-9	0.7500	0.2500	0.5708	0.4292	0.3879
MMA-HEMA-10	0.8000	0.2000	0.5236	0.4764	0.2759
MMA-HEMA-11	0.8500	0.1500	0.6316	0.3684	0.2659
MMA-HEMA-12	0.9000	0.1000	0.7742	0.2258	0.3311
HEMA	1	0	1	0	-

3.21 Copolymerisation of 2-ethylhexyl methacrylate (EHMA) and 2-hydroxyethyl methacrylate (HEMA)

3.21.1 Synthesis of poly(EHMA-*co*-HEMA)

Copolymers of EHMA-HEMA of different composition were synthesised as described earlier in Section 3.5.1. The feed compositions of the monomers are presented in Table 3.34. Synthesis of statistical copolymers poly(EHMA-*co*-HEMA) is depicted in Scheme 3.17.

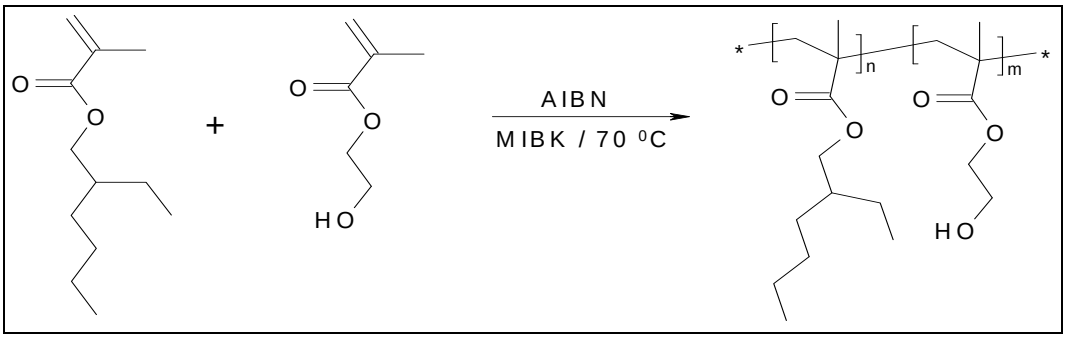

Scheme 3.17: Synthesis of poly (EHMA-*co*-HEMA)

3.21.2 Determination of unreacted monomers by gas chromatography (GC)

The unreacted monomers concentrations were determined using GC-FID method as described in Section 3.4.1.

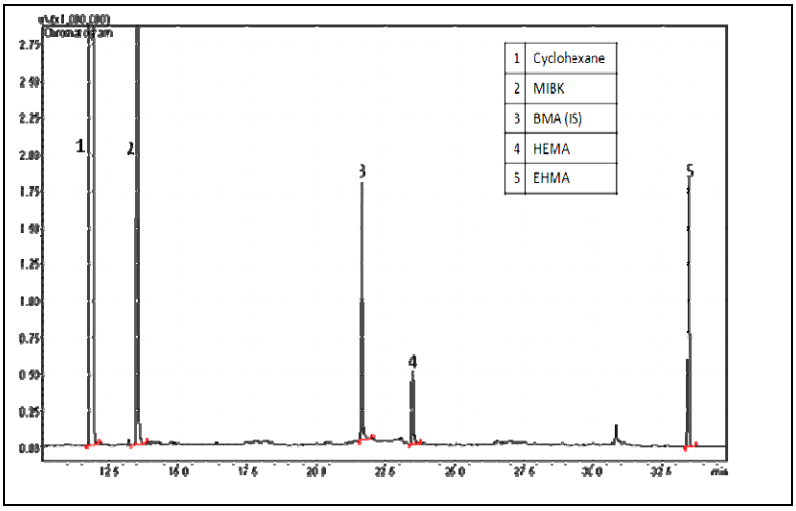

Figure 3.17: Representative GC chromatogram showing separation of cyclohexane (solvent), MIBK, BMA (IS), HEMA and EHMA.

Table 3.33: Response factor (R_f) of monomer EHMA and HEMA

Sr. No.	Monomer	Retention time R_t (min.)	Mean R_f	% RSD R_f
1.	2-Hydroxyethyl methacrylate (HEMA)	24.19	1.53	1.83
2.	2-Ethyl hexyl methacrylate (EHMA)	33.72	0.82	1.27

Concentration of unreacted monomer was calculated by using above response factors.

Table 3.34: Composition data for copolymerisation of EHMA with HEMA

Polymer code	Mole fraction				Weight fraction conversion
	In feed		In polymer		
	M_1	M_2	m_1	m_2	
EHMA	0	1	0	1	-
EHMA-HEMA-1	0.1000	0.9000	0.0679	0.9321	0.7628
EHMA-HEMA-2	0.2000	0.8000	0.1199	0.8801	0.6195
EHMA-HEMA-3	0.3500	0.6500	0.2979	0.7021	0.7691
EHMA-HEMA-4	0.4000	0.6000	0.2966	0.7034	0.4640
EHMA-HEMA-5	0.4500	0.5500	0.3448	0.6552	0.4253
EHMA-HEMA-6	0.5000	0.5000	0.4334	0.5666	0.5835
EHMA-HEMA-7	0.5500	0.4500	0.4784	0.5216	0.5457
EHMA-HEMA-8	0.6000	0.4000	0.5191	0.4809	0.4503
EHMA-HEMA-9	0.6500	0.3500	0.5551	0.4449	0.4174
EHMA-HEMA-10	0.7000	0.3000	0.6305	0.3695	0.4624
EHMA-HEMA-11	0.7500	0.2500	0.6782	0.3218	0.4145
EHMA-HEMA-12	0.8500	0.1500	0.8064	0.1936	0.4913
HEMA	1	0	1	0	-

3.22 Copolymerisation of 2-hydroxypropyl methacrylate (HPMA) and 2-hydroxyethyl methacrylate (HEMA)

3.22.1 Synthesis of poly(HPMA-*co*-HEMA)

Copolymers of HPMA-HEMA of different composition were synthesised as described in Section 3.5.1. The feed compositions of monomers are presented in Table 3.36. Synthesis of statistical copolymers poly(HPMA-*co*-HEMA) is depicted in Scheme 3.18.

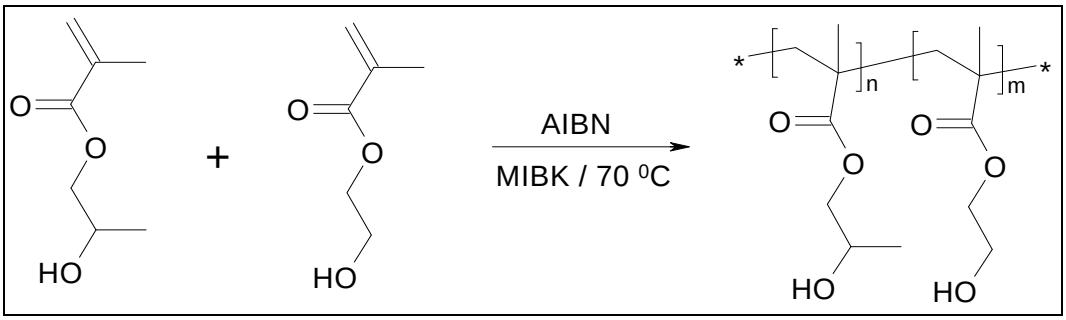

Scheme 3.18: Synthesis of poly (HPMA-*co*-HEMA)

3.22.2 Determination of unreacted monomers by Gas Chromatography (GC)

The unreacted monomer concentrations were determined using GC-FID method as described in Section 3.4.1.

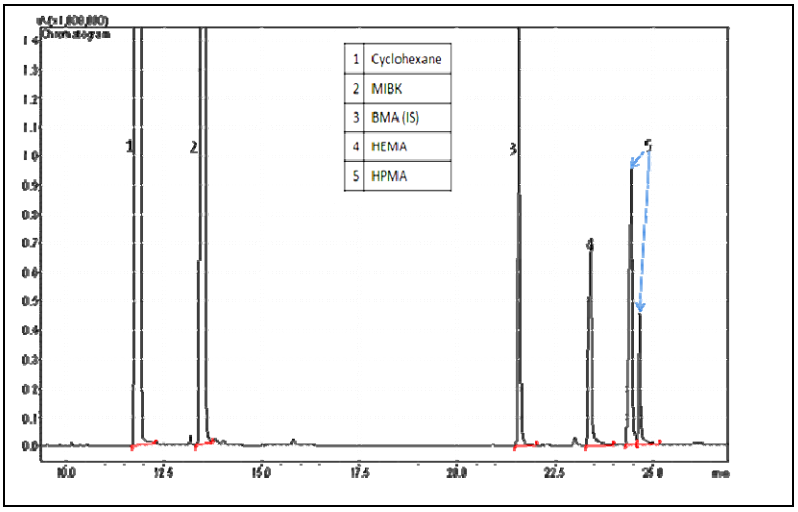

Figure 3.18: Representative GC chromatogram showing separation of cyclohexane, MIBK, BMA (IS), HEMA and HPMA.

Table 3.35: Response factor (R_f) of monomer HPMA and HEMA

Sr. No.	Monomer	Retention time R_t (min.)	Mean R_f	% RSD R_f
1.	2-Hydroxyethyl methacrylate (HEMA)	24.19	1.46	0.81
2.	2-Hydroxypropyl methacrylate (HPMA)	24.93	1.32	0.43

Concentration of unreacted monomer was calculated by using above response factors for respective monomers.

Table 3.36: Composition data for copolymerisation of HPMA with HEMA

Polymer code	Mole fraction				Weight fraction conversion
	In feed		In polymer		
	M_1	M_2	m_1	m_2	
HEMA	0	1	0	1	-
HPMA-HEMA-1	0.1000	0.9000	0.0984	0.9016	0.6537
HPMA-HEMA-2	0.1500	0.8500	0.1448	0.8552	0.6590
HPMA-HEMA-3	0.2000	0.8000	0.1907	0.8093	0.7111
HPMA-HEMA-4	0.2500	0.7500	0.2295	0.7705	0.6000
HPMA-HEMA-5	0.3000	0.7000	0.2750	0.7250	0.5765
HPMA-HEMA-6	0.3500	0.6500	0.3300	0.6700	0.6744
HPMA-HEMA-7	0.4000	0.6000	0.3650	0.6350	0.4297
HPMA-HEMA-8	0.4500	0.5500	0.4200	0.5800	0.5380
HPMA-HEMA-9	0.5000	0.5000	0.4659	0.5341	0.3753
HPMA-HEMA-10	0.5500	0.4500	0.5248	0.4752	0.5725
HPMA-HEMA-11	0.6000	0.4000	0.5780	0.4220	0.5367
HPMA-HEMA-12	0.6500	0.3500	0.6069	0.3931	0.3976
HPMA-HEMA-13	0.7000	0.3000	0.6735	0.3265	0.4650
HPMA-HEMA-14	0.7500	0.2500	0.7189	0.2811	0.3435
HPMA-HEMA-15	0.8000	0.2000	0.7598	0.2402	0.2917
HPMA-HEMA-16	0.8500	0.1500	0.8213	0.1787	0.3818
HPMA-HEMA-17	0.9000	0.1000	0.8746	0.1254	0.4057
HEMA	1	0	1	0	-

3.23 Copolymerisation of methyl acrylate (MA) and 2-hydroxypropyl methacrylate (HPMA)

3.23.1 Synthesis of poly(MA-*co*-HPMA)

Copolymers of MA-HPMA were synthesised as described in Section 3.5.1. The feed compositions of the monomers are presented in Table 3.38. Synthesis of statistical copolymers poly(MA-*co*-HPMA) is depicted in Scheme 3.19.

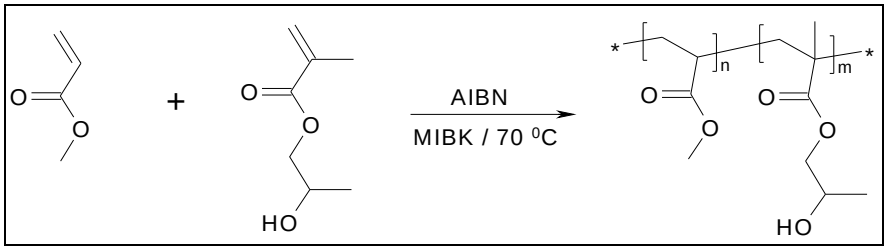

Scheme 3.19: Synthesis of poly (MA-*co*-HPMA)

3.23.2 Determination of unreacted monomers by gas chromatography (GC)

The unreacted monomer concentrations were determined using GC-FID analysis methodologies as described in Section 3.4.1.

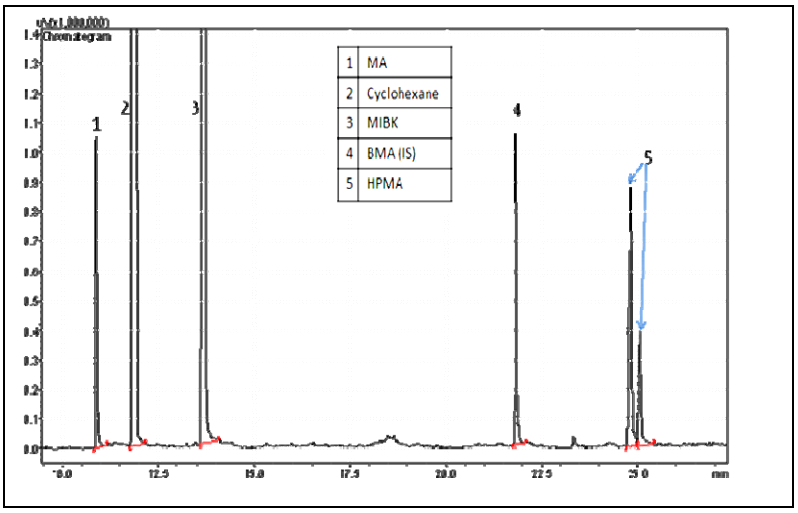

Figure 3.19: Representative GC chromatogram showing separation of MA, cyclohexane, MIBK, BMA (IS), and HPMA.

Table 3.37: Response factor (R_f) of monomer MA and HPMA

No.	Monomer	R_t (min.)	Mean R_f	% RSD R_f
1.	Methyl acrylate (MA)	10.89	2.67	2.84
2.	2-Hydroxypropyl methacrylate (HPMA)	24.93	1.30	1.72

Concentration of unreacted monomer was calculated by using above response factors.

Table 3.38: Composition data for copolymerisation of MA with HPMA

Polymer code	Mole fraction				Weight fraction conversion
	In feed		In polymer		
	M_1	M_2	m_1	m_2	
MA	0	1	0	1	--
MA-HPMA-1	0.1000	0.9000	0.0678	0.9322	0.6719
MA-HPMA-2	0.1500	0.8500	0.1170	0.8830	0.3449
MA-HPMA-3	0.2000	0.8000	0.1717	0.8283	0.3814
MA-HPMA-4	0.3000	0.7000	0.2444	0.7556	0.3974
MA-HPMA-5	0.3500	0.6500	0.3402	0.6598	0.3983
MA-HPMA-6	0.4500	0.5500	0.3849	0.6151	0.2703
MA-HPMA-7	0.6500	0.3500	0.6919	0.3081	0.3305
MA-HPMA-8	0.7000	0.3000	0.7302	0.2698	0.2520
MA-HPMA-9	0.7500	0.2500	0.8065	0.1935	0.3937
MA-HPMA-10	0.9000	0.1000	0.9427	0.0573	0.3171
HPMA	1	0	1	0	--

3.24 Copolymerisation of butyl acrylate (BA) and 2-hydroxypropyl methacrylate (HPMA)

3.24.1 Synthesis of poly(BA-*co*-HPMA)

Copolymers of BA-HPMA were synthesised as described in earlier Section 3.5.1. The feed compositions of the monomers are presented in Table 3.40. Synthesis of statistical copolymers poly(BA-*co*-HPMA) is depicted in Scheme 3.20.

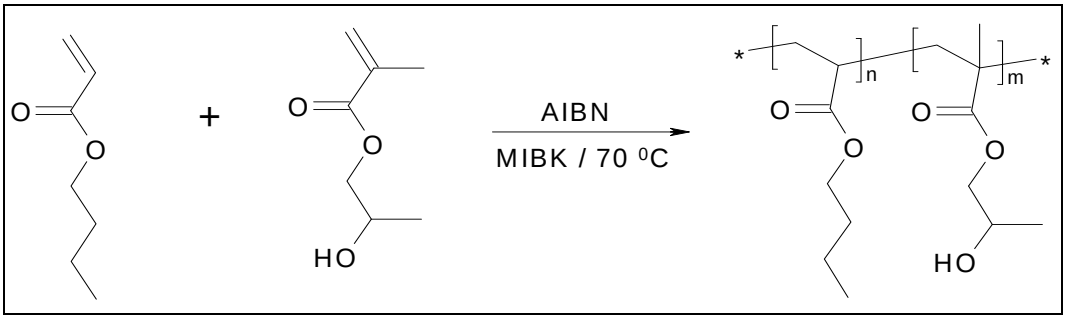

Scheme 3.20: Synthesis of poly (BA-*co*-HPMA)

3.24.2 Determination of unreacted monomers by gas chromatography (GC)

The unreacted monomer concentrations were determined as described in Section 3.4.1.

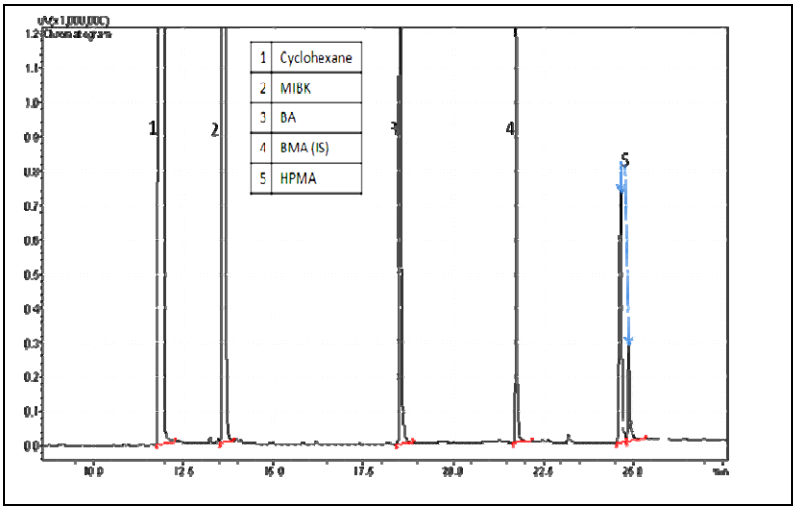

Figure 3.20: Representative GC chromatogram showing separation of cyclohexane, MIBK, BA, BMA (IS), and HPMA.

Table 3.39: Response factor (R_f) of monomer BA and HPMA

Sr. No.	Monomer	Retention time R_t (min.)	Mean R_f	% RSD R_f
1.	Butyl acrylate (BA)	18.60	1.10	0.83
2.	2-Hydroxypropyl methacrylate (HPMA)	24.93	1.30	1.74

Concentration of unreacted monomer was calculated by using above response factors for respective monomers

Table 3.40: Composition data for copolymerisation of BA with HPMA

Polymer code	Mole fraction				Weight fraction conversion
	In feed		In polymer		
	M_1	M_2	m_1	m_2	
BA	0	1	0	1	-
BA-HPMA-1	0.1000	0.9000	0.0702	0.9298	0.7791
BA-HPMA-2	0.1500	0.8500	0.1047	0.8953	0.7392
BA-HPMA-3	0.2000	0.8000	0.1419	0.8581	0.6398
BA-HPMA-4	0.2500	0.7500	0.1633	0.8367	0.4972
BA-HPMA-5	0.3000	0.7000	0.2257	0.7743	0.6467
BA-HPMA-6	0.3500	0.6500	0.2412	0.7588	0.4715
BA-HPMA-7	0.4000	0.6000	0.3258	0.6742	0.5961
BA-HPMA-8	0.4500	0.5500	0.3242	0.6758	0.4477
BA-HPMA-9	0.5000	0.5000	0.3566	0.6434	0.4531
BA-HPMA-10	0.5500	0.4500	0.4172	0.5828	0.4316
BA-HPMA-11	0.6000	0.4000	0.4588	0.5412	0.3889
BA-HPMA-12	0.6500	0.3500	0.4817	0.5183	0.2598
BA-HPMA-13	0.7000	0.3000	0.4885	0.5115	0.1986
BA-HPMA-14	0.7500	0.2500	0.5623	0.4377	0.1387
BA-HPMA-15	0.9000	0.1000	0.7648	0.2352	0.1912
HPMA	1	0	1	0	-

3.25 Copolymerisation of 2-ethylhexyl acrylate (EHA) and 2-hydroxypropyl methacrylate (HPMA)

3.25.1 Synthesis of poly(EHA-*co*-HPMA)

Copolymers of EHA-HPMA of different composition were synthesised as described in Section 3.5.1. The feed compositions of the monomers are presented in Table 3.42. Synthesis of statistical copolymers poly(EHA-*co*-HPMA) is depicted in Scheme 3.21.

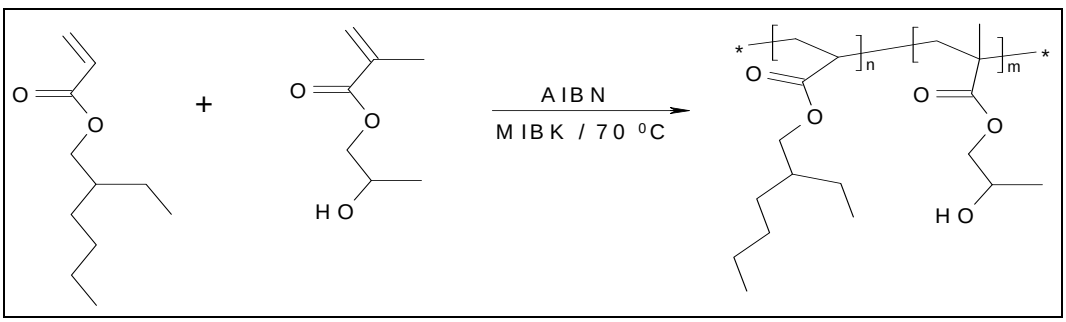

Scheme 3.21: Synthesis of poly (EHA-*co*-HPMA)

3.25.2 Determination of unreacted monomers by gas chromatography (GC)

The unreacted monomers were determined as described in Section 3.4.1.

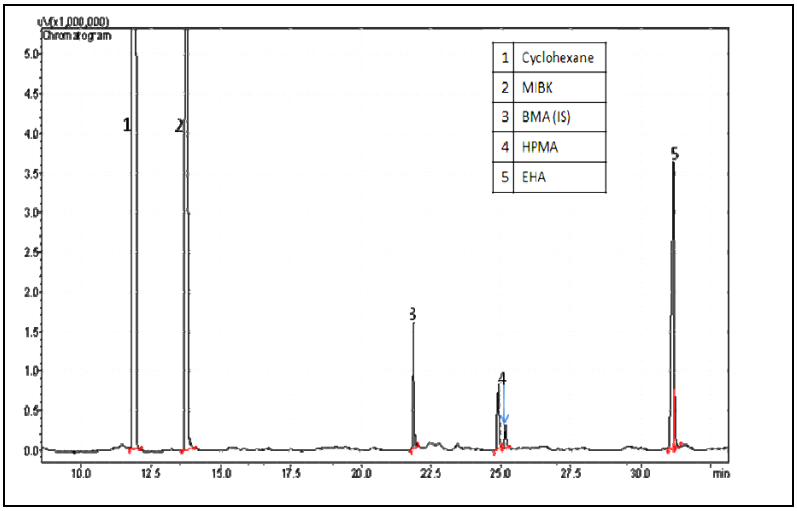

Figure 3.23: Representative GC chromatogram showing separation of cyclohexane, MIBK, BMA (IS), HPMA and EHA.

Table 3.41: Response factor (R_f) of monomer EHA and HPMA

No.	Monomer	R_t (min.)	Mean R_f	% RSD R_f
1.	2-Hydroxypropyl methacrylate (HPMA)	24.93	1.41	2.22
2.	2-Ethylhexyl acrylate (EHA)	31.19	0.84	1.94

Concentration of unreacted monomer was calculated by using above response factors.

Table 3.42: Composition data for copolymerisation of EHA with HPMA

Polymer code	Mole fraction				Weight fraction conversion
	In feed		In polymer		
	M_1	M_2	m_1	m_2	
HPMA	0	1	0	1	-
EHA-HPMA-1	0.1000	0.9000	0.0359	0.9641	0.6281
EHA-HPMA-2	0.1500	0.8500	0.0599	0.9401	0.4901
EHA-HPMA-3	0.2000	0.8000	0.0719	0.9281	0.4272
EHA-HPMA-4	0.2500	0.7500	0.0797	0.9203	0.4146
EHA-HPMA-5	0.3000	0.7000	0.1570	0.8430	0.5210
EHA-HPMA-6	0.4000	0.6000	0.2274	0.7726	0.4250
EHA-HPMA-7	0.4500	0.5500	0.1923	0.8077	0.3467
EHA-HPMA-8	0.5000	0.5000	0.2034	0.7966	0.3313
EHA-HPMA-9	0.5500	0.4500	0.2543	0.7457	0.3111
EHA-HPMA-10	0.6500	0.3500	0.4259	0.5741	0.1914
EHA-HPMA-11	0.7500	0.2500	0.4930	0.5070	0.1595
EHA-HPMA-12	0.8500	0.1500	0.6303	0.3697	0.0885
EHA-HPMA-13	0.9000	0.1000	0.7272	0.2728	0.1162
EHA	1	0	1	0	-

3.26 Copolymerisation of methyl methacrylate (MMA) and 2-hydroxypropyl methacrylate (HPMA)

3.26.1 Synthesis of poly(MMA-*co*-HPMA)

Copolymers of MMA-HPMA were synthesised as described in earlier Section 3.5.1. The feed compositions of the monomers are presented in Table 3.44. Synthesis of statistical copolymers poly(MMA-*co*-HPMA) is depicted in Scheme 3.22.

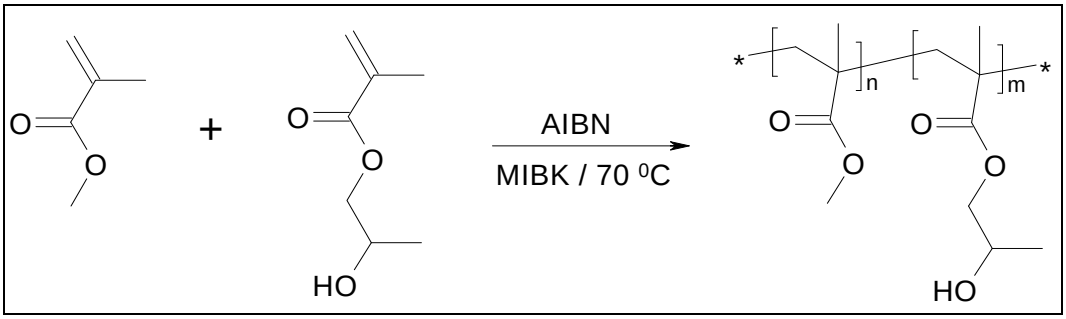

Scheme 3.22: Synthesis of poly (MMA-*co*-HPMA)

3.26.2 Determination of unreacted monomers by gas chromatography (GC)

The unreacted monomer concentrations were determined as described in Section 3.4.1.

Table 3.43: Response factor (R_f) of monomer MMA and HPMA

Sr. No.	Monomer	Retention time R_t (min.)	Mean R_f	% RSD R_f
1.	Methyl methacrylate (MMA)	21.73	1.71	2.01
2.	2-Hydroxypropyl methacrylate (HPMA)	24.93	0.98	1.24

Concentration of unreacted monomer was calculated by using above response factors.

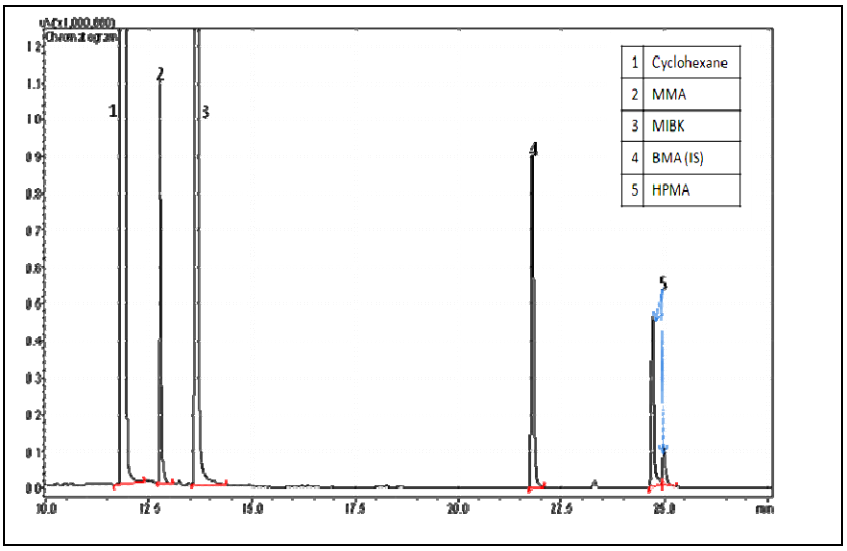

Figure 3.24: Representative GC chromatogram showing separation of cyclohexane, MMA, MIBK, BMA (IS), and HPMA.

Table 3.44: Composition data for copolymerisation of MMA with HPMA

Polymer code	Mole fraction				Weight fraction conversion
	In feed		In polymer		
	M_1	M_2	m_1	m_2	
MMA	0	1	0	1	-
MMA-HPMA-1	0.1000	0.9000	0.0816	0.9184	0.7786
MMA-HPMA-2	0.1500	0.8500	0.1370	0.8630	0.9689
MMA-HPMA-3	0.2000	0.8000	0.1888	0.8112	0.9589
MMA-HPMA-4	0.2500	0.7500	0.2129	0.7871	0.8636
MMA-HPMA-5	0.3000	0.7000	0.2697	0.7303	0.9184
MMA-HPMA-6	0.3500	0.6500	0.2902	0.7098	0.7956
MMA-HPMA-7	0.4000	0.6000	0.3482	0.6518	0.8071
MMA-HPMA-8	0.4500	0.5500	0.3761	0.6239	0.7137
MMA-HPMA-9	0.5000	0.5000	0.3994	0.6006	0.5958
MMA-HPMA-10	0.5500	0.4500	0.4497	0.5503	0.5585
MMA-HPMA-11	0.6000	0.4000	0.5131	0.4869	0.6029
MMA-HPMA-12	0.6500	0.3500	0.5189	0.4811	0.5006
MMA-HPMA-13	0.7500	0.2500	0.6297	0.3703	0.4556
MMA-HPMA-14	0.8000	0.2000	0.6708	0.3292	0.4362
MMA-HPMA-15	0.9000	0.1000	0.8076	0.1924	0.2877
HPMA	1	0	1	0	-

3.27 Copolymerisation of 2-ethylhexyl methacrylate (EHMA) and 2-hydroxypropyl methacrylate (HPMA)

3.27.1 Synthesis of poly(EHMA-*co*-HPMA)

Copolymers of EHMA-HPMA of different composition were synthesised as described in earlier Section 3.5.1. The feed compositions of the monomers are presented in Table 3.46. Synthesis of statistical copolymers poly(EHMA-*co*-HPMA) is depicted in Scheme 3.23.

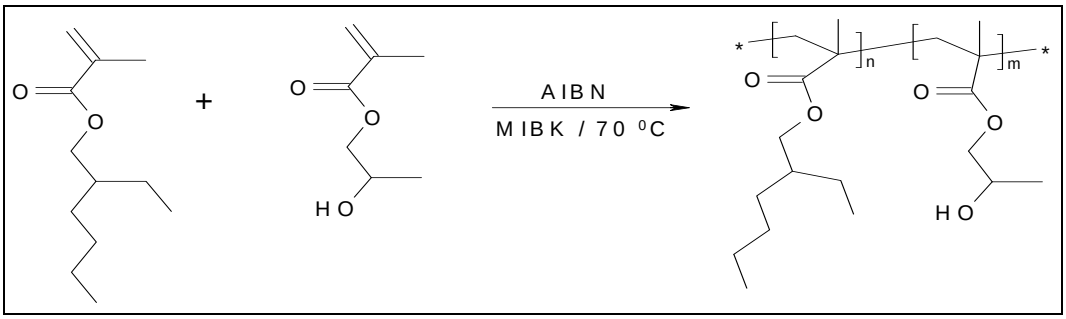

Scheme 3.23: Synthesis of poly (EHMA-*co*-HPMA)

3.27.2 Determination of unreacted monomers by gas chromatography (GC)

The unreacted monomers were determined as described in Section 3.4.1.

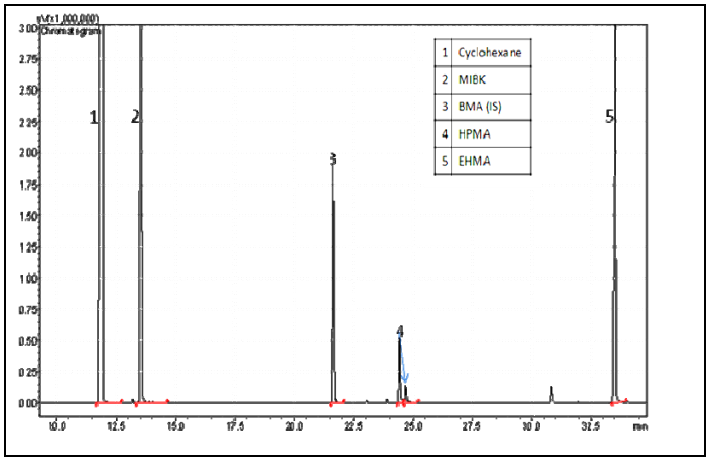

Figure 3.23: Separation of cyclohexane, MIBK, BMA (IS), HPMA and EHMA.

Table 3.45: Response factor (R_f) of monomer EHMA and HPMA

No.	Monomer	R_t (min.)	Mean R_f	% RSD R_f
1.	2-Hydroxypropyl methacrylate (HPMA)	24.93	1.34	1.95
2.	2-Ethylhexyl methacrylate (EHMA)	33.72	0.81	1.21

Concentration of unreacted monomer was calculated by using above response factors.

Table 3.46: Composition data for copolymerisation of EHMA with HPMA

Polymer code	Mole fraction				Weight fraction conversion
	In feed		In polymer		
	M_1	M_2	m_1	m_2	
EHMA	0	1	0	1	-
EHMA-HPMA-1	0.1000	0.9000	0.0864	0.9136	0.8782
EHMA-HPMA-2	0.1500	0.8500	0.1401	0.8599	0.9049
EHMA-HPMA-3	0.2000	0.8000	0.1829	0.8171	0.9003
EHMA-HPMA-4	0.2500	0.7500	0.2315	0.7685	0.9078
EHMA-HPMA-5	0.3000	0.7000	0.2816	0.7184	0.9083
EHMA-HPMA-6	0.3500	0.6500	0.3322	0.6678	0.9187
EHMA-HPMA-7	0.4000	0.6000	0.3728	0.6272	0.8910
EHMA-HPMA-8	0.4500	0.5500	0.4243	0.5757	0.8959
EHMA-HPMA-9	0.5000	0.5000	0.4604	0.5396	0.8022
EHMA-HPMA-10	0.5500	0.4500	0.5212	0.4788	0.8665
EHMA-HPMA-11	0.6500	0.3500	0.6121	0.3879	0.6387
EHMA-HPMA-12	0.7000	0.3000	0.6830	0.3170	0.8692
EHMA-HPMA-13	0.7500	0.2500	0.7356	0.2644	0.8407
EHMA-HPMA-14	0.8000	0.2000	0.7906	0.2094	0.8685
EHMA-HPMA-15	0.8500	0.1500	0.8408	0.1592	0.8786
EHMA-HPMA-16	0.9000	0.1000	0.8975	0.1025	0.8799
HPMA	1	0	1	0	-

3.28 Copolymerisation of 2-hydroxyethyl acrylate (HEA) and 2-hydroxypropyl methacrylate (HPMA)

3.28.1 Synthesis of poly(HEA-*co*-HPMA)

Copolymers of HEA-HPMA were synthesized as described in Section 3.5.1. The feed compositions of the monomers are presented in Table 3.48. Synthesis of statistical copolymers poly(HEA-*co*-HPMA) is depicted in Scheme 3.24.

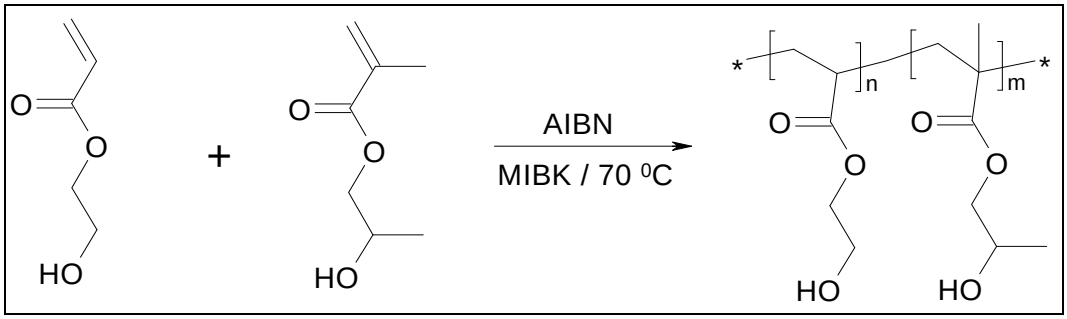

Scheme 3.24: Synthesis of poly (HEA-*co*-HPMA)

3.28.2 Determination of unreacted monomers by gas chromatography (GC)

The unreacted monomer concentrations were determined using GC-FID analysis methodologies as described in Section 3.4.1.

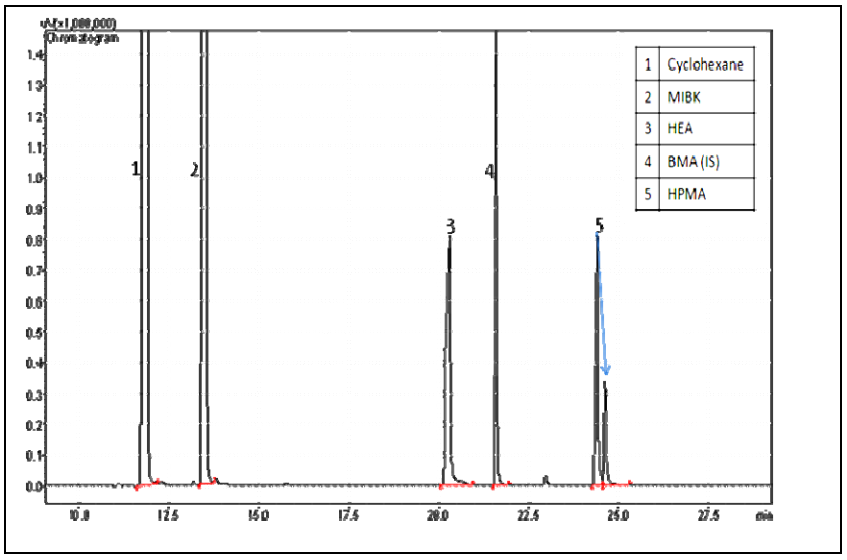

Figure 3.24: Representative GC chromatogram showing separation of cyclohexane, MIBK, HEA, BMA (IS), and HPMA.

Table 3.47: Response factor (R_f) of monomer HEA and HPMA

Sr. No.	Monomer	Retention time R_t (min.)	Mean R_f	% RSD R_f
1.	2-Hydroxyethyl acrylate (HEA)	20.80	1.82	1.13
2.	2-Hydroxypropyl methacrylate (HPMA)	24.93	1.32	0.25

Concentration of unreacted monomer was calculated by using above response factors.

Table 3.48: Composition data for copolymerisation of HEA with HPMA

Polymer code	Mole fraction				Weight fraction conversion
	In feed		In polymer		
	M_1	M_2	m_1	m_2	
HEA	0	1	0	1	-
HEA-HPMA-1	0.1000	0.9000	0.1345	0.8655	0.4149
HEA-HPMA-2	0.1500	0.8500	0.1815	0.8185	0.6249
HEA-HPMA-3	0.2000	0.8000	0.2438	0.7562	0.3084
HEA-HPMA-4	0.2500	0.7500	0.2600	0.7400	0.2778
HEA-HPMA-5	0.3000	0.7000	0.3081	0.6919	0.2637
HEA-HPMA-6	0.4000	0.6000	0.3949	0.6051	0.2675
HEA-HPMA-7	0.4500	0.5500	0.4182	0.5818	0.2077
HEA-HPMA-8	0.5000	0.5000	0.4625	0.5375	0.2533
HEA-HPMA-9	0.5500	0.4500	0.5704	0.4296	0.2322
HEA-HPMA-10	0.6000	0.4000	0.5491	0.4509	0.3625
HEA-HPMA-11	0.6500	0.3500	0.6400	0.3600	0.3742
HEA-HPMA-12	0.7000	0.3000	0.6590	0.3410	0.2188
HEA-HPMA-13	0.8500	0.1500	0.7975	0.2025	0.1489
HPMA	1	0	1	0	-

3.29 Copolymerisation of 2-hydroxypropyl acrylate (HPA) and 2-hydroxypropyl methacrylate (HPMA)

3.29.1 Synthesis of poly(HPA-*co*-HPMA)

Copolymers of HPA-HPMA were synthesised as described in Section 3.5.1. The feed compositions of the monomers are presented in Table 3.50. Synthesis of statistical copolymers poly(HPA-*co*-HPMA) is depicted in Scheme 3.25.

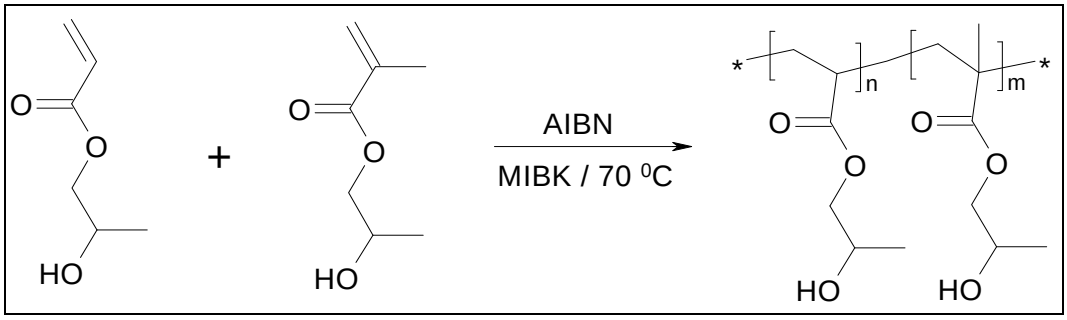

Scheme 3.25: Synthesis of poly (HPA-*co*-HPMA)

3.29.2 Determination of unreacted monomers by gas chromatography (GC)

The unreacted monomer concentrations were determined using GC-FID analysis methodologies as described in Section 3.4.1.

Table 3.49: Response factor (R_f) of monomer HPA and HPMA

Sr. No.	Monomer	Retention time R_t(min.)	Mean R_f	% RSD R_f
1.	2-Hydroxypropyl acrylate (HPA)	21.96	1.42	3.12
2.	2-Hydroxypropyl methacrylate (HPMA)	24.93	1.19	1.74

Concentration of unreacted monomer was calculated by using above response factors for respective monomers.

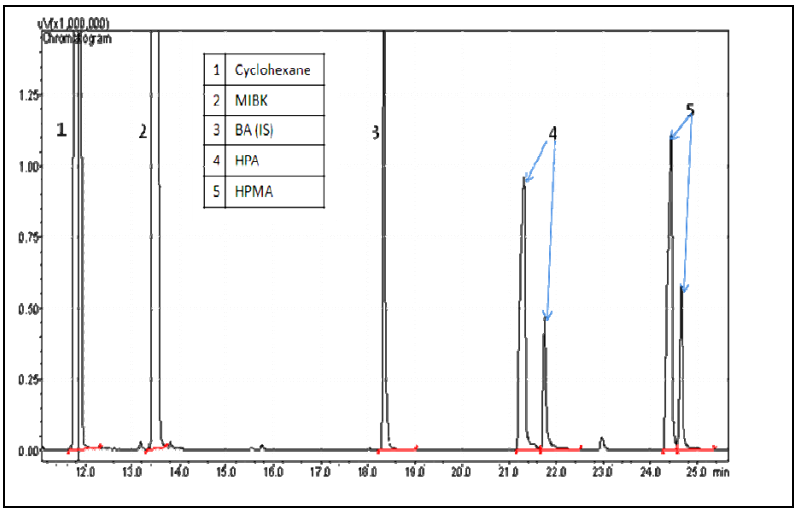

Figure 3.25: Representative GC chromatogram showing separation of cyclohexane, MIBK, BMA (IS), HPA and HPMA.

Table 3.50: Composition data for copolymerisation of HPA with HPMA

Polymer code	Mole fraction				Weight fraction conversion
	In feed		In polymer		
	M_1	M_2	m_1	m_2	
HPA	0	1	0	1	-
HPA-HPMA-1	0.1000	0.9000	0.1127	0.8873	0.2715
HPA-HPMA-2	0.1500	0.8500	0.1676	0.8324	0.3028
HPA-HPMA-3	0.2000	0.8000	0.1984	0.8016	0.3348
HPA-HPMA-4	0.2500	0.7500	0.2315	0.7685	0.2622
HPA-HPMA-5	0.3000	0.7000	0.2729	0.7271	0.2687
HPA-HPMA-6	0.3500	0.6500	0.3265	0.6735	0.4015
HPA-HPMA-7	0.4000	0.6000	0.3842	0.6158	0.1576
HPA-HPMA-8	0.4500	0.5500	0.3921	0.6079	0.1977
HPA-HPMA-9	0.7000	0.3000	0.6929	0.3071	0.1853
HPA-HPMA-10	0.8500	0.1500	0.8786	0.1214	0.1801
HPA-HPMA-11	0.9000	0.1000	0.9185	0.0815	0.1503
HPMA	1	0	1	0	-

3.30 References:

[1] D. A. Tirrell, H. Mark, N. M. Bikales, C. G. Overberger and G. Menges, *Encyclopedia of Polymer Science and Engineering*, Vol. 4, 2nd *Edition*. John Wiley & Sons, New York, **1985.**

[2] N. L. Zutty and J. A. Faucher, *J. Polym. Sci.*, **1962**, 60, 536.

[3] G. Stergiou, P. Dousikos and M. Pitsikalis, *Euro. Poly. J.,* **2002,** 38, 1963.

[4] O. S. Young, S. K. Nam and S. D. Seul, *J. Ind. Eng. Chem.*, **2000,** Vol.6, 236.

[5] S. H. Kandil and M. A. El-Gamal, *J. Polym. Sci., Part A: Polym. Chem.,* **1986,** 24, 2765.

[6] *S.* Mori, *J. Appl. Polym. Sci.*, **1989**, 38, 547.

[7] B. M. Gallo and S. Russo, *J. Macromol. Sci. Chem.,* **1974**, 521.

[8] D. A. Netzel, *Dev. Appl. Spect.,* **1970**, 7B, 147.

[9] A. Petit and J. Neel, *J. Appl. Polym. Sci.,* **1990,** 41, 267.

[10] S. Mori, *J. Chromatog.,* **1980,** 194, 163.

[11] S. Paul and A. B. W. Becker, *J. Coat. Technol.,* **1980**, 52, 47.

[12] M. Blazso, E. J. T. Szekely, B. Plage and H. R. Schulten, *J. Polym. Sci., Part A: Polym. Chem.,* **1989**, 27, 1027.

[13] D. O. Hummel, H. D. Schuddemage and K. Rubenacker, *Polymer Spectroscopy, Verlag Chemie*, Munich **1974**, 355.

[14] A. K. Lee and R. D. Sedgwick, *J. Polym. Sci.: Polym. Chem. Ed.,* **1978,** 16, 685**.**

[15] G. C. Odian, *Principles of Polymerisation: 3rd Edition*, John Wiley and Sons Inc., New York. **1991**.

[16]. C. Hagiopol, *Copolymerisation: Towards a Systematic Approach*, Kluwer Academic Plenum Publishers, New York, **1999**.

[17] P. J. Flory, *Principles of Polymer Chemistry*, Cornell University Press, Ithaca, **1953**.

[18] M. Fineman and S. D. Ross, J. *Polym. Sci.,* **1950**, 5, 249.

[19] T. Kelen and F. Tudos, *J. Macro. Sci. Chem*., A9, **1975,** 1, 1-27.

[20] F. Tudos and T. Kelen, T. *J. Macromol. Sci.: Part A,* **1981,** *16*, 1283.

[21] R. Mao, M. B. Huglin, *Polymer,* **1993**, 34, 1709.

[22] D. A. Skoog, D. M. West and F. J. Holler, *Fundamentals of Analytical Chemistry,* Saunders College Pub., **1988**.

[23] G. D. Christian, *Analytical Chemistry, 6th Edition*, John Wiley and Sons Inc., Singapore, **2004**.

Chapter IV

Results and Discussion

Part A: Reactivity Ratio

4.1 Poly(methyl acrylate-*co*-2-hydroxyethyl acrylate) System

There are no reports on the estimation of copolymerization kinetic parameters, namely monomer reactivity ratios for the two monomers methyl acrylate with 2-hydroxyethyl acrylate. Poly(methyl acrylate-*co*-2-hydroxyethyl acrylate) [poly(MA-*co*-HEA)] hydrogels are known to form interpenetrating networks (IPN).[1] Polypyrrole/crosslinked poly(MA-*co*-HEA) conductive composite films have been prepared by vapour phase polymerisation of pyrrole within crosslinked poly(MA-*co*-HEA) networks using anhydrous ferric chloride as oxidant.[2] The physiochemical properties of these hydrogels make them suitable as scleral buckling implants for retinal detachment surgery. The base crosslinked hydrogels were prepared by terpolymerisation of 2-hydroxyethyl acrylate, methyl acrylate and ethylene diacrylate.[3] These were also evaluated for their physico-chemical properties,[4] miscibility with phenoxy resins,[5] reactivity with acrylonitrile[6] and as moisture barrier sheets.[7]

4.1.1 Reactivity ratio determination for poly(MA-*co*-HEA) system

The reactivity ratios of MA and HEA were determined from the monomer feed ratios and the copolymer composition, by Finemann-Ross (FR), Kelen-Tudos (KT), extended Kelen-Tudos (ext. KT) and Mao-Huglin (MH) methods.[8-11] The parameters of FR and KT for the copolymers are presented in Table 4.1 and that of extended KT is given in Table 4.2. The reactivity ratios of MA and HEA are denoted as r_{MA} (or r_1) and r_{HEA} (or r_2), respectively, and the values obtained from various methods are presented in Table 4.4.

Table 4.1: FR and KT parameters for poly(MA-*co*-HEA) system

Copolymer Code	$F=M_1/M_2$	$f=m_1/m_2$	$H=F^2/f$	$G=F(f-1)/f$	$\xi=H/(\alpha+H)$	$\eta=G/(\alpha+H)$
MA-HEA -1	0.1111	0.0763	0.1618	-1.3447	0.1284	-1.0671
MA-HEA -2	0.1765	0.1280	0.2434	-1.2026	0.1815	-0.8963
MA-HEA-3	0.2501	0.1715	0.3646	-1.2081	0.2493	-0.8258
MA-HEA-4	0.3334	0.2434	0.4567	-1.0365	0.2938	-0.6665
MA-HEA-5	0.5386	0.4237	0.6846	-0.7325	0.3840	-0.4108
MA-HEA-6	0.6668	0.5154	0.8627	-0.6270	0.4400	-0.3197
MA-HEA-7	0.8183	0.7546	0.8874	-0.2661	0.4470	-0.1340
MA-HEA-8	1.0002	0.9893	1.0112	-0.0108	0.4794	-0.0051
MA-HEA-9	1.2225	1.4642	1.0207	0.3875	0.4818	0.1829
MA-HEA-10	2.3338	2.1971	2.4790	1.2716	0.6930	0.3555
MA-HEA-11	9.0018	10.8659	7.4575	8.1734	0.8717	0.9553

Table 4.2: Extended Kelen-Tudos parameters for poly(MA-*co*-HEA) system

Copolymer Code	ζ_1	ζ_2	Z	H	G	ξ	η
MA-HEA -1	0.4272	0.6220	0.5728	0.2326	-1.6124	0.1544	-1.0701
MA-HEA -2	0.4525	0.6241	0.6157	0.3376	-1.4162	0.2094	-0.8787
MA-HEA-3	0.3692	0.5384	0.5961	0.4826	-1.3899	0.2747	-0.7912
MA-HEA-4	0.3234	0.4431	0.6676	0.5461	-1.1334	0.3000	-0.6226
MA-HEA-5	0.3576	0.4545	0.7301	0.7948	-0.7893	0.3842	-0.3815
MA-HEA-6	0.2879	0.3725	0.7286	0.9708	-0.6651	0.4324	-0.2963
MA-HEA-7	0.1461	0.1585	0.9156	0.9001	-0.2680	0.4140	-0.1232
MA-HEA-8	0.1338	0.1353	0.9883	1.0129	-0.0108	0.4429	-0.0047
MA-HEA-9	0.1711	0.1429	1.2174	0.9880	0.3813	0.4367	0.1685
MA-HEA-10	0.1219	0.1295	0.9375	2.5001	1.2770	0.6624	0.3383
MA-HEA-11	0.2967	0.2458	1.2477	6.9800	7.9074	0.8456	0.9580

The graphical copolymerisation plots of FR, KT and extended KT are presented in Figures 4.1 (a-c). The plots are linear for all graphical methods, indicating that these follow conventional copolymerisation kinetics and that the reactivity of a polymer radical is determined only by the terminal monomer unit. As moderate conversions were noted for some copolymer compositions the kinetic data were analysed by extended KT and Mao-Huglin methods as well.

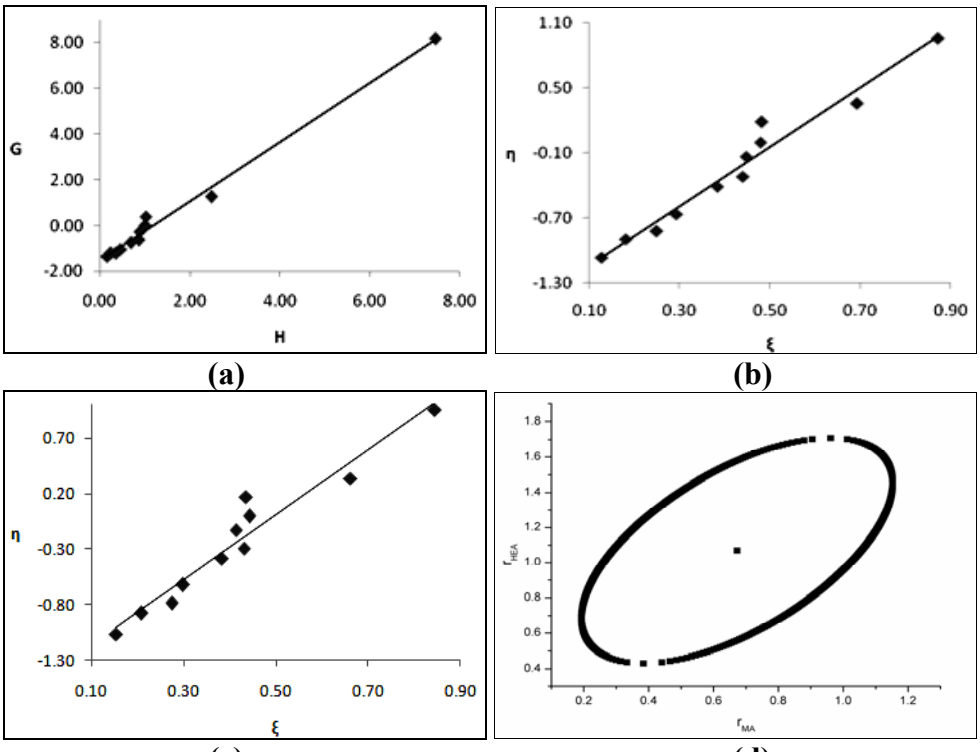

(a) **(b)**

(c) **(d)**

Figure 4.1: (a) FR, (b) KT, (c) Ext. KT plots for poly(MA-*co*-HEA) system and (d) 95% Joint confidence interval calculated by MH method

The 95 % joint confidence limit of the reactivity ratio values, calculated by Mao-Huglin method, is plotted in Figure 4.1 (d). Its equation is,

$4.4507(r_1-0.6729)^2 - 4.0220\ (r_1-0.6729)\ (r_2-1.0695) + 2.5113(r_2- 1.0695)^2=0.6542$

Table 4.3: Structural data for poly(MA-*co*-HEA)

Copolymer code	M_{MA}-M_{MA}	M_{HEA}-M_{HEA}	M_{MA}-M_{HEA}	μ_{MA}	μ_{HEA}
MA-HEA -1	0.0101	0.8682	0.1217	1.15	16.27
MA-HEA -2	0.0238	0.7969	0.1793	1.25	10.61
MA-HEA-3	0.0375	0.7448	0.2177	1.35	7.78
MA-HEA-4	0.0624	0.6710	0.2666	1.46	6.09
MA-HEA-5	0.1277	0.5325	0.3397	1.75	4.15
MA-HEA-6	0.1598	0.4796	0.3606	1.93	3.54
MA-HEA-7	0.2361	0.3759	0.3880	2.14	3.07
MA-HEA-8	0.3001	0.3055	0.3944	2.39	2.70
MA-HEA-9	0.4028	0.2144	0.3828	2.70	2.39
MA-HEA-10	0.5133	0.1389	0.3478	4.24	1.73
MA-HEA-11	0.8453	0.0138	0.1409	13.51	1.19

In order to gain further information related to the copolymer structure, the statistical distribution of the sequences of two monomers (dyad) were calculated using method due to Igarashi[12] and mean sequence lengths were estimated as well. The data is presented in Table 4.3, and the variation of the dyad fractions with the mole fraction of BA in the copolymers is displayed in Figure 4.2.

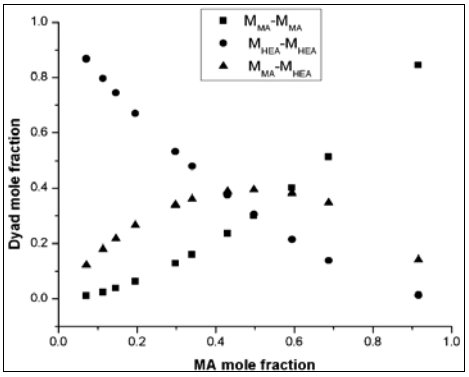

Figure 4.2: Dyad monomer sequence fractions verses the MA mole fractions for the copolymers.

Table 4.4: Reactivity ratios of MA and HEA computed by different models

Method	r_{MA}	r_{HEA}
Finemann-Ross	1.2933	1.5272
Kelen-Tudos	1.3241	1.5542
Extended Kelen-Tudos	1.4670	1.8552
Mao-Huglin	1.4753	1.8495
Average	1.3898	1.6965

The reactivity ratio estimations are presented in Table 4.4. The r_{MA} and r_{HEA} values obtained depend on the method used. The differential and integral forms yield values which are similar within themselves but differ from each other. The average value of r_{MA} is equal to 1.3898 and that of r_{HEA} is equal to 1.6965, which indicates the higher incorporation of HEA units in the copolymer than that in the feed. The product of the reactivity ratios of two monomers $r_{MA} \bullet r_{HEA}$ values are greater than 1, suggesting that there is a marginal tendency towards the formation of block copolymers.

4.1.2 Thermal analysis of poly(MA-*co*-HEA) system

The glass transition temperatures (T_g) the three copolymer compositions poly(MA_{25}-HEA_{75}), poly(MA_{50}-HEA_{50}), and poly(MA_{75}-HEA_{25}) were investigated using DSC.

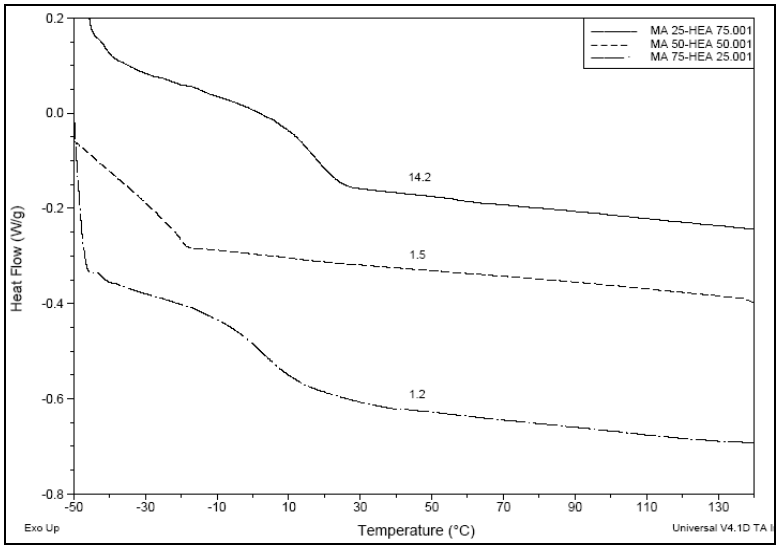

Figure 4.3: DSC thermograms of poly(MA_{25}-HEA_{75}), poly(MA_{50}-HEA_{50}), and poly(MA_{75}-HEA_{25}).

The differential scanning calorimetry (DSC) thermograms of copolymers, with T_g values, are presented in Figure 4.3. The T_g of homopolymers of methyl acrylate (MA) and 2-hydroxyethyl acrylate (HEA) are 10°C and 2°C, respectively. The data presented here show that glass transition temperature (T_g) of copolymers (14.2, 1.5 and 1.2°C) differ from that of the homopolymers and are dependent on composition.

4.2 Poly(butyl acrylate-*co*-2-hydroxyethyl acrylate) System

Polymers comprised of 2-hydroxylethyl acrylate (HEA) and butyl acrylate (BA) find application as adhesive tapes for semiconducting coatings.[13] The adhesive compositions have good durability and curability. The polymers also find application

as polarising plates, in liquid crystal displays[14] and are peelable.[15] These monomers have been copolymerised with styrene,[16,17] crosslinked with diisocyanate.[18]

4.2.1 Reactivity ratio determination for poly(BA-*co*-HEA) system

The reactivity ratios of BA and HEA were determined by Finemann-Ross (FR), Kelen-Tudos (KT), extended Kelen-Tudos (Ext. KT) and Mao-Huglin (MH) methods. The parameters of FR and KT for the copolymers are presented in Table 4.5 and that of Extended KT is shown in Table 4.6.

Table 4.5: FR and KT parameters for poly(BA-*co*-HEA) system

Copolymer Code	$F=M_1/M_2$	$f=m_1/m_2$	$H=F^2/f$	$G=F(f-1)/f$	$\xi=H/(\alpha+H)$	$\eta=G/(\alpha+H)$
BA-HEA -1	0.1111	0.0538	0.2295	-1.9548	0.1096	-0.9331
BA-HEA -2	0.1765	0.0987	0.3154	-1.6107	0.1446	-0.7386
BA-HEA-3	0.2500	0.1521	0.4110	-1.3939	0.1805	-0.6123
BA-HEA-4	0.3333	0.2157	0.5152	-1.2122	0.2164	-0.5092
BA-HEA-5	0.4286	0.2727	0.6734	-1.1428	0.2653	-0.4501
BA-HEA-6	0.5385	0.3493	0.8301	-1.0031	0.3080	-0.3722
BA-HEA-7	0.6667	0.4255	1.0445	-0.9001	0.3590	-0.3093
BA-HEA-8	0.8182	0.5652	1.1845	-0.6295	0.3884	-0.2064
BA-HEA-9	1.0000	0.7095	1.4094	-0.4094	0.4304	-0.1250
BA-HEA-10	1.2222	0.7989	1.8700	-0.3077	0.5006	-0.0824
BA-HEA-11	1.5000	0.8406	2.6765	-0.2843	0.5893	-0.0626
BA-HEA-12	1.8571	1.1860	2.9080	0.2913	0.6092	0.0610
BA-HEA-13	3.0000	1.6417	5.4822	1.1726	0.7461	0.1596
BA-HEA-14	9.0000	5.3427	15.1609	7.3155	0.8904	0.4297

Table 4.6: Extended Kelen-Tudos parameters for poly(BA-*co*-HEA) system

Copolymer Code	ζ_1	ζ_2	Z	H	G	ξ	η
BA-HEA -1	0.2636	0.5445	0.3890	0.3553	-2.4321	0.1216	-0.8324
BA-HEA -2	0.3416	0.6105	0.4433	0.5025	-2.0332	0.1637	-0.6625
BA-HEA-3	0.3235	0.5318	0.5150	0.5733	-1.6463	0.1826	-0.5243
BA-HEA-4	0.4021	0.6214	0.5295	0.7693	-1.4813	0.2306	-0.4441
BA-HEA-5	0.3741	0.5879	0.5286	0.9760	-1.3757	0.2755	-0.3884
BA-HEA-6	0.3006	0.4634	0.5744	1.0588	-1.1329	0.2921	-0.3125
BA-HEA-7	0.2888	0.4525	0.5658	1.3293	-1.0154	0.3412	-0.2606
BA-HEA-8	0.3037	0.4397	0.6250	1.4471	-0.6958	0.3605	-0.1734
BA-HEA-9	0.1605	0.2263	0.6822	1.5246	-0.4258	0.3727	-0.1041
BA-HEA-10	0.1989	0.3043	0.6112	2.1386	-0.3291	0.4545	-0.0699
BA-HEA-11	0.1521	0.2714	0.5211	3.0959	-0.3058	0.5467	-0.0540
BA-HEA-12	0.1043	0.1633	0.6178	3.1079	0.3012	0.5477	0.0531
BA-HEA-13	0.1605	0.2933	0.5040	6.4638	1.2733	0.7158	0.1410
BA-HEA-14	0.2195	0.3697	0.5368	18.5391	8.0895	0.8784	0.3833

The graphical copolymerisation plots of FR, KT and Extended KT are presented in Figures 4.4 (a-c). The plots are not linear for all graphical methods,

indicating that these may not follow conventional copolymerisation kinetics. The reactivity ratios of BA and HEA are denoted as r_{MA} (or r_1) and r_{HEA} (or r_2), respectively and the values obtained from various methods are presented in Table 4.8.

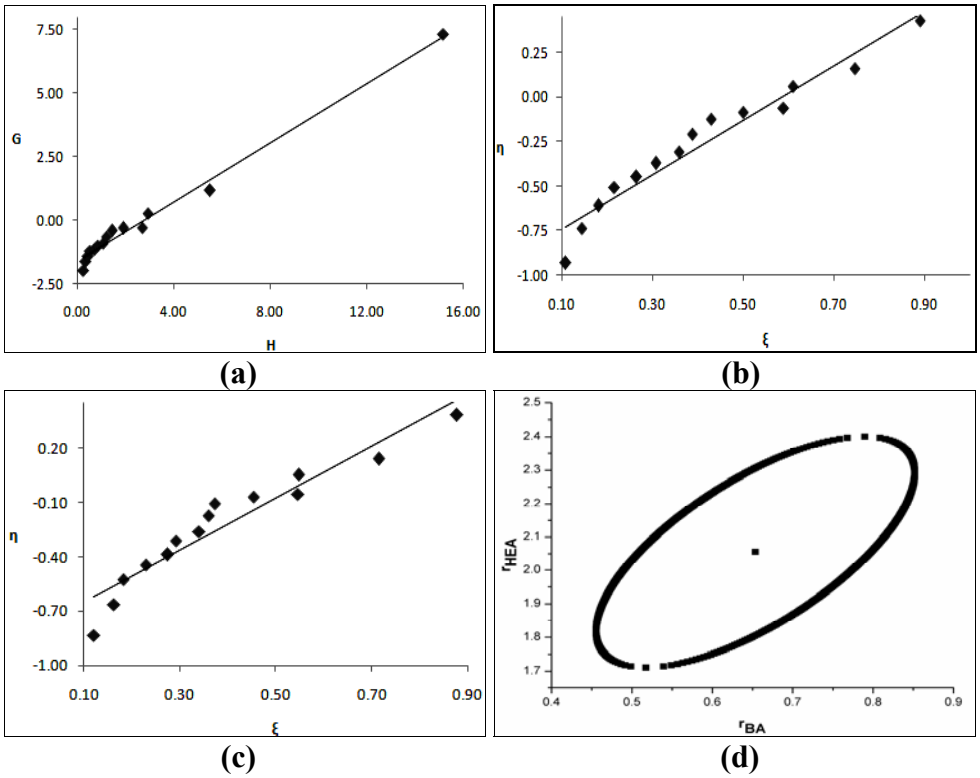

Figure 4.4: (a) FR, (b) KT, (c) Ext. KT plots for the poly(BA-*co*-HEA) system and (d) 95% Joint confidence interval calculated by MH method

The 95 % joint confidence limit of the reactivity ratio, as calculated by Mao-Huglin method, are plotted in Fig. 4.4 (d). Its equation is,

$2.9314\ (r1 - 0.6536)^2 - 2.3145(r1 - 0.6536)\ (r2 - 2.0556) + 0.9688(r2 - 2.0556)^2 = 0.0608$

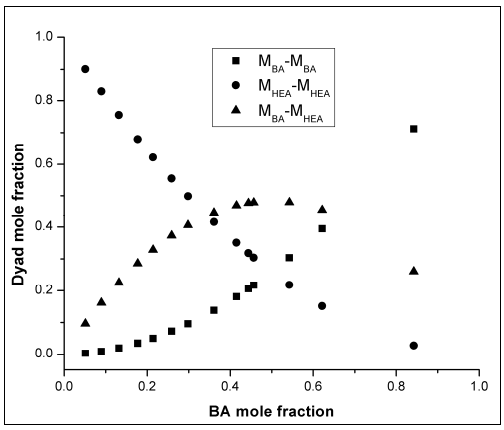

Figure 4.5: Dyad monomer sequence fractions verses the BA mole fractions for the copolymers.

The statistical distribution of the sequences of two monomers (dyad) M_{BA}-M_{BA}, M_{HEA}-M_{HEA} and M_{BA}-M_{HEA} were calculated by using the Igarashi method. Mean sequence lengths μ_{BA} and μ_{HEA} were also calculated. The data presented in Table 4.7, and the variation of the dyad fractions with the BA mole fraction is shown in Fig.4.5.

Table 4.7: Structural data for poly(BA-*co*-HEA)

Copolymer Code	M_{BA}-M_{BA}	M_{HEA}-M_{HEA}	M_{BA}-M_{HEA}	μ_{BA}	μ_{HEA}
BA-HEA -1	0.0030	0.9009	0.0962	1.0698	17.5456
BA-HEA -2	0.0091	0.8293	0.1616	1.1108	11.4176
BA-HEA-3	0.0194	0.7554	0.2252	1.1570	8.3536
BA-HEA-4	0.0346	0.6798	0.2856	1.2094	6.5152
BA-HEA-5	0.0501	0.6215	0.3284	1.2692	5.2896
BA-HEA-6	0.0724	0.5546	0.3730	1.3382	4.4142
BA-HEA-7	0.0955	0.4985	0.4060	1.4187	3.7576
BA-HEA-8	0.1381	0.4159	0.4460	1.5139	3.2469
BA-HEA-9	0.1808	0.3507	0.4686	1.6281	2.8384
BA-HEA-10	0.2060	0.3178	0.4762	1.7677	2.5041
BA-HEA-11	0.2174	0.3040	0.4785	1.9422	2.2256
BA-HEA-12	0.3032	0.2181	0.4787	2.1665	1.9899
BA-HEA-13	0.3942	0.1513	0.4545	2.8843	1.6128
BA-HEA-14	0.7122	0.0275	0.2604	6.6529	1.2043

Table 4.8: Reactivity ratios of BA and HEA computed by different models

Method	r_{BA}	r_{HEA}
Finemann-Ross	0.5821	1.5914
Kelen-Tudos	0.6382	1.6732
Extended Kelen-Tudos	0.6384	2.0332
Mao-Huglin	0.6536	2.0556
Average	0.6281	1.8384

The r_{BA} values obtained by all methods are similar but that obtained for r_{HEA} differ for the differential and integral forms. The value of r_{BA} is equal to 0.6281 and that of r_{HEA} is equal to 1.8384, which indicates the higher incorporation of HEA units in the copolymer than in feed. The product of the reactivity ratios of two monomers $r_{BA} \bullet r_{HEA}$ values again exceed 1, suggesting that there is tendency towards the formation of block copolymer.

4.2.2 Thermal analysis of the poly(BA-*co*-HEA)

The glass transition temperature (T_g) of poly(BA_{25}-HEA_{75}), poly(BA_{50}-HEA_{50}), and poly(BA_{75}-HEA_{25}) were estimated by DSC and data (-14.7, -15.4 and -14.2°C) is represented in Figure 4.6. The T_g of homopolymer of butyl acrylate (BA) and 2-hydroxyethyl acrylate (HEA) are known to be -50°C and 2°C, respectively. The

results shows that glass transition temperature (T_g) of copolymers are nearly invariant with respect to copolymer composition and differ considerably from those of parent homopolymers.

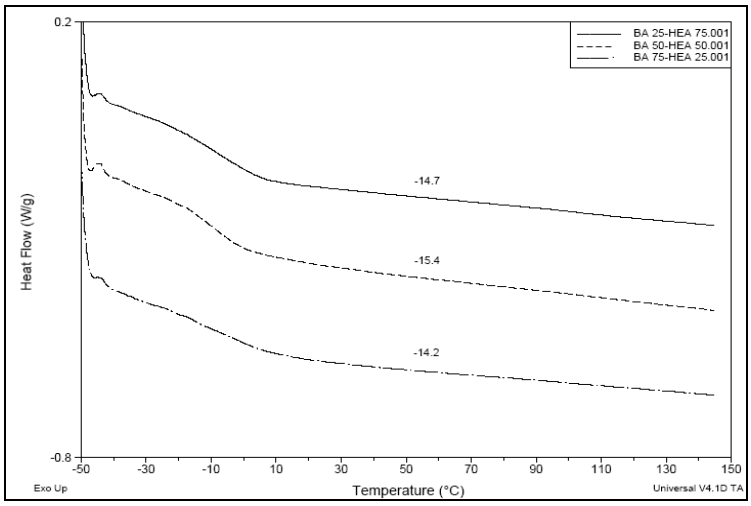

Figure 4.6: DSC thermograms of poly(BA_{25}-HEA_{75}), poly(BA_{50}-HEA_{50}), and poly(BA_{75}-HEA_{25}).

4.3 Poly(2-ethylhexyl acrylate-*co*-2-hydroxyethyl acrylate) System

The poly(2-ethylhexyl acrylate-*co*-2-hydroxyethyl acrylate) [poly(2EHA-*co*-HEA)] system is commercially pertinent. Copolymers based on 2-ethyl hexyl acrylate and 2-hydroxyethyl acrylate monomers are used as pressure sensitive adhesive sheets in electronic components.[19] These are radiation curable and have good coatability, adhesion reliability, repeelability and are antifouling.[20,21] Coumarin functionalised poly(2-ethyl hexyl acrylate-*co*-hydroxyethyl acrylate) are used as light deactivatable pressure sensitive adhesives (PSA) via photodimerization.[22] These polymers are also used in storage stable transdermal preparations containing drugs.[23]

4.3.1 Reactivity ratio determination for poly(EHA-*co*-HEA) system

The kinetic parameter, monomer reactivity ratios were determined by Finemann-Ross (FR), Kelen-Tudos (KT), extended Kelen-Tudos (Ext. KT) and Mao-Huglin (MH) methods. The parameters of FR and KT for the copolymers are presented in Table 4.9 and that of Ext. KT is shown in Table 4.10. The graphical copolymerisation plots of FR, KT and extended KT are presented in Figures 4.7 (a-c). The plots are some what linear for graphical methods, indicating that these follow conventional copolymerisation kinetics. The reactivity ratios of EHA and HEA are denoted as r_{EHA} (or r_1) and r_{HEA} (or r_2) respectively and the values obtained from various methods are presented in Table 4.12.

Table 4.9: FR and KT parameters for Poly(EHA-*co*-HEA) system

Copolymer Code	$F=M_1/M_2$	$f=m_1/m_2$	$H=F^2/f$	$G=F(f-1)/f$	$\xi=H/(\alpha+H)$	$\eta=G/(\alpha+H)$
EHA-HEA -1	0.1765	0.1552	0.2006	-0.9604	0.1112	-0.5321
EHA-HEA -2	0.2500	0.2290	0.2729	-0.8418	0.1454	-0.4484
EHA-HEA-3	0.4286	0.3973	0.4623	-0.6502	0.2237	-0.3146
EHA-HEA-4	0.5385	0.4473	0.6482	-0.6654	0.2878	-0.2954
EHA-HEA-5	0.6667	0.4958	0.8964	-0.6779	0.3584	-0.2711
EHA-HEA-6	1.2222	0.9195	1.6246	-0.1070	0.5031	-0.0331
EHA-HEA-7	1.5000	1.1446	1.9658	0.1894	0.5506	0.0531
EHA-HEA-8	1.8571	1.5057	2.2906	0.6237	0.5881	0.1601
EHA-HEA-9	3.0000	2.4478	3.6767	1.7744	0.6962	0.3360
EHA-HEA-10	9.0000	6.3122	12.8323	7.5742	0.8889	0.5246

Table 4.10: Extended Kelen-Tudos parameters for Poly(EHA-*co*-HEA) system

Copolymer Code	ζ_1	ζ_2	Z	H	G	ξ	η
EHA-HEA -1	0.7778	0.8843	0.6974	0.3191	-1.2113	0.0936	-0.3551
EHA-HEA -2	0.8199	0.8952	0.7601	0.3964	-1.0144	0.1136	-0.2908
EHA-HEA-3	0.8666	0.9349	0.7374	0.7307	-0.8174	0.1911	-0.2138
EHA-HEA-4	0.8028	0.9665	0.4782	1.9563	-1.1560	0.3875	-0.2290
EHA-HEA-5	0.6650	0.8942	0.4870	2.0910	-1.0354	0.4034	-0.1998
EHA-HEA-6	0.6631	0.8814	0.5103	3.5312	-0.1578	0.5332	-0.0238
EHA-HEA-7	0.6647	0.8711	0.5334	4.0233	0.2710	0.5654	0.0381
EHA-HEA-8	0.6634	0.8182	0.6386	3.6923	0.7919	0.5442	0.1167
EHA-HEA-9	0.6410	0.7856	0.6653	5.5308	2.1763	0.6414	0.2524
EHA-HEA-10	0.6124	0.8732	0.4590	29.9612	11.5735	0.9065	0.3501

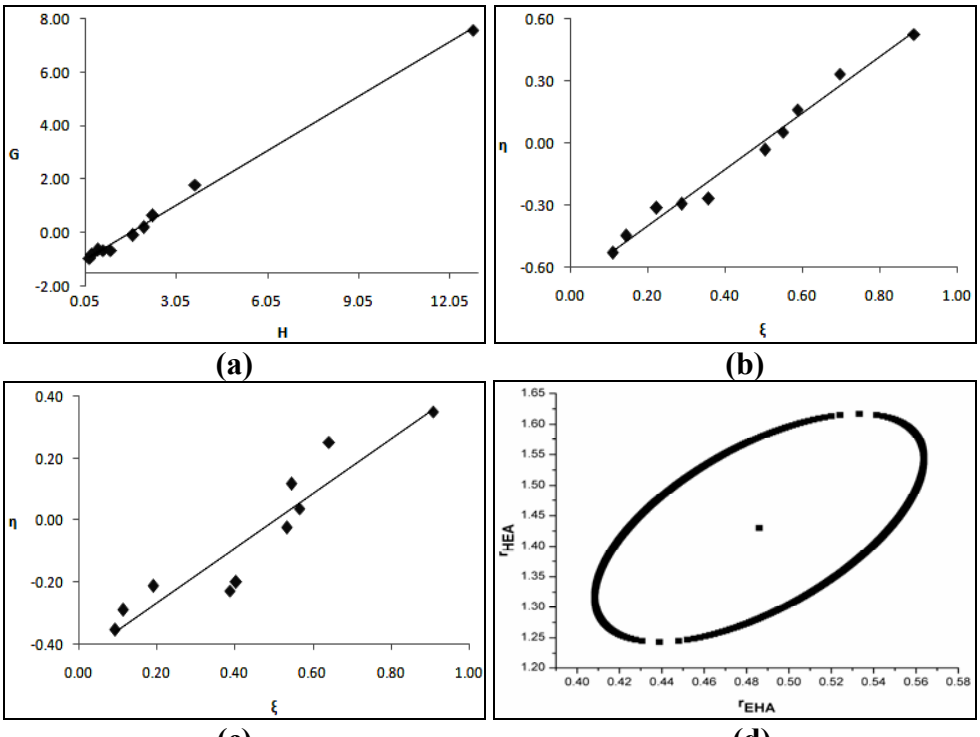

Figure 4.7: (a) FR, (b) KT, (c) Ext. KT plots for the Poly(EHA-*co*-HEA) system and (d) 95% Joint confidence interval calculated by MH method

The 95 % joint confidence limit of reactivity ratios are plotted in Figure 4.7 (d). Its equation is,

$2.5008(r_1 - 0.4860)^2 - 1.2631(r_1 - 0.4860)(r_2 - 1.4300) + 0.4319(r_2 - 1.4300)^2 = 0.0095$

In order to gain further information related to the copolymer structure, the statistical distribution of the sequences of two monomers (dyad) M_{EHA}-M_{EHA}, M_{HEA}-M_{HEA} and M_{EHA}-M_{HEA} were calculated as described earlier. Mean sequence lengths μ_{EHA} and μ_{HEA} were also calculated. The data is presented in Table 4.11, and the variation of the dyad fractions with the BA mole fraction in the copolymers is displayed in Figure 4.8.

Table 4.11: Structural data for Poly(EHA-*co*-HEA) system

Copolymer Code	M_{EHA}-M_{EHA}	M_{HEA}-M_{HEA}	M_{EHA}-M_{HEA}	μ_{EHA}	μ_{HEA}
EHA-HEA -1	0.0138	0.7451	0.2411	1.1013	8.0029
EHA-HEA -2	0.0274	0.6547	0.3179	1.1435	5.9432
EHA-HEA-3	0.0671	0.4985	0.4344	1.2460	3.8835
EHA-HEA-4	0.0803	0.4622	0.4575	1.3091	3.2951
EHA-HEA-5	0.0934	0.4305	0.4761	1.3827	2.8537
EHA-HEA-6	0.2082	0.2501	0.5418	1.7017	2.0111
EHA-HEA-7	0.2637	0.1962	0.5401	1.8612	1.8239
EHA-HEA-8	0.3415	0.1397	0.5187	2.0662	1.6654
EHA-HEA-9	0.4900	0.0701	0.4399	2.7223	1.4119
EHA-HEA-10	0.7408	0.0143	0.2448	6.1669	1.1373

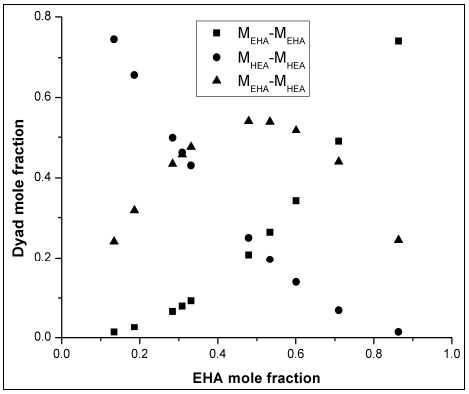

Figure 4.8: Dyad monomer sequence fractions verses the EHA mole fractions for the copolymers.

Table 4.12: Reactivity ratios of EHA and HEA computed by different models

Method	r_{EHA}	r_{HEA}
Finemann-Ross	0.6792	1.0623
Kelen-Tudos	0.6894	1.0846
Extended Kelen-Tudos	0.4424	1.3667
Mao-Huglin	0.4844	1.4299
Average	0.5741	1.2359

The values of r_{EHA} were similar but r_{HEA} varied with the method, and indicated the higher incorporation of HEA units in the copolymer than that added in the feed. In this system too, the product of the reactivity ratios of two monomers $r_{MA} \bullet r_{HEA}$ values is less than 1, indicating tendency to form random copolymer.

4.3.2 Thermal analysis of poly(EHA-*co*-HEA)

The glass transition temperature (T_g) of the three copolymer compositions such as poly(EHA_{25}-HEA_{75}), poly(EHA_{50}-HEA_{50}), and poly(EHA_{75}-HEA_{25}) were investigated by using DSC and T_g values data is presented in Figure 4.9.

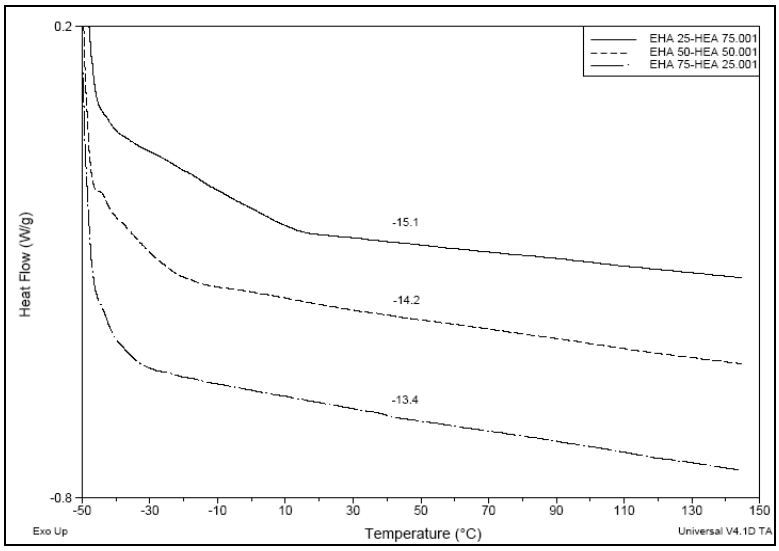

Figure 4.9: DSC thermograms of poly(EHA_{25}-HEA_{75}), poly(EHA_{50}-HEA_{50}), and poly(EHA_{75}-HEA_{25}).

The T_g of poly(EHA_{25}-HEA_{75}), poly(EHA_{50}-HEA_{50}), and poly(EHA_{75}-HEA_{25}) are quite low, -15.1, -14.2 and -13.4 ^oC respectively**.** The T_g of parent homopolymers of EHA and HEA are 12 ºC and 2 ºC. These copolymers are elastomers and meet the primary criteria required for applications as flexible intraocular lense.

4.4 Poly(methyl methacrylate-*co*-hydroxyethyl acrylate) System

Poly(methyl methacrylate-*co*-hydroxyethyl acrylate) [Poly(MMA-*co*-HEA)] have been studied in preparation of nano-silica composites,[24] waterborne varnish,[25,26] and liquid crystal displays.[27] The thermal degradation of poly(2-hydroxyethyl acrylate)-*co*-methyl methacrylate/SiO_2 nanohybrids has been studied.[28] The polymers are found to be self-reinforcing hydrogels.[29] This system has been studied for the kinetic estimation of monomer reactivity ratios.[30]

4.4.1 Reactivity ratio determination for poly(MMA-*co*-HEA) system

The reactivity ratios of MMA and HEA were determined by Finemann-Ross (FR), Kelen-Tudos (KT), Extended Kelen-Tudos (Ext. KT) and Mao-Huglin (MH) methods. These are presented in Table 4.13 and Table 4.14, respectively. The graphical copolymerisation plots of FR, KT and Ext. KT are presented in Figures 4.10 (a-c). The plots are generally linear for all graphical methods, indicating that these follow conventional copolymerisation kinetics. The reactivity ratios of MMA and HEA are denoted as r_{MMA} (or r_1) and r_{HEA} (or r_2) resp. and the values are presented in Table 4.16.

Table 4.13: FR and KT parameters for poly(MMA-*co*-HEA) system

Copolymer Code	$F=M_1/M_2$	$f=m_1/m_2$	$H=F^2/f$	$G=F(f-1)/f$	$\xi=H/(\alpha+H)$	$\eta=G/(\alpha+H)$
MMA-HEA -1	0.1111	0.1122	0.1100	-0.8789	0.0561	-0.4482
MMA-HEA -2	0.1765	0.1436	0.2169	-1.0527	0.1049	-0.5091
MMA-HEA-3	0.2500	0.2365	0.2642	-0.8069	0.1249	-0.3815
MMA-HEA-4	0.3333	0.2695	0.4123	-0.9035	0.1822	-0.3992
MMA-HEA-5	0.4286	0.3082	0.5959	-0.9618	0.2435	-0.3931
MMA-HEA-6	0.5385	0.4565	0.6352	-0.6412	0.2555	-0.2579
MMA-HEA-7	0.6667	0.4805	0.9249	-0.7207	0.3332	-0.2596
MMA-HEA-8	0.8182	0.4920	1.3607	-0.8449	0.4237	-0.2631
MMA-HEA-9	1.0000	0.6077	1.6456	-0.6456	0.4706	-0.1846
MMA-HEA-10	1.2222	0.7347	2.0334	-0.4415	0.5235	-0.1137
MMA-HEA-11	1.5000	0.8158	2.7581	-0.3387	0.5984	-0.0735
MMA-HEA-12	1.8571	0.9613	3.5877	-0.0747	0.6597	-0.0137
MMA-HEA-13	4.0000	1.7223	9.2899	1.6775	0.8339	0.1506
MMA-HEA-14	9.0000	2.6008	31.1442	5.5395	0.9439	0.1679

Table 4.14: Extended Kelen-Tudos parameters for poly(MMA-*co*-HEA) system

Copolymer Code	ζ_1	ζ_2	Z	H	G	ξ	η
MMA-HEA -1	0.4659	0.4612	1.0140	0.1091	-0.8755	0.0317	-0.2539
MMA-HEA -2	0.3545	0.4358	0.7649	0.2454	-1.1197	0.0685	-0.3124
MMA-HEA-3	0.4989	0.5273	0.9222	0.2782	-0.8279	0.0769	-0.2289
MMA-HEA-4	0.2927	0.3620	0.7705	0.4540	-0.9481	0.1197	-0.2500
MMA-HEA-5	0.2397	0.3333	0.6760	0.6745	-1.0233	0.1681	-0.2550
MMA-HEA-6	0.2097	0.2474	0.8281	0.6656	-0.6564	0.1662	-0.1639
MMA-HEA-7	0.2552	0.3541	0.6741	1.0573	-0.7706	0.2405	-0.1753
MMA-HEA-8	0.1849	0.3074	0.5564	1.5891	-0.9130	0.3225	-0.1853
MMA-HEA-9	0.1908	0.3140	0.5618	1.9255	-0.6983	0.3658	-0.1327
MMA-HEA-10	0.2464	0.4099	0.5363	2.5544	-0.4948	0.4335	-0.0840
MMA-HEA-11	0.2413	0.4437	0.4709	3.6788	-0.3912	0.5242	-0.0557
MMA-HEA-12	0.3093	0.5976	0.4066	5.8153	-0.0951	0.6353	-0.0104
MMA-HEA-13	0.2267	0.5265	0.3439	14.5643	2.1004	0.8135	0.1173
MMA-HEA-14	0.2351	0.8136	0.1596	102.1662	10.0332	0.9684	0.0951

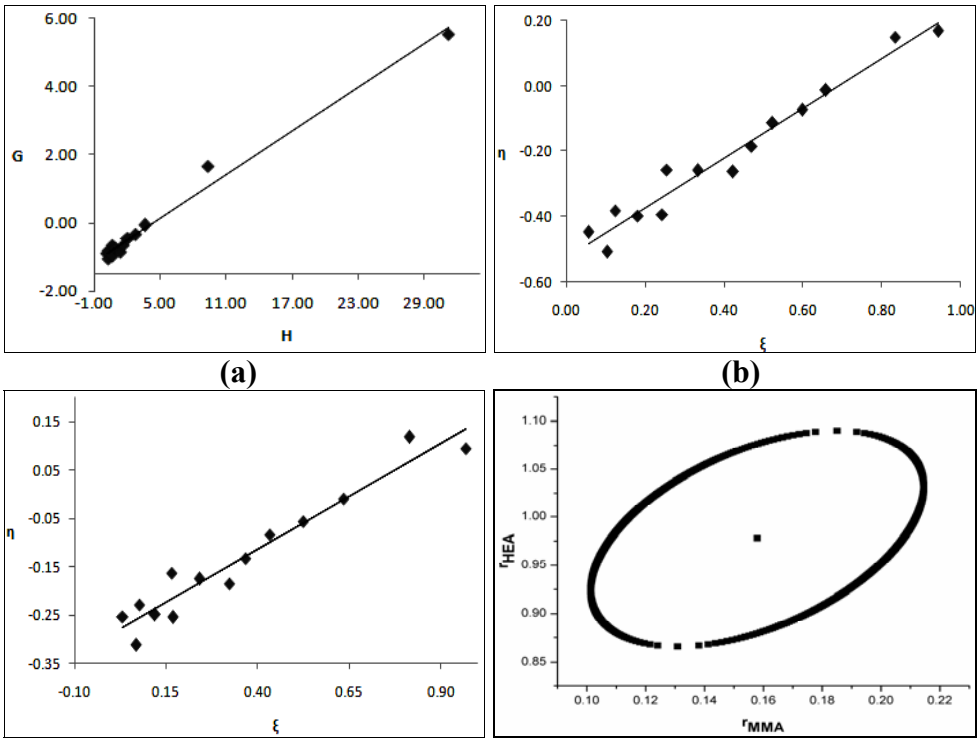

Figure 4.10: (a) FR, (b) KT, (c) Ext. KT plots for the poly(MMA-*co*-HEA) system and (d) 95% Joint confidence interval calculated by MH method

The 95 % joint confidence limit of the reactivity ratio calculated using Mao-Huglin method is presented in Figure 4.10 (d). Its equation is,

$3.0380(r_1 - 0.1579)^2 - 1.4662(r_1 - 0.1579)(r_2 - 0.9779) + 0.7709(r_2 - 0.9779)^2 = 0.0075$

The statistical distribution of the sequences of two monomers (dyad) M_{MMA}-M_{MMA}, M_{HEA}-M_{HEA} and M_{MMA}-M_{HEA} and mean sequence lengths μ_{MMA} and μ_{HEA} were calculated. The data is presented in Table 4.15, and the variation of the dyad fractions with the BA mole fraction in the copolymers is displayed in Figure 4.11.

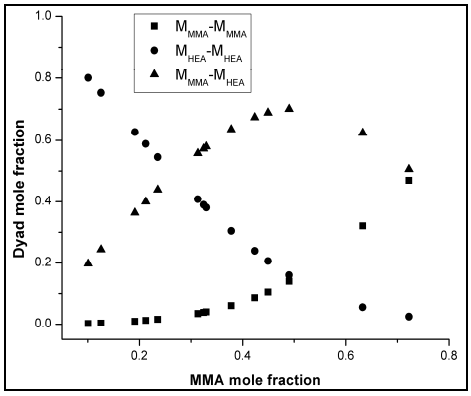

Figure 4.11: Dyad monomer sequence fractions verses the MMA mole fractions for the copolymers.

Table 4.15: Structural data for poly(MMA-*co*-HEA) system

Copolymer Code	M_{MMA}-M_{MMA}	M_{HEA}-M_{HEA}	M_{MMA}-M_{MMA}	μ_{MMA}	μ_{HEA}
MMA-HEA -1	0.0022	0.8004	0.1974	1.0211	9.6175
MMA-HEA -2	0.0036	0.7525	0.2439	1.0335	6.4258
MMA-HEA-3	0.0096	0.6270	0.3634	1.0475	4.8300
MMA-HEA-4	0.0124	0.5878	0.3998	1.0633	3.8725
MMA-HEA-5	0.0161	0.5449	0.4391	1.0814	3.2342
MMA-HEA-6	0.0346	0.4078	0.5575	1.1023	2.7782
MMA-HEA-7	0.0383	0.3892	0.5725	1.1266	2.4363
MMA-HEA-8	0.0401	0.3806	0.5793	1.1554	2.1703
MMA-HEA-9	0.0603	0.3043	0.6354	1.1899	1.9575
MMA-HEA-10	0.0864	0.2393	0.6743	1.2321	1.7834
MMA-HEA-11	0.1047	0.2062	0.6891	1.2849	1.6383
MMA-HEA-12	0.1398	0.1596	0.7006	1.3527	1.5156
MMA-HEA-13	0.3206	0.0552	0.6242	1.7596	1.2394
MMA-HEA-14	0.4694	0.0248	0.5059	2.7091	1.1064

Table 4.16: Reactivity ratios of MMA and HEA computed by different models

Method	r_{MMA}	r_{HEA}
Finemann-Ross	0.2123	0.9141
Kelen-Tudos	0.2355	0.9699
Extended Kelen-Tudos	0.1542	0.9682
Mao-Huglin	0.1579	0.9779
Average	0.1899	0.9575

The value of r_{MMA} is 0.1899 and that of r_{HEA} is 0.9575. This indicates that HEA had greater tendency to enter the copolymer chain. The product of the reactivity ratios of two monomers $r_{MMA} \bullet r_{HEA}$ value is less than 1, suggesting that there is tendency to form random copolymers. Thus, interestingly, this system gives rise to azeotropic copolymer at a particular feed composition of the monomers. This was calculated using the equation 4.1. Here, $r_2 = r_{HEA}$ and $r_1 = r_{MMA}$.

$$N_1 = \frac{(1 - r_2)}{(2 - r_1 - r_2)} \qquad 4.1$$

The azeotropic composition will be an excellent hydrogel since the hydrophobic (MMA) component is 0.0498.

4.4.2 Thermal analysis of the poly(MMA-*co*-HEA)

The glass transition temperatures (T_g) of three copolymer compositions poly(EHA_{25}-HEA_{75}), poly(EHA_{50}-HEA_{50}), and poly(EHA_{75}-HEA_{25}) were investigated using DSC. The DSC thermograms and T_g values of copolymers are given in Figure 4.12.

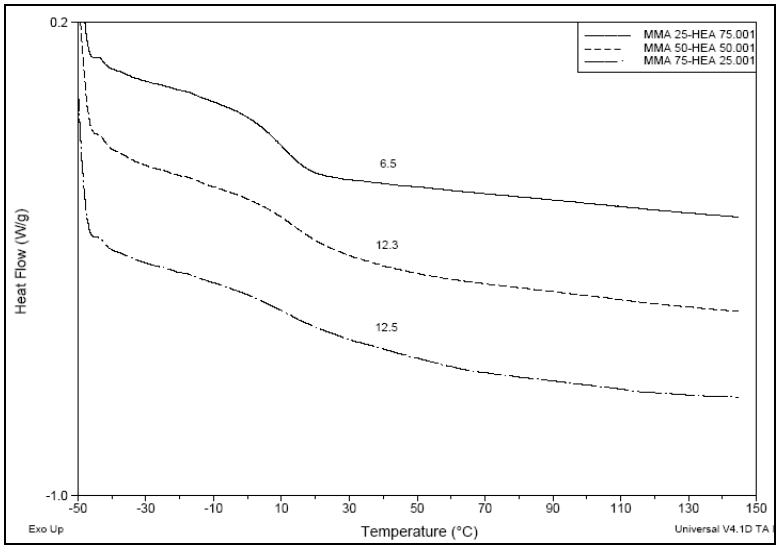

Figure 4.12: DSC thermograms of poly(MMA_{25}-HEA_{75}), poly(MMA_{50}-HEA_{50}), and poly(MMA_{75}-HEA_{25}).

The T_g values of poly(MMA_{25}-HEA_{75}), poly(MMA_{50}-HEA_{50}), and poly(MMA_{75}-HEA_{25}) were 6.5, 12.3 and 12.5 ^oC, respectively. The T_g values of respective homopolymers of MMA and HEA are 95ºC and 2ºC respectively. This copolymer system is ideally suited for evaluation as hydrogels.

4.5 Poly(2-ethylhexyl methacrylate-*co*-2-hydroxyethyl acrylate) System

This copolymer, Poly(2-ethylhexyl methacrylate-*co*-2-hydroxyethyl acrylate) [poly(EHMA-*co*-HEA)] has been evaluated as dispersant for encapsulating pigment,[31] thermosetting coatings[32,33] and for cationic electrodeposition.[34] The polymer is also used in multi-component composite coatings that provide improved durability, acid resistance, particularly for plastic automotive parts.[35]

4.5.1 Reactivity ratio determination for poly(EHMA-*co*-HEA) system

As indicated earlier, the reactivity ratios of MMA and HEA, determined by Finemann-Ross (FR), Kelen-Tudos (KT), Extended Kelen-Tudos (Ext. KT) and Mao-Huglin (MH) methods, are presented in Tables 4.17 and 4.18. The graphical copolymerisation plots of FR, KT and Extended KT are presented in Figures 4.13 (a-c). The plots are linear for all graphical methods, indicating that these follow conventional copolymerisation kinetics. The reactivity ratios of EHMA and HEA are denoted as r_{EHMA} (or r_1) and r_{HEA} (or r_2) respectively and the values obtained from various methods are presented in Table 4.20.

Table 4.17: FR and KT parameters for poly(EHMA-*co*-HEA) system

Copolymer Code	$F=M_1/M_2$	$f=m_1/m_2$	$H=F^2/f$	$G=F(f-1)/f$	$\xi=H/(\alpha+H)$	$\eta=G/(\alpha+H)$
EHMA-HEA -1	0.1111	0.0872	0.1416	-1.1636	0.1088	-0.8938
EHMA-HEA -2	0.1765	0.1725	0.1805	-0.8463	0.1346	-0.6312
EHMA-HEA-3	0.2500	0.2512	0.2488	-0.7454	0.1766	-0.5290
EHMA-HEA-4	0.3333	0.3355	0.3312	-0.6603	0.2221	-0.4428
EHMA-HEA-5	0.4286	0.4294	0.4277	-0.5695	0.2694	-0.3586
EHMA-HEA-6	0.5385	0.5349	0.5421	-0.4682	0.3184	-0.2751
EHMA-HEA-7	0.6667	0.6522	0.6815	-0.3556	0.3700	-0.1931
EHMA-HEA-8	0.8182	0.7980	0.8389	-0.2072	0.4196	-0.1036
EHMA-HEA-9	1.0000	0.9598	1.0419	-0.0419	0.4731	-0.0190
EHMA-HEA-10	1.2222	1.1597	1.2881	0.1684	0.5261	0.0688
EHMA-HEA-11	1.5000	1.4119	1.5936	0.4376	0.5787	0.1589
EHMA-HEA-12	1.8571	1.7580	1.9618	0.8008	0.6284	0.2565
EHMA-HEA-13	2.3333	2.1674	2.5120	1.2568	0.6841	0.3422
EHMA-HEA-14	3.0000	2.7861	3.2304	1.9232	0.7358	0.4380
EHMA-HEA-15	4.0000	3.7029	4.3210	2.9198	0.7883	0.5327
EHMA-HEA-16	5.6667	5.1644	6.2177	4.5694	0.8427	0.6193
EHMA-HEA-17	9.0000	8.5208	9.5062	7.9438	0.8912	0.7447

Table 4.18: Extended Kelen-Tudos parameters for poly(EHMA-*co*-HEA) system

Copolymer Code	ζ_1	ζ_2	Z	H	G	ξ	η
EHMA-HEA -1	0.4964	0.6328	0.6848	0.1859	-1.3331	0.1071	-0.7683
EHMA-HEA -2	0.8638	0.8834	0.9274	0.2006	-0.8922	0.1146	-0.5099
EHMA-HEA-3	0.9278	0.9235	1.0225	0.2402	-0.7323	0.1343	-0.4093
EHMA-HEA-4	0.8979	0.8922	1.0243	0.3197	-0.6488	0.1711	-0.3472
EHMA-HEA-5	0.9283	0.9264	1.0097	0.4212	-0.5651	0.2138	-0.2868
EHMA-HEA-6	0.9536	0.9599	0.9542	0.5875	-0.4874	0.2750	-0.2281
EHMA-HEA-7	0.9418	0.9628	0.8643	0.8731	-0.4025	0.3605	-0.1662
EHMA-HEA-8	0.9023	0.9252	0.8971	0.9915	-0.2252	0.3903	-0.0886
EHMA-HEA-9	0.8883	0.9255	0.8439	1.3477	-0.0477	0.4652	-0.0165
EHMA-HEA-10	0.6589	0.6944	0.9073	1.4088	0.1761	0.4763	0.0595
EHMA-HEA-11	0.8294	0.8812	0.8302	2.0483	0.4961	0.5694	0.1379
EHMA-HEA-12	0.8673	0.9162	0.8146	2.6492	0.9305	0.6310	0.2216
EHMA-HEA-13	0.8261	0.8894	0.7946	3.4325	1.4691	0.6890	0.2949
EHMA-HEA-14	0.8170	0.8797	0.8018	4.3335	2.2275	0.7367	0.3787
EHMA-HEA-15	0.8628	0.9320	0.7388	6.7841	3.6585	0.8141	0.4390
EHMA-HEA-16	0.8330	0.9140	0.7295	9.7058	5.7090	0.8624	0.5072
EHMA-HEA-17	0.8697	0.9186	0.8124	12.9090	9.2570	0.8929	0.6403

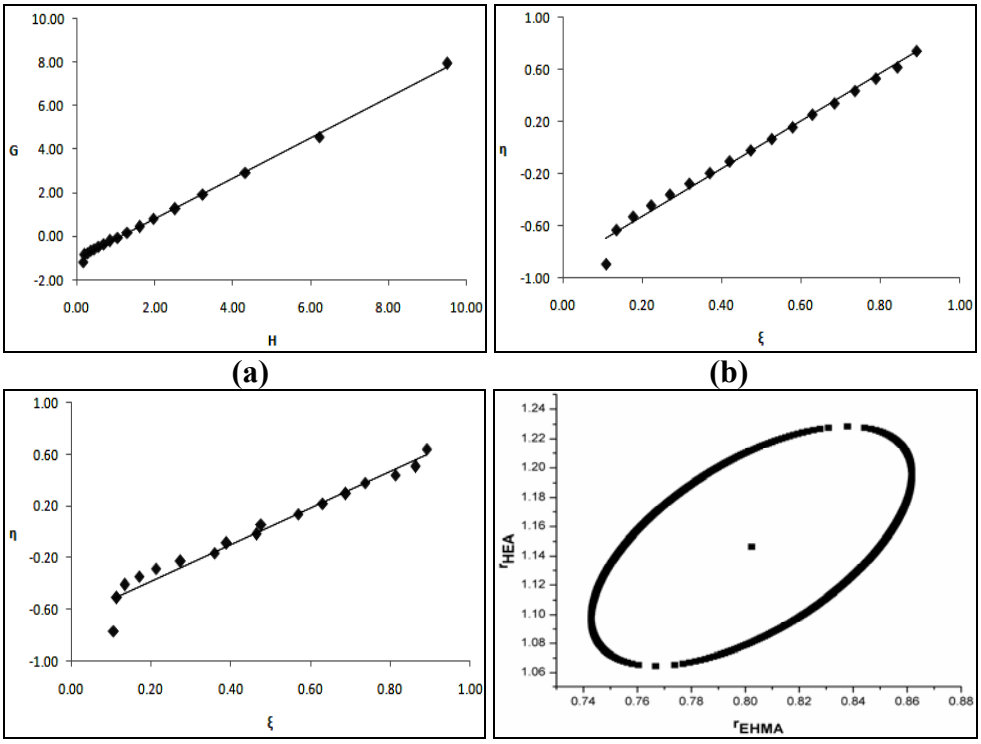

Figure 4.13: (a) FR, (b) KT, (c) Ext. KT plots for EHMA and HEA copolymer system and (d) 95% Joint confidence interval calculated by MH method

Similarly, the 95 % joint confidence limit of the reactivity ratio is plotted in Figure 4.13 (d). Its equation is,

$5.1212(r_1 - 0.8023)^2 - 4.4415(r_1 - 0.8023)(r_2 - 1.1465) + 2.6883(r_2 - 1.1465)^2 = 0.0116$

The statistical distribution of the sequences of two monomers (dyad) M_{EHMA}-M_{EHMA}, M_{HEA}-M_{HEA} and M_{EHMA}-M_{HEA} and mean sequence lengths μ_{EHMA} and μ_{HEA} calculated are presented in Table 4.19. The variation of the dyad fractions with the EHMA mole fraction in the copolymers is displayed in Figure 4.14.

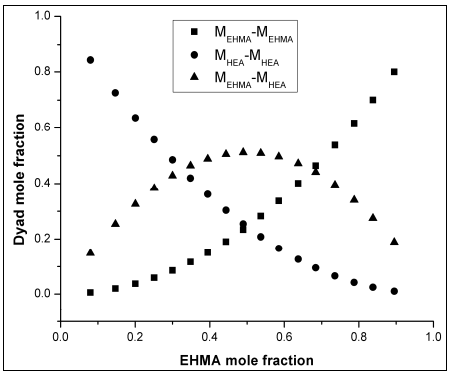

Figure 4.14: Dyad monomer sequence fractions verses the EHMA mole fractions for the copolymers.

Table 4.19: Structural data for poly(EHMA-*co*-HEA) system

Copolymer Code	M_{EHMA}-M_{EHMA}	M_{HEA}-M_{HEA}	M_{EHMA}-M_{MMA}	μ_{EHMA}	μ_{HEA}
EHMA-HEA -1	0.0059	0.8456	0.1485	1.0949	10.5751
EHMA-HEA -2	0.0202	0.7259	0.2539	1.1508	7.0288
EHMA-HEA-3	0.0379	0.6364	0.3257	1.2136	5.2556
EHMA-HEA-4	0.0598	0.5574	0.3829	1.2848	4.1917
EHMA-HEA-5	0.0861	0.4852	0.4287	1.3662	3.4824
EHMA-HEA-6	0.1165	0.4196	0.4639	1.4601	2.9758
EHMA-HEA-7	0.1504	0.3609	0.4887	1.5696	2.5959
EHMA-HEA-8	0.1912	0.3035	0.5053	1.6991	2.3003
EHMA-HEA-9	0.2339	0.2544	0.5117	1.8544	2.0639
EHMA-HEA-10	0.2825	0.2085	0.5091	2.0443	1.8705
EHMA-HEA-11	0.3371	0.1663	0.4966	2.2816	1.7093
EHMA-HEA-12	0.4012	0.1264	0.4724	2.5867	1.5729
EHMA-HEA-13	0.4638	0.0953	0.4409	2.9936	1.4560
EHMA-HEA-14	0.5379	0.0662	0.3959	3.5632	1.3546
EHMA-HEA-15	0.6173	0.0426	0.3401	4.4176	1.2660
EHMA-HEA-16	0.7002	0.0246	0.2753	5.8416	1.1877
EHMA-HEA-17	0.8001	0.0102	0.1896	8.6896	1.1182

Table 4.20: Reactivity ratios of EHMA and HEA computed by different models

Method	r_{EHMA}	r_{HEA}
Finemann-Ross	0.9294	1.0371
Kelen-Tudos	0.9370	1.0419
Extended Kelen-Tudos	0.7490	1.0301
Mao-Huglin	0.8023	1.1465
Average	0.8544	1.0639

This system is suitable for extensive investigation. The r_{EHMA} is 0.8544 and r_{HEA} is 1.0639. Thus HEA units add marginally faster to the copolymer chain. The product of the reactivity ratios of two monomers $r_{EHMA} \bullet r_{HEA}$ value is less than 1. Hence the copolymer formed has a random distribution of the two monomers.

4.5.2 Thermal analysis of the poly(EHMA-*co*-HEA)

The glass transition temperature (T_g) behaviour of three compositions, poly($EHMA_{25}$-HEA_{75}), poly($EHMA_{50}$-HEA_{50}), and poly($EHMA_{75}$-HEA_{25}), were investigated using DSC. The DSC thermograms of copolymers, with glass transition temperature (T_g), are presented in Fig. 4.15.

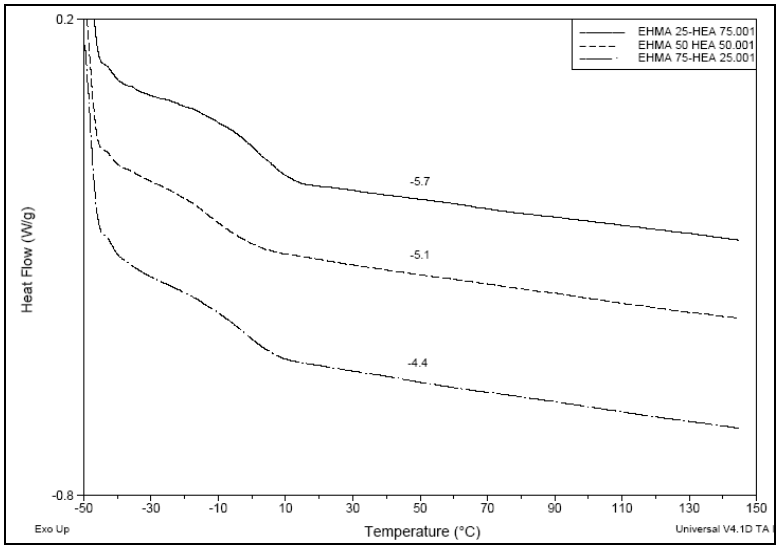

Figure 4.15: DSC thermograms of poly($EHMA_{25}$-HEA_{75}), poly($EHMA_{50}$-HEA_{50}), and poly($EHMA_{75}$-HEA_{25}).

The T_g three compositions, poly($EHMA_{25}$-HEA_{75}), poly($EHMA_{50}$-HEA_{50}), and poly($EHMA_{75}$-HEA_{25}), were determined as -5.7, -5.1 and -4.4°C, respectively. These are quite independent of composition but fall within the T_g of parent homopolymers of 2-ethyl hexyl methacrylate (EHMA) and 2-hydroxyethyl acrylate (HEA) which are -10 °C and 2 °C respectively. These copolymers are elastomers suitable for optical evaluations.

4.6 Poly(2-hydroxyethyl methacrylate-*co*-2-hydroxyethyl acrylate) System

Poly(2-hydroxyethyl methacrylate-*co*-2-hydroxyethyl acrylate) [poly(HEMA-*co*-HEA)] are used in high speed UV curable digital jet inks. These have good adhesive strength when printed onto the hard (glass, ceramic, etc.) as well as soft materials (PET, PC, etc.).[36] Formulations consisting of these monomers are used in applications such as stain resistant UV curable coating and water borne thermally foamed adhesive plates.[37-39] The copolymers are added to compositions used in photocurable hydrophilic coatings,[40] laminating adhesives[41,42] and in coating films having high nonvolatile content.[43] Other evaluations have been as carriers for immobilisation of microorganisms.[44] Water absorption capacity has also been investigated.[45]

4.6.1 Reactivity ratio determination for poly(HEMA-*co*-HEA) system

The kinetic estimates of reactivity ratios of HEMA and HEA were determined as described in Section 4.1.1. The Finemann-Ross (FR) and Kelen-Tudos (KT) parameters for the copolymers are presented in Table 4.21 and Extended Kelen-Tudos

is shown in Table 4.22. The graphical copolymerisation plots of FR, KT and Extended KT are presented in Figures 4.16 (a-c). The plots are linear for all graphical methods, indicating that these follow conventional copolymerisation kinetics. The reactivity ratios of HEMA and HEA are denoted as r_{HEMA} (or r_1) and r_{HEA} (or r_2) respectively and the values obtained from various methods are presented in Table 4.24.

Table 4.21: FR and KT parameters for poly(HEMA-*co*-HEA) system

Copolymer Code	$F=M_1/M_2$	$f=m_1/m_2$	$H=F^2/f$	$G=F(f-1)/f$	$\xi=H/(\alpha+H)$	$\eta=G/(\alpha+H)$
HEMA-HEA -1	0.1111	0.1739	0.0710	-0.5279	0.0802	-0.5960
HEMA-HEA -2	0.3333	0.4141	0.2683	-0.4717	0.2478	-0.4355
HEMA-HEA-3	0.4286	0.5349	0.3434	-0.3727	0.2965	-0.3218
HEMA-HEA-4	0.5385	0.7053	0.4111	-0.2250	0.3354	-0.1835
HEMA-HEA-5	0.6667	0.8160	0.5446	-0.1503	0.4007	-0.1106
HEMA-HEA-6	0.8182	0.9761	0.6858	-0.0200	0.4571	-0.0134
HEMA-HEA-7	1.0000	1.1219	0.8914	0.1086	0.5225	0.0637
HEMA-HEA-8	1.2222	1.3195	1.1322	0.2959	0.5815	0.1520
HEMA-HEA-9	1.5000	1.6026	1.4039	0.5640	0.6328	0.2542
HEMA-HEA-10	1.8571	2.0227	1.7051	0.9390	0.6767	0.3726
HEMA-HEA-11	2.3333	2.4328	2.2379	1.3742	0.7331	0.4502
HEMA-HEA-12	3.0000	3.0105	2.9895	2.0035	0.7858	0.5267
HEMA-HEA-13	4.0000	3.9731	4.0271	2.9932	0.8317	0.6182
HEMA-HEA-14	5.6667	5.4839	5.8555	4.6333	0.8779	0.6946
HEMA-HEA-15	9.0000	8.6638	9.3492	7.9612	0.9198	0.7833

Table 4.22: Extended Kelen-Tudos parameters for poly(HEMA-*co*-HEA) system

Copolymer Code	ζ_1	ζ_2	Z	H	G	ξ	η
HEMA-HEA -1	0.4307	0.2752	1.7501	0.0568	-0.4720	0.0668	-0.5550
HEMA-HEA -2	0.4269	0.3437	1.3220	0.2369	-0.4432	0.2299	-0.4300
HEMA-HEA-3	0.5061	0.4055	1.3565	0.2907	-0.3429	0.2681	-0.3162
HEMA-HEA-4	0.5093	0.3888	1.4459	0.3374	-0.2038	0.2983	-0.1802
HEMA-HEA-5	0.5745	0.4694	1.3486	0.4487	-0.1364	0.3612	-0.1098
HEMA-HEA-6	0.5067	0.4247	1.2780	0.5976	-0.0187	0.4295	-0.0134
HEMA-HEA-7	0.5931	0.5287	1.1954	0.7851	0.1020	0.4973	0.0646
HEMA-HEA-8	0.6797	0.6296	1.1463	1.0042	0.2787	0.5585	0.1550
HEMA-HEA-9	0.6701	0.6272	1.1239	1.2687	0.5362	0.6151	0.2600
HEMA-HEA-10	0.6700	0.6152	1.1610	1.5007	0.8809	0.6541	0.3839
HEMA-HEA-11	0.8055	0.7726	1.1056	1.9902	1.2959	0.7149	0.4655
HEMA-HEA-12	0.8573	0.8543	1.0108	2.9466	1.9891	0.7878	0.5318
HEMA-HEA-13	0.7984	0.8038	0.9833	4.1093	3.0236	0.8381	0.6167
HEMA-HEA-14	0.8554	0.8839	0.8981	6.7995	4.9929	0.8955	0.6575
HEMA-HEA-15	0.8511	0.8841	0.8837	11.0955	8.6729	0.9332	0.7295

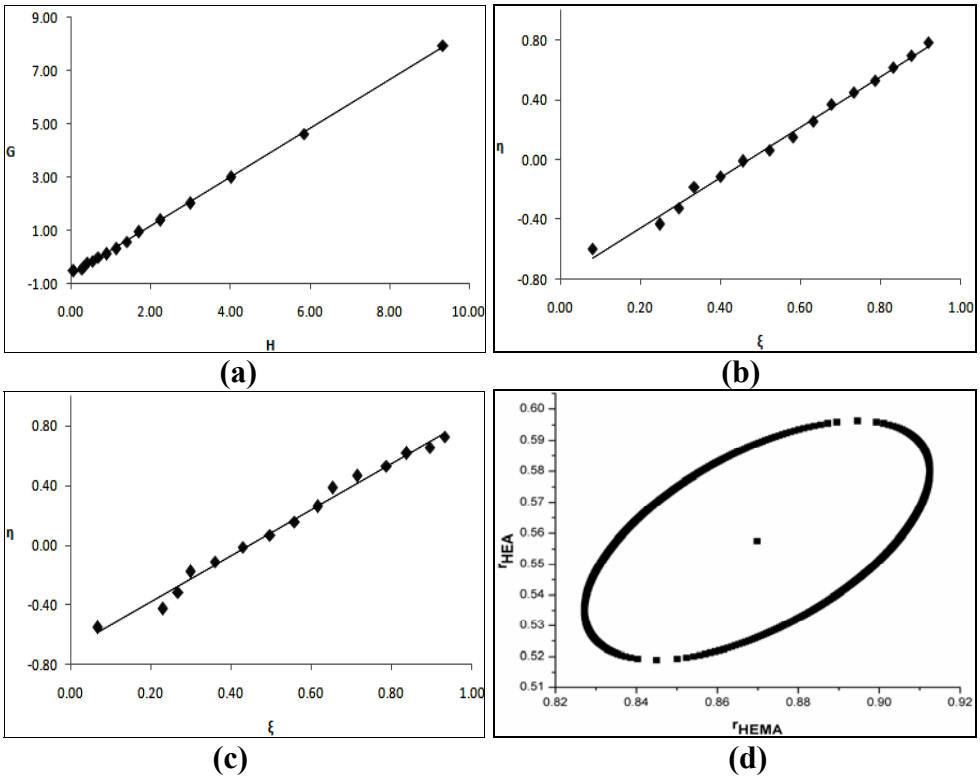

Figure 4.16: (a) FR, (b) KT, (c) Ext. KT plots for the poly(HEMA-*co*-HEA) system and (d) 95% Joint confidence interval calculated by MH method

The 95 % joint confidence limit of the reactivity ratio values are plotted in Figure 4.16 (d). Its equation is,

$5.4585(r_1 - 0.8698)^2 - 7.0150(r_1 - 0.8698)(r_2 - 0.5576) + 6.6426(r_2 - 0.5576)^2 = 0.0066$

The statistical distribution of the sequences of two monomers (dyad) M_{HEMA}-M_{HEMA}, M_{HEA}-M_{HEA} and M_{HEMA}-M_{HEA} and mean sequence lengths μ_{HEMA} and μ_{HEA} are presented in Table 4.23, and the variation is represented Figure 4.17.

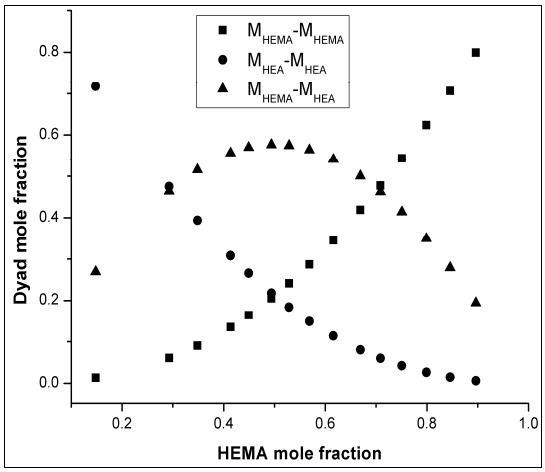

Figure 4.17: Dyad monomer sequence fractions verses the HEMA mole fractions for the copolymers.

Table 4.23: Structural data for poly(HEMA-*co*-HEA) system

Copolymer Code	M_{HEMA}-M_{HEMA}	M_{HEA}-M_{HEA}	M_{HEMA}-M_{HEA}	μ_{HEMA}	μ_{HEA}
HEMA-HEA -1	0.0136	0.7173	0.2691	1.0984	6.4621
HEMA-HEA -2	0.0608	0.4752	0.4639	1.2951	2.8207
HEMA-HEA-3	0.0907	0.3937	0.5156	1.3794	2.4161
HEMA-HEA-4	0.1352	0.3080	0.5568	1.4767	2.1271
HEMA-HEA-5	0.1643	0.2656	0.5700	1.5902	1.9104
HEMA-HEA-6	0.2055	0.2176	0.5769	1.7243	1.7418
HEMA-HEA-7	0.2413	0.1839	0.5748	1.8853	1.6069
HEMA-HEA-8	0.2868	0.1491	0.5641	2.0820	1.4966
HEMA-HEA-9	0.3453	0.1138	0.5409	2.3280	1.4046
HEMA-HEA-10	0.4188	0.0804	0.5008	2.6441	1.3268
HEMA-HEA-11	0.4775	0.0601	0.4624	3.0657	1.2601
HEMA-HEA-12	0.5437	0.0423	0.4140	3.6559	1.2023
HEMA-HEA-13	0.6241	0.0263	0.3496	4.5412	1.1517
HEMA-HEA-14	0.7063	0.0148	0.2789	6.0167	1.1071
HEMA-HEA-15	0.7994	0.0063	0.1943	8.9677	1.0674

Table 4.24: Reactivity ratios of HEMA and HEA computed by different models

Method	r_{HEMA}	r_{HEA}
Finemann-Ross	0.9163	0.6764
Kelen-Tudos	0.8950	0.6444
Extended Kelen-Tudos	0.8600	0.5492
Mao-Huglin	0.8698	0.5576
Average	0.8853	0.6069

The average value of r_{HEMA} is equal to 0.8853 and that of r_{HEA} is equal to 0.6069, which indicates the higher incorporation of HEMA units in the copolymer than in feed. The product of the reactivity ratios of two monomers $r_{HEMA} \bullet r_{HEA}$ value is 0.5373 which is less than 1, suggesting that there is tendency for the formation of random copolymer system. Since the r_1 and r_2 values are less than one, this system gives rise to azeotropic polymerisation at a particular composition of the monomers which is calculated using the equation 4.1. The azeotropic polymerisation forms at a particular composition 0.7753, when the mole fraction of the monomer HEMA in the feed is 0.7753, the copolymer formed will have the same composition as that of the feed.

4.6.2 Thermal analysis of the poly(HEMA-*co*-HEA)

The glass transition temperature (T_g) of three copolymer compositions such as poly($HEMA_{25}$-HEA_{75}), poly($HEMA_{50}$-HEA_{50}), and poly($HEMA_{75}$-HEA_{25}) were 28.6,

42.3 and 54.3, respectively, as established with DSC. The DSC thermograms of copolymers with T_g values are presented in Figure 4.18.

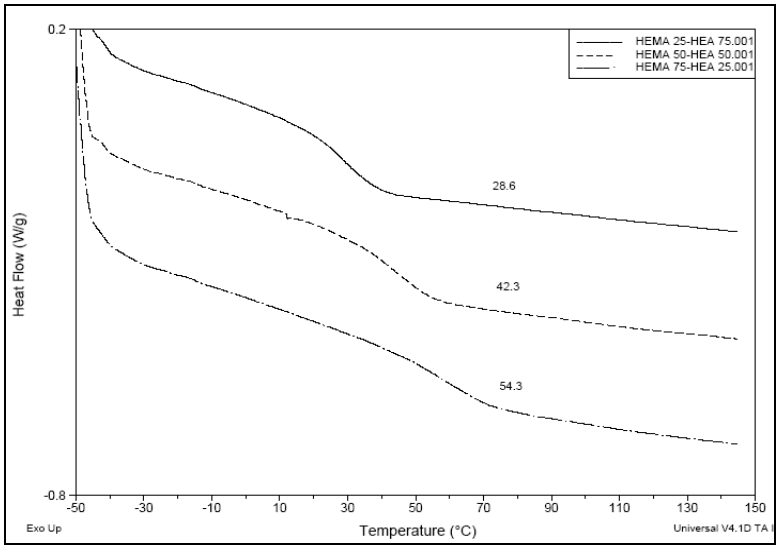

Figure 4.18: DSC thermograms of poly($HEMA_{25}$-HEA_{75}), poly($HEMA_{50}$-HEA_{50}), and poly($HEMA_{75}$-HEA_{25}).

Both monomers used in this copolymerization are hydrophilic. Thus, the copolymer would be a good hydrogel. The T_g of the hydrogels will be much lower than that reported here for dry copolymer samples.

4.7 Poly(methyl acrylate-*co*-2-hydroxypropyl acrylate) System

The copolymer system is reported in literature, though the reactivity ratio has not been estimated, hitherto. The copolymers have been evaluated to estimate the yield stress relative to composition.[46]

4.7.1 Reactivity ratio determination for poly(MA-*co*-HPA) system

The kinetic parameters used to estimate reactivity ratios of MA and HPA determined by Finemann-Ross (FR) and Kelen-Tudos (KT) are presented in Table 4.25, while that by Extended Kelen-Tudos (Ext. KT) is shown in Table 4.26. The graphical copolymerisation plots of FR, KT and extended KT are presented in Figures 4.19 (a-c). The plots are highly scattered for all graphical methods, indicating that these may not follow conventional copolymerisation kinetics. The reactivity ratios of MA and HPA are denoted as r_{MA} (or r_1) and r_{HPA} (or r_2) respectively and the values obtained from various methods are presented in Table 4.28.

Table 4.25: FR and KT parameters for poly(MA-*co*-HPA) system

Copolymer Code	$F=M_1/M_2$	$f=m_1/m_2$	$H=F^2/f$	$G=F(f-1)/f$	$\xi=H/(\alpha+H)$	$\eta=G/(\alpha+H)$
MA-HPA -1	0.1111	0.1573	0.0785	-0.5951	0.0986	-0.7476
MA-HPA -2	0.2500	0.2350	0.2660	-0.8140	0.2705	-0.8276
MA-HPA -3	0.3333	0.3425	0.3244	-0.6400	0.3114	-0.6142
MA-HPA -4	0.4286	0.5793	0.3170	-0.3112	0.3065	-0.3008
MA-HPA -5	0.5385	0.6250	0.4639	-0.3231	0.3927	-0.2735
MA-HPA -6	0.6667	1.0597	0.4194	0.0376	0.3689	0.0330
MA-HPA -7	0.8182	1.0043	0.6665	0.0035	0.4816	0.0025
MA-HPA -8	4.0000	6.4412	2.4840	3.3790	0.7759	1.0554
MA-HPA -9	9.0000	12.3504	6.5585	8.2713	0.9014	1.1368

Table 4.26: Extended Kelen-Tudos parameters for poly(MA-*co*-HPA) system

Copolymer Code	ζ_1	ζ_2	Z	H	G	ξ	η
MA-HPA -1	0.3247	0.2293	1.5073	0.0693	-0.5591	0.0951	-0.7676
MA-HPA -2	0.4243	0.4514	0.9196	0.2779	-0.8320	0.2966	-0.8879
MA-HPA -3	0.3313	0.3225	1.0337	0.3205	-0.6361	0.3272	-0.6493
MA-HPA -4	0.3687	0.2728	1.4442	0.2778	-0.2913	0.2965	-0.3109
MA-HPA -5	0.3224	0.2778	1.1960	0.4369	-0.3136	0.3986	-0.2861
MA-HPA -6	0.2092	0.1316	1.6633	0.3830	0.0359	0.3676	0.0344
MA-HPA -7	0.2395	0.1951	1.2613	0.6313	0.0034	0.4892	0.0027
MA-HPA -8	0.2490	0.1546	1.7047	2.2166	3.1920	0.7708	1.1100
MA-HPA -9	0.1461	0.1065	1.4030	6.2740	8.0899	0.9049	1.1669

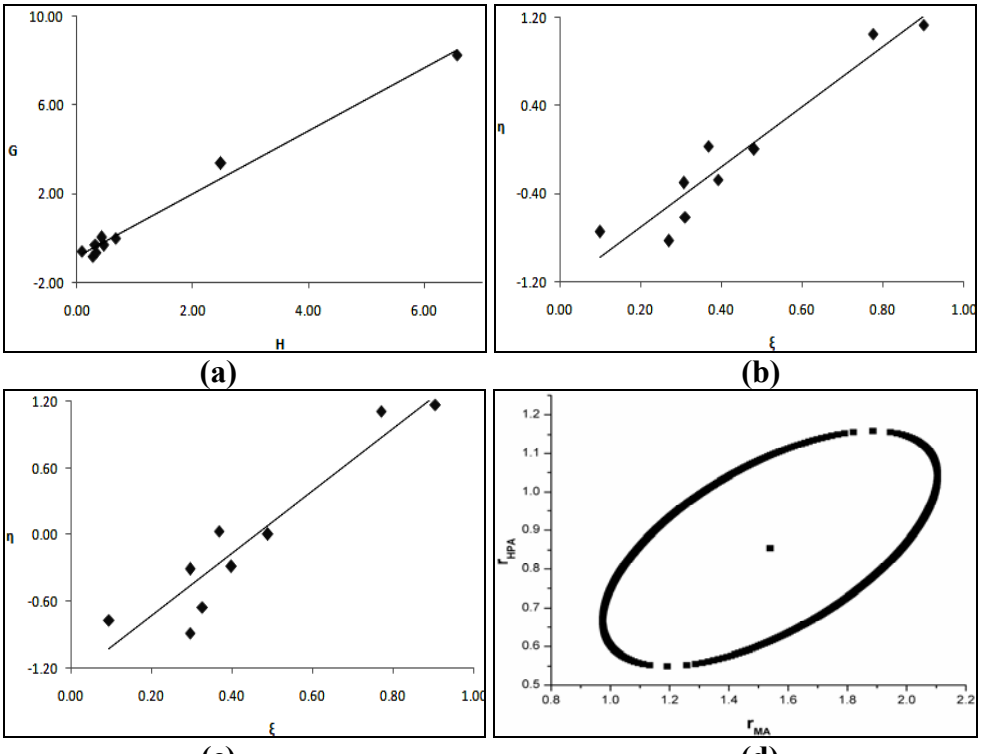

Figure 4.19: (a) FR, (b) KT, (c) Ext. KT plots for poly(MA-*co*-HPA) system and (d) 95% Joint confidence interval calculated by MH method

The 95 % joint confidence limit of the reactivity ratio by Mao-Huglin method is plotted in Figure 4.19 (d). Its equation is,

$2.1730(r_1\text{-}1.5391)^2 - 4.9485(r_1\text{-}1.5391)(r_2\text{-}0.8544) + 7.4616(r_2\text{-}0.8544)^2 = 0.4317$

The statistical distribution of the sequences of two monomers (dyad) M_{MA}-M_{MA}, M_{HPA}-M_{HPA} and M_{MA}-M_{HPA} and mean sequence lengths μ_{MA} and μ_{HPA} are presented in Table 4.27, and the variation of the dyad fractions with the MA mole fraction in the copolymers is displayed in Figure 4.20.

Table 4.27: Structural data for poly(MA-*co*-HPA) system

Copolymer Code	M_{MA}-M_{MA}	M_{HPA}-M_{HPA}	M_{MA}-M_{HPA}	μ_{MA}	μ_{HPA}
MA-HPA -1	0.0221	0.7502	0.2277	1.1655	8.7157
MA-HPA -2	0.0423	0.6617	0.2960	1.3724	4.4292
MA-HPA -3	0.0741	0.5639	0.3619	1.4965	3.5719
MA-HPA -4	0.1478	0.4142	0.4380	1.6384	3.0004
MA-HPA -5	0.1617	0.3925	0.4458	1.8021	2.5921
MA-HPA -6	0.2799	0.2510	0.4691	1.9931	2.2860
MA-HPA -7	0.2663	0.2642	0.4695	2.2188	2.0478
MA-HPA -8	0.7528	0.0216	0.2256	6.9584	1.2143
MA-HPA -9	0.8571	0.0069	0.1360	14.4064	1.0953

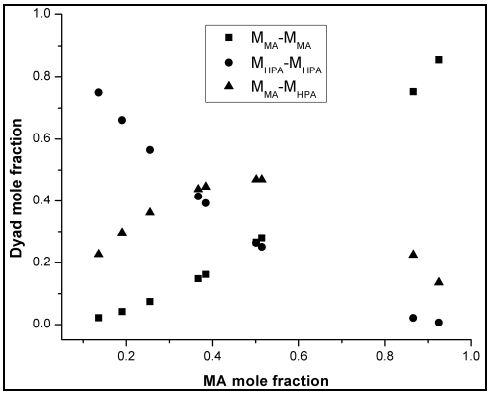

Figure 4.20: Dyad monomer sequence fractions verses the MA mole fractions for the copolymers.

Table 4.28: Reactivity ratios of MA and HPA computed by different models

Method	r_{MA}	r_{HPA}
Finemann-Ross	1.4221	0.8284
Kelen-Tudos	1.4832	0.8911
Extended Kelen-Tudos	1.5142	0.8555
Mao-Huglin	1.5391	0.8544
Average	1.4896	0.8573

The value of r_{MA} is 1.4896 and that of r_{HPA} is 0.8573. Thus, MA units enter the copolymer chain at a faster rate. The product of the reactivity ratios of two monomers

$r_{MA} \bullet r_{HPA}$ value is 1.2770 which is greater than 1, indicating a tendency for the formation long sequence of each in the copolymer.

4.7.2 Thermal analysis of poly(MA-*co*-HPA)

Thermal behaviour of poly(MA_{25}-HPA_{75}), poly(MA_{50}-HPA_{50}), and poly(MA_{75}-HPA_{25}) were investigated by DSC. The DSC thermograms of copolymers are presented in Figure 4.21.

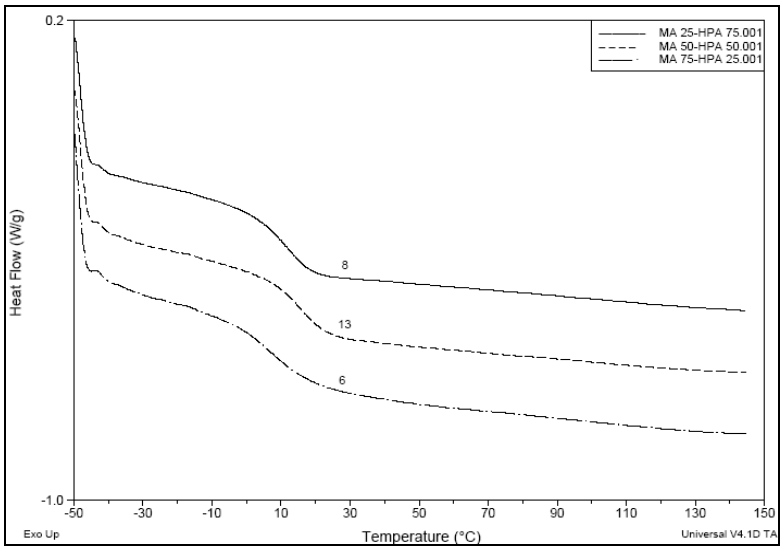

Figure 4.21: DSC thermograms of poly(MA_{25}-HPA_{75}), poly(MA_{50}-HPA_{50}), and poly(MA_{75}-HPA_{25}).

The T_g values (8, 13, 6 ºC) show an interesting trend in that the highest value is opposite was what could be expected for a 50:50 composition. The T_g of homopolymer of MA and HPA are 3 ºC and 14 ºC respectively.

4.8 Poly(butyl acrylate-*co*-2-hydroxypropyl acrylate) System

Butyl acrylate and 2-hydroxypropyl acrylate are used in coating compositions that exhibit increased humidity resistance.[47] Copolymers with fluorinated monomers are used to form hydrophobic non-wetting coatings on glass and cotton fabrics.[48,49]

4.8.1 Reactivity ratio determination for poly(BA-*co*-HPA) system

The kinetic estimates of reactivity ratios for BA and HPA determined by Finemann-Ross (FR), Kelen-Tudos (KT), Extended Kelen-Tudos (Ext. KT) are presented in Tables 4.29 and 4.30. The graphical copolymerisation plots of FR, KT and Extended KT are presented in Figures 4.22 (a-c). The plots are highly scattered for all graphical methods, indicating that these do not follow conventional

copolymerisation kinetics. The reactivity ratios of BA and HPA are denoted as r_{BA} (or r_1) and r_{HPA} (or r_2) respectively. The reactivity ratios are presented in Table 4.32.

Table 4.29: FR and KT parameters for poly(BA-*co*-HPA) system

Copolymer Code	$F=M_1/M_2$	$f=m_1/m_2$	$H=F^2/f$	$G=F(f-1)/f$	$\xi=H/(\alpha+H)$	$\eta=G/(\alpha+H)$
BA-HPA-1	0.2500	0.2497	0.2503	-0.7514	0.0696	-0.2090
BA-HPA-2	0.3333	0.3947	0.2815	-0.5111	0.0776	-0.1409
BA-HPA-3	0.4286	0.2778	0.6612	-1.1142	0.1650	-0.2781
BA-HPA-4	0.5385	0.4182	0.6932	-0.7490	0.1717	-0.1855
BA-HPA-5	0.8182	0.4208	1.5909	-1.1262	0.3223	-0.2282
BA-HPA-6	1.0000	0.5980	1.6724	-0.6724	0.3333	-0.1340
BA-HPA-7	1.2222	0.7656	1.9512	-0.3743	0.3684	-0.0707
BA-HPA-8	2.3333	0.8353	6.5178	-0.4600	0.6608	-0.0466
BA-HPA-9	4.0000	1.4558	10.9906	1.2524	0.7667	0.0874
BA-HPA-10	9.0000	1.8120	44.7027	4.0330	0.9304	0.0839

Table 4.30: Extended Kelen-Tudos parameters for poly(BA-*co*-HPA) system

Copolymer Code	ζ_1	ζ_2	Z	H	G	ξ	η
BA-HPA-1	0.0710	0.0711	0.9986	0.2504	-0.7514	0.0621	-0.1865
BA-HPA-2	0.0178	0.0151	1.1859	0.2807	-0.5104	0.0692	-0.1257
BA-HPA-3	0.0690	0.1065	0.6352	0.6885	-1.1369	0.1541	-0.2545
BA-HPA-4	0.1423	0.1832	0.7585	0.7269	-0.7670	0.1614	-0.1702
BA-HPA-5	0.0140	0.0271	0.5109	1.6124	-1.1338	0.2991	-0.2103
BA-HPA-6	0.1321	0.2209	0.5675	1.8565	-0.7084	0.3295	-0.1257
BA-HPA-7	0.1352	0.2159	0.5974	2.1451	-0.3924	0.3622	-0.0662
BA-HPA-8	0.0492	0.1373	0.3413	7.1723	-0.4826	0.6550	-0.0441
BA-HPA-9	0.0553	0.1521	0.3452	12.2199	1.3205	0.7638	0.0825
BA-HPA-10	0.0529	0.2629	0.1783	57.0091	4.5545	0.9378	0.0749

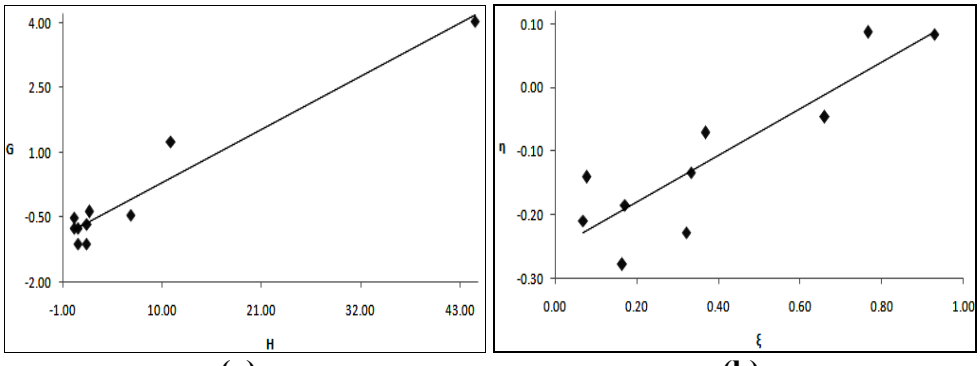

(a) **(b)**

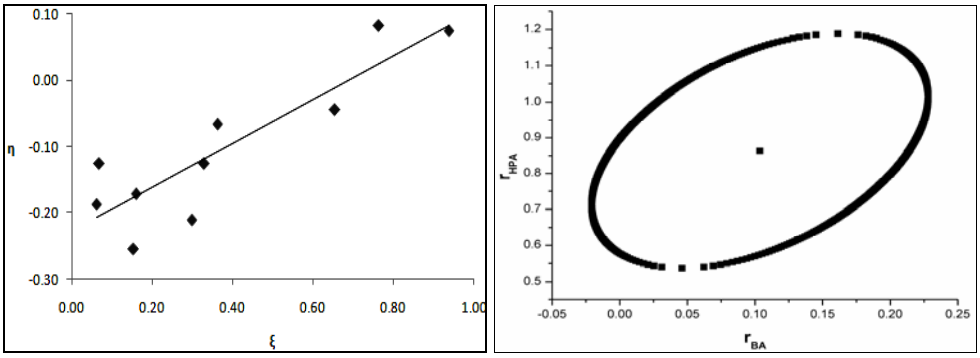

(c) **(d)**

Figure 4.22: (a) FR, (b) KT, (c) Ext. KT plots for poly(BA-*co*-HPA) system and (d) 95% Joint confidence interval calculated by MH method

The 95 % joint confidence limit of the reactivity ratio values calculated by Mao-Huglin method is shown in Figure 4.22 (d). Its equation is,

$$2.2886(r_1-0.1037)^2 - 0.8087(r_1-0.1037)(r_2-0.8630) + 0.3329(r_2-0.8630)^2 = 0.0278$$

The statistical distribution of the sequences of two monomers (dyad) M_{BA}-M_{BA}, M_{HPA}-M_{HPA} and M_{BA}-M_{HPA} and mean sequence lengths μ_{BA} and μ_{HPA} are presented in Table 4.31, and the variation of the dyad fractions with the BA mole fraction in the copolymers is displayed in Figure 4.23.

Table 4.31: Structural data for poly(BA-*co*-HPA) system

Copolymer Code	M_{BA}-M_{BA}	M_{HPA}-M_{HPA}	M_{BA}-M_{HPA}	μ_{BA}	μ_{HPA}
BA-HPA-1	0.0057	0.6062	0.3881	1.0271	4.3964
BA-HPA-2	0.0148	0.4487	0.5365	1.0361	3.5473
BA-HPA-3	0.0071	0.5723	0.4206	1.0465	2.9812
BA-HPA-4	0.0167	0.4269	0.5564	1.0584	2.5769
BA-HPA-5	0.0169	0.4246	0.5585	1.0887	2.0378
BA-HPA-6	0.0365	0.2880	0.6755	1.1084	1.8491
BA-HPA-7	0.0639	0.1967	0.7393	1.1325	1.6947
BA-HPA-8	0.0780	0.1678	0.7542	1.2529	1.3639
BA-HPA-9	0.2355	0.0499	0.7146	1.4336	1.2123
BA-HPA-10	0.3192	0.0305	0.6503	1.9756	1.0943

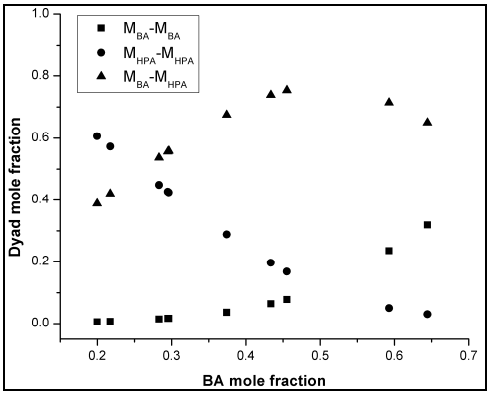

Figure 4.23: Dyad monomer sequence fractions verses the BA mole fractions for the copolymers.

Table 4.32: Reactivity ratios of BA and HPA computed by different models

Method	r_{BA}	r_{HPA}
Finemann-Ross	0.1111	0.8224
Kelen-Tudos	0.1153	0.8496
Extended Kelen-Tudos	0.1034	0.8614
Mao-Huglin	0.1037	0.8630
Average	0.1084	0.8491

The r_{BA} and r_{HPA} values obtained from four methods are in good agreement with each other. The value of r_{BA} is equal to 0.1084 and that of r_{HPA} is equal to 0.8491, which indicates the higher incorporation of HPA units in the copolymer than in feed. The product of the reactivity ratios of two monomers $r_{BA} \bullet r_{HPA}$ value is 0.0920 which is much less than 1. This system gives rise to azeotropic composition. This is estimated from equation 4.1 as to occur when the mole fraction of the monomer BA in the feed is 0.1447.

4.8.2 Thermal analysis of poly(BA-*co*-HPA)

Glass transition temperature of poly(BA_{25}-HPA_{75}), poly(BA_{50}-HPA_{50}), and poly(BA_{75}-HPA_{25}) estimated by DSC were -15.5, -13.2 and 1.1ºC, respectively. The DSC thermograms and T_g values are presented in Figure 4.24.

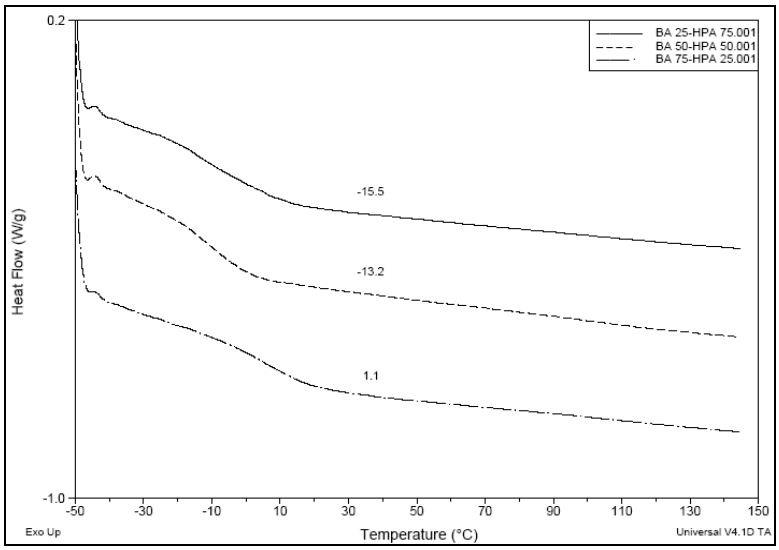

Figure 4.24: DSC thermograms of poly(BA_{25}-HPA_{75}), poly(BA_{50}-HPA_{50}), and poly(BA_{75}-HPA_{25}).

The thermal analysis shows that the copolymer is an elastomeric hydrogel at ambient temperature.

4.9 Poly(2-ethylhexyl acrylate-*co*-2-hydroxypropyl acrylate) System

2-Ethyl hexyl acrylate (EHA) and 2-hydroxypropyl acrylate (HPA) are used in combination in the preparation of wafer processing tapes and radiation-inactive adhesive tapes for dicing semiconductor wafers[50,51] and in preparation of contact adhesives.[52,53] Crosslinking of these polymers with isocyanates gave adhesive materials with high shear strength.[54]

4.9.1 Reactivity ratio determination for poly(EHA-*co*-HPA) system

The kinetic estimates EHA and HPA were determined by Finemann-Ross (FR), Kelen-Tudos (KT), Extended Kelen-Tudos (Ext. KT) and Mao-Huglin (MH) methods. The FR and KT data is presented in Table 4.33 and extended KT is shown in Table 4.34.

Table 4.33: FR and KT parameters for poly(EHA-*co*-HPA) system

Copolymer Code	$F=M_1/M_2$	$f=m_1/m_2$	$H=F^2/f$	$G=F(f-1)/f$	$\xi=H/(\alpha+H)$	$\eta=G/(\alpha+H)$
EHA:HPA-1	0.1111	0.0862	0.1431	-1.1772	0.1234	-1.0149
EHA:HPA-2	0.2500	0.2391	0.2614	-0.7956	0.2045	-0.6225
EHA:HPA-3	0.3333	0.2800	0.3968	-0.8571	0.2807	-0.6064
EHA:HPA-4	0.4285	0.3808	0.4822	-0.6969	0.3217	-0.4649
EHA:HPA-5	0.5385	0.3796	0.7639	-0.8802	0.4290	-0.4943
EHA:HPA-6	0.6666	0.5030	0.8836	-0.6588	0.4650	-0.3467
EHA:HPA-7	1.2222	1.1106	1.3450	0.1217	0.5695	0.0515
EHA:HPA-8	1.4998	1.1424	1.9690	0.1869	0.6595	0.0626
EHA:HPA-9	2.3333	2.0192	2.6963	1.1778	0.7262	0.3172
EHA:HPA-10	4.0000	3.1565	5.0688	2.7328	0.8329	0.4491
EHA:HPA-11	5.6666	4.4458	7.2227	4.3920	0.8766	0.5331

Table 4.34: Extended Kelen-Tudos parameters for poly(EHA-*co*-HPA) system

Copolymer Code	ζ_1	ζ_2	Z	H	G	ξ	η
EHA:HPA-1	0.6626	0.8536	0.5654	0.2698	-1.6160	0.1277	-0.7653
EHA:HPA-2	0.8683	0.9079	0.8500	0.3309	-0.8951	0.1523	-0.4120
EHA:HPA-3	0.6055	0.7208	0.7291	0.5268	-0.9876	0.2224	-0.4169
EHA:HPA-4	0.8633	0.9715	0.5592	1.2174	-1.1073	0.3979	-0.3619
EHA:HPA-5	0.3737	0.5302	0.6195	0.9890	-1.0015	0.3494	-0.3538
EHA:HPA-6	0.2041	0.2705	0.7237	0.9602	-0.6867	0.3427	-0.2451
EHA:HPA-7	0.1763	0.1940	0.8992	1.3735	0.1230	0.4272	0.0382
EHA:HPA-8	0.1220	0.1602	0.7454	2.0561	0.1910	0.5275	0.0490
EHA:HPA-9	0.5076	0.5865	0.8021	3.1384	1.2706	0.6302	0.2551
EHA:HPA-10	0.4246	0.5380	0.7156	6.1633	3.0134	0.7699	0.3764
EHA:HPA-11	0.6509	0.8297	0.5946	12.5750	5.7952	0.8722	0.4020

The graphical copolymerisation plots of FR, KT and Extended KT are presented in Figures 4.25 (a-c). The plots are substantially linear for all graphical methods, indicating that these follow conventional copolymerisation kinetics. The reactivity ratios of EHA and HPA, denoted as r_{EHA} (or r_1) and r_{HPA} (or r_2) are presented in Table 4.36.

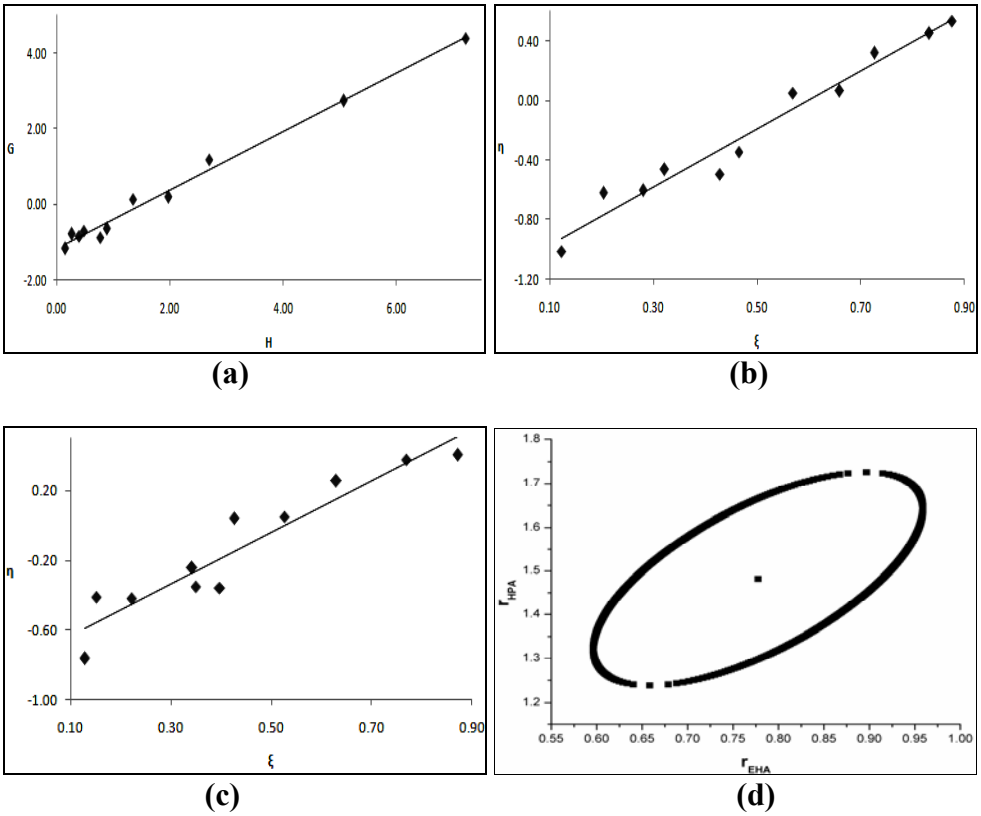

Figure 4.25: (a) FR, (b) KT, (c) Ext. KT plots for poly(EHA-*co*-HPA) system and (d) 95% Joint confidence interval calculated by MH method

The 95 % joint confidence limit calculated by Mao-Huglin method is plotted in Figure 4.25 (d). Its equation is,

$$3.0664(r_1 - 0.7776)^2 - 2.9964(r_1 - 0.7776)(r_2 - 1.4819) + 1.6908(r_2 - 1.4819)^2 = 0.0571$$

The statistical distribution of the sequences of two monomers (dyad) M_{EHA}-M_{EHA}, M_{HPA}-M_{HPA} and M_{EHA}-M_{HPA} and mean sequence lengths μ_{EHA} and μ_{HPA} are presented in Table 4.35, and the variation of the dyad fractions with the BA mole fraction in the copolymers is displayed in Figure 4.26.

Table 4.35: Structural data for poly(EHA-*co*-HPA) system

Copolymer Code	M_{BA}-M_{BA}	M_{HPA}-M_{HPA}	M_{BA}-M_{HPA}	μ_{BA}	μ_{HPA}
EHA-HPA-1	0.0063	0.8475	0.1462	1.0843	12.8650
EHA-HPA-2	0.0372	0.6513	0.3114	1.1896	6.2733
EHA-HPA-3	0.0479	0.6103	0.3418	1.2529	4.9549
EHA-HPA-4	0.0760	0.5245	0.3994	1.3251	4.0765
EHA-HPA-5	0.0757	0.5254	0.3989	1.4085	3.4483
EHA-HPA-6	0.1120	0.4427	0.4453	1.5057	2.9775
EHA-HPA-7	0.2769	0.2245	0.4986	1.9271	2.0787
EHA-HPA-8	0.2843	0.2179	0.4978	2.1377	1.8790
EHA-HPA-9	0.4473	0.1097	0.4430	2.7701	1.5650
EHA-HPA-10	0.5767	0.0579	0.3654	4.0344	1.3296
EHA-HPA-11	0.6665	0.0337	0.2998	5.2987	1.2326

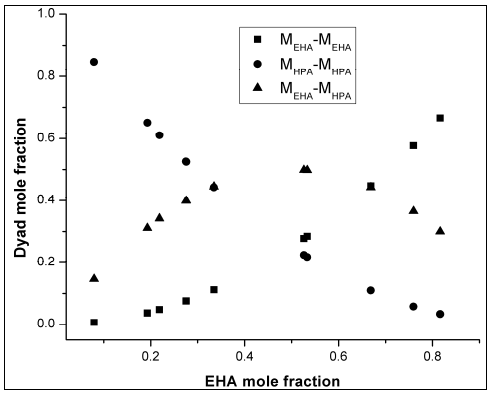

Figure 4.26: Dyad monomer sequence fractions verses the EHA mole fractions for the copolymers.

Table 4.36: Reactivity ratios of EHA and HPA computed by different models

Method	r_{EHA}	r_{HPA}
Finemann-Ross	0.7763	1.1764
Kelen-Tudos	0.7801	1.1836
Extended Kelen-Tudos	0.7003	1.4313
Mao-Huglin	0.7776	1.4819
Average	0.7586	1.3183

The r_{EHA} is 0.7586 and r_{HPA} is dependent on method used for estimation, with an average of 1.3183, which indicates the higher incorporation of HPA units in the copolymer than in feed. It is interesting to note that the product of the reactivity ratios of two monomers $r_{EHA} \bullet r_{HPA}$ value is 1.0000 which indicates the formation of ideal copolymer.

4.9.2 Thermal analysis of poly(EHA-*co*-HPA)

Glass transition temperature (T_g) of poly(EHA_{25}-HPA_{75}), poly(EHA_{50}-HPA_{50}), and poly(EHA_{75}-HPA_{25}) estimated by DSC were 1.5, -15.2 and -14.3ºC. The DSC thermograms are presented in Figure 4.27.

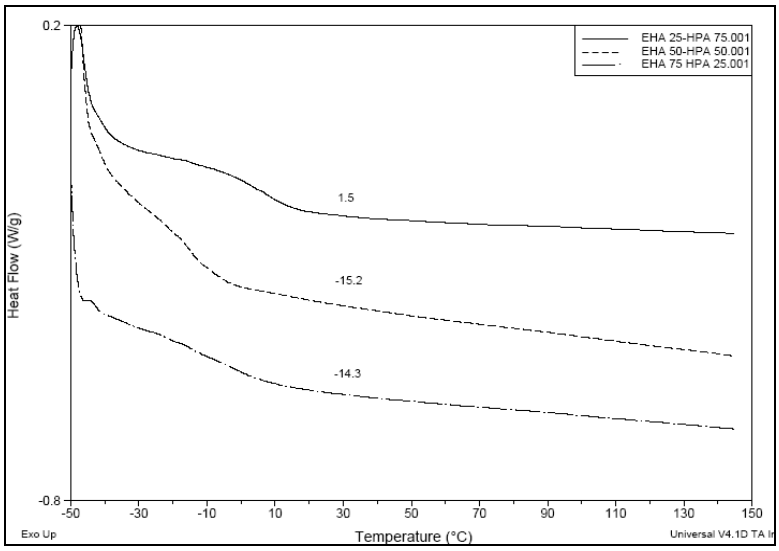

Figure 4.27: DSC thermograms of poly(EHA_{25}-HPA_{75}), poly(EHA_{50}-HPA_{50}), and poly(EHA_{75}-HPA_{25}).

The T_g values of copolymers are much lower than those of the parent EHA and HPA homopolymers which are 12ºC and 14ºC respectively. This copolymer system too is elastomeric.

4.10 Poly(methyl methacrylate-*co*-2-hydroxypropyl acrylate) System

Methyl methacrylate (MMA) and 2-hydroxypropyl acrylate (HPA) copolymers form hybrid materials with silica when MMA and HPA are copolymerized in presence of tetraethyl orthosilicate.[55]

4.10.1 Reactivity ratio determination for poly(MMA-*co*-HPA) System

The kinetic parameters for determination of reactivity ratios of MMA and HPA by Finemann-Ross (FR) and Kelen-Tudos (KT) are presented in Table 4.37. The data for Extended KT is shown in Table 4.38. The graphical copolymerisation plots of FR, KT and Extended KT are presented in Figures 4.28 (a-c). The plots are linear for all graphical methods, indicating that these follow conventional copolymerisation kinetics. The reactivity ratios of MMA and HPA are denoted as r_{MMA} (or r_1) and r_{HPA} (or r_2) respectively and the values obtained by various methods are presented in Table 4.40.

Table 4.37: FR and KT parameters for poly(MMA-*co*-HPA) system

Copolymer Code	$F=M_1/M_2$	$f=m_1/m_2$	$H=F^2/f$	$G=F(f-1)/f$	$\xi=H/(\alpha+H)$	$\eta=G/(\alpha+H)$
MMA-HPA-1	0.1111	0.1500	0.0823	-0.6296	0.0858	-0.6564
MMA-HPA-2	0.1765	0.2451	0.1270	-0.5434	0.1265	-0.5413
MMA-HPA-3	0.2500	0.3179	0.1966	-0.5365	0.1832	-0.4997
MMA-HPA-4	0.3333	0.3477	0.3196	-0.6254	0.2671	-0.5227
MMA-HPA-5	0.4286	0.5081	0.3615	-0.4148	0.2919	-0.3350
MMA-HPA-6	0.5385	0.5991	0.4840	-0.3603	0.3556	-0.2648
MMA-HPA-7	0.6667	0.7377	0.6025	-0.2371	0.4073	-0.1602
MMA-HPA-8	0.8182	1.0461	0.6399	0.0360	0.4219	0.0238
MMA-HPA-9	1.0000	1.1987	0.8342	0.1658	0.4875	0.0969
MMA-HPA-10	1.2222	1.4781	1.0106	0.3954	0.5354	0.2095
MMA-HPA-11	1.5000	1.6372	1.3743	0.5838	0.6105	0.2593
MMA-HPA-12	1.8571	2.2059	1.5635	1.0153	0.6407	0.4160
MMA-HPA-13	2.3333	2.5298	2.1522	1.4110	0.7105	0.4658
MMA-HPA14	3.0000	3.0838	2.9185	2.0272	0.7690	0.5341
MMA-HPA-15	4.0000	3.9114	4.0906	2.9774	0.8235	0.5994
MMA-HPA-16	5.6667	5.9564	5.3910	4.7153	0.8601	0.7523
MMA-HPA-17	9.0000	8.6688	9.3439	7.9618	0.9142	0.7790

Table 4.38: Extended Kelen-Tudos parameters for poly(MMA-*co*-HPA) system

Copolymer Code	ζ_1	ζ_2	Z	H	G	ξ	η
MMA-HPA-1	0.5238	0.3880	1.5110	0.1500	-0.5626	0.1163	-0.4360
MMA-HPA-2	0.5576	0.4014	1.5892	0.2451	-0.4750	0.1769	-0.3428
MMA-HPA-3	0.5439	0.4278	1.4064	0.3179	-0.4850	0.2180	-0.3326
MMA-HPA-4	0.6965	0.6677	1.0821	0.3477	-0.6028	0.2337	-0.4051
MMA-HPA-5	0.5676	0.4787	1.2870	0.5081	-0.3822	0.3083	-0.2318
MMA-HPA-6	0.5522	0.4963	1.1715	0.5991	-0.3422	0.3444	-0.1967
MMA-HPA-7	0.6505	0.5879	1.1859	0.7377	-0.2212	0.3928	-0.1178
MMA-HPA-8	0.4743	0.3710	1.3871	1.0461	0.0332	0.4784	0.0152
MMA-HPA-9	0.4547	0.3793	1.2715	1.1987	0.1563	0.5125	0.0668
MMA-HPA-10	0.4090	0.3382	1.2742	1.4781	0.3753	0.5645	0.1433
MMA-HPA-11	0.4321	0.3959	1.1226	1.6372	0.5676	0.5894	0.2044
MMA-HPA-12	0.3959	0.3333	1.2432	2.2059	0.9700	0.6592	0.2899
MMA-HPA-13	0.3885	0.3584	1.1085	2.5298	1.3800	0.6893	0.3760
MMA-HPA14	0.2594	0.2524	1.0326	3.0838	2.0181	0.7300	0.4778
MMA-HPA-15	0.4196	0.4291	0.9706	3.9114	2.9998	0.7743	0.5938
MMA-HPA-16	0.4112	0.3912	1.0673	5.9564	4.6438	0.8393	0.6544
MMA-HPA-17	0.3938	0.4089	0.9522	8.6688	8.0539	0.8838	0.8211

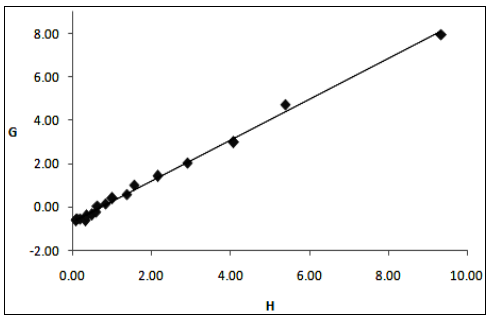

(a)

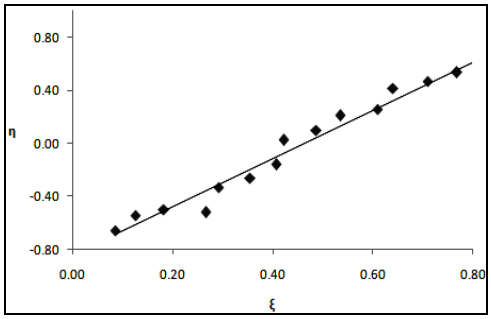

(b)

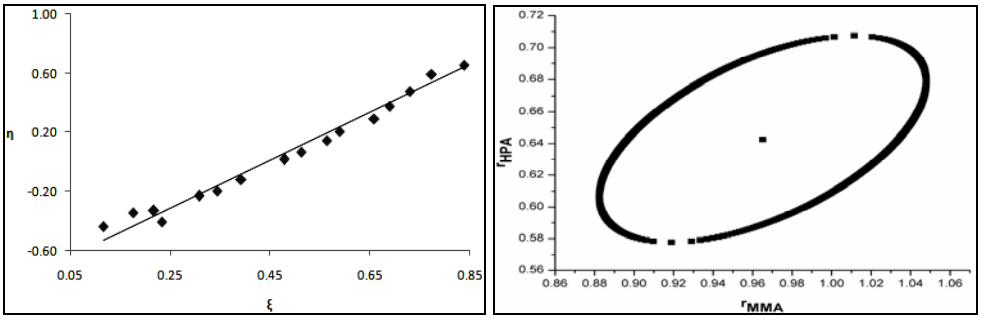

(c) **(d)**

Figure 4.28: (a) FR, (b) KT, (c) Ext. KT plots for poly(MMA-*co*-HPA) system and (d) 95% Joint confidence interval calculated by MH method

The 95 % joint confidence limit of the reactivity ratio values by Mao-Huglin method are plotted in Figure 4.28 (d). Its equation is,

$$5.4166(r_1-0.9652)^2-7.7277(r_1-0.9652)\,(r_2-0.6426)+8.8154\,(r_2-0.6426)^2=0.0255$$

The statistical distribution of the sequences of two monomers (dyad) M_{MMA}-M_{MMA}, M_{HPA}-M_{HPA} and M_{MMA}-M_{HPA} and mean sequence lengths μ_{MMA} and μ_{HPA} are presented in Table 4.39. The variation of the dyad fractions with the MMA mole fraction in the copolymers is displayed in Figure 4.29.

Table 4.39: Structural data for poly(MMA-*co*-HPA) system

Copolymer Code	M_{MMA}-M_{MMA}	M_{HPA}-M_{HPA}	M_{MMA}-M_{HPA}	μ_{MMA}	μ_{HPA}
MMA-HPA-1	0.0126	0.7517	0.2356	1.1052	7.4971
MMA-HPA-2	0.0299	0.6362	0.3339	1.1671	5.0908
MMA-HPA-3	0.0461	0.5637	0.3901	1.2367	3.8876
MMA-HPA-4	0.0533	0.5373	0.4094	1.3156	3.1657
MMA-HPA-5	0.0950	0.4211	0.4839	1.4057	2.6844
MMA-HPA-6	0.1198	0.3705	0.5097	1.5098	2.3407
MMA-HPA-7	0.1577	0.3086	0.5337	1.6311	2.0829
MMA-HPA-8	0.2377	0.2152	0.5471	1.7746	1.8823
MMA-HPA-9	0.2739	0.1836	0.5425	1.9467	1.7219
MMA-HPA-10	0.3340	0.1410	0.5250	2.1571	1.5906
MMA-HPA-11	0.3646	0.1230	0.5124	2.4201	1.4813
MMA-HPA-12	0.4565	0.0803	0.4632	2.7582	1.3887
MMA-HPA-13	0.4986	0.0652	0.4362	3.2090	1.3094
MMA-HPA14	0.5579	0.0476	0.3944	3.8401	1.2406
MMA-HPA-15	0.6249	0.0321	0.3429	4.7868	1.1805
MMA-HPA-16	0.7279	0.0155	0.2566	6.3646	1.1274
MMA-HPA-17	0.8010	0.0078	0.1912	9.5203	1.0802

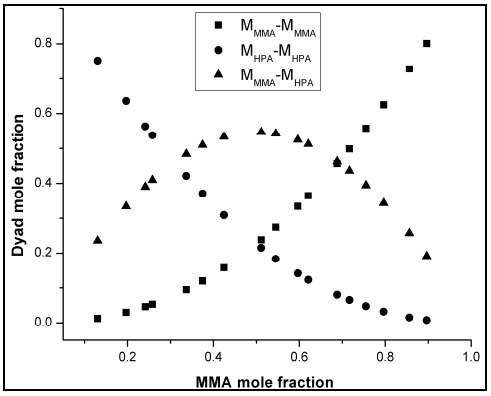

Figure 4.29: Dyad monomer sequence fractions verses the MMA mole fractions for the copolymers.

Table 4.40: Reactivity ratios of MMA and HPA computed by different models

Method	r_{MMA}	r_{HPA}
Finemann-Ross	0.9423	0.6902
Kelen-Tudos	0.9769	0.7356
Extended Kelen-Tudos	0.9023	0.8192
Mao-Huglin	0.9652	0.6426
Average	0.9467	0.7219

The r_{MMA} and r_{HPA} values obtained from four methods are in good agreement. The value of r_{MMA} is 0.9467 and that of r_{HPA} is 0.7219, which indicates greater incorporation of MMA units in the copolymer than in feed. The product of the reactivity ratios of two monomers $r_{MMA} \bullet r_{HPA}$ value is 0.6834. This being less than 1, suggests the tendency to form random copolymers. Since the r_1 and r_2 values are less than one, this system gives rise to azeotropic composition (equation 4.1) when the mole fraction of the monomer MMA in the feed is 0.8392.

4.10.2 Thermal analysis of poly(MMA-*co*-HPA)

The glass transition temperature (T_g) of poly(MMA_{25}-HPA_{75}), poly(MMA_{50}-HPA_{50}), and poly(MMA_{75}-HPA_{25}) were estimated by DSC as 15.2, 19.5 and 14.6ºC. The DSC thermograms and T_g of copolymers are given in Figure 4.30. These copolymers are suitable for evaluation as hydrogels.

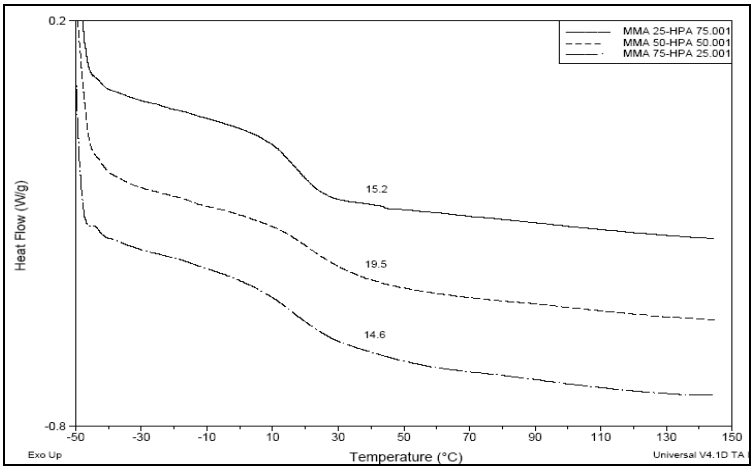

Figure 4.30: DSC thermograms of poly(MMA_{25}-HPA_{75}), poly(MMA_{50}-HPA_{50}), and poly(MMA_{75}-HPA_{25}).

4.11 Poly(2-ethylhexyl methacrylate-*co*-2-hydroxypropyl acrylate) System

The monomers EHMA and HPA are used in the preparation of multilayered films and chip-resistant multilayered coating films,[56] cationic electrodeposition coatings[57] and sealing of perforated articles.[58]

4.11.1 Reactivity ratio determination for poly(EHMA-*co*-HPA) system

The kinetic estimates of reactivity ratios of EHMA and HPA by Finemann-Ross (FR) and Kelen-Tudos (KT) are presented in Table 4.41. Similarly, the data for Extended Kelen-Tudos (Ext. KT) and Mao-Huglin (MH) methods.

Table 4.41: FR and KT parameters for poly(EHMA-*co*-HPA) system

Copolymer Code	$F=M_1/M_2$	$f=m_1/m_2$	$H=F^2/f$	$G=F(f-1)/f$	$\xi=H/(\alpha+H)$	$\eta=G/(\alpha+H)$
EHMA-HPA-1	0.1111	0.1121	0.1101	-0.8801	0.0967	-0.7724
EHMA-HPA-2	0.1765	0.1843	0.1690	-0.7811	0.1410	-0.6519
EHMA-HPA-3	0.2500	0.2431	0.2571	-0.7783	0.1999	-0.6051
EHMA-HPA-4	0.3333	0.3281	0.3386	-0.6826	0.2476	-0.4990
EHMA-HPA-5	0.4286	0.4219	0.4353	-0.5872	0.2972	-0.4009
EHMA-HPA-6	0.5385	0.5227	0.5547	-0.4917	0.3502	-0.3104
EHMA-HPA-7	0.6667	0.6513	0.6824	-0.3569	0.3987	-0.2085
EHMA-HPA-8	0.8182	0.7703	0.8691	-0.2440	0.4578	-0.1285
EHMA-HPA-9	1.0000	0.9819	1.0185	-0.0185	0.4974	-0.0090
EHMA-HPA-10	1.2222	1.1631	1.2843	0.1714	0.5551	0.0741
EHMA-HPA-11	1.5000	1.4613	1.5397	0.4735	0.5994	0.1843
EHMA-HPA-12	1.8571	1.7503	1.9705	0.7961	0.6569	0.2654
EHMA-HPA-13	2.3333	2.2134	2.4598	1.2791	0.7050	0.3666
EHMA-HPA14	3.0000	2.7202	3.3086	1.8971	0.7627	0.4373
EHMA-HPA-15	4.0000	3.5962	4.4491	2.8877	0.8121	0.5271
EHMA-HPA-16	5.6667	5.3510	6.0009	4.6077	0.8536	0.6554
EHMA-HPA-17	9.0000	8.4192	9.6209	7.9310	0.9034	0.7447

Table 4.42: Extended Kelen-Tudos parameters for poly(EHMA-*co*-HPA) system

Copolymer Code	ζ_1	ζ_2	Z	H	G	ξ	H
EHMA-HPA-1	0.8923	0.8844	1.0327	0.1051	-0.8598	0.0821	-0.6713
EHMA-HPA-2	0.9456	0.9055	1.2341	0.1210	-0.6610	0.0933	-0.5098
EHMA-HPA-3	0.8591	0.8834	0.9120	0.2923	-0.8299	0.1991	-0.5654
EHMA-HPA-4	0.9454	0.9605	0.9000	0.4050	-0.7465	0.2562	-0.4723
EHMA-HPA-5	0.9359	0.9507	0.9130	0.5062	-0.6332	0.3010	-0.3765
EHMA-HPA-6	0.8816	0.9082	0.8935	0.6548	-0.5342	0.3577	-0.2919
EHMA-HPA-7	0.8829	0.9037	0.9165	0.7755	-0.3805	0.3975	-0.1950
EHMA-HPA-8	0.8248	0.8761	0.8342	1.1070	-0.2754	0.4850	-0.1206
EHMA-HPA-9	0.8508	0.8665	0.9447	1.1001	-0.0192	0.4834	-0.0084
EHMA-HPA-10	0.8431	0.8860	0.8531	1.5983	0.1912	0.5762	0.0689
EHMA-HPA-11	0.7871	0.8079	0.9375	1.6625	0.4920	0.5858	0.1734
EHMA-HPA-12	0.8282	0.8787	0.8349	2.5112	0.8987	0.6811	0.2438
EHMA-HPA-13	0.7995	0.8428	0.8684	2.9350	1.3972	0.7140	0.3399
EHMA-HPA14	0.8011	0.8835	0.7511	4.8212	2.2901	0.8040	0.3819
EHMA-HPA-15	0.8372	0.9312	0.6781	7.8207	3.8286	0.8693	0.4256
EHMA-HPA-16	0.8516	0.9019	0.8219	7.9210	5.2938	0.8708	0.5819
EHMA-HPA-17	0.8429	0.9011	0.8002	13.1499	9.2722	0.9179	0.6473

The significance of the parameters of FR and KT for the method is shown in Table 4.41. The graphical copolymerisation plots of FR, KT and extended KT are presented in Figures 4.31 (a-c). The plots are linear for all graphical methods, indicating that these follow conventional copolymerisation kinetics. The reactivity ratios of EHMA and HPA are denoted as r_{EHMA} (or r_1) and r_{HPA} (or r_2) respectively and the values obtained from various methods are presented in Table 4.44.

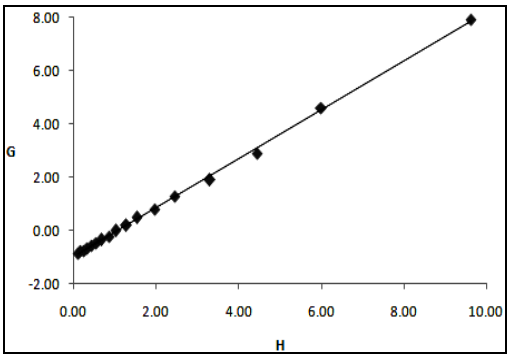

(a)

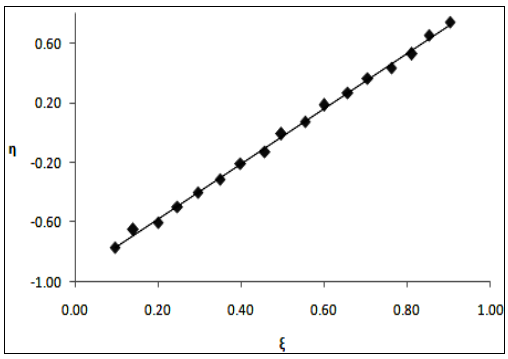

(b)

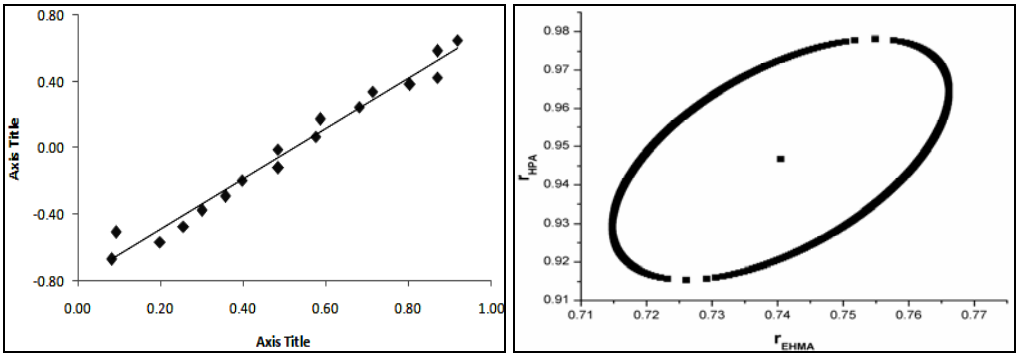

(c) **(d)**

Figure 4.31: (a) FR, (b) KT, (c) Ext. KT plots for poly(EHMA-*co*-HPA) system, and (d) 95% Joint confidence interval calculated by MH method

The 95 % joint confidence limit of the reactivity ratio calculated by Mao-Huglin method is plotted in Figure 4.31 (d). Its equation is,

$$5.4431(r_1\text{-}0.7405)^2\text{-}5.0022(r_1\text{-}0.7405)\,(r_2\text{-}0.9468) + 3.6428(r_2\text{-}0.9468)^2 = 0.0025$$

The statistical distribution of the sequences of two monomers (dyad) M_{EHMA}-M_{EHMA}, M_{HPA}-M_{HPA} and M_{EHMA}-M_{HPA} and mean sequence lengths μ_{EHMA} and μ_{HPA} are presented in Table 4.43. The variation of the dyad fractions with the EHMA mole fraction in the copolymers is displayed in Figure 4.32.

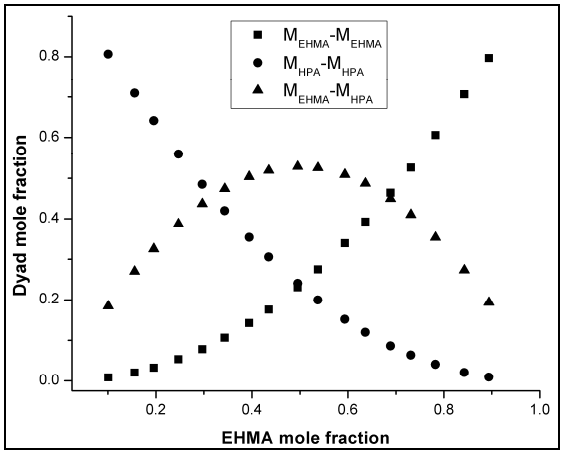

Figure 4.32: Dyad monomer sequence fractions verses the EHMA mole fractions for the copolymers.

Table 4.43: Structural data for poly(EHMA-*co*-HPA) system

Copolymer Code	M_{EHMA}-M_{EHMA}	M_{HPA}-M_{HPA}	M_{EHMA}-M_{HPA}	μ_{EHMA}	μ_{HPA}
EHMA-HPA-1	0.0084	0.8068	0.1848	1.0914	9.7012
EHMA-HPA-2	0.0205	0.7093	0.2703	1.1451	6.4785
EHMA-HPA-3	0.0328	0.6417	0.3255	1.2056	4.8672
EHMA-HPA-4	0.0533	0.5593	0.3874	1.2742	3.9004
EHMA-HPA-5	0.0783	0.4848	0.4369	1.3525	3.2559
EHMA-HPA-6	0.1063	0.4198	0.4739	1.4429	2.7955
EHMA-HPA-7	0.1426	0.3537	0.5037	1.5483	2.4502
EHMA-HPA-8	0.1755	0.3053	0.5192	1.6730	2.1816
EHMA-HPA-9	0.2311	0.2403	0.5286	1.8225	1.9668
EHMA-HPA-10	0.2750	0.1996	0.5254	2.0053	1.7910
EHMA-HPA-11	0.3392	0.1518	0.5090	2.2338	1.6445
EHMA-HPA-12	0.3929	0.1201	0.4871	2.5275	1.5206
EHMA-HPA-13	0.4641	0.0865	0.4494	2.9192	1.4143
EHMA-HPA14	0.5260	0.0636	0.4103	3.4675	1.3223
EHMA-HPA-15	0.6058	0.0409	0.3532	4.2900	1.2417
EHMA-HPA-16	0.7061	0.0210	0.2730	5.6608	1.1706
EHMA-HPA-17	0.7970	0.0094	0.1936	8.4025	1.1074

Table 4.44: Reactivity ratios of EHMA and HPA computed by different models

Method	r_{EHMA}	r_{HPA}
Finemann-Ross	0.9203	1.0044
Kelen-Tudos	0.9048	0.9802
Extended Kelen-Tudos	0.7243	0.9358
Mao-Huglin	0.7405	0.9468
Average	0.8225	0.9668

The value average value of r_{EHMA} is equal to 0.8225 and that of r_{HPA} is equal to 0.9668, which indicates the higher incorporation of HPA units in the copolymer than in feed. The product of the reactivity ratios of two monomers $r_{EHMA} \bullet r_{HPA}$ value is 0.7952. This value is indicative of the tendency towards the formation of random copolymers. Since the r_1 and r_2 values are less than one, this system gives rise to azeotropic polymerisation at a particular composition of the monomers which is calculated equation 4.1 as when the mole fraction of the EHMA in the feed is 0.1576. The copolymer formed will have the same composition as that of the feed.

4.11.2 Thermal analysis of poly(EHMA-*co*-HPA)

Glass transition temperature (T_g) of poly($EHMA_{25}$-HPA_{75}), poly($EHMA_{50}$-HPA_{50}), and poly($EHMA_{75}$-HPA_{25}) estimated by DSC were 8.5, -15.2 and -15.8, respectively. The DSC thermograms of copolymers are given in Figure 4.33. The T_g

values of homopolymer of EHMA and HPA are -10 ºC and 14 ºC respectively. This copolymer is suitable for evaluation as hydrogel.

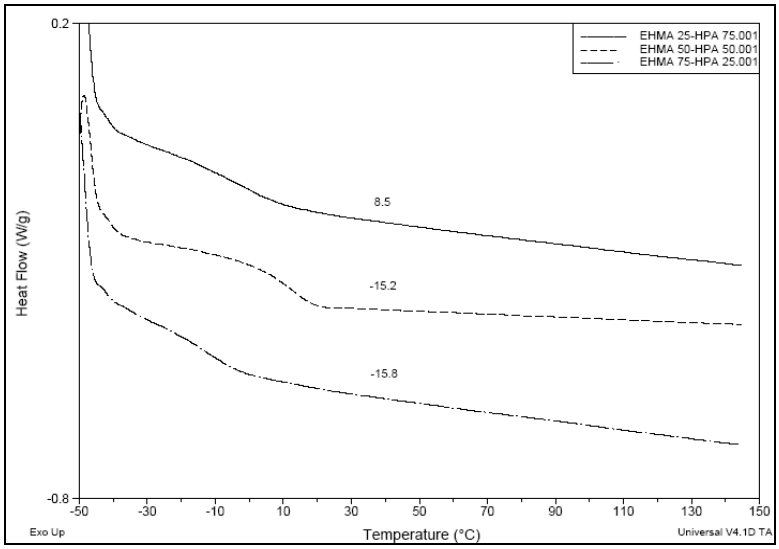

Figure 4.33: DSC thermograms of poly($EHMA_{25}$-HPA_{75}), poly($EHMA_{50}$-HPA_{50}), and poly($EHMA_{75}$-HPA_{25}).

4.12 Poly(2-hydroxyethyl acrylate-*co*-2-hydroxypropyl acrylate) System

2-Hydroxyethyl acrylate and 2-hydroxypropyl acrylate are used in alcohol-soluble acrylic thermoplastic resin,[59] UV curable inks,[60] iron-silicon-modified water-soluble acrylic resin dispersion,[61] and in liquid curable urethane acrylate compositions to display good blocking resistance after cure for applications in optical fibres.[62]

4.12.1 Reactivity ratio determination for poly(HEA-*co*-HPA) system

The reactivity ratios of HEA and HPA were estimated by Finemann-Ross (FR), Kelen-Tudos (KT), Extended Kelen-Tudos (Ext. KT) and Mao-Huglin (MH) methods. The parameters of FR and KT for the copolymers are presented in Table 4.45 and of Extended KT is shown in Table 4.46. The graphical copolymerisation plots of FR, KT and extended KT are presented in Figures 4.34 (a-c). The plots are all highly scattered for all graphical methods, indicating that these do not follow conventional copolymerisation kinetics. The reactivity ratios of HEA and HPA are denoted as r_{HEA} (or r_1) and r_{HPA} (or r_2) respectively and the values obtained from various methods are presented in Table 4.48.

Table 4.45: FR and KT parameters for poly(HEA-*co*-HPA) system

Copolymer Code	$F=M_1/M_2$	$f=m_1/m_2$	$H=F^2/f$	$G=F(f-1)/f$	$\xi=H/(\alpha+H)$	$\eta=G/(\alpha+H)$
HEA-HPA-1	0.1765	0.2137	0.1457	-0.6491	0.0538	-0.2396
HEA-HPA-2	0.2500	0.2703	0.2312	-0.6749	0.0827	-0.2415
HEA-HPA-3	0.3333	0.4184	0.2655	-0.4633	0.0938	-0.1637
HEA-HPA-4	0.5385	0.5563	0.5212	-0.4295	0.1689	-0.1392
HEA-HPA-5	0.6667	0.7254	0.6127	-0.2523	0.1929	-0.0794
HEA-HPA-6	0.8182	0.8239	0.8125	-0.1749	0.2407	-0.0518
HEA-HPA-7	1.5000	0.9193	2.4474	-0.1316	0.4884	-0.0263
HEA-HPA-8	1.8571	0.9601	3.5924	-0.0772	0.5835	-0.0125
HEA-HPA-9	5.6667	1.2363	25.9733	1.0832	0.9102	0.0380
HEA-HPA-10	9.0000	1.7954	45.1141	3.9873	0.9462	0.0836

Table4.46: Extended Kelen-Tudos parameters for poly(HEA-*co*-HPA) system

Copolymer Code	ζ_1	ζ_2	Z	H	G	ξ	H
HEA-HPA-1	0.5096	0.4207	1.3050	0.1255	-0.6025	0.0481	-0.2308
HEA-HPA-2	0.6933	0.6413	1.1530	0.2033	-0.6329	0.0756	-0.2354
HEA-HPA-3	0.2466	0.1964	1.2947	0.2496	-0.4492	0.0913	-0.1642
HEA-HPA-4	0.2814	0.2724	1.0393	0.5151	-0.4269	0.1717	-0.1423
HEA-HPA-5	0.0713	0.0655	1.0915	0.6089	-0.2516	0.1968	-0.0813
HEA-HPA-6	0.0525	0.0521	1.0071	0.8122	-0.1749	0.2463	-0.0530
HEA-HPA-7	0.0306	0.0500	0.6068	2.4969	-0.1329	0.5012	-0.0267
HEA-HPA-8	0.0432	0.0836	0.5061	3.7489	-0.0789	0.6013	-0.0127
HEA-HPA-9	0.0226	0.1038	0.2090	28.2981	1.1306	0.9193	0.0367
HEA-HPA-10	0.0206	0.1032	0.1910	49.2230	4.1649	0.9519	0.0805

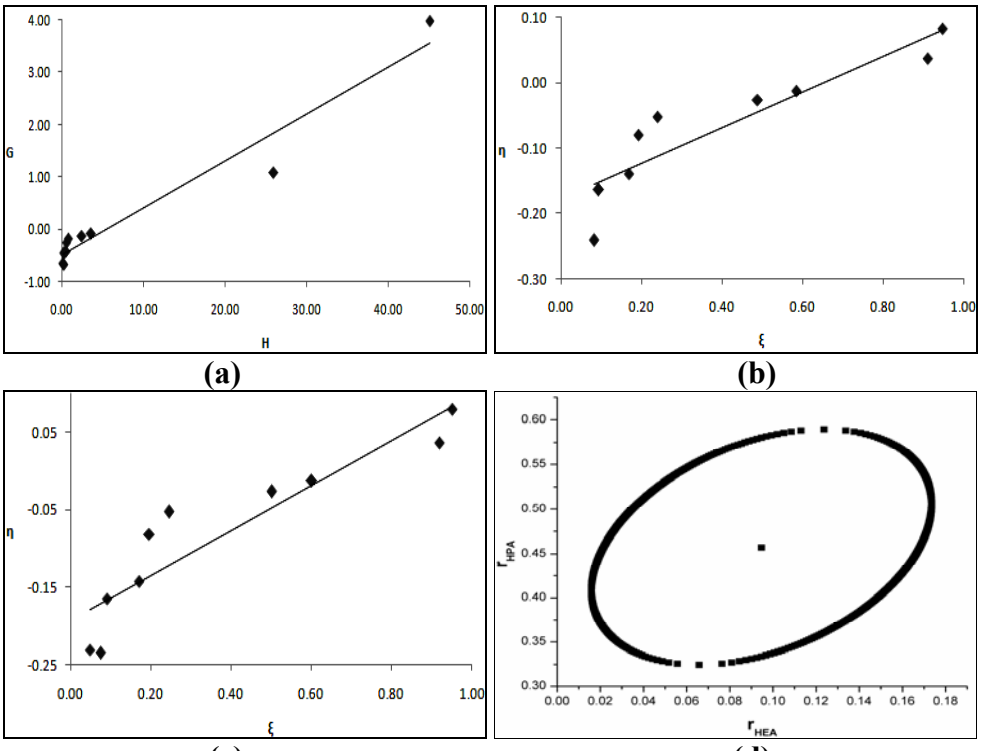

(a) **(b)**

(c) **(d)**

Figure 4.34: (a) FR, (b) KT, (c) Ext. KT plots for poly(HEA-*co*-HPA) system and (d) 95% Joint confidence interval calculated by MH method

The 95 % joint confidence limit of the reactivity ratio values by Mao-Huglin method is plotted in Figure 4.34 (d). Its equation is,

$$2.5851(r_1-0.0947)^2-1.1299(r_1-0.0947)\,(r_2-0.4570)+0.9144(r_2-0.4570)^2=0.0139$$

The statistical distribution of the sequences of two monomers (dyad) M_{HEA}-M_{HEA}, M_{HPA}-M_{HPA} and M_{HEA}-M_{HPA} and mean sequence lengths μ_{EHMA} and μ_{HPA} are presented in Table 4.47, and the variation of the dyad fractions with the HEA mole fraction in the copolymers is displayed in Figure 4.35.

Table 4.47: Structural data for poly(HEA-*co*-HPA) system

Copolymer Code	M_{HEA}-M_{HEA}	M_{HPA}-M_{HPA}	M_{HEA}-M_{HPA}	μ_{HEA}	μ_{HPA}
HEA-HPA-1	0.0021	0.6499	0.3481	1.0167	3.6730
HEA-HPA-2	0.0034	0.5778	0.4188	1.0236	2.8868
HEA-HPA-3	0.0087	0.4187	0.5726	1.0315	2.4151
HEA-HPA-4	0.0171	0.3022	0.6808	1.0508	1.8760
HEA-HPA-5	0.0343	0.1934	0.7722	1.0629	1.7076
HEA-HPA-6	0.0494	0.1460	0.8047	1.0772	1.5765
HEA-HPA-7	0.0682	0.1102	0.8216	1.1416	1.3145
HEA-HPA-8	0.0774	0.0978	0.8248	1.1753	1.2540
HEA-HPA-9	0.1525	0.0468	0.8007	1.5349	1.0832
HEA-HPA-10	0.3017	0.0171	0.6812	1.8496	1.0524

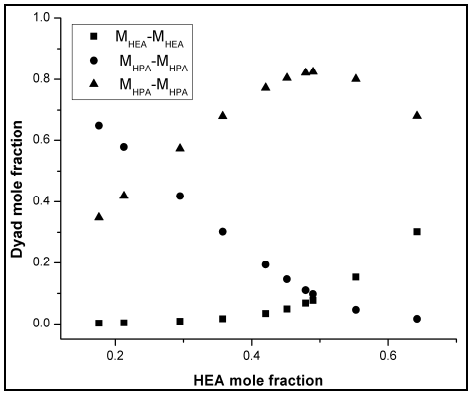

Figure 4.35: Dyad monomer sequence fractions verses the HEA mole fractions for the copolymers.

Table 4.48: Reactivity ratios of HEA and HPA computed by different models

Method	r_{HEA}	r_{HPA}
Finemann-Ross	0.0902	0.4964
Kelen-Tudos	0.0964	0.4564
Extended Kelen-Tudos	0.0975	0.4772
Mao-Huglin	0.0947	0.4570
Average	0.0944	0.4717

The r_{HEA} and r_{HPA} values obtained from four methods are quite similar. The average value of r_{HEA} is 0.0944 and that of r_{HPA} is 0.4717, which indicates the higher incorporation of HPA units in the copolymer than that in the feed. The product of the reactivity ratios of two monomers $r_{HEA} \bullet r_{HPA}$ value is 0.0445 suggesting the formation of random copolymers. Since the r_1 and r_2 values are less than one, this system gives rise to azeotropic polymerisation at a particular composition, it was calculated to occur, using equation 4.1, when the mole fraction of the monomer HEA in the feed is 0.3684.

4.12.2 Thermal analysis of poly(HEA-*co*-HPA)

Glass transition temperature (T_g) of poly(HEA_{25}-HPA_{75}), poly(HEA_{50}-HPA_{50}), and poly(HEA_{75}-HPA_{25}) were determined using DSC as -8.9, -8.4 and -8.4ºC. The DSC thermograms of copolymers are presented in Figure 4.36.

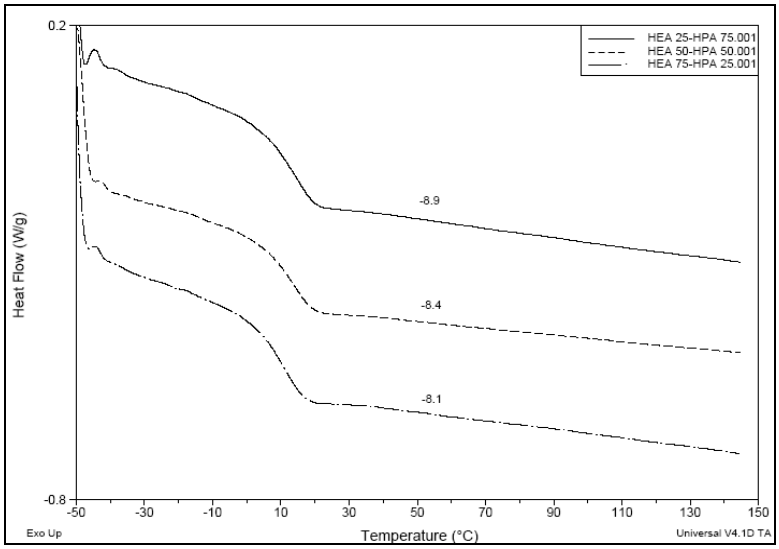

Figure 4.36: DSC thermograms of poly(HEA_{25}-HPA_{75}), poly(HEA_{50}-HPA_{50}), and poly(HEA_{75}-HPA_{25}).

The T_g values of parent homopolymers of HEA and HPA are 2 ºC and 14 ºC respectively. The copolymerization depresses the T_g below that of the homopolymers over a wide composition range. This shows that this copolymer series is suited to further evaluation as hydrogels.

4.13 Poly(methyl acrylate-*co*-2-hydroxyethyl methacrylate) System

Methyl acrylate and 2-hydroxyethyl methacrylate polymers have been studied before microstructural features.[63] These polymers are used as temporary skin substitutes and studies showed that increase in methyl acrylate content in the copolymer, the equilibrium water content, equilibrium water retention, water vapour

transmission, glass transition temperature and tensile stress at break all decrease.[64] Copolymerisation of 2-hydroxyethyl methacrylate with methyl acrylate in ethanol gave a ternary copolymer due to the formation of a hydrophobic third monomer by ester exchange during the polymerisation while that in N,N'-dimethyl acetamide as solvent did not give a terpolymer structure.[65]

4.13.1 Reactivity ratio determination for poly(MA-*co*-HEMA) system

The reactivity ratios of MA and HEMA were determined by Finemann-Ross (FR), Kelen-Tudos (KT), extended Kelen-Tudos (Ext..KT) and Mao-Huglin (MH) methods. The kinetic parameters of FR, KT and ext.KT for copolymers are presented in Tables 4.49 and 4.50. The graphical copolymerisation plots of FR, KT and extended KT are presented in Figures 4.37 (a-c). The plots are some what scattered for all graphical methods, indicating that these may not follow conventional copolymerisation kinetics. The reactivity ratios of MA and HEMA are denoted as r_{MA} (or r_1) and r_{HEMA} (or r_2) respectively and the values obtained from various methods are presented in Table 4.52.

Table 4.49: FR and KT parameters for poly(MA-*co*-HEMA) system

Copolymer Code	$F=M_1/M_2$	$f=m_1/m_2$	$H=F^2/f$	$G=F(f-1)/f$	$\xi=H/(\alpha+H)$	$\eta=G/(\alpha+H)$
MA-HEMA-1	0.1111	0.0421	0.2933	-2.5282	0.1064	-0.9173
MA-HEMA-2	0.1765	0.0841	0.3704	-1.9221	0.1308	-0.6783
MA-HEMA-3	0.2501	0.1114	0.5613	-1.9947	0.1856	-0.6595
MA-HEMA-4	0.3334	0.1286	0.8646	-2.2598	0.2598	-0.6792
MA-HEMA-5	0.5386	0.1699	1.7071	-2.6310	0.4094	-0.6310
MA-HEMA-6	1.2225	0.4842	3.0867	-1.3025	0.5562	-0.2347
MA-HEMA-7	1.8575	0.9492	3.6352	-0.0995	0.5961	-0.0163
MA-HEMA-8	4.0008	1.7041	9.3930	1.6530	0.7923	0.1394
MA-HEMA-9	5.6678	2.4296	13.2218	3.3350	0.8430	0.2127
MA-HEMA-10	9.0018	3.9184	20.6799	6.7045	0.8936	0.2897

Table 4.50: Extended Kelen-Tudos parameters for poly(MA-*co*-HEMA) system

Copolymer Code	ζ_1	ζ_2	Z	H	G	ξ	H
MA-HEMA-1	0.2634	0.6952	0.2573	0.6360	-3.7228	0.1387	-0.8119
MA-HEMA-2	0.3427	0.7191	0.3304	0.7704	-2.7716	0.1632	-0.5872
MA-HEMA-3	0.3171	0.7118	0.3066	1.1854	-2.8984	0.2309	-0.5645
MA-HEMA-4	0.2450	0.6354	0.2786	1.6566	-3.1281	0.2955	-0.5580
MA-HEMA-5	0.1732	0.5490	0.2389	2.9782	-3.4752	0.4299	-0.5016
MA-HEMA-6	0.1296	0.3272	0.3502	3.9477	-1.4729	0.4999	-0.1865
MA-HEMA-7	0.1223	0.2393	0.4768	4.1744	-0.1066	0.5138	-0.0131
MA-HEMA-8	0.1486	0.3488	0.3750	12.1200	1.8779	0.7542	0.1169
MA-HEMA-9	0.1205	0.2811	0.3891	16.0503	3.6753	0.8025	0.1838
MA-HEMA-10	0.1109	0.2548	0.3997	24.5249	7.3012	0.8613	0.2564

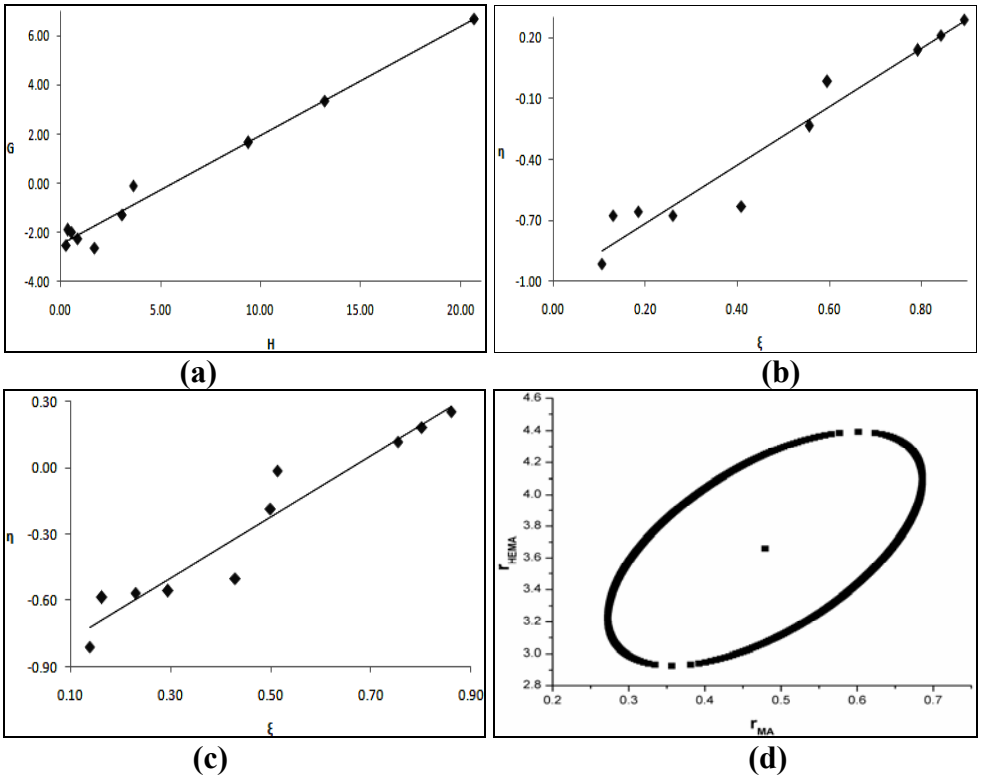

Figure 4.37: (a) FR, (b) KT, (c) Ext. KT plots for poly(MA-*co*-HEMA) system and (d) 95% Joint confidence interval calculated by MH method

The 95 % joint confidence limit of the reactivity ratio by Mao-Huglin method is plotted in Figure 4.37 (d). Its equation is,

$$2.8752(r_1-0.4791)^2 - 0.9602(r_1-0.4791)(r_2-3.6598) + 0.2279(r_2-3.6598)^2 = 0.0796$$

The statistical distribution of the sequences of two monomers (dyad) M_{MA}-M_{MA}, M_{HEMA}-M_{HEMA} and M_{MA}-M_{HEMA} and mean sequence lengths μ_{MA} and μ_{HEMA} are presented in Table 4.51, and the variation of the dyad fractions with the MA mole fraction in the copolymers is displayed in Figure 4.38.

Table 4.51: Structural data for poly(MA-*co*-HEMA) system

Copolymer Code	M_{MA}-M_{HEMA}	M_{HEMA}-M_{HEMA}	M_{MA}-M_{HEMA}	μ_{MA}	μ_{HEMA}
MA-HEMA-1	0.0182	0.9374	0.0444	1.0508	28.5497
MA-HEMA-2	0.0358	0.8806	0.0836	1.0807	18.3431
MA-HEMA-3	0.0469	0.8464	0.1067	1.1143	13.2429
MA-HEMA-4	0.0538	0.8259	0.1203	1.1523	10.1832
MA-HEMA-5	0.0700	0.7795	0.1505	1.2461	6.6849
MA-HEMA-6	0.1783	0.5259	0.2958	1.5586	3.5045
MA-HEMA-7	0.3015	0.3276	0.3709	1.8487	2.6483
MA-HEMA-8	0.4409	0.1805	0.3787	2.8280	1.7653
MA-HEMA-9	0.5322	0.1153	0.3525	3.5898	1.5402
MA-HEMA-10	0.6508	0.0574	0.2918	5.1129	1.3401

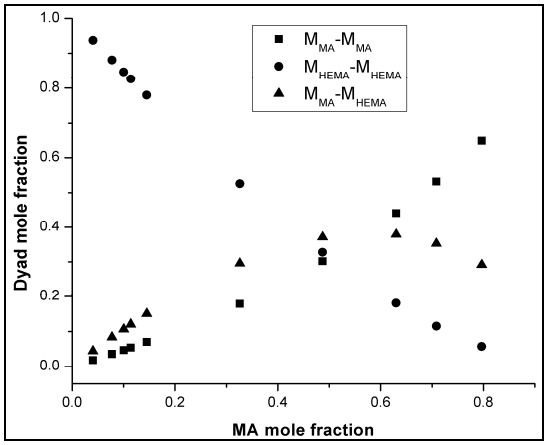

Figure 4.38: Dyad monomer sequence fractions verses the MA mole fractions for the copolymers.

Table 4.52: Reactivity ratios of MA and HEMA computed by different models

Method	r_{MA}	r_{HEMA}
Finemann-Ross	0.4451	2.4991
Kelen-Tudos	0.4343	2.4702
Extended Kelen-Tudos	0.4692	3.6177
Mao-Huglin	0.4791	3.6598
Average	0.4569	3.0617

The r_{MA} and r_{HEMA} values obtained from differential form and integrated forms differ, especially for the more reactive comonomer, HEMA. The average value of r_{MA} is 0.4569 and that of r_{HEMA} is 3.0617, which indicates the higher incorporation of HEMA units in the copolymer than in feed. The product of the reactivity ratios of two monomers $r_{MA} \bullet r_{HEMA}$ value is 1.3989 which suggests a tendency for the formation of long sequence length in the copolymer chain.

4.13.2 Thermal analysis of poly(MA-*co*-HEMA)

Glass transition temperature (T_g) of poly(MA_{25}-$HEMA_{75}$), poly(MA_{50}-$HEMA_{50}$), and poly(MA_{75}-$HEMA_{25}$) determined by DSC were 71.1, 55.4 and 18.4°C. The DSC thermograms with T_g values of copolymers are given in Figure 4.39. The T_g of poly(MA) is 10°C, and that of poly(HEMA) is 76°C. The results indicate that T_g decreases with increase MA mole fraction in copolymer.

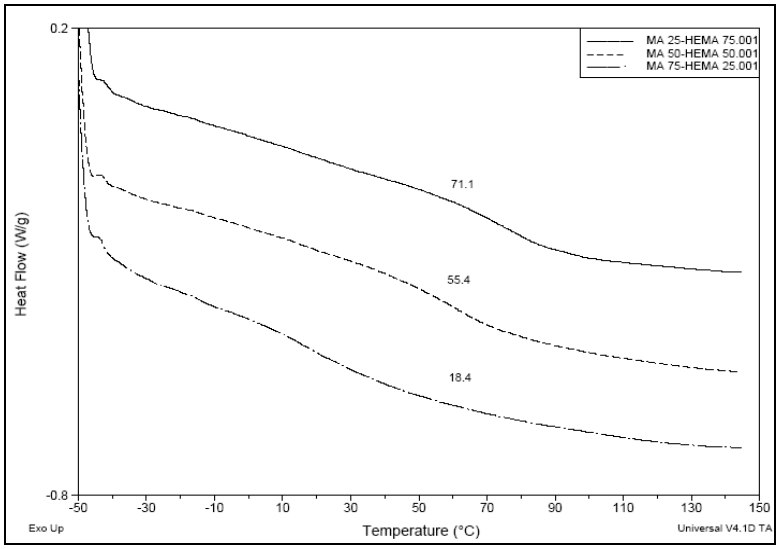

Figure 4.39: DSC thermograms of poly(MA_{25}-$HEMA_{75}$), poly(MA_{50}-$HEMA_{50}$), and poly(MA_{75}-$HEMA_{25}$).

4.14 Poly(butyl acrylate-*co*-2-hydroxyethyl methacrylate) System

Butyl acrylate-*co*-2-hydroxyethyl methacrylate block copolymer can be grafted on carbon fibre by controlled polymerisation.[66] These polymers are used in the preparation of acrylic adhesive compositions that have reduced oxygen polymerization inhibition and good low-temperature curability.[67] Thin polymer films of poly(butyl acrylate) and poly(hydroxyethyl methacrylate) generate well-ordered arrays of functional patterned polymeric nanostructures.[68] Poly(BA-*co*-HEMA) has been used to evaluate the effect of solvent on free radical copolymerisation,[69,70] non-seeded emulsion polymerisation,[71] structural analysis,[72] reactivity ratio[73]etc. These polymers have also been evaluated for drug release including *in vitro* kinetics and release mechanism of pentoxifylline from coated pellets and compacts.[74]

4.14.1 Reactivity ratio determination for poly(BA-*co*-HEMA) system

The reactivity ratios of BA and HEMA were determined by Finemann-Ross (FR), Kelen-Tudos (KT), Extended Kelen-Tudos (Ext. KT) and Mao-Huglin (MH) methods. The kinetic parameters of FR and KT are presented in Table 4.53 and that for Extended KT is shown in Table 4.54. The graphical copolymerisation plots of FR, KT and Extended KT are presented in Figures 4.40 (a-c). The plots are highly scattered for all graphical methods, indicating that these do not follow conventional copolymerisation kinetics. The reactivity ratios of BA and HEMA are denoted as r_{BA} (or r_1) and r_{HEMA} (or r_2) respectively and the values obtained from various methods are presented in Table 4.56.

Table 4.53: FR and KT parameters for poly(BA-*co*-HEMA) system

Copolymer Code	$F=M_1/M_2$	$f=m_1/m_2$	$H=F^2/f$	$G=F(f-1)/f$	$\xi=H/(\alpha+H)$	$\eta=G/(\alpha+H)$
BA-HEMA-1	0.1111	0.0429	0.2876	-2.4777	0.1207	-1.0393
BA-HEMA-2	0.1765	0.0953	0.3269	-1.6760	0.1349	-0.6916
BA-HEMA-3	0.2500	0.0953	0.6561	-2.3744	0.2384	-0.8627
BA-HEMA-4	0.3333	0.1680	0.6613	-1.6505	0.2398	-0.5985
BA-HEMA-5	0.4286	0.2281	0.8054	-1.4506	0.2775	-0.4999
BA-HEMA-6	0.5385	0.2535	1.1436	-1.5853	0.3530	-0.4893
BA-HEMA-7	0.6667	0.2489	1.7858	-2.0120	0.4600	-0.5183
BA-HEMA-8	0.8182	0.2411	2.7761	-2.5748	0.5698	-0.5284
BA-HEMA-9	1.0000	0.3033	3.2973	-2.2973	0.6113	-0.4259
BA-HEMA-10	1.2222	0.4077	3.6644	-1.7760	0.6361	-0.3083
BA-HEMA-11	1.8571	0.7970	4.3275	-0.4731	0.6737	-0.0736
BA-HEMA-12	2.3333	0.9668	5.6313	-0.0801	0.7287	-0.0104
BA-HEMA-13	4.0000	2.1176	7.5557	2.1111	0.7828	0.2187
BA-HEMA-14	9.0000	5.3013	15.2793	7.3023	0.8794	0.4203

Table 4.54: Extended Kelen-Tudos parameters for poly(BA-*co*-HEMA) system

Copolymer Code	ζ_1	ζ_2	Z	H	G	ξ	H
BA-HEMA-1	0.2742	0.7099	0.2590	0.6399	-3.6954	0.1664	-0.9611
BA-HEMA-2	0.3826	0.7087	0.3909	0.6233	-2.3143	0.1628	-0.6045
BA-HEMA-3	0.2638	0.6924	0.2598	1.4114	-3.4825	0.3057	-0.7544
BA-HEMA-4	0.3502	0.6947	0.3633	1.2729	-2.2899	0.2843	-0.5114
BA-HEMA-5	0.3781	0.7105	0.3832	1.5535	-2.0147	0.3265	-0.4234
BA-HEMA-6	0.2818	0.5985	0.3628	1.9268	-2.0578	0.3755	-0.4010
BA-HEMA-7	0.2011	0.5387	0.2902	2.9553	-2.5883	0.4797	-0.4202
BA-HEMA-8	0.1152	0.3908	0.2469	3.9553	-3.0734	0.5524	-0.4292
BA-HEMA-9	0.1293	0.4264	0.2491	4.8861	-2.7966	0.6039	-0.3456
BA-HEMA-10	0.1138	0.3412	0.2895	4.8643	-2.0462	0.6028	-0.2536
BA-HEMA-11	0.1013	0.2361	0.3967	5.0651	-0.5118	0.6125	-0.0619
BA-HEMA-12	0.0797	0.1924	0.3888	6.3965	-0.0854	0.6662	-0.0089
BA-HEMA-13	0.0625	0.1181	0.5137	8.0240	2.1755	0.7146	0.1937
BA-HEMA-14	0.0965	0.1638	0.5672	16.4792	7.5836	0.8372	0.3853

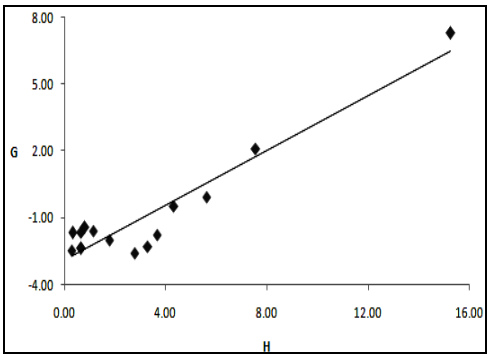

(a)

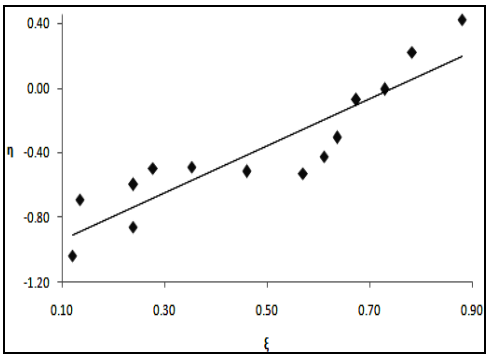

(b)

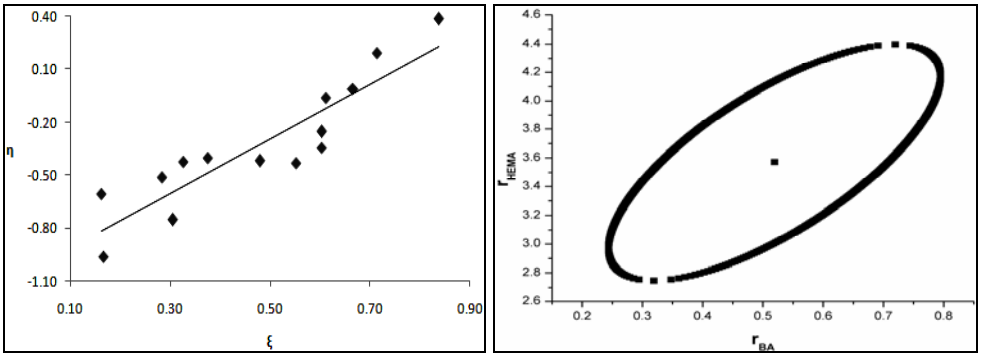

(c) **(d)**

Figure 4.40: (a) FR, (b) KT, (c) Extended KT plots for poly(BA-*co*-HEMA) system and (d) 95% Joint confidence interval calculated by MH method

The 95 % joint confidence limit of the reactivity ratio calculated by Mao-Huglin method is plotted in Figure 4.40 (d). Its equation is,

$$3.7365(r_1-0.5193)^2 - 1.8145(r_1-0.5193)(r_2-3.5721) + 0.4160(r_2-3.5721)^2 = 0.1333$$

The statistical distribution of the sequences of two monomers (dyad) M_{BA}-M_{BA}, M_{HEMA}-M_{HEMA} and M_{BA}-M_{HEMA} and mean sequence lengths μ_{BA} and μ_{HEMA} are presented in Table 4.55, and the variation of the dyad fractions with the BA mole fraction in the copolymers is displayed in Figure 4.41.

Table 4.55: Structural data for poly(BA-*co*-HEMA) system

Copolymer Code	M_{BA}-M_{BA}	M_{HEMA}-M_{HEMA}	M_{BA}-M_{HEMA}	μ_{BA}	μ_{HEMA}
BA-HEMA-1	0.0025	0.9202	0.0774	1.0553	28.4149
BA-HEMA-2	0.0106	0.8366	0.1528	1.0878	18.2612
BA-HEMA-3	0.0106	0.8366	0.1528	1.1245	13.1844
BA-HEMA-4	0.0277	0.7400	0.2324	1.1659	10.1383
BA-HEMA-5	0.0447	0.6733	0.2819	1.2133	8.1076
BA-HEMA-6	0.0525	0.6480	0.2995	1.2680	6.6570
BA-HEMA-7	0.0511	0.6525	0.2964	1.3319	5.5692
BA-HEMA-8	0.0487	0.6601	0.2912	1.4073	4.7230
BA-HEMA-9	0.0681	0.6027	0.3291	1.4978	4.0461
BA-HEMA-10	0.1020	0.5228	0.3751	1.6084	3.4923
BA-HEMA-11	0.2220	0.3350	0.4430	1.9245	2.6402
BA-HEMA-12	0.2675	0.2844	0.4480	2.1615	2.3055
BA-HEMA-13	0.4816	0.1231	0.3954	2.9912	1.7615
BA-HEMA-14	0.7159	0.0333	0.2508	5.4802	1.3385

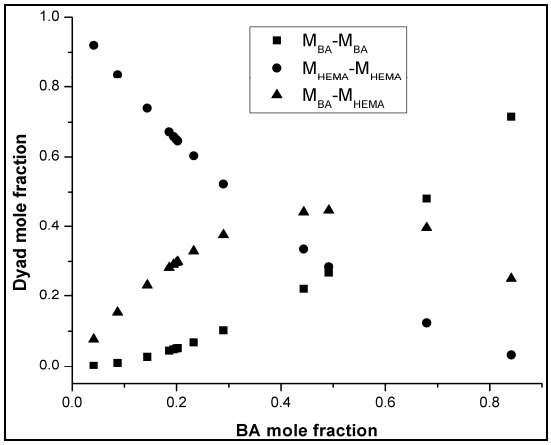

Figure 4.41: Dyad monomer sequence fractions verses the BA mole fractions for the copolymers.

Table 4.56: Reactivity ratios of BA and HEMA computed by different models

Method	r_{BA}	r_{HEMA}
Finemann-Ross	0.6152	2.9051
Kelen-Tudos	0.3734	2.2743
Extended Kelen-Tudos	0.4833	3.4322
Mao-Huglin	0.5193	3.5721
Average	0.4978	3.0461

The r_{BA} and r_{HEMA} values obtained from four methods show a wide scatter for both monomers to each other. All four kinetic estimates point to faster incorporation of HEMA units into the copolymer chain. The product of the reactivity ratios of two monomers $r_{BA} \bullet r_{HEMA}$ value is 1.5163 there is a tendency to form long sequences of HEMA along the copolymer chain.

4.14.2 Thermal analysis of poly(BA-*co*-HEMA) system

Glass transition temperature (T_g) of poly(BA_{25}-$HEMA_{75}$), poly(BA_{50}-$HEMA_{50}$), and poly(BA_{75}-$HEMA_{25}$) were determined using DSC. DSC thermograms and T_g values of copolymers (64.1, 42.4 and 13.3°C) are given in Figure 4.42. The T_g of poly(BA) is -50°C, and that of poly(HEMA) is 76°C. The results indicate that the T_g values of the copolymers are very high, close to that of poly(HEMA) and decrease with increase in BA mole fraction in copolymer.

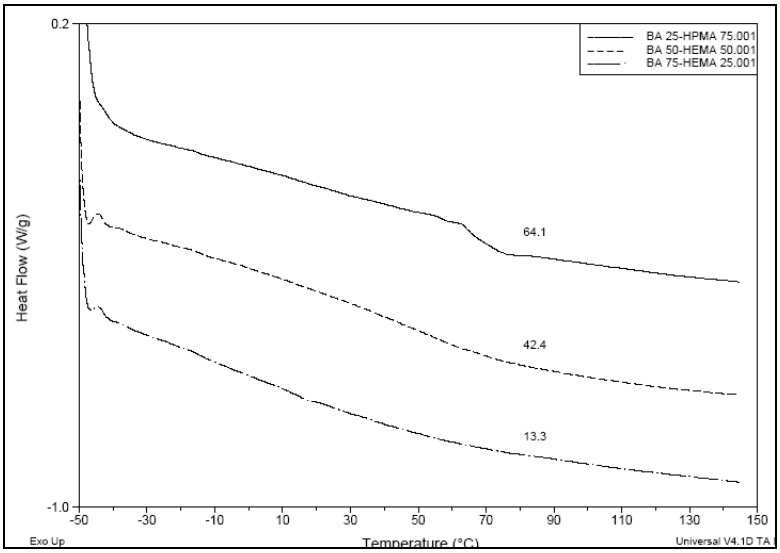

Figure 4.42: DSC thermograms of poly(BA_{25}-$HEMA_{75}$), poly(BA_{50}-$HEMA_{50}$), and poly(BA_{75}-$HEMA_{25}$).

4.15 Poly(2-ethylhexyl acrylate-*co*-2-hydroxyethyl methacrylate) System

Poly(2-ethylhexyl acrylate-*co*-hydroxyethyl methacrylate) find applications as components in surface protection films of optical components and as pressure-sensitive adhesives having with good thermal conductivity and flexibility.[75-77]These polymers are used in compositions for deep fluorination of teeth,[78] in preparation of organic solvent free aqueous primers for lamp reflectors.[79] Copolymer kinetic estimates are also reported.[80]

4.15.1 Reactivity ratio determination for poly(EHA-*co*-HEMA) system

The reactivity ratios of EHA and HEMA were determined by Finemann-Ross (FR), Kelen-Tudos (KT), Extended Kelen-Tudos (Ext. KT) and Mao-Huglin (MH) methods. The kinetic parameters of FR and KT are presented in Table 4.57 and that of Extended KT is shown in Table 4.58. The graphical copolymerisation plots of FR, KT and extended KT are presented in Figures 4.43 (a-c). The plots are scattered for all graphical methods, indicating that these may not follow conventional copolymerisation kinetics. The reactivity ratios of EHA and HEMA are denoted as r_{EHA} (or r_1) and r_{HEMA} (or r_2) respectively and the values obtained from various methods are presented in Table 4.60.

Table 4.57: FR and KT parameters for poly(EHA-*co*-HEMA) system

Copolymer Code	$F=M_1/M_2$	$f=m_1/m_2$	$H=F^2/f$	$G=F(f-1)/f$	$\xi=H/(\alpha+H)$	$\eta=G/(\alpha+H)$
EHA-HEMA-1	0.1111	0.0460	0.2686	-2.3066	0.1531	-1.3144
EHA-HEMA-2	0.1765	0.0647	0.4814	-2.5516	0.2447	-1.2968
EHA-HEMA-3	0.2500	0.0912	0.6855	-2.4919	0.3156	-1.1475
EHA-HEMA-4	0.3333	0.1257	0.8841	-2.3188	0.3730	-0.9783
EHA-HEMA-5	0.4286	0.1951	0.9415	-1.7683	0.3878	-0.7284
EHA-HEMA-6	0.6667	0.2741	1.6216	-1.7657	0.5218	-0.5682
EHA-HEMA-7	0.8182	0.4225	1.5843	-1.1182	0.5160	-0.3642
EHA-HEMA-8	1.0000	0.4853	2.0604	-1.0604	0.5810	-0.2990
EHA-HEMA-9	1.2222	0.6063	2.4640	-0.7938	0.6238	-0.2009
EHA-HEMA-10	1.5000	0.8989	2.5031	-0.1688	0.6275	-0.0423
EHA-HEMA-11	1.8571	1.0443	3.3025	0.0789	0.6896	0.0165
EHA-HEMA-12	2.3333	1.7197	3.1660	0.9765	0.6805	0.2099
EHA-HEMA-13	3.0000	1.8917	4.7576	1.4141	0.7620	0.2265
EHA-HEMA-14	4.0000	2.3200	6.8966	2.2758	0.8227	0.2715
EHA-HEMA-15	5.6667	3.9049	8.2232	4.2155	0.8469	0.4342

Table 4.58: Extended Kelen-Tudos parameters for poly(EHA-*co*-HEMA) system

Copolymer Code	ζ_1	ζ_2	Z	H	G	ξ	H
EHA-HEMA-1	0.3289	0.7951	0.2516	0.7262	-3.7925	0.2216	-1.1573
EHA-HEMA-2	0.3038	0.8287	0.2052	1.5361	-4.5577	0.3758	-1.1152
EHA-HEMA-3	0.2749	0.7537	0.2294	1.7328	-3.9620	0.4045	-0.9249
EHA-HEMA-4	0.2918	0.7739	0.2321	2.3335	-3.7673	0.4777	-0.7713
EHA-HEMA-5	0.3375	0.7415	0.3044	2.1055	-2.6443	0.4522	-0.5679
EHA-HEMA-6	0.2365	0.5751	0.3152	2.7593	-2.3033	0.5196	-0.4337
EHA-HEMA-7	0.2694	0.5217	0.4257	2.3321	-1.3566	0.4776	-0.2778
EHA-HEMA-8	0.2350	0.4841	0.4046	2.9641	-1.2719	0.5375	-0.2306
EHA-HEMA-9	0.1953	0.3938	0.4342	3.2159	-0.9068	0.5577	-0.1573
EHA-HEMA-10	0.2951	0.4925	0.5156	3.3807	-0.1961	0.5699	-0.0331
EHA-HEMA-11	0.3299	0.5867	0.4531	5.0867	0.0979	0.6660	0.0128
EHA-HEMA-12	0.4464	0.6057	0.6354	4.2598	1.1327	0.6255	0.1663
EHA-HEMA-13	0.2526	0.4006	0.5689	5.8454	1.5675	0.6962	0.1867
EHA-HEMA-14	0.1630	0.2810	0.5393	7.9771	2.4476	0.7577	0.2325
EHA-HEMA-15	0.1589	0.2306	0.6602	8.9604	4.4004	0.7784	0.3823

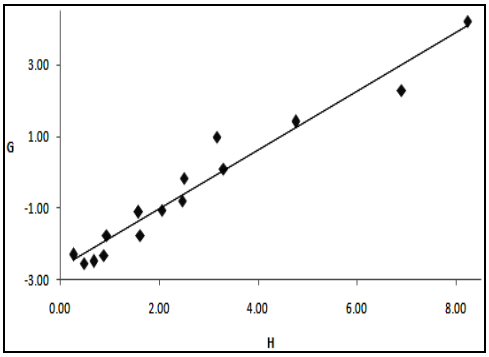

(a)

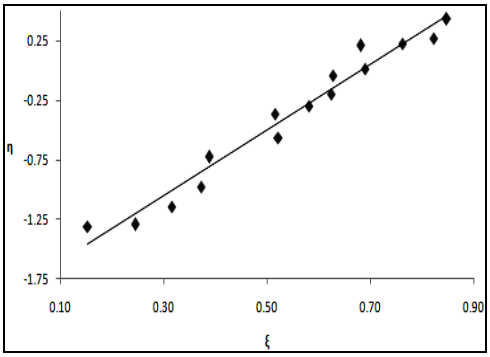

(b)

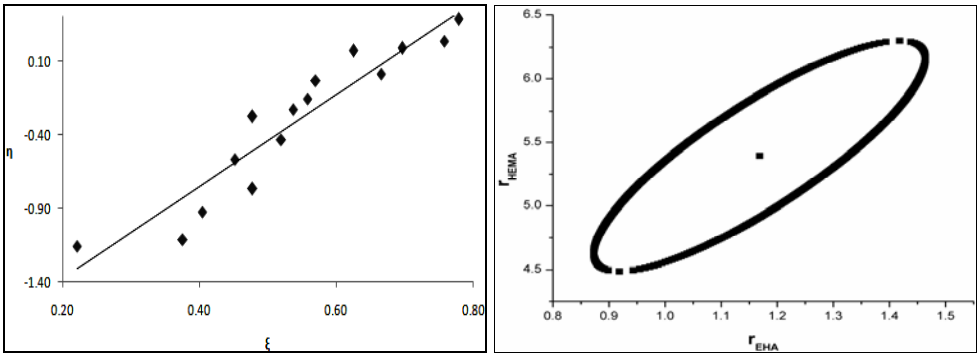

(c) **(d)**

Figure 4.43: (a) FR, (b) KT, (c) Ext. KT plots for poly(EHA-*co*-HEMA) system and (d) 95% Joint confidence interval calculated by MH method

The 95 % joint confidence limit of the reactivity ratio by Mao-Huglin method is plotted in Figure 4.43 (d). Its equation is,

$$4.6659(r_1-1.1685)^2 - 2.5690(r_1-1.1685)(r_2-5.3942) + 0.4946(r_2-5.3942)^2 = 0.1161$$

The statistical distribution of the sequences of two monomers (dyad) M_{EHA}-M_{EHA}, M_{HEMA}-M_{HEMA} and M_{EHA}-M_{HEMA} and mean sequence lengths μ_{EHA} and μ_{HEMA} are presented in Table 4.59, and the variation of the dyad fractions with the EHA mole fraction in the copolymers is displayed in Figure 4.44.

Table 4.59: Structural data for poly(EHA-*co*-HEMA) system

Copolymer Code	M_{EHA}-M_{EHA}	M_{HEMA}-M_{HEMA}	M_{EHA}-M_{HEMA}	μ_{EHA}	μ_{HEMA}
EHA-HEMA-1	0.0062	0.9183	0.0755	1.1111	37.0252
EHA-HEMA-2	0.0111	0.8896	0.0993	1.1765	23.6825
EHA-HEMA-3	0.0194	0.8522	0.1284	1.2501	17.0112
EHA-HEMA-4	0.0317	0.8084	0.1599	1.3334	13.0084
EHA-HEMA-5	0.0592	0.7327	0.2081	1.4287	10.3399
EHA-HEMA-6	0.0919	0.6616	0.2465	1.6669	7.0042
EHA-HEMA-7	0.1517	0.5576	0.2907	1.8184	5.8923
EHA-HEMA-8	0.1755	0.5220	0.3025	2.0003	5.0028
EHA-HEMA-9	0.2184	0.4635	0.3180	2.2226	4.2750
EHA-HEMA-10	0.3071	0.3604	0.3325	2.5005	3.6685
EHA-HEMA-11	0.3443	0.3226	0.3331	2.8577	3.1554
EHA-HEMA-12	0.4746	0.2099	0.3155	3.3340	2.7155
EHA-HEMA-13	0.4997	0.1913	0.3090	4.0009	2.3343
EHA-HEMA-14	0.5526	0.1550	0.2925	5.0012	2.0007
EHA-HEMA-15	0.6767	0.0844	0.2389	6.6684	1.7064

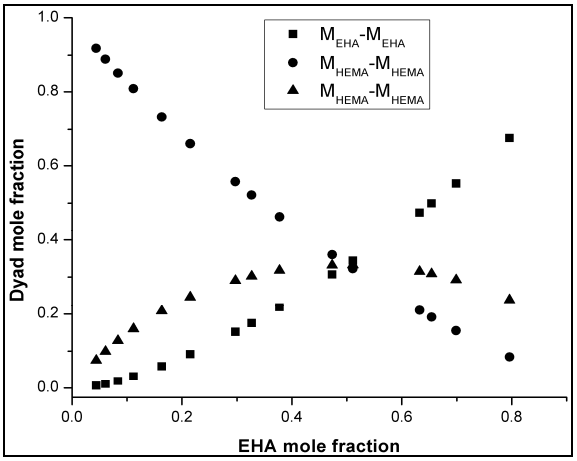

Figure 4.44: Dyad monomer sequence fractions verses the EHA mole fractions for the copolymers.

Table 4.60: Reactivity ratios of EHA and HEMA computed by different models

Method	r_{EHA}	r_{HEMA}
Finemann-Ross	0.8241	2.6821
Kelen-Tudos	0.8801	2.8074
Extended Kelen-Tudos	1.1273	5.1273
Mao-Huglin	1.1685	5.3942
Average	1.0003	4.0028

In this system as well there is a clear divergence in the reactivity ratios determined by differential and integral forms of kinetic estimates. Interestingly, the two methodologies are in agreement within themselves. The overall indication points to the higher incorporation of HEMA units in the copolymer than in feed. The product of the reactivity ratios of two monomers $r_{EHA} \bullet r_{HEMA}$ value is 4.0036 which is far in excess of 1, indicating a tendency towards block copolymer formation.

4.15.2 Thermal analysis of poly(EHA-*co*-HEMA)

The glass transition temperature (T_g) of poly(EHA_{25}-$HEMA_{75}$), poly(EHA_{50}-$HEMA_{50}$), and poly(EHA_{75}-$HEMA_{25}$) estimated by DSC, were 8.5, -15.2 and -15.8ºC, and hence very composition dependent. The DSC thermograms of copolymers with T_g values are given in Figure 4.45. The T_g values decreases well below that of parent homopolymer of EHA and HEMA, which are 12ºC and 76ºC respectively.

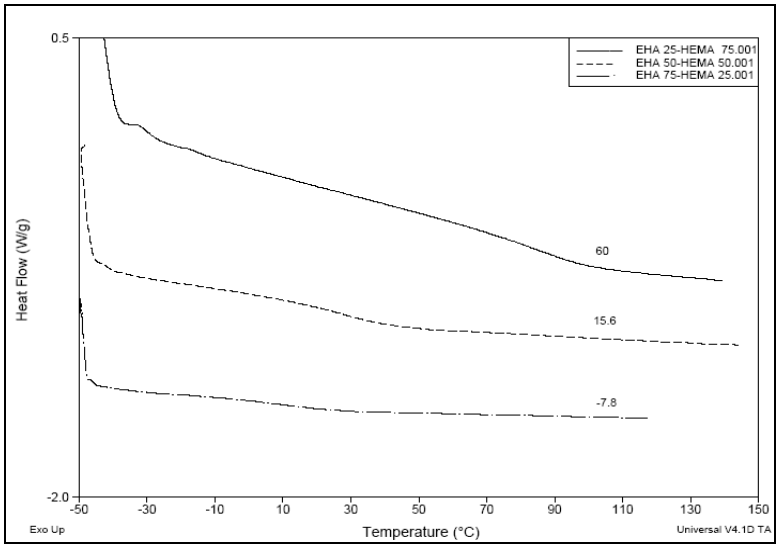

Figure 4.45: DSC thermogram of poly(EHA_{25}-$HEMA_{75}$), poly(EHA_{50}-$HEMA_{50}$), and poly(EHA_{75}-$HEMA_{25}$).

4.16 Poly(methyl methacrylate-*co*-2-hydroxyethyl methacrylate) System

Thses polymers find extensive use in biomedical applications such as dental treatment,[81] ultrastructural evaluation of *in vitro* mineralised calcium phosphate phase,[82] *in vitro* mineralisation and cell adhesion on surface modified polymer,[83] biomimetically modified polymer for hard tissue regeneration,[84] hydrogel tubes as nerve guidance channels,[85] hydrogel hollow fibre membranes,[86] and cell microencapsulation.[87] Poly(MMA-*co*-HEMA) are used in immobilization of α-amylase[88,89] and type-I collagen and basic fibroblast growth factor (bFGF) to improve cytocompatibility.[90] Physical, chemical and dyeing properties of Bombyx mori silks grafted with the copolymer have also been studied.[91] The viscoelastic behaviour of water swollen copolymers,[92] their thermal behaviour,[93] water diffusion and mechanical properties[94] and water sorption and desorption properties.[95,96] have been investigated.

4.16.1 Reactivity ratio determination for poly(MMA-*co*-HEMA) system

The reactivity ratios of MMA and HEMA were determined by Finemann-Ross (FR), Kelen-Tudos (KT), extended Kelen-Tudos (ext. KT) and Mao-Huglin (MH) methods. The kinetic parameters of FR and KT are presented in Table 4.61 and that of extended KT is shown in Table 4.62. The graphical copolymerisation plots of FR, KT and extended KT are presented in Figures 4.46 (a-c). The plots are highly for all graphical methods, indicating that these do not follow conventional copolymerisation kinetics. The reactivity ratios of MMA and HEMA are denoted as r_{MMA} (or r_1) and

r_{HEMA} (or r_2) respectively and the values obtained from various methods are presented in Table 4.64.

Table 4.61: FR and KT parameters for poly(MMA-*co*-HEMA) system

Copolymer Code	$F=M_1/M_2$	$f=m_1/m_2$	$H=F^2/f$	$G=F(f-1)/f$	$\xi=H/(\alpha+H)$	$\eta=G/(\alpha+H)$
MMA-HEMA-1	0.1111	0.0574	0.2149	-1.8232	0.0871	-0.7386
MMA-HEMA-2	0.2500	0.1249	0.5005	-1.7520	0.1817	-0.6362
MMA-HEMA-3	0.3333	0.1461	0.7604	-1.9477	0.2523	-0.6463
MMA-HEMA-4	0.4286	0.1853	0.9913	-1.8844	0.3055	-0.5808
MMA-HEMA-5	0.6667	0.3137	1.4166	-1.4582	0.3860	-0.3973
MMA-HEMA-6	1.0000	0.6092	1.6414	-0.6414	0.4214	-0.1647
MMA-HEMA-7	1.2222	0.6627	2.2542	-0.6222	0.5001	-0.1380
MMA-HEMA-8	1.8571	0.9695	3.5574	-0.0584	0.6122	-0.0100
MMA-HEMA-9	3.0000	1.3299	6.7677	0.7441	0.7502	0.0825
MMA-HEMA-10	4.0000	1.0989	14.5595	0.3601	0.8660	0.0214
MMA-HEMA-11	5.6667	1.7147	18.7275	2.3618	0.8926	0.1126
MMA-HEMA-12	9.0000	3.4279	23.6295	6.3745	0.9129	0.2463

Table 4.62: Extended Kelen-Tudos parameters for poly(MMA-*co*-HEMA) system

Copolymer Code	ζ_1	ζ_2	Z	H	G	ξ	H
MMA-HEMA-1	0.3740	0.7234	0.3644	0.4325	-2.5863	0.0904	-0.5407
MMA-HEMA-2	0.3772	0.7551	0.3365	1.1026	-2.6004	0.2022	-0.4769
MMA-HEMA-3	0.2994	0.6830	0.3097	1.5232	-2.7568	0.2593	-0.4694
MMA-HEMA-4	0.2752	0.6366	0.3180	1.8323	-2.5619	0.2964	-0.4144
MMA-HEMA-5	0.3082	0.6549	0.3463	2.6157	-1.9815	0.3755	-0.2844
MMA-HEMA-6	0.4581	0.7520	0.4395	3.1543	-0.8892	0.4203	-0.1185
MMA-HEMA-7	0.3639	0.6712	0.4067	4.0058	-0.8294	0.4794	-0.0993
MMA-HEMA-8	0.3356	0.6429	0.3971	6.1482	-0.0767	0.5856	-0.0073
MMA-HEMA-9	0.2368	0.5342	0.3537	10.6284	0.9325	0.7096	0.0623
MMA-HEMA-10	0.1282	0.4666	0.2183	23.0658	0.4533	0.8413	0.0165
MMA-HEMA-11	0.1465	0.4843	0.2393	29.9470	2.9866	0.8732	0.0871
MMA-HEMA-12	0.2338	0.6138	0.2799	43.7590	8.6746	0.9096	0.1803

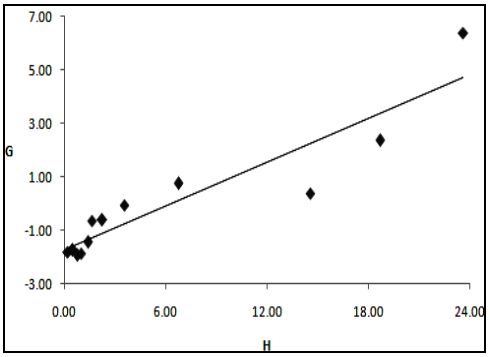

(a)

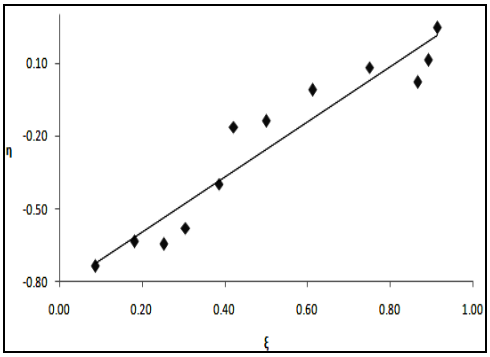

(b)

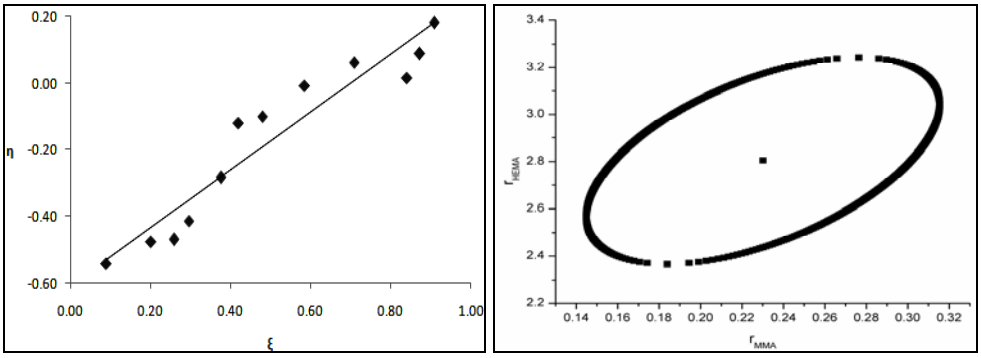

(c) **(d)**

Figure 4.46: (a) FR, (b) KT, (c) Ext. KT plots for poly(MMA-*co*-HEMA) system and (d) 95% Joint confidence interval calculated by MH method

The 95 % joint confidence limit of the reactivity ratio estimated by Mao-Huglin method is plotted in Figure 4.46 (d). Its equation is,

$4.0543(r_1\text{-}0.2301)^2 - 0.8551(r_1\text{-}0.2301)(r_2\text{-}2.8048) + 0.1533(r_2\text{-}2.8048)^2 = 0.0208$

The statistical distribution of the sequences of two monomers (dyad) M_{MMA}-M_{MMA}, M_{HEMA}-M_{HEMA} and M_{MMA}-M_{HEMA} and mean sequence lengths μ_{MMA} and μ_{HEMA} are presented in Table 4.63, and the variation of the dyad fractions with the MMA mole fraction in the copolymers is displayed in Figure 4.47.

Table 4.63: Structural data for poly(MMA-*co*-HEMA) system

Copolymer Code	M_{MMA}-M_{MMA}	M_{HEMA}-M_{HEMA}	M_{MMA}-M_{HEMA}	μ_{MMA}	μ_{HEMA}
MMA-HEMA-1	0.0040	0.8954	0.1006	1.0834	18.1486
MMA-HEMA-2	0.0162	0.7942	0.1897	1.1876	8.6216
MMA-HEMA-3	0.0211	0.7661	0.2128	1.2501	6.7162
MMA-HEMA-4	0.0312	0.7185	0.2503	1.3215	5.4459
MMA-HEMA-5	0.0694	0.5917	0.3389	1.5001	3.8581
MMA-HEMA-6	0.1632	0.4061	0.4307	1.7502	2.9054
MMA-HEMA-7	0.1795	0.3823	0.4382	1.9169	2.5590
MMA-HEMA-8	0.2646	0.2801	0.4554	2.3932	2.0260
MMA-HEMA-9	0.3473	0.2057	0.4471	3.2506	1.6351
MMA-HEMA-10	0.2963	0.2492	0.4545	4.0008	1.4764
MMA-HEMA-11	0.4185	0.1552	0.4263	5.2511	1.3362
MMA-HEMA-12	0.6108	0.0625	0.3267	7.7518	1.2117

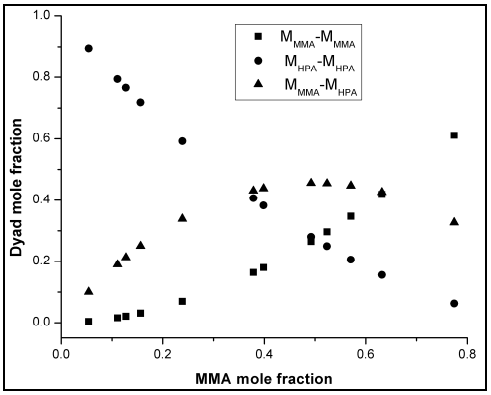

Figure 4.47: Dyad monomer sequence fractions verses the MMA mole fractions for the copolymers.

Table 4.64: Reactivity ratios of MMA and HEMA computed by different models

Method	r_{MMA}	r_{HEMA}
Finemann-Ross	0.7782	1.6153
Kelen-Tudos	0.7721	1.5733
Extended Kelen-Tudos	0.7400	2.2337
Mao-Huglin	0.2301	2.8048
Average	0.6301	2.0568

The values obtained by the differential form of the kinetic estimates were similar while integral forms show differences. The four estimates all indicate a faster reaction for HEMA into the copolymer chain. The product of the reactivity ratios of two monomers $r_{MMA} \bullet r_{HEMA}$ value is 1.2960 suggesting that there is tendency for the formation of sequences of HEMA interposed by single MMA units along the copolymer chain.

4.16.2 Thermal analysis of poly(MMA-*co*-HEMA)

The glass transition temperature (T_g) of poly(MMA_{25}-$HEMA_{75}$), poly(MMA_{50}-$HEMA_{50}$), and poly(MMA_{75}-$HEMA_{25}$) were estimated by DSC and values are 76.5, 82.5 and 71.5ºC respectively shown in Figure 4.48. The T_g of homopolymers poly(MMA) is 95 °C, and that of poly(HEMA) is 76 °C. The results indicate that T_g values of two copolymers are close to that of poly(HEMA).

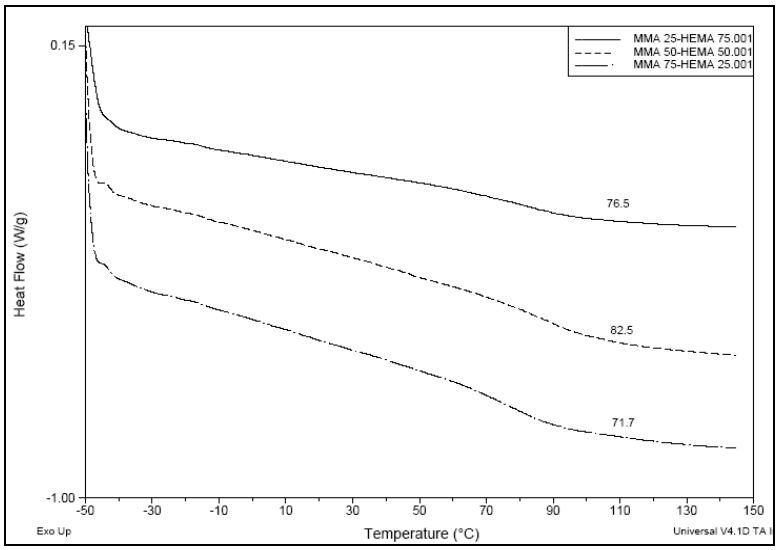

Figure 4.48: DSC thermograms of poly(MMA_{25}-$HEMA_{75}$), poly(MMA_{50}-$HEMA_{50}$), and poly(MMA_{75}-$HEMA_{25}$).

4.17 Poly(2-ethylhexyl methacrylate-*co*-2-hydroxyethyl methacrylate) System

These polymers are used in lacquers for chip and humidity resistant adhesive coatings,[97] in resin particles for cathodic electrodeposition coating compositions

having balanced smoothness and defect resistance,[98] in photocuring transfer sheets for optical information recording medium[99] and in moisture resistant multiple coating layers.[100] These monomers are constituents of sheet used for temporary fixation, which when laminated with a silicon wafer, show good dicing workability.[101]

4.17.1 Reactivity ratio determination for poly(EHMA-*co*-HEMA) system

The reactivity ratios of EHMA and HEMA were determined by Finemann-Ross (FR), Kelen-Tudos (KT), Extended Kelen-Tudos (Ext. KT) and Mao-Huglin (MH) methods. The kinetic parameters of FR and KT for the copolymers are presented in Table 4.65 and that of Ext. KT is shown in Table 4.66. The graphical copolymerisation plots of FR, KT and Extended KT are presented in Figures 4.49 (a-c). The plots are linear for all graphical methods, indicating that these follow conventional copolymerisation kinetics. The reactivity ratios of EHMA and HEMA are denoted as r_{EHMA} (or r_1) and r_{HEMA} (or r_2) respectively and the values obtained from various methods are presented in Table 4.68.

Table 4.65: FR and KT parameters for poly(EHMA-*co*-HEMA) system

Copolymer Code	$F=M_1/M_2$	$f=m_1/m_2$	$H=F^2/f$	$G=F(f-1)/f$	$\xi=H/(\alpha+H)$	$\eta=G/(\alpha+H)$
EHMA-HEMA-1	0.1111	0.0729	0.1694	-1.4137	0.1291	-1.0774
EHMA-HEMA-2	0.2500	0.1362	0.4590	-1.5859	0.2865	-0.9901
EHMA-HEMA-3	0.5385	0.4244	0.6832	-0.7303	0.3741	-0.4000
EHMA-HEMA-4	0.6667	0.4217	1.0539	-0.9142	0.4798	-0.4162
EHMA-HEMA-5	0.8182	0.5262	1.2721	-0.7366	0.5268	-0.3050
EHMA-HEMA-6	1.0000	0.7650	1.3072	-0.3072	0.5336	-0.1254
EHMA-HEMA-7	1.2222	0.9170	1.6290	-0.1106	0.5877	-0.0399
EHMA-HEMA-8	1.5000	1.0793	2.0848	0.1102	0.6459	0.0341
EHMA-HEMA-9	1.8571	1.2478	2.7641	0.3688	0.7075	0.0944
EHMA-HEMA-10	2.3333	1.7063	3.1908	0.9658	0.7363	0.2229
EHMA-HEMA-11	3.0000	2.1079	4.2696	1.5768	0.7889	0.2913
EHMA-HEMA-12	5.6667	4.1648	7.7101	4.3061	0.8709	0.4864

Table 4.66: Ext. Kelen-Tudos parameters for poly(EHMA-*co*-HEMA) system

Copolymer Code	ζ_1	ζ_2	Z	H	G	ξ	η
EHMA-HEMA-1	0.5265	0.8028	0.4604	0.3437	-2.0136	0.1513	-0.8865
EHMA-HEMA-2	0.3859	0.7085	0.3955	0.8703	-2.1839	0.3111	-0.7805
EHMA-HEMA-3	0.6702	0.8503	0.5841	1.2441	-0.9855	0.3922	-0.3107
EHMA-HEMA-4	0.3602	0.5694	0.5300	1.5012	-1.0911	0.4378	-0.3182
EHMA-HEMA-5	0.3411	0.5303	0.5520	1.7268	-0.8582	0.4725	-0.2348
EHMA-HEMA-6	0.5202	0.6800	0.6445	1.8418	-0.3647	0.4886	-0.0967
EHMA-HEMA-7	0.4889	0.6516	0.6365	2.2633	-0.1304	0.5400	-0.0311
EHMA-HEMA-8	0.4026	0.5595	0.6283	2.7339	0.1262	0.5865	0.0271
EHMA-HEMA-9	0.3702	0.5509	0.5774	3.7422	0.4291	0.6600	0.0757
EHMA-HEMA-10	0.4279	0.5852	0.6347	4.2354	1.1128	0.6872	0.1806
EHMA-HEMA-11	0.3852	0.5482	0.6122	5.6236	1.8096	0.7447	0.2396
EHMA-HEMA-12	0.4735	0.6443	0.6207	10.8108	5.0989	0.8487	0.4003

The 95 % joint confidence limit of the reactivity ratio by Mao-Huglin method is plotted in Figure 4.49 (d). Its equation is,

$$3.9048(r_1 - 0.7994)^2 - 2.7704(r_1 - 0.7994)(r_2 - 2.3448) + 0.8501(r_2 - 2.3448)^2 = 0.0290$$

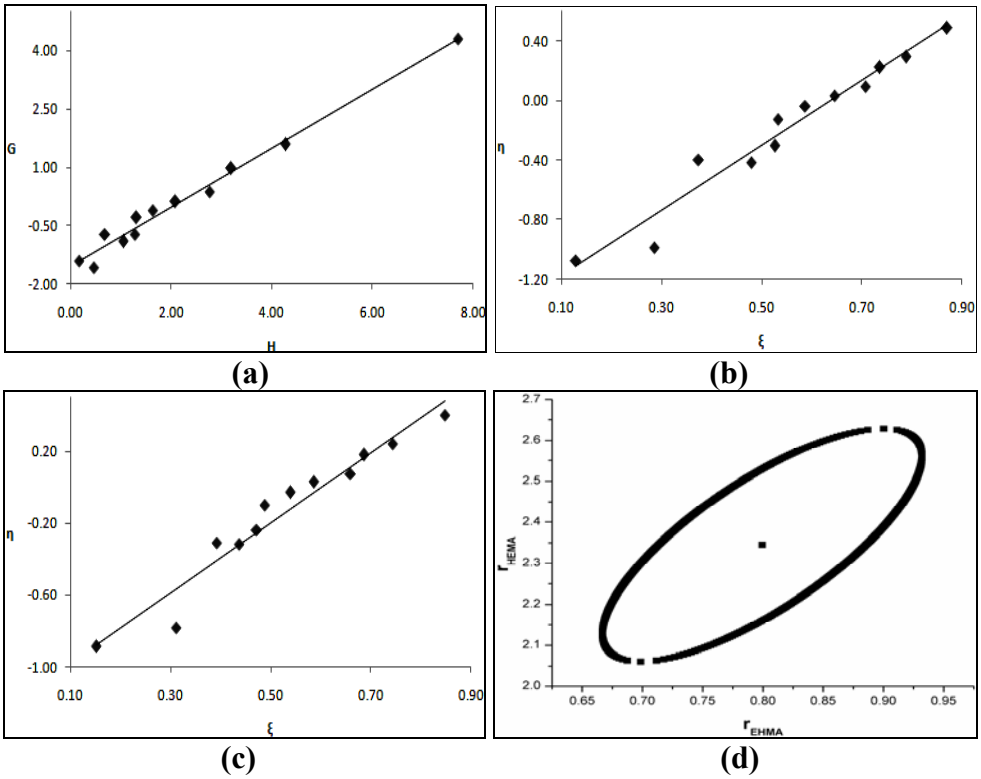

Figure 4.49: (a) FR, (b) KT, (c) Ext. KT plots for the poly(EHMA-*co*-HEMA) system and (d) 95% Joint confidence interval calculated by MH method

The statistical distribution of the sequences of two monomers (dyad) M_{EHMA}-M_{EHMA}, M_{HEMA}-M_{HEMA} and M_{EHMA}-M_{HEMA} and mean sequence lengths μ_{EHMA} and μ_{HEMA} are presented in Table 4.67, and the variation of the dyad fractions with the EHMA mole fraction in the copolymers is displayed in Figure 4.50.

Table 4.67: Structural data for poly(EHMA-*co*-HEMA) system

Copolymer Code	M_{EHMA}-M_{EHMA}	M_{HEMA}-M_{HEMA}	M_{EHMA}-M_{HEMA}	μ_{EHMA}	μ_{HEMA}
EHMA-HEMA-1	0.0065	0.8707	0.1228	1.0866	18.4258
EHMA-HEMA-2	0.0195	0.7798	0.2007	1.1948	8.7448
EHMA-HEMA-3	0.1073	0.5114	0.3813	1.4196	4.5958
EHMA-HEMA-4	0.1064	0.5132	0.3804	1.5195	3.9043
EHMA-HEMA-5	0.1402	0.4506	0.4092	1.6376	3.3665
EHMA-HEMA-6	0.2127	0.3458	0.4415	1.7793	2.9362
EHMA-HEMA-7	0.2544	0.2976	0.4480	1.9525	2.5842
EHMA-HEMA-8	0.2950	0.2569	0.4482	2.1690	2.2908
EHMA-HEMA-9	0.3332	0.2230	0.4438	2.4473	2.0426
EHMA-HEMA-10	0.4201	0.1591	0.4209	2.8184	1.8298
EHMA-HEMA-11	0.4800	0.1235	0.3965	3.3379	1.6454
EHMA-HEMA-12	0.6610	0.0482	0.2908	5.4160	1.3417

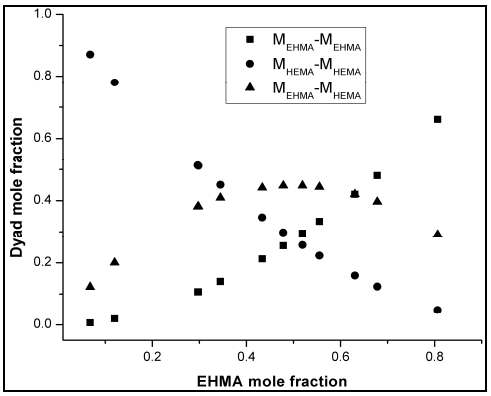

Figure 4.50: Dyad monomer sequence fractions verses the EHMA mole fractions for the copolymers.

Table 4.68: Reactivity ratios of EHMA and HEMA computed by different models

Method	r_{EHMA}	r_{HEMA}
Finemann-Ross	0.7583	1.5521
Kelen-Tudos	0.7842	1.5965
Extended Kelen-Tudos	0.7752	2.2516
Mao-Huglin	0.7994	2.3448
Average	0.7793	1.9362

All four methods determine the similar values for the less reactive comonomer, EHMA, while they differ with respect to the more reactive comonomer, HEMA. The two differential forms, FR and KT, indicate a similar value for HEMA, which differ appreciably from the similar values brought forth by the integral form of the copolymer reactivity ratios methods, namely extended KT and Mao-Huglin methods. All point to the higher incorporation of HEMA units in the copolymer than in the feed. The product of the reactivity ratios of two monomers $r_{EHMA} \bullet r_{HEMA}$ value is 1.5089 which is greater than 1, suggesting that there is tendency for the formation of long sequence of HEMA in the copolymer chain.

4.17.2 Thermal analysis of poly(EHMA-*co*-HEMA)

The glass transition (T_g) of poly($EHMA_{25}$-$HEMA_{75}$), poly($EHMA_{50}$-$HEMA_{50}$), and poly($EHMA_{75}$-$HEMA_{25}$) were estimated by DSC as 78.4, 27.3 and -10.5°C, which vary very widely with composition. The DSC thermograms with T_g values of copolymers are given in Figure 4.51. The T_g of poly(EHMA) is -10 °C, and that of poly(HEMA) is 76 °C. The results clearly indicate that the T_g values of copolymers decreases with increasing EHMA content in copolymer.

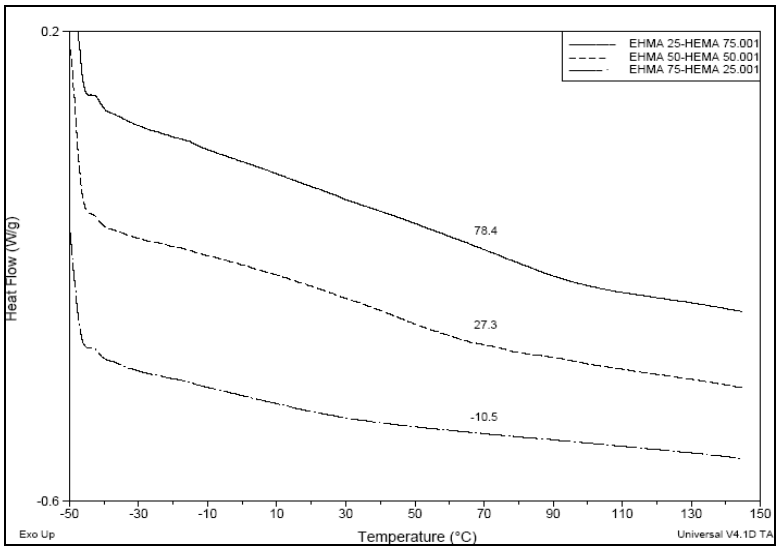

Figure 4.51: DSC thermograms of poly(EHMA$_{25}$-HEMA$_{75}$), poly(EHMA$_{50}$-HEMA$_{50}$), and poly(EHMA$_{75}$-HEMA$_{25}$).

4.18 Poly(2-hydroxypropyl methacrylate-*co*-2-hydroxyethyl methacrylate) System

2-Hydroxypropyl methacrylate, 2-hydroxylethyl methacrylate are used in covering hollow microsphere emulsion used in printing coating applications.[102] The polymers are also used as polyacrylate-polyurethane resin binder in preparation of single-fluid general plastic gravure alcohol and water-soluble compound ink.[103]

4.18.1 Reactivity ratio determination for poly(HPMA-*co*-HEMA) system

The reactivity ratios of HEMA and HPMA were determined by Finemann-Ross (FR), Kelen-Tudos (KT), Extended Kelen-Tudos (Ext. KT) and Mao-Huglin (MH) methods. The kinetic parameters of FR and KT are presented in Table 4.69 and that of Extended KT is shown in Table 4.70. The graphical copolymerisation plots of FR, KT and Extended KT are presented in Figures 4.52 (a-c). The plots are linear for all graphical methods, indicating that these follow conventional copolymerisation kinetics. The reactivity ratios of HPMA and HEMA are denoted as r_{HPMA} (or r_1) and r_{HEMA} (or r_2) respectively and the values obtained from various methods are presented in Table 4.72.

Table 4.69: FR and KT parameters for poly(HPMA-*co*-HEMA) system

Copolymer Code	$F=M_1/M_2$	$f=m_1/m_2$	$H=F^2/f$	$G=F(f-1)/f$	$\xi=H/(\alpha+H)$	$\eta=G/(\alpha+H)$
HPMA-HEMA-1	0.1111	0.1091	0.1131	-0.9069	0.0898	-0.7201
HPMA-HEMA-2	0.1765	0.1693	0.1839	-0.8658	0.1383	-0.6509
HPMA-HEMA-3	0.2500	0.2357	0.2652	-0.8108	0.1879	-0.5744
HPMA-HEMA-4	0.3333	0.2978	0.3731	-0.7858	0.2456	-0.5172
HPMA-HEMA-5	0.4286	0.3792	0.4843	-0.7015	0.2970	-0.4302
HPMA-HEMA-6	0.5385	0.4926	0.5885	-0.5545	0.3393	-0.3197
HPMA-HEMA-7	0.6667	0.5747	0.7734	-0.4934	0.4029	-0.2570
HPMA-HEMA-8	0.8182	0.7241	0.9245	-0.3118	0.4465	-0.1506
HPMA-HEMA-9	1.0000	0.8722	1.1465	-0.1465	0.5001	-0.0639
HPMA-HEMA-10	1.2222	1.1043	1.3527	0.1155	0.5413	0.0462
HPMA-HEMA-11	1.5000	1.3696	1.6429	0.4048	0.5890	0.1451
HPMA-HEMA-12	1.8571	1.5439	2.2339	0.6543	0.6609	0.1936
HPMA-HEMA-13	2.3333	2.0624	2.6398	1.2020	0.6973	0.3175
HPMA-HEMA-14	3.0000	2.5574	3.5191	1.8270	0.7543	0.3916
HPMA-HEMA-15	4.0000	3.1638	5.0572	2.7357	0.8152	0.4410
HPMA-HEMA-16	5.6667	4.5973	6.9848	4.4341	0.8590	0.5453
HPMA-HEMA-17	9.0000	6.9726	11.6169	7.7092	0.9102	0.6040

Table 4.70: Extended Kelen-Tudos parameters for poly(HPMA-*co*-HEMA) system

Copolymer Code	ζ_1	ζ_2	Z	H	G	ξ	η
HPMA-HEMA-1	0.6434	0.6549	0.9690	0.1162	-0.9194	0.0834	-0.6597
HPMA-HEMA-2	0.6365	0.6634	0.9293	0.1960	-0.8939	0.1331	-0.6067
HPMA-HEMA-3	0.6788	0.7201	0.8920	0.2962	-0.8568	0.1882	-0.5446
HPMA-HEMA-4	0.5520	0.6178	0.8349	0.4273	-0.8410	0.2507	-0.4934
HPMA-HEMA-5	0.5298	0.5987	0.8264	0.5553	-0.7512	0.3030	-0.4099
HPMA-HEMA-6	0.6373	0.6966	0.8504	0.6812	-0.5966	0.3478	-0.3046
HPMA-HEMA-7	0.3935	0.4565	0.8202	0.8543	-0.5186	0.4008	-0.2433
HPMA-HEMA-8	0.5036	0.5691	0.8320	1.0460	-0.3316	0.4502	-0.1427
HPMA-HEMA-9	0.3509	0.4023	0.8397	1.2371	-0.1522	0.4920	-0.0605
HPMA-HEMA-10	0.5477	0.6061	0.8515	1.5232	0.1225	0.5439	0.0438
HPMA-HEMA-11	0.5182	0.5676	0.8711	1.8049	0.4243	0.5856	0.1376
HPMA-HEMA-12	0.3729	0.4485	0.7840	2.5117	0.6938	0.6629	0.1831
HPMA-HEMA-13	0.4486	0.5075	0.8404	2.9199	1.2641	0.6957	0.3012
HPMA-HEMA-14	0.3303	0.3874	0.8180	3.8222	1.9040	0.7495	0.3734
HPMA-HEMA-15	0.2782	0.3517	0.7521	5.5927	2.8769	0.8141	0.4188
HPMA-HEMA-16	0.3700	0.4561	0.7588	7.9851	4.7409	0.8621	0.5118
HPMA-HEMA-17	0.3952	0.5101	0.7047	14.0406	8.4754	0.9166	0.5533

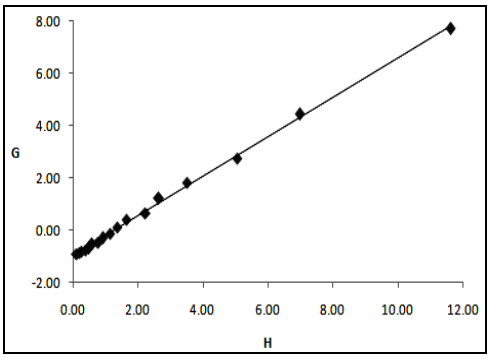

(a)

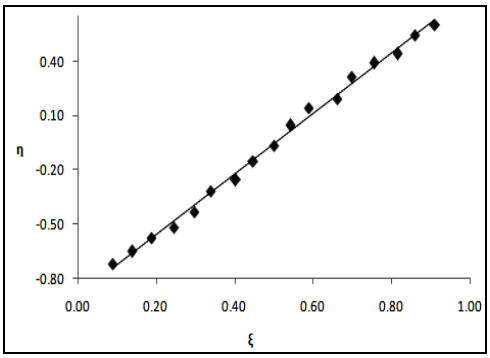

(b)

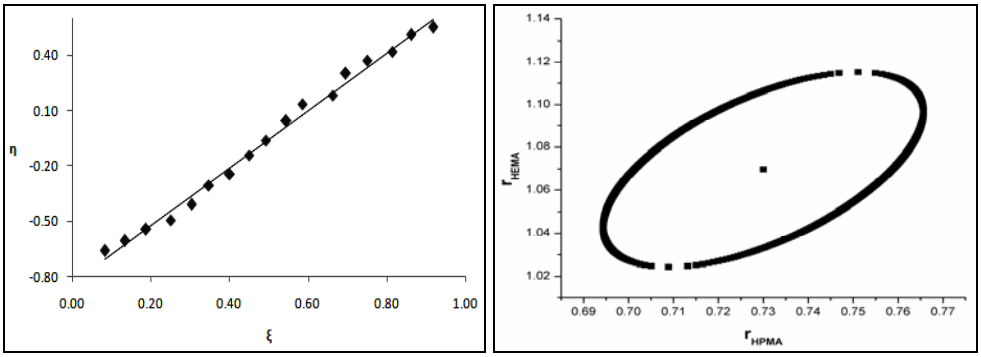

(c) **(d)**

Figure 4.52: (a) FR, (b) KT, (c) Ext. KT plots for poly(HPMA-*co*-HEMA) system and (d) 95% Joint confidence interval calculated by MH method

The 95 % joint confidence limit of the reactivity ratio calculated by Mao-Huglin method is plotted in Figure 4.52 (d). Its equation is,

$5.3036(r_1 - 0.7300)^2 - 4.9226(r_1 - 0.7300)(r_2 - 1.0697) + 3.2605(r_2 - 1.0697)^2 = 0.0044$

The statistical distribution of the sequences of two monomers (dyad) M_{HPMA}-M_{HPMA}, M_{HEMA}-M_{HEMA} and M_{HPMA}-M_{HEMA} and mean sequence lengths μ_{HPMA} and μ_{HEMA} are presented in Table 4.71, and the variation of the dyad fractions with the HPMA mole fraction in the copolymers is displayed in Figure 4.53.

Table 4.71: Structural data for poly(HPMA-*co*-HEMA) system

Copolymer Code	M_{HPMA}-M_{HPMA}	M_{HEMA}-M_{HEMA}	M_{HPMA}-M_{HEMA}	μ_{HPMA}	μ_{HEMA}
HPMA-HEMA-1	0.0079	0.8110	0.1811	1.0833	10.3276
HPMA-HEMA-2	0.0173	0.7277	0.2549	1.1322	6.8729
HPMA-HEMA-3	0.0307	0.6492	0.3202	1.1873	5.1456
HPMA-HEMA-4	0.0451	0.5861	0.3688	1.2498	4.1092
HPMA-HEMA-5	0.0658	0.5159	0.4183	1.3211	3.4183
HPMA-HEMA-6	0.0968	0.4367	0.4665	1.4035	2.9247
HPMA-HEMA-7	0.1198	0.3899	0.4904	1.4995	2.5546
HPMA-HEMA-8	0.1614	0.3215	0.5171	1.6131	2.2667
HPMA-HEMA-9	0.2014	0.2697	0.5289	1.7493	2.0364
HPMA-HEMA-10	0.2597	0.2101	0.5302	1.9158	1.8480
HPMA-HEMA-11	0.3191	0.1631	0.5178	2.1240	1.6909
HPMA-HEMA-12	0.3540	0.1402	0.5057	2.3916	1.5581
HPMA-HEMA-13	0.4415	0.0946	0.4639	2.7484	1.4442
HPMA-HEMA-14	0.5068	0.0690	0.4243	3.2479	1.3455
HPMA-HEMA-15	0.5692	0.0496	0.3812	3.9972	1.2591
HPMA-HEMA-16	0.6694	0.0268	0.3038	5.2460	1.1829
HPMA-HEMA-17	0.7620	0.0129	0.2251	7.7437	1.1152

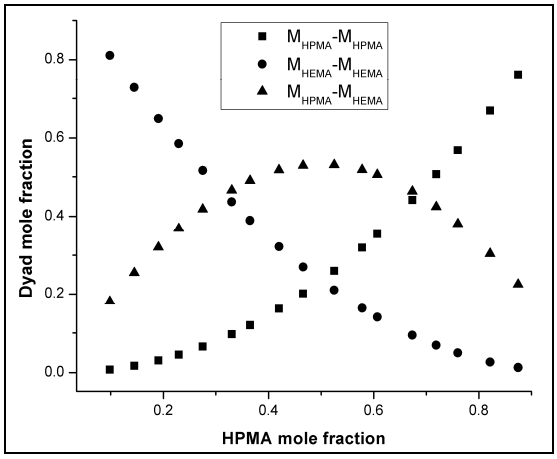

Figure 4.53: Dyad monomer sequence fractions verses the HPMA mole fractions for the copolymers.

Table 4.72: Reactivity ratios of HPMA and HEMA computed by different models

Method	r_{HPMA}	r_{HEMA}
Finemann-Ross	0.7579	0.9844
Kelen-Tudos	0.7812	1.0246
Extended Kelen-Tudos	0.7282	1.0669
Mao-Huglin	0.7300	1.0697
Average	0.7493	1.0364

All methods show similar values for the reactivity ratios of the two monomers. The average value of r_{HPMA} to 0.7493 and that of r_{HEMA} is 1.0364, which indicates the higher incorporation of HEMA units in the copolymer than in feed. The product of the reactivity ratios of two monomers $r_{HPMA} \bullet r_{HEMA}$ value is 0.7766 suggesting the tendency towards the formation of random copolymer system.

4.18.2 Thermal analysis of poly(HPMA-*co*-HEMA)

The glass transition temperature (T_g) of poly($HPMA_{25}$-$HEMA_{75}$), poly($HPMA_{50}$-$HEMA_{50}$), and poly($HPMA_{75}$-$HEMA_{25}$) were determined by DSC as 67.4, 76.3 and 56.3ºC, respectively. The DSC thermograms with T_g values of copolymers are given in Figure 4.54. The T_g of poly(HPMA) is 76°C, and that of poly(HEMA) is 76°C. T_g values of copolymers are varies with the composition.

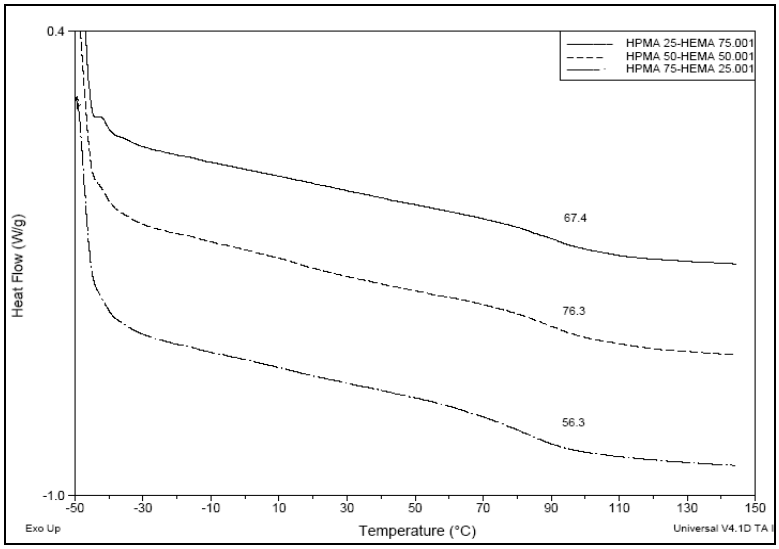

Figure 4.54: DSC thermograms of poly(HPMA$_{25}$-HEMA$_{75}$), poly(HPMA$_{50}$-HEMA$_{50}$), and poly(HPMA$_{75}$-HEMA$_{25}$).

4.19 Poly(methyl acrylate-*co*-2-hydroxypropyl methacrylate) System

Poly(methyl acrylate-*co*-hydroxypropyl methacrylate) have been evaluated for swelling characteristics.[104]

4.19.1 Reactivity ratio determination for poly(MA-*co*-HPMA) system

The reactivity ratios of MA and HPMA were determined by Finemann-Ross (FR), Kelen-Tudos (KT), Extended Kelen-Tudos (Ext. KT) and Mao-Huglin (MH) methods. The kinetic parameters of FR and KT are presented in Table 4.73 and that of Extended KT is shown in Table 4.74. The graphical copolymerisation plots of FR, KT and Extended KT are presented in Figures 4.55 (a-c). The plots are linear for all graphical methods, indicating that these follow conventional copolymerisation kinetics. The reactivity ratios of MA and HPMA are denoted as r_{MA} (or r_1) and r_{HPMA} (or r_2) respectively and the values obtained from various methods are presented in Table 4.76.

Table 4.73: FR and KT parameters for poly(MA-*co*-HPMA) system

Copolymer Code	$F=M_1/M_2$	$f=m_1/m_2$	$H=F^2/f$	$G=F(f-1)/f$	$\xi=H/(\alpha+H)$	$\eta=G/(\alpha+H)$
MA-HPMA-1	0.1111	0.0727	0.1698	-1.4167	0.1566	-1.3071
MA-HPMA-2	0.1765	0.1325	0.2351	-1.1558	0.2046	-1.0057
MA-HPMA-3	0.2500	0.2074	0.3014	-0.9557	0.2480	-0.7862
MA-HPMA-4	0.4286	0.3235	0.5677	-0.8962	0.3831	-0.6048
MA-HPMA-5	0.5385	0.5155	0.5624	-0.5060	0.3809	-0.3427
MA-HPMA-6	0.8182	0.6256	1.0700	-0.4896	0.5393	-0.2468
MA-HPMA-7	1.8571	2.2454	1.5360	1.0301	0.6269	0.4204
MA-HPMA-8	2.3333	2.7059	2.0120	1.4710	0.6876	0.5027
MA-HPMA-9	3.0000	4.1667	2.1600	2.2800	0.7026	0.7417
MA-HPMA-10	9.0000	16.4568	4.9220	8.4531	0.8434	1.4484

Table 4.74: Extended Kelen-Tudos parameters for poly(MA-*co*-HPMA) system

Copolymer Code	ζ_1	ζ_2	Z	H	G	ξ	η
MA-HPMA-1	0.4494	0.6866	0.5143	0.2749	-1.8029	0.2102	-1.3785
MA-HPMA-2	0.2652	0.3533	0.7070	0.2650	-1.2272	0.2042	-0.9454
MA-HPMA-3	0.3235	0.3901	0.7906	0.3318	-1.0026	0.2431	-0.7346
MA-HPMA-4	0.3158	0.4183	0.7003	0.6596	-0.9659	0.3897	-0.5707
MA-HPMA-5	0.3853	0.4025	0.9451	0.5772	-0.5126	0.3585	-0.3184
MA-HPMA-6	0.2240	0.2930	0.7316	1.1689	-0.5117	0.5309	-0.2324
MA-HPMA-7	0.3600	0.2978	1.2626	1.4085	0.9864	0.5769	0.4040
MA-HPMA-8	0.2674	0.2306	1.1871	1.9202	1.4371	0.6502	0.4866
MA-HPMA-9	0.4376	0.3150	1.5208	1.8015	2.0822	0.6356	0.7346
MA-HPMA-10	0.3414	0.1867	2.0208	4.0298	7.6487	0.7960	1.5108

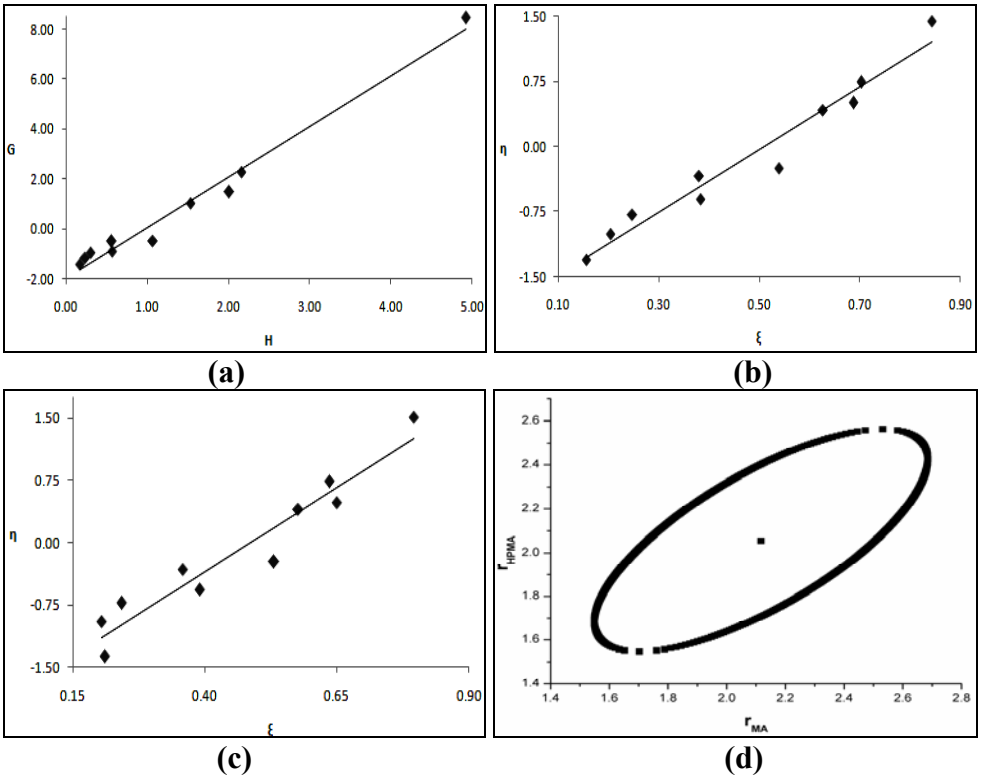

(a) **(b)** **(c)** **(d)**

Figure 4.55: (a) FR, (b) KT, (c) Ext. KT plots for poly(MA-*co*-HPMA) system and (d) 95% Joint confidence interval calculated by MH method

The 95 % joint confidence limit of the reactivity ratio by Mao-Huglin method is plotted in Figure 4.55 (d). Its equation is,

$$2.4976(r_1 - 2.1171)^2 - 4.0737(r_1 - 2.1171)(r_2 - 2.0546) + 3.1188(r_2 - 2.0546) = 0.3765$$

The statistical distribution of the sequences of two monomers (dyad) M_{MA}-M_{MA}, M_{HPA}-M_{HPA} and M_{MA}-M_{HPA} and mean sequence lengths μ_{MA} and μ_{HPA} are presented in Table 4.75, and the variation of the dyad fractions with the MA mole fraction in the copolymers is displayed in Figure 4.56.

Table 4.75: Structural data for poly(MA-*co*-HPMA) system

Copolymer Code	M_{MA}-M_{MA}	M_{HPMA}-M_{HPMA}	M_{MA}-M_{HPMA}	μ_{MA}	μ_{HPMA}
MA-HPMA-1	0.0132	0.8776	0.1093	1.2222	18.3970
MA-HPMA-2	0.0336	0.7997	0.1667	1.3529	11.9537
MA-HPMA-3	0.0632	0.7197	0.2170	1.4999	8.7320
MA-HPMA-4	0.1109	0.6220	0.2671	1.8570	5.5103
MA-HPMA-5	0.1848	0.5045	0.3107	2.0767	4.5899
MA-HPMA-6	0.2231	0.4534	0.3235	2.6360	3.3626
MA-HPMA-7	0.5426	0.1588	0.2986	4.7135	2.0408
MA-HPMA-8	0.5897	0.1294	0.2810	5.6657	1.8284
MA-HPMA-9	0.6895	0.0766	0.2338	6.9988	1.6443
MA-HPMA-10	0.8952	0.0098	0.0951	18.9964	1.2148

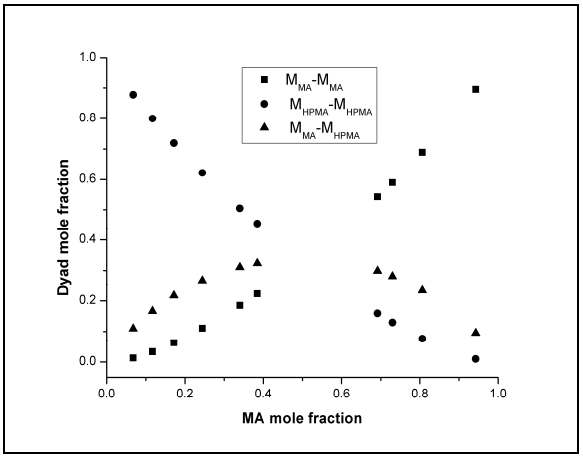

Figure 4.56: Dyad monomer sequence fractions verses the MA mole fractions for the copolymers.

Table 4.76: Reactivity ratios of MA and HPMA computed by different models

Method	r_{MA}	r_{HPMA}
Finemann-Ross	2.0261	1.9621
Kelen-Tudos	1.7662	1.6813
Extended Kelen-Tudos	2.0892	2.0341
Mao-Huglin	2.1171	2.0546
Average	1.9996	1.9330

All methods except KT show similar values. The data reveals that these two monomers have low tendency to copolymerise with each other.

4.19.2 Thermal analysis of poly(MA-*co*-HPMA)

The glass transition temperature (T_g) poly(MA_{25}-$HPMA_{75}$), poly(MA_{50}-$HPMA_{50}$), and poly(MA_{75}-$HPMA_{25}$) were determined by DSC as 58.6, 48.5 and 32.3°C, respectively. The DSC thermograms are presented in Figure 4.57. The T_g of poly(MA) is 3.0°C, and that of poly(HEMA) is 76°C. The data indicates that T_g of copolymers decreases with increasing mole fraction of MA.

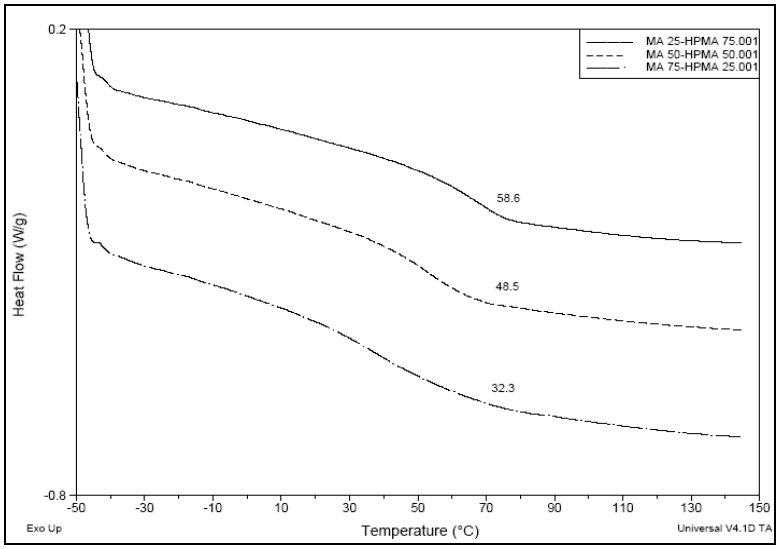

Figure 4.57: DSC thermograms of poly(MA_{25}-$HPMA_{75}$), poly(MA_{50}-$HPMA_{50}$), and poly(MA_{75}-$HPMA_{25}$).

4.20 Poly(butyl acrylate-*co*-2-hydroxypropyl methacrylate) System

There are reports on the use of poly(butyl acrylate-*co*-2-hydroxypropyl methacrylate) in thermosetting powdered coating.[105] The copolymer has also been investigated for their general properties.[106]

4.20.1 Reactivity ratio determination for poly(BA-*co*-HPMA) system

The reactivity ratios of BA and HPMA were determined by Finemann-Ross (FR), Kelen-Tudos (KT), Extended Kelen-Tudos (Ext. KT) and Mao-Huglin (MH) methods. The parameters of FR and KT are presented in Table 4.77 and that of Extended KT is shown in Table 4.78.

Table 4.77: FR and KT parameters for poly(BA-*co*-HPMA) system

Copolymer Code	$F=M_1/M_2$	$f=m_1/m_2$	$H=F^2/f$	$G=F(f-1)/f$	$\xi=H/(\alpha+H)$	$\eta=G/(\alpha+H)$
BA-HPMA-1	0.1111	0.0755	0.1635	-1.3602	0.0749	-0.6236
BA-HPMA-2	0.1765	0.1169	0.2664	-1.3330	0.1166	-0.5836
BA-HPMA-3	0.2500	0.1653	0.3781	-1.2623	0.1578	-0.5268
BA-HPMA-4	0.3333	0.1952	0.5691	-1.3740	0.2200	-0.5311
BA-HPMA-5	0.4286	0.2915	0.6302	-1.0419	0.2380	-0.3935
BA-HPMA-6	0.5385	0.3178	0.9123	-1.1558	0.3114	-0.3945
BA-HPMA-7	0.6667	0.4833	0.9196	-0.7127	0.3131	-0.2426
BA-HPMA-8	0.8182	0.4796	1.3957	-0.8876	0.4089	-0.2600
BA-HPMA-9	1.0000	0.5541	1.8046	-0.8046	0.4721	-0.2105
BA-HPMA-10	1.2222	0.7159	2.0866	-0.4850	0.5084	-0.1182
BA-HPMA-11	1.5000	0.8477	2.6543	-0.2695	0.5681	-0.0577
BA-HPMA-12	1.8571	0.9294	3.7111	-0.1411	0.6478	-0.0246
BA-HPMA-13	2.3333	0.9551	5.7006	-0.1098	0.7386	-0.0142
BA-HPMA-14	3.0000	1.2847	7.0057	0.6648	0.7764	0.0737
BA-HPMA-15	9.0000	3.2522	24.9062	6.2326	0.9251	0.2315

Table 4.78: Extended Kelen-Tudos parameters for poly(BA-*co*-HPMA) system

Copolymer Code	ζ_1	ζ_2	Z	H	G	ξ	η
BA-HPMA-1	0.5452	0.8022	0.4862	0.3194	-1.9013	0.0855	-0.5088
BA-HPMA-2	0.5132	0.7746	0.4831	0.5009	-1.8278	0.1278	-0.4665
BA-HPMA-3	0.4508	0.6818	0.5235	0.6033	-1.5946	0.1500	-0.3966
BA-HPMA-4	0.3217	0.5492	0.4871	0.8228	-1.6521	0.1940	-0.3896
BA-HPMA-5	0.4824	0.7093	0.5330	1.0260	-1.3294	0.2309	-0.2992
BA-HPMA-6	0.3209	0.5436	0.4932	1.3063	-1.3831	0.2765	-0.2928
BA-HPMA-7	0.4814	0.6640	0.6020	1.3336	-0.8583	0.2807	-0.1806
BA-HPMA-8	0.3178	0.5422	0.4896	2.0012	-1.0629	0.3693	-0.1962
BA-HPMA-9	0.3178	0.5734	0.4488	2.7511	-0.9934	0.4460	-0.1610
BA-HPMA-10	0.3223	0.5503	0.4869	3.0199	-0.5834	0.4691	-0.0906
BA-HPMA-11	0.2925	0.5176	0.4747	3.7621	-0.3209	0.5240	-0.0447
BA-HPMA-12	0.1887	0.3771	0.4418	4.7615	-0.1599	0.5822	-0.0195
BA-HPMA-13	0.1351	0.3302	0.3623	7.2753	-0.1240	0.6804	-0.0116
BA-HPMA-14	0.1017	0.2375	0.3955	8.2110	0.7197	0.7061	0.0619
BA-HPMA-15	0.1599	0.4424	0.2982	36.5694	7.5523	0.9145	0.1889

The graphical copolymerisation plots of FR, KT and Extended KT are presented in Figures 4.58 (a-c). The plots are linear for all graphical methods, indicating that these follow conventional copolymerisation kinetics. The reactivity ratios of BA and HPMA are denoted as r_{BA} (or r_1) and r_{HPMA} (or r_2) respectively and the values obtained from various methods are presented in Table 4.80.

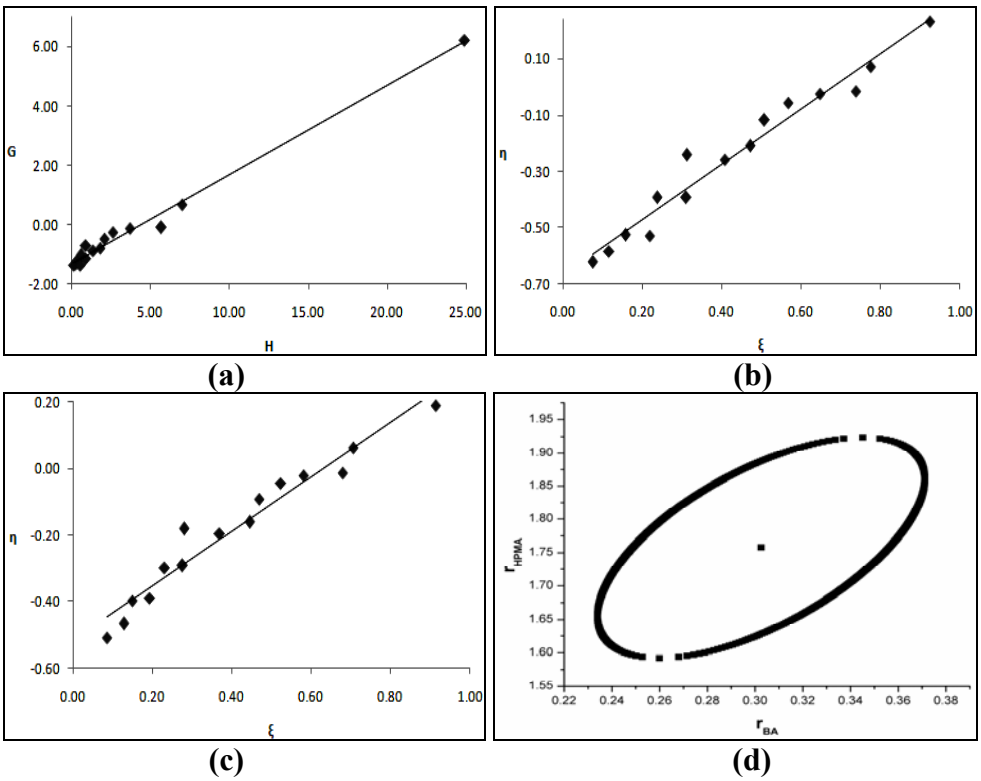

Figure 4.58: (a) FR, (b) KT (c) Extended KT plots for poly(BA-*co*-HPMA) system and (d) 95% Joint confidence interval calculated by MH method

The 95 % joint confidence limit of the reactivity ratio by Mao-Huglin method is plotted in Figure 4.58 (d). Its equation is,

$2.2886(r_1-0.1037)^2 - 0.8087(r_1-0.1037)(r_2-0.8630) + 0.3329(r_2-0.8630)^2 = 0.0278$

The statistical distribution of the sequences of two monomers (dyad) M_{BA}-M_{BA}, M_{HPA}-M_{HPA} and M_{BA}-M_{HPA} and mean sequence lengths μ_{BA} and μ_{HPA} are presented in Table 4.79, and the variation of the dyad fractions with the BA mole fraction in the copolymers is displayed in Figure 4.59.

Table 4.79: Structural data for poly(BA-*co*-HPMA) system

Copolymer Code	M_{BA}-M_{BA}	M_{HPMA}-M_{HPMA}	M_{BA}-M_{HPMA}	μ_{BA}	μ_{HPMA}
BA-HPMA-1	0.0025	0.8621	0.1354	1.0338	14.9608
BA-HPMA-2	0.0058	0.7965	0.1977	1.0538	9.7901
BA-HPMA-3	0.0111	0.7274	0.2615	1.0762	7.2048
BA-HPMA-4	0.0151	0.6884	0.2965	1.1015	5.6536
BA-HPMA-5	0.0309	0.5796	0.3895	1.1305	4.6195
BA-HPMA-6	0.0359	0.5536	0.4104	1.1640	3.8808
BA-HPMA-7	0.0722	0.4206	0.5072	1.2031	3.3268
BA-HPMA-8	0.0714	0.4231	0.5056	1.2492	2.8959
BA-HPMA-9	0.0895	0.3764	0.5341	1.3046	2.5512
BA-HPMA-10	0.1308	0.2964	0.5728	1.3723	2.2692
BA-HPMA-11	0.1649	0.2474	0.5877	1.4569	2.0341
BA-HPMA-12	0.1859	0.2225	0.5917	1.5657	1.8353
BA-HPMA-13	0.1924	0.2154	0.5922	1.7107	1.6648
BA-HPMA-14	0.2716	0.1470	0.5814	1.9138	1.5171
BA-HPMA-15	0.5636	0.0339	0.4025	3.7414	1.1724

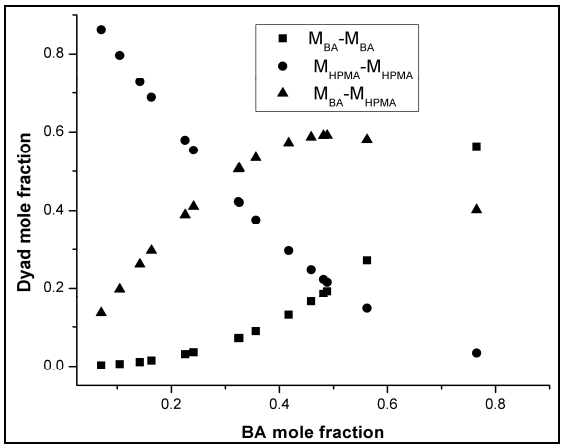

Figure 4.59: Dyad monomer sequence fractions verses the BA mole fractions for the copolymers.

Table 4.80: Reactivity ratios of BA and HPMA computed by different models

Method	r_{BA}	r_{HPMA}
Finemann-Ross	0.3001	1.3331
Kelen-Tudos	0.3142	1.3499
Extended Kelen-Tudos	0.3015	1.7639
Mao-Huglin	0.3026	1.7579
Average	0.3046	1.5512

The four methods show a general agreement for reactivity ratio r_{BA} and differ in their estimates for r_{HPA}. The differential forms and integral forms agree within themselves. The average value of r_{BA} is 0.3046 and that of r_{HPMA} is 1.5512, which indicates the faster incorporation of HPMA units in the copolymer than in feed. The product of the reactivity ratios of two monomers $r_{BA} \bullet r_{HPMA}$ is 0.4725 which suggests that there is tendency to form random copolymers.

4.20.2 Thermal analysis of poly(BA-*co*-HPMA)

The glass transition temperature (T_g) of poly(BA_{25}-$HPMA_{75}$), poly(BA_{50}-$HPMA_{50}$), and poly(BA_{75}-$HPMA_{25}$) were determined by DSC as 56.5, 38.5 and 3.4°C, respectively. The DSC thermograms are presented in Figure 4.60.

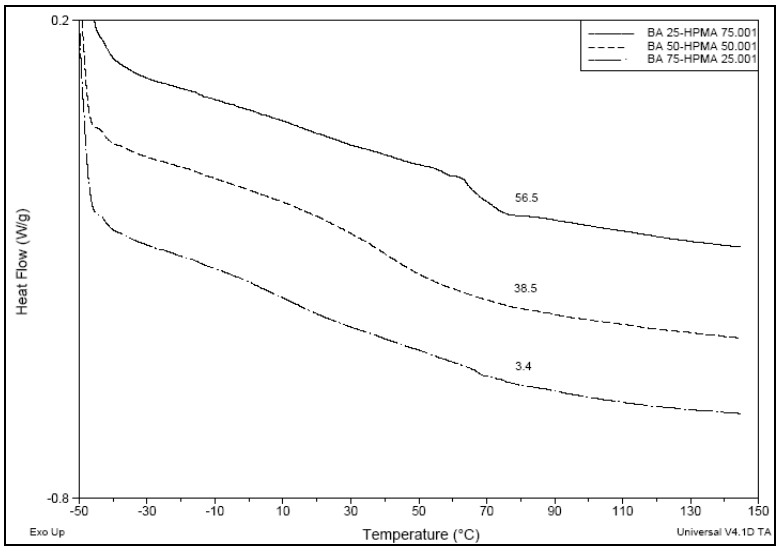

Figure 4.60: DSC thermograms of poly(BA_{25}-$HPMA_{75}$), poly(BA_{50}-$HPMA_{50}$), and poly(BA_{75}-$HPMA_{25}$).

The T_g of poly(BA) is -50°C, and that of poly(HEMA) is 76°C. The T_g values of copolymers decrease with increasing BA mole fraction in the copolymer.

4.21 Poly(2-ethylhexyl acrylate-*co*-2-hydroxypropyl methacrylate) System

This combination of monomers are used in coating formulations to provide good adhesion, impact and solvent resistance to aluminium cans.[107] The adhesives having good adhesion, and are useful for laminating phase contrast and polarising plates to form elliptic polarizing plates.[108]

4.21.1 Reactivity ratio determination for poly(EHA-*co*-HPMA) system

The reactivity ratios of EHA and HPMA were determined by Finemann-Ross (FR), Kelen-Tudos (KT), Extended Kelen-Tudos (Ext. KT) and Mao-Huglin (MH)

methods. The kinetic parameters of FR and KT for the copolymers are presented in Table 4.81 and that of Extended KT is shown in Table 4.82. The graphical copolymerisation plots of FR, KT and Extended KT are presented in Figures 4.61 (a-c). The plots are highly scattered for all graphical methods, indicating that these may not follow conventional copolymerisation kinetics. The reactivity ratios of EHA and HPMA are denoted as r_{EHA} (or r_1) and r_{HPMA} (or r_2) respectively and the values obtained from various methods are presented in Table 4.84.

Table 4.81: FR and KT parameters for poly(EHA-*co*-HPMA) system

Copolymer Code	$F=M_1/M_2$	$f=m_1/m_2$	$H=F^2/f$	$G=F(f-1)/f$	$\xi=H/(\alpha+H)$	$\eta=G/(\alpha+H)$
EHA-HPMA-1	0.1111	0.0372	0.3316	-2.8737	0.0946	-0.8197
EHA-HPMA-2	0.1765	0.0637	0.4890	-2.5946	0.1335	-0.7083
EHA-HPMA-3	0.2500	0.0774	0.8072	-2.9789	0.2027	-0.7482
EHA-HPMA-4	0.3333	0.0866	1.2833	-3.5165	0.2879	-0.7889
EHA-HPMA-5	0.4285	0.1863	0.9857	-1.8719	0.2370	-0.4500
EHA-HPMA-6	0.6666	0.2943	1.5102	-1.5987	0.3224	-0.3413
EHA-HPMA-7	0.8182	0.2381	2.8113	-2.6179	0.4697	-0.4374
EHA-HPMA-8	1.0000	0.2554	3.9158	-2.9158	0.5523	-0.4113
EHA-HPMA-9	1.2222	0.3411	4.3791	-2.3608	0.5798	-0.3126
EHA-HPMA-10	1.8571	0.7419	4.6490	-0.6462	0.5943	-0.0826
EHA-HPMA-11	3.0000	0.9724	9.2558	-0.0853	0.7446	-0.0069
EHA-HPMA-12	5.6666	1.7048	18.8353	2.3428	0.8558	0.1064
EHA-HPMA-13	8.9999	2.6657	30.3856	5.6237	0.9054	0.1676

Table 4.82: Extended Kelen-Tudos parameters for poly(EHA-*co*-HPMA) system

Copolymer Code	ζ_1	ζ_2	Z	H	G	ξ	η
EHA-HPMA-1	0.2294	0.6848	0.2257	0.7304	-4.2648	0.1185	-0.6921
EHA-HPMA-2	0.2004	0.5554	0.2760	0.8362	-3.3930	0.1334	-0.5413
EHA-HPMA-3	0.1589	0.5130	0.2405	1.3388	-3.8365	0.1977	-0.5666
EHA-HPMA-4	0.1383	0.5323	0.1958	2.2581	-4.6647	0.2936	-0.6066
EHA-HPMA-5	0.2831	0.6513	0.3159	1.8662	-2.5756	0.2557	-0.3529
EHA-HPMA-6	0.2525	0.5720	0.3429	2.5022	-2.0578	0.3154	-0.2594
EHA-HPMA-7	0.1583	0.5439	0.2195	4.9415	-3.4708	0.4764	-0.3346
EHA-HPMA-8	0.1453	0.5691	0.1865	7.3384	-3.9916	0.5746	-0.3126
EHA-HPMA-9	0.1549	0.5550	0.2078	7.8957	-3.1701	0.5924	-0.2379
EHA-HPMA-10	0.1324	0.3314	0.3527	5.9622	-0.7317	0.5233	-0.0642
EHA-HPMA-11	0.1114	0.3438	0.2804	12.3644	-0.0985	0.6948	-0.0055
EHA-HPMA-12	0.0690	0.2295	0.2744	22.6389	2.5684	0.8065	0.0915
EHA-HPMA-13	0.0977	0.3298	0.2569	40.4027	6.4847	0.8815	0.1415

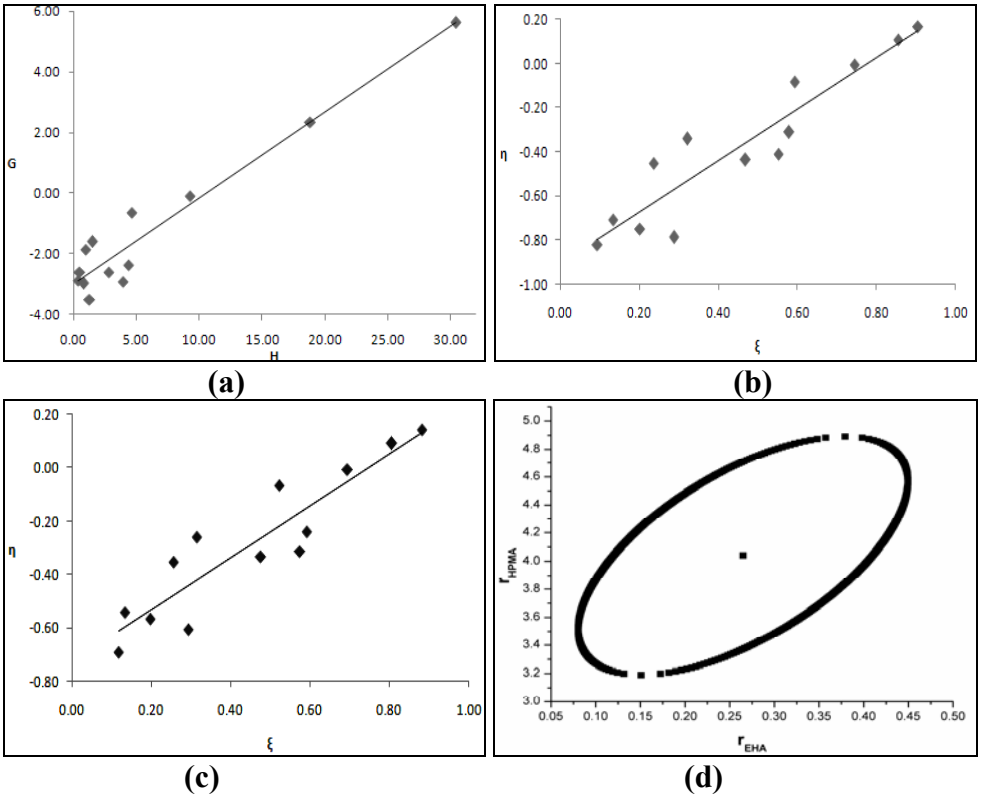

(a) **(b)** **(c)** **(d)**

Figure 4.61: (a) FR, (b) KT, (c) Ext. KT plots for poly(EHA-*co*-HPMA) system and (d) 95% Joint confidence interval calculated by MH method

The 95 % joint confidence limit of the reactivity ratio by Mao-Huglin method and has been plotted in Figure 4.61 (d). Its equation is,

$$3.4480(r_1 - 0.2650)^2 - 0.9248(r_1 - 0.2650)(r_2 - 4.0406) + 0.1621(r_2 - 4.0406)^2 = 0.0725$$

The statistical distribution of the sequences of two monomers (dyad) M_{EHA}-M_{EHA}, M_{HPMA}-M_{HPMA} and M_{EHA}-M_{HPMA} and mean sequence lengths μ_{EHA} and μ_{HPMA} are presented in Table 4.83, and the variation of the dyad fractions with the EHA mole fraction in the copolymers is displayed in Figure 4.62.

Table 4.83: Structural data for poly(EHA-*co*-HPMA) system

Copolymer Code	M_{BA}-M_{BA}	M_{HPMA}-M_{HPMA}	M_{BA}-M_{HPMA}	μ_{BA}	μ_{HPMA}
EHA-HPMA-1	0.0012	0.9294	0.0694	1.0292	32.1633
EHA-HPMA-2	0.0033	0.8836	0.1131	1.0464	20.6223
EHA-HPMA-3	0.0048	0.8610	0.1342	1.0657	14.8504
EHA-HPMA-4	0.0059	0.8465	0.1476	1.0876	11.3875
EHA-HPMA-5	0.0230	0.7090	0.2680	1.1127	9.0805
EHA-HPMA-6	0.0488	0.5941	0.3571	1.1753	6.1939
EHA-HPMA-7	0.0348	0.6501	0.3151	1.2151	5.2320
EHA-HPMA-8	0.0390	0.6321	0.3289	1.2629	4.4625
EHA-HPMA-9	0.0613	0.5527	0.3860	1.3213	3.8331
EHA-HPMA-10	0.1758	0.3240	0.5002	1.4882	2.8644
EHA-HPMA-11	0.2372	0.2512	0.5116	1.7887	2.1542
EHA-HPMA-12	0.3922	0.1316	0.4762	2.4898	1.6110
EHA-HPMA-13	0.5252	0.0708	0.4041	3.3661	1.3847

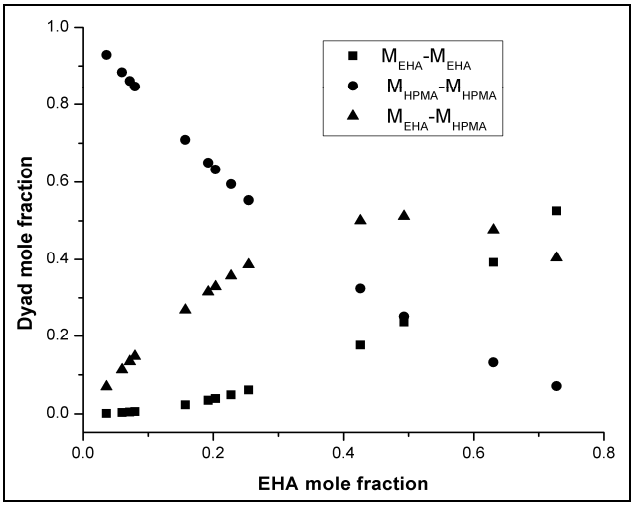

Figure 4.62: Dyad monomer sequence fractions verses the EHA mole fractions for the copolymers.

Table 4.84: Reactivity ratios of EHA and HPMA computed by different models

Method	r_{EHA}	r_{HPMA}
Finemann-Ross	0.2823	2.9694
Kelen-Tudos	0.2591	2.8853
Extended Kelen-Tudos	0.2452	3.9545
Mao-Huglin	0.2650	4.0406
Average	0.2629	3.4625

The methods show agreement for r_{EHA} and differ for r_{HPMA}. The values obtained by the integral form of kinetic estimates are more exact, since the data shows considerable scatter. HPMA is more reactive than EHA. The product of the reactivity ratios of two monomers $r_{EHA} \bullet r_{HPMA}$ is 0.9103, suggesting that there is tendency to form random copolymers.

4.21.2 Thermal analysis of poly(EHA-*co*-HPMA)

The glass transition temperature (T_g) poly(EHA_{25}-$HPMA_{75}$) and poly(EHA_{50}-$HPMA_{50}$), were determined by DSC as 42.3 and 26.5^oC. The DSC thermograms with T_g values of copolymers are given in Figure 4.63. The T_g values decrease with higher mole fractions of HPMA in copolymer.

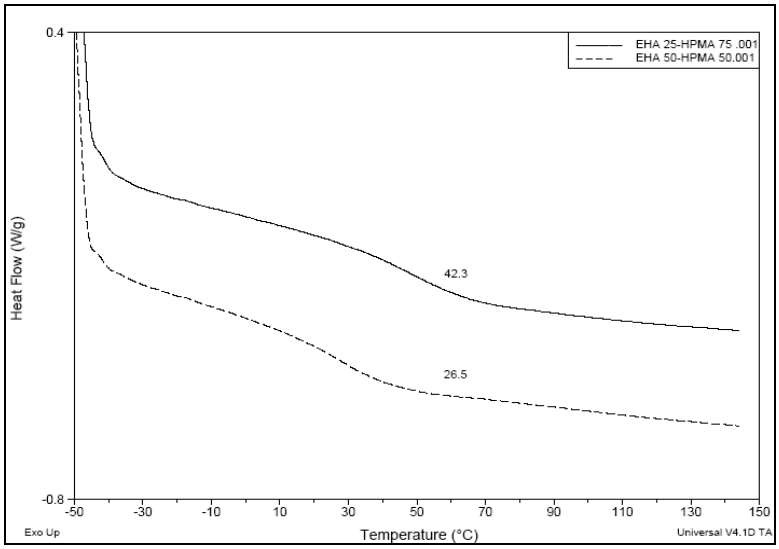

Figure 4.63: DSC thermograms of poly(EHA_{25}-$HPMA_{75}$), poly(EHA_{50}-$HPMA_{50}$).

4.22 Poly(methyl methacrylate-*co*-2-hydroxypropyl methacrylate) System

Poly(methyl methacrylate-*co*-2-hydroxypropyl methacrylate) are used as hosts in laser dyes due to optical homogeneity, transparency in pumping and lasing range, higher damage threshold and better photostability.[109] The effects of composition on the glass transition have been investigated with DSC.[110] The copolymers have been evaluated in acrylic bone cement to obtain ductile materials with reduced polymer shrinkage.[111]

4.22.1 Reactivity ratio determination for poly(MMA-*co*-HPMA) system

The reactivity ratios of MMA and HPMA were determined by Finemann-Ross (FR), Kelen-Tudos (KT), Extended Kelen-Tudos (Ext. KT) and Mao-Huglin (MH) methods. The parameters of FR and KT for the copolymers are presented in Table 4.85 and that of Extended KT is shown in Table 4.86. The graphical copolymerisation plots of FR, KT and Extended KT are presented in Figures 4.64 (a-c). The plots are linear for all graphical methods, indicating that these follow conventional copolymerisation kinetics. The reactivity ratios of MMA and HPMA are denoted as r_{MMA} (or r_1) and r_{HPMA} (or r_2) respectively and the values obtained from various methods are presented in Table 4.88.

Table 4.85: FR and KT parameters for poly(MMA-*co*-HPMA) system

Copolymer Code	$F=M_1/M_2$	$f=m_1/m_2$	$H=F^2/f$	$G=F(f-1)/f$	$\xi=H/(\alpha+H)$	$\eta=G/(\alpha+H)$
MMA-HPMA-1	0.1111	0.0888	0.1390	-1.1397	0.0782	-0.6414
MMA-HPMA-2	0.1765	0.1587	0.1962	-0.9352	0.1070	-0.5099
MMA-HPMA-3	0.2500	0.2328	0.2685	-0.8241	0.1409	-0.4323
MMA-HPMA-4	0.3333	0.2705	0.4108	-0.8991	0.2005	-0.4389
MMA-HPMA-5	0.4286	0.3692	0.4974	-0.7321	0.2330	-0.3429
MMA-HPMA-6	0.5385	0.4088	0.7093	-0.7787	0.3022	-0.3318
MMA-HPMA-7	0.6667	0.5343	0.8319	-0.5811	0.3368	-0.2353
MMA-HPMA-8	0.8182	0.6027	1.1107	-0.5394	0.4041	-0.1962
MMA-HPMA-9	1.0000	0.6650	1.5037	-0.5037	0.4786	-0.1603
MMA-HPMA-10	1.2222	0.8173	1.8278	-0.2733	0.5274	-0.0788
MMA-HMPA-11	1.5000	1.0537	2.1352	0.0765	0.5659	0.0203
MMA-HPMA-12	1.8571	1.0786	3.1975	0.1354	0.6613	0.0280
MMA-HPMA-13	3.0000	1.7007	5.2920	1.2360	0.7636	0.1784
MMA-HPMA-14	4.0000	2.0379	7.8513	2.0372	0.8274	0.2147
MMA-HPMA-15	9.0000	4.1962	19.303	6.8552	0.9218	0.3274

Table 4.86: Extended Kelen-Tudos parameters for poly(MMA-*co*-HPMA) system

Copolymer Code	ζ_1	ζ_2	Z	H	G	ξ	η
MMA-HPMA-1	0.6315	0.7899	0.6399	0.2170	-1.4240	0.0786	-0.5160
MMA-HPMA-2	0.8813	0.9797	0.5470	0.5305	-1.5379	0.1726	-0.5004
MMA-HPMA-3	0.9019	0.9688	0.6698	0.5187	-1.1454	0.1694	-0.3741
MMA-HPMA-4	0.7265	0.8953	0.5744	0.8198	-1.2701	0.2438	-0.3777
MMA-HPMA-5	0.8171	0.9485	0.5729	1.1249	-1.1009	0.3067	-0.3002
MMA-HPMA-6	0.6464	0.8514	0.5452	1.3751	-1.0843	0.3510	-0.2767
MMA-HPMA-7	0.6902	0.8613	0.5933	1.5177	-0.7850	0.3738	-0.1933
MMA-HPMA-8	0.5812	0.7890	0.5594	1.9261	-0.7103	0.4310	-0.1589
MMA-HPMA-9	0.4593	0.6906	0.5241	2.4212	-0.6392	0.4877	-0.1288
MMA-HPMA-10	0.4404	0.6587	0.5402	2.8012	-0.3383	0.5242	-0.0633
MMA-HMPA-11	0.4993	0.7107	0.5577	3.3885	0.0964	0.5713	0.0162
MMA-HPMA-12	0.3806	0.6553	0.4497	5.3326	0.1749	0.6771	0.0222
MMA-HPMA-13	0.3651	0.6440	0.4398	8.7923	1.5932	0.7757	0.1406
MMA-HPMA-14	0.3476	0.6823	0.3725	14.6884	2.7864	0.8524	0.1617
MMA-HPMA-15	0.2485	0.5329	0.3752	29.8021	8.5179	0.9214	0.2633

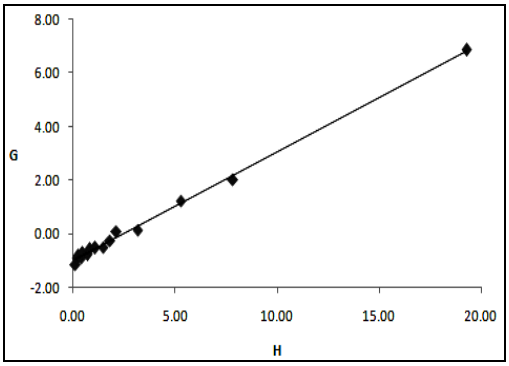

(a)

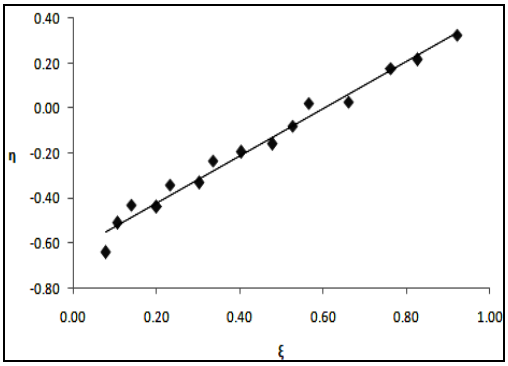

(b)

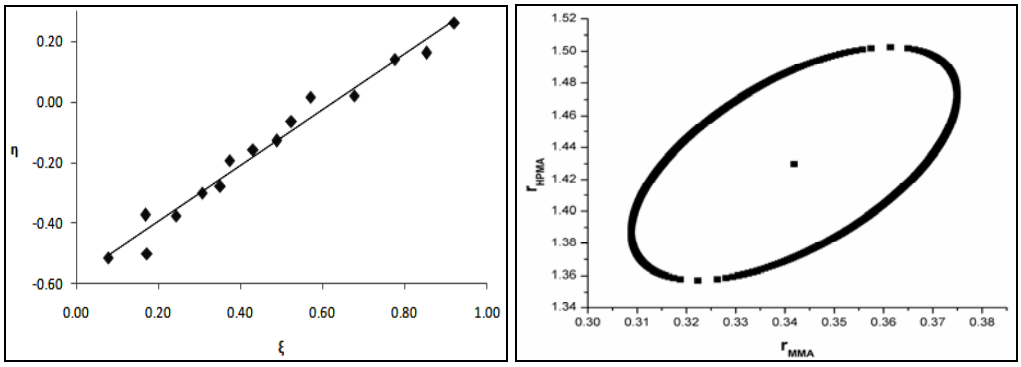

(c) **(d)**

Figure 4.64: (a) FR, (b) KT, (c) Ext. KT plots for poly(MMA-*co*-HPMA) system and (d) 95% Joint confidence interval calculated by MH method

The 95 % joint confidence limit of the reactivity ratio by Mao-Huglin method is plotted in Figure 4.64 (d). Its equation is,

$4.1772(r_1 - 0.3419)^2 - 2.2445(r_1 - 0.3419)(r_2 - 1.4299) + 0.8628(r_2 - 1.4299)^2 = 0.0030$

The statistical distribution of the sequences of two monomers (dyad) M_{MMA}-M_{MMA}, M_{HPMA}-M_{HPMA} and M_{MMA}-M_{HPMA} and mean sequence lengths μ_{MMA} and μ_{HPMA} are presented in Table 4.87, and the variation of the dyad fractions with the MMA mole fraction in the copolymers is displayed in Figure 4.65.

Table 4.87: Structural data for poly(MMA-*co*-HPMA) system

Copolymer Code	M_{MMA}-M_{MMA}	M_{HPMA}-M_{HPMA}	M_{MMA}-M_{HPMA}	μ_{MMA}	μ_{HPMA}
MMA-HPMA-1	0.0034	0.8402	0.1564	1.0419	12.1366
MMA-HPMA-2	0.0102	0.7362	0.2536	1.0666	8.0119
MMA-HPMA-3	0.0206	0.6429	0.3365	1.0943	5.9496
MMA-HPMA-4	0.0269	0.6011	0.3720	1.1257	4.7122
MMA-HPMA-5	0.0461	0.5067	0.4472	1.1617	3.8873
MMA-HPMA-6	0.0546	0.4743	0.4711	1.2031	3.2980
MMA-HPMA-7	0.0840	0.3876	0.5284	1.2515	2.8561
MMA-HPMA-8	0.1011	0.3490	0.5499	1.3086	2.5124
MMA-HPMA-9	0.1170	0.3182	0.5648	1.3772	2.2374
MMA-HPMA-10	0.1564	0.2569	0.5867	1.4610	2.0124
MMA-HMPA-11	0.2163	0.1901	0.5936	1.5658	1.8249
MMA-HPMA-12	0.2224	0.1846	0.5931	1.7005	1.6663
MMA-HPMA-13	0.3568	0.0974	0.5458	2.1316	1.4125
MMA-HPMA-14	0.4151	0.0735	0.5114	2.5088	1.3094
MMA-HPMA-15	0.6365	0.0214	0.3420	4.3948	1.1375

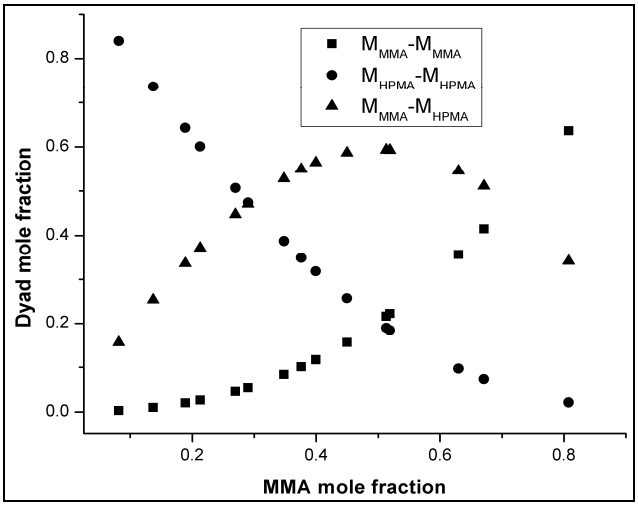

Figure 4.65: Dyad monomer sequence fractions verses the MMA mole fractions for the copolymers

Table 4.88: Reactivity ratios of MMA and HPMA computed by different models

Method	r_{MMA}	r_{HPMA}
Finemann-Ross	0.4061	1.0172
Kelen-Tudos	0.4162	1.0301
Extended Kelen-Tudos	0.3444	1.4724
Mao-Huglin	0.3419	1.4299
Average	0.3772	1.2374

The values obtained by the differential forms (FR and KT) and integral forms (Extended KT and MH) match within themselves. HPMA units add relatively faster to in the copolymer than MMA. The product of the reactivity ratios of two monomers $r_{MMA} \bullet r_{HPMA}$ value is 0.4667 indicating a tendency to form random copolymers.

4.22.2 Thermal analysis of poly(MMA-*co*-HPMA) system

The glass transition temperature (T_g) poly(MMA_{25}-$HPMA_{75}$), poly(MMA_{50}-$HPMA_{50}$), and poly(MMA_{75}-$HPMA_{25}$) were determined by DSC as 83.1, 43.5 and 21.6°C, respectively. The DSC thermograms are presented in Figure 4.66.

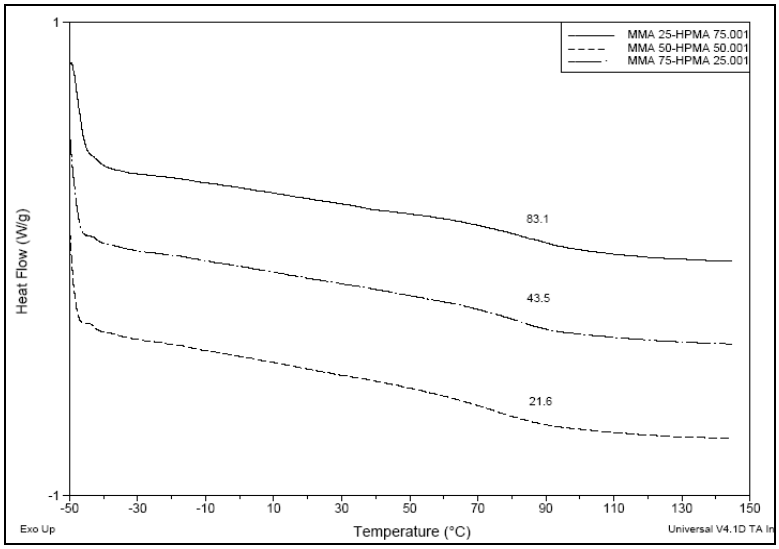

Figure 4.66: DSC thermograms of poly(MMA_{25}-$HPMA_{75}$), poly(MMA_{50}-$HPMA_{50}$), and poly(MMA_{75}-$HPMA_{25}$).

The T_g of poly(MMA) is 95 °C, and that of poly(HPMA) is 76 °C. The results shows that T_g values of copolymers differ and are depressed considerably relative to that of parent homopolymers.

4.23 Poly(2-ethylhexyl methacrylate-*co*-2-hydroxypropyl methacrylate) System

Poly(2-ethylhexyl methacrylate-*co*-2-hydroxypropyl methacrylate) are used in plasma display panels.[112-114] These are also used to prepare storage stable two-component curable adhesives[115] and coatings with improved hardness, acid resistance, crazing resistance and good reflow properties.[116]

4.23.1 Reactivity ratio determination for poly(EHMA-*co*-HPMA) system

The reactivity ratios of EHMA and HPMA were determined by Finemann-Ross (FR), Kelen-Tudos (KT), Extended Kelen-Tudos and Mao-Huglin (MH) methods. The parameters of FR and KT for the copolymers are presented in Table 4.89 and that of Extended KT is shown in Table 4.90. The graphical copolymerisation plots of FR, KT and Extended KT are presented in Figures 4.67 (a-c). The plots are linear for all graphical methods, indicating that these follow conventional copolymerisation kinetics. The reactivity ratios of EHMA and HPMA are denoted as r_{EHMA} (or r_1) and r_{HPMA} (or r_2) respectively and the values obtained from various methods are presented in Table 4.92.

Table 4.89: FR and KT parameters for poly(EHMA-*co*-HPMA) system

Copolymer Code	$F=M_1/M_2$	$f=m_1/m_2$	$H=F^2/f$	$G=F(f-1)/f$	$\xi=H/(\alpha+H)$	$\eta=G/(\alpha+H)$
EHMA-HPMA-1	0.1111	0.0946	0.1305	-1.0631	0.1061	-0.8648
EHMA-HPMA-2	0.1765	0.1629	0.1912	-0.9070	0.1482	-0.7031
EHMA-HPMA-3	0.2500	0.2238	0.2793	-0.8671	0.2027	-0.6292
EHMA-HPMA-4	0.3333	0.3013	0.3688	-0.7731	0.2513	-0.5268
EHMA-HPMA-5	0.4286	0.3919	0.4686	-0.6649	0.2990	-0.4242
EHMA-HPMA-6	0.5385	0.4974	0.5829	-0.5441	0.3466	-0.3235
EHMA-HPMA-7	0.6667	0.5945	0.7476	-0.4548	0.4049	-0.2463
EHMA-HPMA-8	0.8182	0.7369	0.9084	-0.2921	0.4526	-0.1455
EHMA-HPMA-9	1.0000	0.8533	1.1719	-0.1719	0.5161	-0.0757
EHMA-HPMA-10	1.2222	1.0884	1.3725	0.0993	0.5554	0.0402
EHMA-HPMA-11	1.8571	1.5778	2.1860	0.6801	0.6655	0.2070
EHMA-HPMA-12	2.3333	2.1549	2.5266	1.2505	0.6969	0.3449
EHMA-HPMA-13	3.0000	2.7822	3.2348	1.9217	0.7464	0.4434
EHMA-HPMA14	4.0000	3.7746	4.2389	2.9403	0.7941	0.5509
EHMA-HPMA-15	5.6667	5.2818	6.0796	4.5938	0.8469	0.6400
EHMA-HPMA-16	9.0000	8.7534	9.2536	7.9718	0.8939	0.7700

Table 4.90: Extended Kelen-Tudos parameters for poly(EHMA-*co*-HPMA) system

Copolymer Code	ζ_1	ζ_2	Z	H	G	ξ	η
EHMA-HPMA-1	0.7628	0.8958	0.6364	0.2336	-1.4226	0.1285	-0.7827
EHMA-HPMA-2	0.8479	0.9187	0.7505	0.2891	-1.1153	0.1544	-0.5954
EHMA-HPMA-3	0.8282	0.9251	0.6795	0.4847	-1.1423	0.2343	-0.5522
EHMA-HPMA-4	0.8461	0.9361	0.6803	0.6510	-1.0271	0.2913	-0.4596
EHMA-HPMA-5	0.8578	0.9380	0.7014	0.7967	-0.8670	0.3346	-0.3642
EHMA-HPMA-6	0.8771	0.9495	0.7021	1.0090	-0.7158	0.3891	-0.2761
EHMA-HPMA-7	0.8379	0.9397	0.6480	1.4157	-0.6258	0.4720	-0.2086
EHMA-HPMA-8	0.8517	0.9456	0.6554	1.7154	-0.4014	0.5199	-0.1217
EHMA-HPMA-9	0.7481	0.8766	0.6588	1.9661	-0.2226	0.5538	-0.0627
EHMA-HPMA-10	0.8285	0.9304	0.6617	2.4860	0.1336	0.6108	0.0328
EHMA-HPMA-11	0.6084	0.7161	0.7445	2.8464	0.7760	0.6425	0.1752
EHMA-HPMA-12	0.8524	0.9230	0.7462	3.8696	1.5476	0.7096	0.2838
EHMA-HPMA-13	0.8280	0.8928	0.7882	4.4782	2.2611	0.7387	0.3730
EHMA-HPMA-14	0.8606	0.9119	0.8108	5.7416	3.4220	0.7838	0.4671
EHMA-HPMA-15	0.8714	0.9349	0.7509	9.3679	5.7024	0.8554	0.5207
EHMA-HPMA-16	0.8780	0.9028	0.9027	10.7411	8.5887	0.8715	0.6968

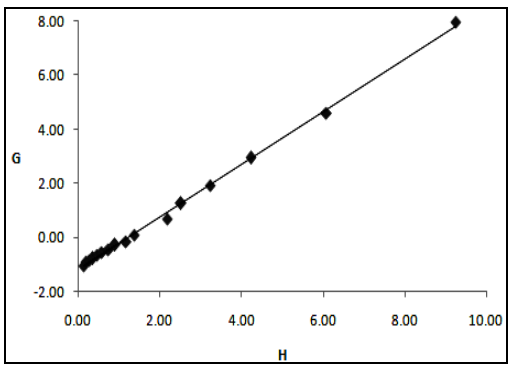

(a)

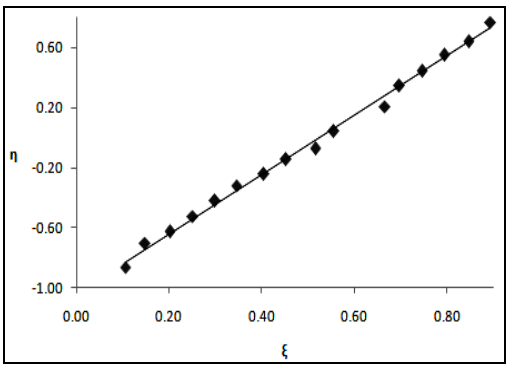

(b)

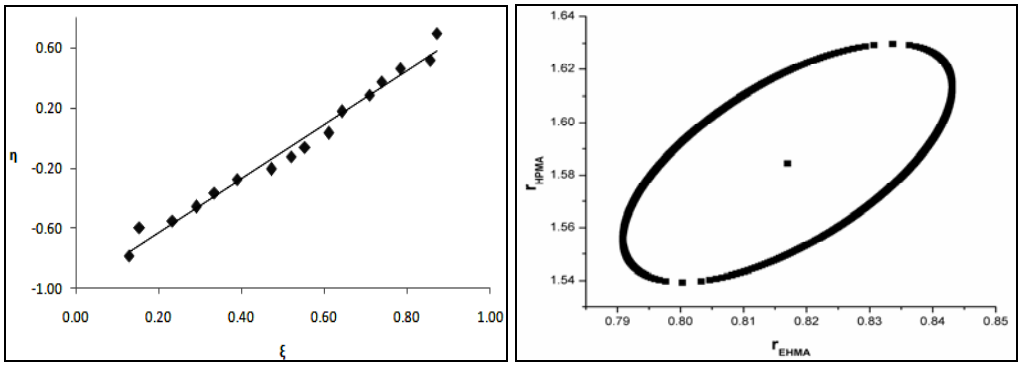

(c) **(d)**

Figure 4.67: (a) FR, (b) KT, (c) Ext. KT plots for poly(EHMA-*co*-HPMA) system and (d) 95% Joint confidence interval calculated by MH method

The 95 % joint confidence limit of the reactivity ratio values by Mao-Huglin method is plotted in Figure 4.67 (d). Its equation is,

$$4.8698(r_1-0.8170)^2 - 3.5938(r_1-0.8170)(r_2-1.5845) + 1.6252(r_2-1.5845)^2 = 0.0020$$

The statistical distribution of the sequences of two monomers (dyad) M_{EHMA}-M_{EHMA}, M_{HPMA}-M_{HPMA} and M_{EHMA}-M_{HPMA} and mean sequence lengths μ_{EHMA} and μ_{HPMA} are presented in Table 4.91, and the variation of the dyad fractions with the EHMA mole fraction in the copolymers is displayed in Figure 4.68.

Table 4.91: Structural data for poly(EHMA-*co*-HPMA) system

Copolymer Code	M_{EHMA}-M_{EHMA}	M_{HPMA}-M_{HPMA}	M_{EHMA}-M_{HPMA}	μ_{EHMA}	μ_{HPMA}
EHMA-HPMA-1	0.0088	0.8359	0.1554	1.0984	13.3336
EHMA-HPMA-2	0.0226	0.7424	0.2350	1.1562	8.7656
EHMA-HPMA-3	0.0379	0.6722	0.2899	1.2214	6.4816
EHMA-HPMA-4	0.0599	0.5968	0.3433	1.2951	5.1112
EHMA-HPMA-5	0.0873	0.5242	0.3885	1.3795	4.1976
EHMA-HPMA-6	0.1200	0.4556	0.4245	1.4768	3.5450
EHMA-HPMA-7	0.1496	0.4040	0.4464	1.5903	3.0556
EHMA-HPMA-8	0.1916	0.3430	0.4654	1.7244	2.6749
EHMA-HPMA-9	0.2239	0.3031	0.4730	1.8854	2.3704
EHMA-HPMA-10	0.2836	0.2413	0.4750	2.0822	2.1212
EHMA-HPMA-11	0.3856	0.1614	0.4530	2.6443	1.7379
EHMA-HPMA-12	0.4757	0.1096	0.4147	3.0659	1.5873
EHMA-HPMA-13	0.5486	0.0774	0.3741	3.6562	1.4568
EHMA-HPMA14	0.6305	0.0493	0.3202	4.5416	1.3426
EHMA-HPMA-15	0.7106	0.0290	0.2605	6.0173	1.2418
EHMA-HPMA-16	0.8072	0.0123	0.1806	8.9686	1.1523

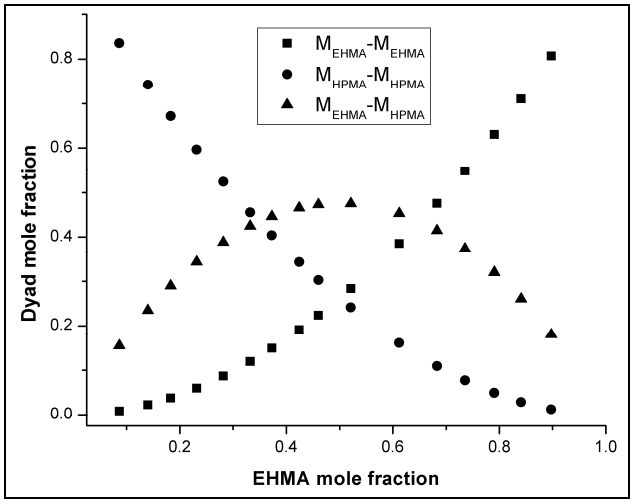

Figure 4.68: Dyad monomer sequence fractions verses the EHMA mole fractions for the copolymers.

Table 4.92: Reactivity ratios of EHMA and HPMA computed by different models

Method	r_{EHMA}	r_{HPMA}
Finemann-Ross	0.9732	1.1954
Kelen-Tudos	0.9382	1.1384
Extended Kelen-Tudos	0.8130	1.5634
Mao-Huglin	0.8170	1.5845
Average	0.8854	1.3704

The values obtained by differential and integral forms differ with each other but agree within themselves. HPMA adds to the copolymer chain faster than EHMA. The product of the reactivity ratios of two monomers $r_{EHMA} \bullet r_{HPMA}$ value is 1.2134 suggesting a tendency to form longer sequences of HPMA in the copolymer chain.

4.23.2 Thermal analysis of poly(EHMA-*co*-HPMA) system

The glass transition temperature (T_g) poly($EHMA_{25}$-$HPMA_{75}$), poly($EHMA_{50}$-$HPMA_{50}$), and poly($EHMA_{75}$-$HPMA_{25}$) were determined by DSC as 39.4, 12.3 and 1.2°C, respectively. The DSC thermograms are presented in Figure 4.69.

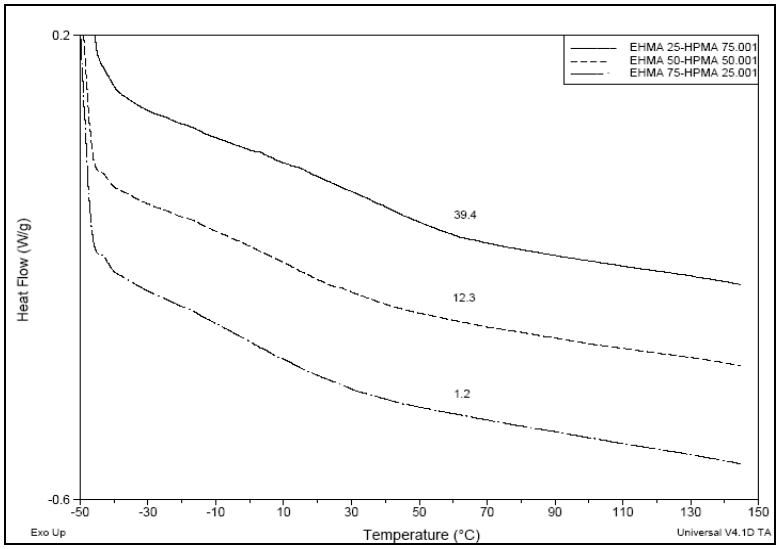

Figure 4.69: DSC thermograms of poly(EHMA$_{25}$-HPMA$_{75}$), poly(EHMA$_{50}$-HPMA$_{50}$), and poly(EHMA$_{75}$-HPMA$_{25}$).

The T_g of poly(EHMA) is -10°C, and that of poly(HPMA) is 76°C. The results shows that T_g values of copolymers decrease with increasing EHMA mole fraction in copolymer.

4.24 Poly(2-hydroxyethyl acrylate-*co*-2-hydroxypropyl methacrylate) System

Poly(2-hydroxyethyl acrylate-*co*-2-hydroxypropyl methacrylate) are used to coat hollow microsphere emulsion in printing coating applications.[117] The polymers are also used in single-fluid general plastic gravure alcohol and water-soluble compound ink.[118]

4.24.1 Reactivity ratio determination for poly(HEA-*co*-HPMA) system

The reactivity ratios of HEA and HPMA were determined by Finemann-Ross (FR), Kelen-Tudos (KT), Extended Kelen-Tudos (Ext. KT) and Mao-Huglin (MH) methods. The parameters of FR and KT for the copolymers are presented in Table 4.93 and that of Extended KT is shown in Table 4.94. The graphical copolymerisation plots of FR, KT and Extended KT are presented in Figures 4.70 (a-c). The plots are some what scattered for all graphical methods, indicating that these may not follow conventional copolymerisation kinetics. The reactivity ratios of HEA and HPMA are denoted as r_{HEA} (or r_1) and r_{HPMA} (or r_2) respectively and the values obtained from various methods are presented in Table 4.96.

Table 4.93: FR and KT parameters for poly(HEA-*co*-HPMA) system

Copolymer Code	$F=M_1/M_2$	$f=m_1/m_2$	$H=F^2/f$	$G=F(f-1)/f$	$\xi=H/(\alpha+H)$	$\eta=G/(\alpha+H)$
HEA-HPMA-1	0.1111	0.1554	0.0794	-0.6039	0.0898	-0.6828
HEA-HPMA-2	0.1765	0.2218	0.1404	-0.6192	0.1485	-0.6550
HEA-HPMA-3	0.2500	0.3225	0.1938	-0.5253	0.1940	-0.5259
HEA-HPMA-4	0.3333	0.3514	0.3162	-0.6152	0.2820	-0.5487
HEA-HPMA-5	0.4286	0.4453	0.4125	-0.5339	0.3388	-0.4385
HEA-HPMA-6	0.6667	0.6526	0.6811	-0.3549	0.4583	-0.2388
HEA-HPMA-7	0.8182	0.7187	0.9315	-0.3203	0.5364	-0.1845
HEA-HPMA-8	1.0000	0.8605	1.1621	-0.1621	0.5908	-0.0824
HEA-HPMA-9	1.2222	1.3279	1.1250	0.3018	0.5829	0.1564
HEA-HPMA-10	1.5000	1.2176	1.8479	0.2681	0.6966	0.1010
HEA-HPMA-11	1.8571	1.7778	1.9401	0.8125	0.7067	0.2960
HEA-HPMA-12	2.3333	1.9328	2.8169	1.1261	0.7777	0.3109
HEA-HPMA-13	5.6667	3.9371	8.1559	4.2274	0.9102	0.4718

Table 4.94: Extended Kelen-Tudos parameters for poly(HEA-*co*-HPMA) system

Copolymer Code	ζ_1	ζ_2	Z	H	G	ξ	η
HEA-HPMA-1	0.5619	0.4018	1.6063	0.0602	-0.5258	0.0766	-0.6687
HEA-HPMA-2	0.7611	0.6056	1.5388	0.0937	-0.5057	0.1143	-0.6169
HEA-HPMA-3	0.3794	0.2941	1.3696	0.1719	-0.4947	0.1914	-0.5509
HEA-HPMA-4	0.2895	0.2746	1.0646	0.3100	-0.6092	0.2992	-0.5880
HEA-HPMA-5	0.2713	0.2611	1.0459	0.4071	-0.5304	0.3592	-0.4680
HEA-HPMA-6	0.2638	0.2695	0.9753	0.6861	-0.3562	0.4858	-0.2523
HEA-HPMA-7	0.1917	0.2183	0.8644	0.9619	-0.3255	0.5698	-0.1928
HEA-HPMA-8	0.2324	0.2701	0.8401	1.2191	-0.1660	0.6267	-0.0854
HEA-HPMA-9	0.2419	0.2226	1.0996	1.0983	0.2982	0.6020	0.1634
HEA-HPMA-10	0.3281	0.4042	0.7679	2.0649	0.2834	0.7398	0.1015
HEA-HPMA-11	0.3676	0.3841	0.9457	1.9877	0.8224	0.7324	0.3030
HEA-HPMA-12	0.2041	0.2464	0.8070	2.9681	1.1559	0.8034	0.3129
HEA-HPMA-13	0.1380	0.1986	0.6707	8.7532	4.3794	0.9234	0.4620

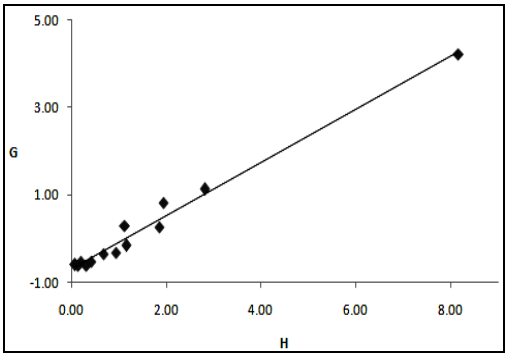

(a)

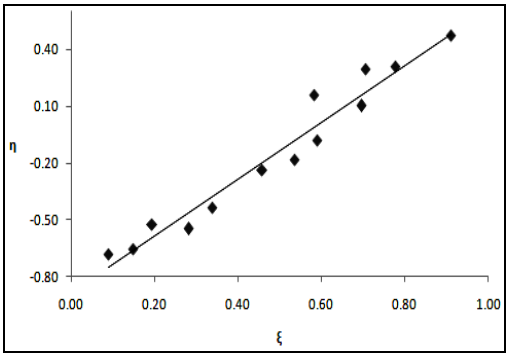

(b)

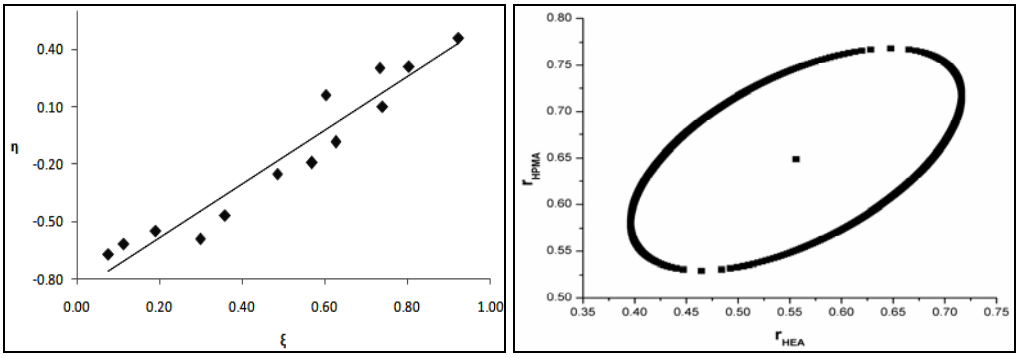

(c) **(d)**

Figure 4.70: (a) FR, (b) KT, (c) Ext. KT plots for poly(HEA-*co*-HPMA) system and (d) 95% Joint confidence interval calculated by MH method

The 95 % joint confidence limit of the reactivity ratio by Mao-Huglin method is plotted in Figure 4.70 (d). Its equation is,

$$4.0614(r_1 - 0.5561)^2 - 6.2208(r_1 - 0.5561)(r_2 - 0.6489) + 7.2829(r_2 - 0.6489)^2 = 0.0700$$

The statistical distribution of the sequences of two monomers (dyad) M_{HEA}-M_{HEA}, M_{HPMA}-M_{HPMA} and M_{HEA}-M_{HPMA} and mean sequence lengths μ_{EHMA} and μ_{HPMA} are presented in Table 4.95, and the variation of the dyad fractions with the HEA mole fraction in the copolymers is displayed in Figure 4.71.

Table 4.95: Structural data for poly(HEA-*co*-HPMA) system

Copolymer Code	M_{HEA}-M_{HEA}	M_{HPA}-M_{HPA}	M_{HEA}-M_{HPA}	μ_{HEA}	μ_{HPA}
HEA-HPMA-1	0.0084	0.7394	0.2522	1.0645	7.0507
HEA-HPMA-2	0.0163	0.6533	0.3304	1.1025	4.8097
HEA-HPMA-3	0.0321	0.5445	0.4234	1.1452	3.6892
HEA-HPMA-4	0.0374	0.5173	0.4453	1.1935	3.0169
HEA-HPMA-5	0.0563	0.4401	0.5037	1.2488	2.5687
HEA-HPMA-6	0.1045	0.3148	0.5807	1.3871	2.0085
HEA-HPMA-7	0.1210	0.2847	0.5942	1.4750	1.8217
HEA-HPMA-8	0.1570	0.2320	0.6110	1.5806	1.6723
HEA-HPMA-9	0.2706	0.1297	0.5997	1.7096	1.5501
HEA-HPMA-10	0.2452	0.1470	0.6078	1.8709	1.4482
HEA-HPMA-11	0.3627	0.0827	0.5545	2.0783	1.3620
HEA-HPMA-12	0.3903	0.0722	0.5375	2.3547	1.2881
HEA-HPMA-13	0.6158	0.0209	0.3633	4.2901	1.1186

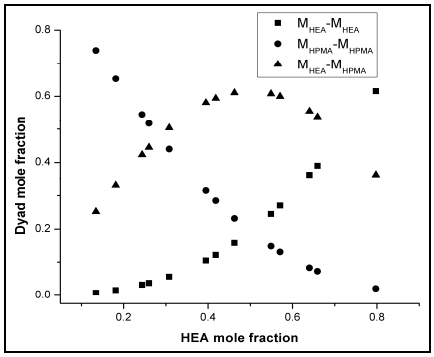

Figure 4.71: Dyad monomer sequence fractions verses the HEA mole fractions for the copolymers.

Table 4.96: Reactivity ratios of HEA and HPMA computed by different models

Method	r_{HEA}	r_{HPMA}
Finemann-Ross	0.6113	0.7011
Kelen-Tudos	0.6162	0.7116
Extended Kelen-Tudos	0.5391	0.6274
Mao-Huglin	0.5561	0.6489
Average	0.5806	0.6723

The average value of r_{HEA} is equal to 0.5806 and that of r_{HPMA} is equal to 0.6723, which indicates that there is slightly higher incorporation of HPMA units in the copolymer than HEA. The product of the reactivity ratios of two monomers $r_{HEA} \bullet r_{HPMA}$ value is 0.3903 which is less than 1, suggesting that there is tendency for the formation of random copolymer system. Since the r_1 and r_2 values are less than one, this system gives rise to azeotropic polymerisation at a particular composition of the monomers which is calculated using equation 4.1 as when the mole fraction of the HEA in the feed is 0.4386.

4.24.2 Thermal analysis of poly(HEA-*co*-HPMA)

The glass transition temperature (T_g) poly(HEA_{25}-$HPMA_{75}$), poly(HEA_{50}-$HPMA_{50}$), and poly(HEA_{75}-$HPMA_{25}$) were determined by DSC as 35.1, 13.2 and 1.1^oC, respectively. The DSC thermograms are presented in Figure 4.72.

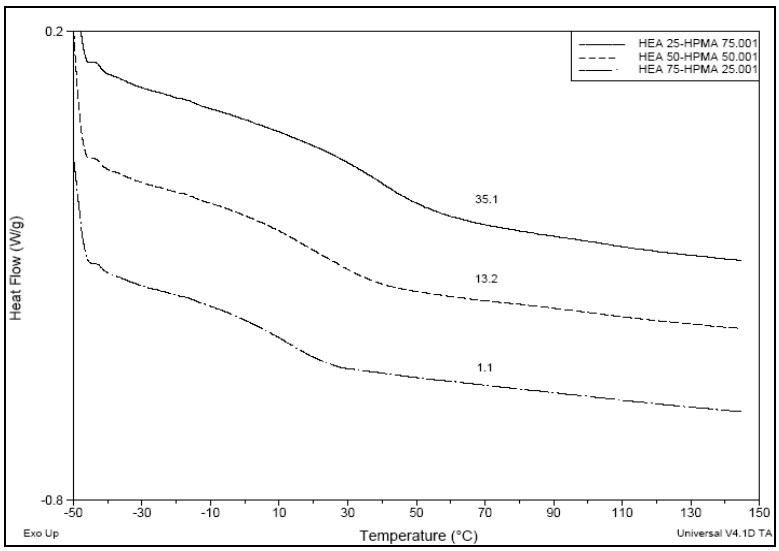

Figure 4.72: DSC thermograms of poly(HEA_{25}-$HPMA_{75}$), poly(HEA_{50}-$HPMA_{50}$), and poly(HEA_{75}-$HPMA_{25}$).

The T_g of poly(HEA) is 2°C, and that of poly(HPMA) is 76°C. The data shows that T_g of copolymers decrease with increase in HEA mole fraction in the

copolymer. In lens application low T_g are required to improve material performance, particularly during the surgical procedures, where some sample folding is required. These copolymers showed relatively low glass transition temperatures (35.1 to 1.1°C), which are desirable.

4.25 Poly(2-hydroxypropyl acrylate-*co*-2-hydroxypropyl methacrylate) System

These copolymers are used in waterproofing and oil-repellent fabric finishing agents,[119] cold curable emulsion adhesive for paper-plastic bonding,[120] room temperature curable translucent material[121] and in preparation of thermosetting liquid coating compositions for aluminium wheels.[122]

4.25.1 Reactivity ratio determination for poly(HPA-*co*-HPMA) system

The reactivity ratios of HPA and HPMA were determined by Finemann-Ross (FR), Kelen-Tudos (KT), extended Kelen-Tudos (ext. KT) and Mao-Huglin (MH) methods. The parameters of FR and KT for the copolymers are presented in Table 4.97 and that of extended KT is shown in Table 4.98.

Table 4.97: FR and KT parameters for poly(HPA-*co*-HPMA) system

Copolymer Code	$F=M_1/M_2$	$f=m_1/m_2$	$H=F^2/f$	$G=F(f-1)/f$	$\xi=H/(\alpha+H)$	$\eta=G/(\alpha+H)$
HPA-HPMA-1	0.1111	0.1271	0.0972	-0.7633	0.1042	-0.8183
HPA-HPMA-2	0.1765	0.2013	0.1547	-0.7000	0.1562	-0.7069
HPA-HPMA-3	0.2500	0.2476	0.2524	-0.7598	0.2320	-0.6983
HPA-HPMA-4	0.3333	0.3012	0.3689	-0.7733	0.3063	-0.6420
HPA-HPMA-5	0.4286	0.3753	0.4894	-0.7133	0.3693	-0.5384
HPA-HPMA-6	0.5385	0.4849	0.5980	-0.5721	0.4171	-0.3991
HPA-HPMA-7	0.6667	0.6239	0.7123	-0.4018	0.4602	-0.2596
HPA-HPMA-8	0.8182	0.6450	1.0379	-0.4504	0.5540	-0.2404
HPA-HPMA-9	2.3333	2.2564	2.4129	1.2992	0.7428	0.3999
HPA-HPMA-10	5.6667	7.2338	4.4390	4.8833	0.8416	0.9258
HPA-HPMA-11	9.0000	11.2716	7.1862	8.2015	0.8958	1.0224

Table 4.98: Ext. Kelen-Tudos parameters for poly(HPA-*co*-HPMA) system

Copolymer Code	ζ_1	ζ_2	Z	H	G	ξ	η
HPA-HPMA-1	0.3065	0.2680	1.1732	0.0923	-0.7441	0.1034	-0.8336
HPA-HPMA-2	0.3389	0.2970	1.1741	0.1460	-0.6802	0.1543	-0.7188
HPA-HPMA-3	0.3321	0.3354	0.9881	0.2536	-0.7615	0.2406	-0.7226
HPA-HPMA-4	0.2424	0.2682	0.8888	0.3813	-0.7862	0.3227	-0.6654
HPA-HPMA-5	0.2438	0.2784	0.8565	0.5116	-0.7294	0.3900	-0.5559
HPA-HPMA-6	0.3737	0.4150	0.8727	0.6366	-0.5903	0.4430	-0.4108
HPA-HPMA-7	0.1511	0.1615	0.9304	0.7209	-0.4042	0.4739	-0.2657
HPA-HPMA-8	0.1713	0.2173	0.7669	1.0966	-0.4629	0.5781	-0.2440
HPA-HPMA-9	0.1833	0.1896	0.9634	2.4309	1.3041	0.7523	0.4036
HPA-HPMA-10	0.1867	0.1462	1.3070	4.2350	4.7698	0.8411	0.9473
HPA-HPMA-11	0.1537	0.1227	1.2746	6.9386	8.0590	0.8966	1.0414

The graphical copolymerisation plots of FR, KT and extended KT are presented in Figures 4.73 (a-c). The plots are some what scattered for all graphical methods, indicating that these may not follow conventional copolymerisation kinetics. The reactivity ratios of HPA and HPMA are denoted as r_{HPA} (or r_1) and r_{HPMA} (or r_2) respectively and the values obtained from various methods are presented in Table 4.100.

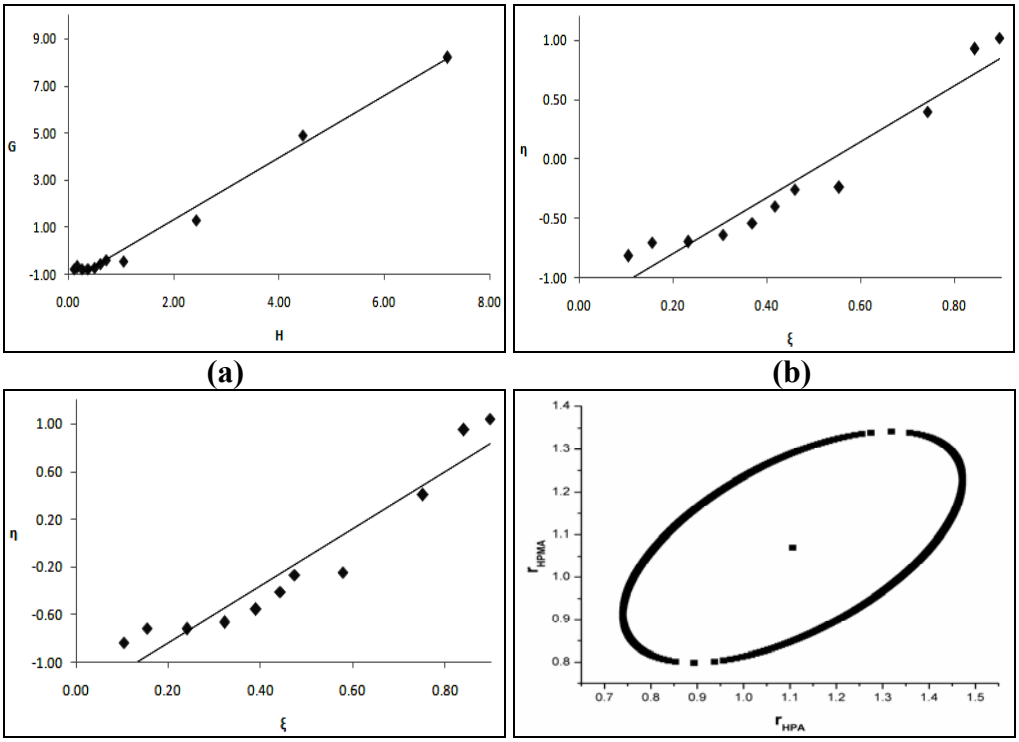

Figure 4.73: (a) FR, (b) KT, (c) Ext. KT plots for poly(HPA-*co*-HPMA) system and (d) 95% Joint confidence interval calculated by MH method

The 95 % joint confidence limit of the reactivity ratio by Mao-Huglin method is plotted in Figure 4.73 (d). Its equation is,

$3.0679(r_1\text{-}1.1060)^2 - 4.8111(r_1\text{-}1.1060)(r_2\text{-}1.0703) + 5.5807(r_2\text{-}1.0703)^2 = 0.2723$

The statistical distribution of the sequences of two monomers (dyad) M_{HPA}-M_{HPA}, M_{HPMA}-M_{HPMA} and M_{HPA}-M_{HPMA} and mean sequence lengths μ_{HPA} and μ_{HPMA} are presented in Table 4.99, and the variation of the dyad fractions with the HPA mole fraction in the copolymers is displayed in Figure 4.74.

Table 4.99: Structural data for poly(HPA-*co*-HPMA) system

Copolymer Code	M_{HPA}-M_{HPA}	M_{HPMA}-M_{HPMA}	M_{HPA}-M_{HPMA}	μ_{HPA}	μ_{HPMA}
HPA-HPMA-1	0.0149	0.7894	0.1957	1.1275	11.0233
HPA-HPMA-2	0.0323	0.6971	0.2707	1.2024	7.3110
HPA-HPMA-3	0.0448	0.6479	0.3074	1.2868	5.4548
HPA-HPMA-4	0.0603	0.5973	0.3424	1.3824	4.3411
HPA-HPMA-5	0.0827	0.5369	0.3804	1.4917	3.5986
HPA-HPMA-6	0.1167	0.4636	0.4197	1.6177	3.0683
HPA-HPMA-7	0.1592	0.3907	0.4501	1.7648	2.6706
HPA-HPMA-8	0.1654	0.3813	0.4533	1.9386	2.3612
HPA-HPMA-9	0.4895	0.1037	0.4067	3.6768	1.4773
HPA-HPMA-10	0.7743	0.0172	0.2084	7.5008	1.1965
HPA-HPMA-11	0.8449	0.0079	0.1472	11.3248	1.1237

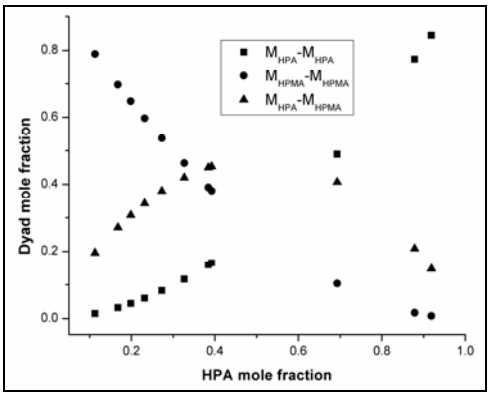

Figure 4.74: Dyad monomer sequence fractions verses the HPA mole fractions for the copolymers.

Table 4.100: Reactivity ratios of HPA and HPMA computed by different models

Method	r_{HPA}	r_{HPMA}
Finemann-Ross	1.3092	1.2723
Kelen-Tudos	1.0941	1.0604
Extended Kelen-Tudos	1.0793	1.0516
Mao-Huglin	1.1060	1.0703
Average	1.1472	1.1137

The average value of r_{HPA} is equal to 1.1472 and that of r_{HPMA} is equal to 1.1137, which indicates that there is slightly higher incorporation of HPMA units in the copolymer than HEA in the copolymer. The product of the reactivity ratios of two monomers $r_{HPA} \bullet r_{HPMA}$ value is 1.2776 which is greater than 1, suggesting that there is a marginal tendency to form block copolymers.

4.25.2 Thermal analysis of poly(HPA-*co*-HPMA)

The glass transition temperature (T_g) of poly(HPA_{25}-$HPMA_{75}$), poly(HPA_{50}-$HPMA_{50}$), and poly(HPA_{75}-$HPMA_{25}$) were determined by DSC as 29.7, 37.2 and 7.3ºC, respectively. The DSC thermograms are presented in Figure 4.75.

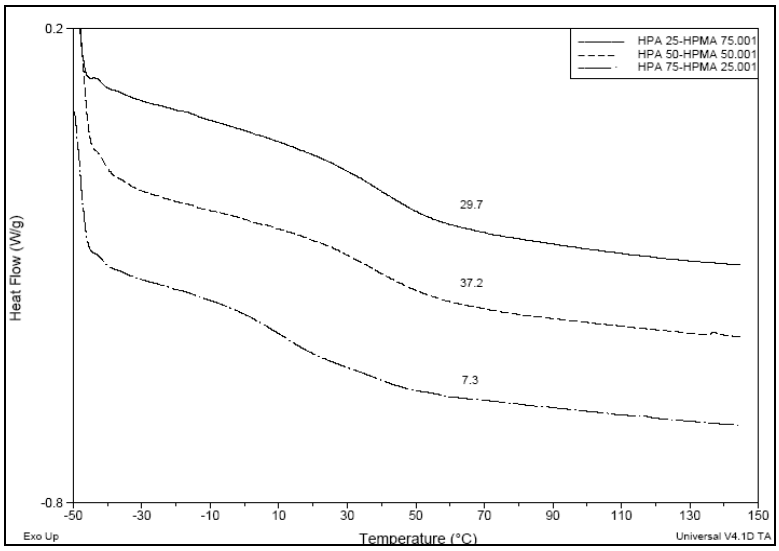

Figure 4.75: DSC thermograms of poly(HPA_{25}-$HPMA_{75}$), poly(HPA_{50}-$HPMA_{50}$), and poly(HPA_{75}-$HPMA_{25}$).

The T_g of poly(HPA) is 14 °C, and that of poly(HPMA) is 76 °C. The results shows that T_g values of copolymers are lower than HPMA and go through a maxia relative to HPA content in the copolymer.

4.26 Comparative Evaluation of Copolymers

These copolymers were studied to determine how each monomer adds to the copolymer chain relative to each other and ultimately whether any of these systems have properities that merit further technical evaluation. Some of these properties are (i) what are the reactivity ratios; (ii) which of these combinations are capable of forming azeotropic compositions; (iii) what is the glass transition temperature of the copolymer with equimolar amounts of the two respective comonomers.

The primary objective of this research was also to determine which, if any of these copolymers could be suitable as (a) hydrogels, (b) contact lens, (c) intraocular lens and (d) scaffold materials for tissue engineering. While technological implications are beyond the scope of this research, a comparative study of basic data presented in Sections 4.1 through 4.25 are presented here.

4.26.1 Copolymers of hydroxyethyl acrylate

A set of 5 copolymers investigated within these series are poly(2-hydroxyethyl acrylate-*co*-methyl acrylate), poly(2-hydroxyethyl acrylate-*co*-butyl acrylate), poly(2-hydroxyethyl acrylate-*co*-2-ethylhexyl acrylate), poly(2-hydroxyethyl acrylate-*co*-methyl methacrylate) and poly(2-hydroxyethyl acrylate-*co*-2-ethylhexyl methacrylate). The monomer reactivity ratio based on extended form of Kelen-Tudos was used in the analysis. Similarly, the copolymers whose glass transition temperatures were compared are poly(HEA_{50}-MA_{50}), poly(HEA_{50}-BA_{50}), poly(HEA_{50}-EHA_{50}), poly(HEA_{50}-MMA_{50}) and poly(HEA_{50}-$EHMA_{50}$). The data is presented in Table 4.101. In all monomer reactivity ratio data r_1 is r_{HEA} and r_2 represents the respective comonomer (MA, BA, EHA, MMA and EHMA, respectively).

Table 4.101: Reactivity ratios of HEA copolymers and their T_g values

Copolymer	r_{HEA}	r_2	T_g, °C
HEA-MA	1.855	1.467	1.5
HEA-BA	2.033	0.638	-15.4
HEA-EHA	1.367	0.442	-14.2
HEA-MMA	0.968	0.154	12.3
HEA-EHMA	1.030	0.749	-5.1

The data shows that, within the relative accuracy of the some what scattered data collection in this study, 2-hydroxyethyl acrylate adds at a higher rate in all copolymers relative to the other acrylate and methacrylate comonomers. Changing methyl acrylate with butyl acrylate (pendent group with single carbon to four carbons) increases the relative reactivity of 2-hydroxyethyl acrylate. Further increase in pendent chain length as well as branching (butyl to 2-ethylhexyl unit) has a mariginal influence. The T_g values are decreased considerably and then is relatively unchanged (within experimental error). Changing the hydrogen in methyl acrylate with methyl unit in methyl methacrylate is known to increase hydrophobic interaction. This is seen to stiffen the polymer chain, as seen in the increase in T_g from 1.5 to 12.3^oC. Interestingly, a change from EHA to EHMA increases the reactivity of the comonomer relative to 2-hydroxyethyl acrylate. EHA is a more reactive monomer in homopolymerisation relative to EHMA. The effect is the opposite in copolymerisation. The other interesting feature is that the copolymer chain is less stiffer, as seen from the decrease in T_g from 1.5 to -5.1^oC. Both these are opposite to

what would have been predicted on the basis of general structural considerations. The poly(2-hydroxyethyl acrylate-*co*-methyl methacrylate) is capable of forming azeotropic composition, which merits further examination from application perspectives.

4.26.2 Copolymers of hydroxypropyl acrylate

A set of 5 copolymers investigated within these series are poly(2-hydroxypropyl acrylate-*co*-methyl acrylate), poly(2-hydroxypropyl acrylate-*co*-butyl acrylate), poly(2-hydroxypropyl acrylate-*co*-2-ethylhexyl acrylate), poly(2-hydroxypropyl acrylate-*co*-methyl methacrylate) and poly(2-hydroxypropyl acrylate-*co*-2-ethylhexyl methacrylate). Again, monomer reactivity ratio based on extended form of Kelen-Tudos was used in the analysis. The copolymers whose glass transition temperatures were compared are poly(HPA_{50}-MA_{50}), poly(HPA_{50}-BA_{50}), poly(HPA_{50}-EHA_{50}), poly(HPA_{50}-MMA_{50}) and poly(HPA_{50}-$EHMA_{50}$). The data is presented in Table 4.102. In all monomer reactivity ratio data r_1 is r_{HPA} and r_2 represents the comonomer (MA, BA, EHA, MMA and EHMA, respectively).

Table 4.102: Reactivity ratios of HPA copolymers and their T_g values

Copolymer	r_{HPA}	r_2	T_g, °C
HPA-MA	0.856	1.514	13.0
HPA-BA	0.861	0.103	-13.2
HPA-EHA	1.431	0.700	-15.2
HPA-MMA	0.819	0.902	19.5
HPA-EHMA	0.936	0.724	-15.2

The data shows that 2-hydroxypropyl acrylate adds at a higher rate relative to only butyl acrylate, 2-ethylhexyl acrylate and 2-ethylhexyl methacrylate. Changing methyl acrylate with butyl acrylate (pendent group with single carbon to four carbons) considerably increases the relative reactivity of 2-hydroxypropyl acrylate. Further increase in pendent chain length as well as branching (butyl to 2-ethylhexyl unit) has a marginal influence. The T_g values are decreased considerably and then very marginally (within experimental error). Changing the hydrogen in methyl acrylate with methyl unit in methyl methacrylate is known to increase hydrophobic interaction. This is seen to stiffen the polymer chain, as seen in the increase in T_g from 13.0 to 19.5^oC. Interestingly, yet again, a change from EHA to EHMA increases the reactivity of the comonomer relative to 2-hydroxypropyl acrylate. The other interesting feature is that the stiffness of copolymer chain is unchanged, as seen from similar T_g of -

15.2°C. Three copolymers within series poly(2-hydroxypropyl acrylate-*co*-butyl acrylate), poly(2-hydroxypropyl acrylate-*co*-methyl methacrylate) and poly(2-hydroxypropyl acrylate-*co*-2-ethylhexyl methacrylate) are capable of forming azeotropic compositions, which merit further examination.

4.26.3 Copolymers of hydroxyethyl methacrylate

A set of 5 copolymers investigated within these series are poly(2-hydroxyethyl methacrylate-*co*-methyl acrylate), poly(2-hydroxyethyl methacrylate-*co*-butyl acrylate), poly(2-hydroxyethyl methacrylate-*co*-2-ethylhexyl acrylate), poly(2-hydroxyethyl methacrylate-*co*-methyl methacrylate) and poly(2-hydroxyethyl methacrylate-*co*-2-ethylhexyl methacrylate). Again, monomer reactivity ratio based on extended form of Kelen-Tudos was used in the analysis. The copolymers whose glass transition temperatures were compared are poly($HEMA_{50}$-MA_{50}), poly($HEMA_{50}$-BA_{50}), poly($HEMA_{50}$-EHA_{50}), poly($HEMA_{50}$-MMA_{50}) and poly($HEMA_{50}$-$EHMA_{50}$). The data is presented in Table 4.103. In all monomer reactivity ratio data r_1 is r_{HEMA} and r_2 represents the comonomer (MA, BA, EHA, MMA and EHMA respectively).

Table 4.103: Reactivity ratios of HEMA copolymers and their T_g values

Copolymer	r_{HEMA}	r_2	T_g, °C
HEMA-MA	3.618	0.469	55.4
HEMA-BA	3.432	0.483	42.4
HEMA-EHA	5.127	1.127	15.6
HEMA-MMA	2.234	0.740	82.5
HEMA-EHMA	2.252	0.775	27.3

The data shows that 2-hydroxyethyl methacrylate adds at a higher rate relative to other comonomers. Changing methyl acrylate with butyl acrylate (pendent group with single carbon to four carbons) did not increase the relative reactivity of 2-hydroxyethyl methacrylate. Further increase in pendent chain length as well as branching (butyl to 2-ethylhexyl unit) has a mariginal influence. The T_g values are decreased marginally and then considerably (within experimental error). Changing the hydrogen in methyl acrylate with methyl unit in methyl methacrylate is seen to stiffen the polymer chain, as seen in the increase in T_g from 55.4 to 82.5°C. Interestingly, yet again a change from EHA to EHMA increases stiffness of copolymer chain as seen from increase in T_g from 15.6 to 27.3°C. None of the copolymers within series are capable of forming azeotropic compositions.

4.26.4 Copolymers of hydroxypropyl methacrylate

A set of 5 copolymers investigated within these series are poly(2-hydroxypropyl methacrylate-*co*-methyl acrylate), poly(2-hydroxypropyl methacrylate-*co*-butyl acrylate), poly(2-hydroxypropyl methacrylate-*co*-2-ethylhexyl acrylate), poly(2-hydroxypropyl methacrylate-*co*-methyl methacrylate) and poly(2-hydroxypropyl methacrylate-*co*-2-ethylhexyl methacrylate). Monomer reactivity ratio based on extended form of Kelen-Tudos was used in the analysis. The copolymers whose glass transition temperatures were compared are poly($HPMA_{50}$-MA_{50}), poly($HPMA_{50}$-BA_{50}), poly($HPMA_{50}$-EHA_{50}), poly($HPMA_{50}$-MMA_{50}) and poly($HPMA_{50}$-$EHMA_{50}$). The data is presented in Table 4.104. In all monomer reactivity ratio data r_1 is r_{HPMA} and r_2 represents the comonomer (MA, BA, EHA, MMA and EHMA respectively).

Table 4.104: Reactivity ratios of HPMA copolymers and their T_g values

Copolymer	r_{HPMA}	r_2	T_g, °C
HPMA-MA	2.034	2.089	48.5
HPMA-BA	1.764	0.302	38.5
HPMA-EHA	3.955	0.245	26.5
HPMA-MMA	1.472	0.344	43.5
HPMA-EHMA	1.563	0.813	12.3

The data shows that surprisingly 2-hydroxypropyl methacrylate adds to the copolymer chain at a higher rate relative to other comonomers. Changing methyl acrylate with butyl acrylate (pendent group with single carbon to four carbons) considerably increases the relative reactivity of 2-hydroxypropyl methacrylate. Further increase in pendent chain length as well as branching (butyl to 2-ethylhexyl unit) increases the relative reactivity of 2-hydroxypropyl methacrylate. The T_g values are decreased with each successive substitution. Changing the hydrogen in methyl acrylate with methyl unit in methyl methacrylate has a marginal role as seen in shift of T_g from 48.5 to 43.5^oC. Interestingly, yet again a change from EHA to EHMA increases the reactivity of the comonomer relative to 2-hydroxypropyl methacrylate. The other interesting feature is that the stiffness of copolymer chain, unaccountably, decreases, as seen from decrease in T_g from 26.5 to 12.3^oC. None of the copolymers within this series is capable of forming azeotropic compositions.

4.26.5 Hydrophilic copolymers of varying hydrophobicity

A set of 5 copolymers investigated within these series are poly(2-hydroxyethyl acrylate-*co*-2-hydroxypropyl acrylate), poly(2-hydroxyethyl acrylate-*co*-2-hydroxyethyl methacrylate), poly(2-hydroxyethyl acrylate-*co*-2-hydroxypropyl methacrylate), poly(2-hydroxypropyl acrylate-*co*-2-hydroxypropyl methacrylate) and poly(2-hydroxyethyl methacrylate-*co*-2-hydroxypropyl methacrylate). Monomer reactivity ratio based on extended form of Kelen-Tudos was used in the analysis. Similarly, the copolymers whose glass transition temperatures were compared are poly(HEA_{50}-HPA_{50}), poly(HEA_{50}-$HEMA_{50}$), poly(HEA_{50}-$HPMA_{50}$), poly(HPA_{50}-$HPMA_{50}$) and poly($HEMA_{50}$-$HPMA_{50}$). The data is presented in Table 4.105. In all monomer reactivity ratio data, the respective monomers are indicated for clarity.

Table 4.105: Reactivity ratios of hydrophilic monomers relative to changes in hydrophobicity and their T_g values

Copolymer	r_1	r_2	T_g, °C
HEA(r_1)-HPA(r_2)	0.098	0.477	-8.4
HEA(r_1)-HEMA(r_2)	0.549	0.860	42.3
HEA(r_1)-HPMA(r_2)	0.539	0.627	13.2
HPA(r_1)-HPMA(r_2)	1.079	1.052	37.2
HEMA(r_1)-HPMA(r_2)	1.067	0.728	76.3

The data clearly points to the fact that pendent hydroxy group plays a predominant role in influencing monomer reactivity ratios. The monomer expected to have the highest reactivity, HEA, has the lowest reactivity relative to the other hydroxy monomers. The chain stiffness of copolymers of 2-hydroyethyl acrylate are determined considerably by substitutions in the main chain. Thus, a change from HEA-HPA to HEA-HPMA increases the T_g by 21.6°C. However, a decrease from propyl to ethyl (HEA-HPMA to HEA-HEMA) increases the T_g further by 29.1°C. While the all trends are along predictable lines, it is difficult to understand the steep increase in T_g of 63.1°C for the HEMA-HPMA system over the HEA-HPMA copolymer system, in the absence of a more detailed study. Three copolymers within series poly(2-hydroxyethyl acrylate-*co*-2-hydroxypropyl acrylate), poly(2-hydroxyethyl acrylate-*co*-hydroxyethyl methacrylate) and poly(2-hydroxypropyl acrylate-*co*-hydroxypropyl methacrylate) are capable of forming azeotropic compositions, which merits further examination.

Similarly, relative evaluations of copolymers of each of the hydrophobic monomers (methyl acrylate, butyl acrylate, 2-ethylhexyl acrylate, methyl methacrylate and 2-ethylhexyl methacrylate) with the four different hydrophilic monomers can also be made. The trend lines as seen by the data presented before are along predictable ones. Though all systems can be examined in great detail, particularly seven of the 25 copolymer systems investigated in depth merit further examination as hydrogels.

4.27 References

[1] J. L.Gomez Ribelles, M. Monleon Pradas, G. Gallego Ferrer and N. Peidro Torres, *J. Polym. Sci., Part B: Polym. Phys*., **1999**, 37, 1587.

[2] Y. Wusheng, L. Hongwu, Y. Benong, Y. Tingjuan and G. Tiren, *Eur. Polym. J.,* **1998,** 34, 779.

[3] M. F. Refojo and F. L. Leong, *J. Biomed. Mater. Res.*, **1981**, 15, 497.

[4] P. I. Urkimbaeva, *Seriya Khimicheskaya*, **2010**, 2, 49.

[5] W. Chengpei, W. Yiliang and Z. Ruiyun, *Zhongguo Kexue Jishu Daxue Xuebao,* **1998**, 28, 216.

[6] M. P. Hong, B. J. Lee and Y.T. Jeon, *Pollimo*, **1993**, 17, 399.

[7] Y.Yamamori, *Jpn. Kokai Tokkyo Koho JP* 2005112426 A2 **2005**.

[8] M. Fineman and S. D. Ross, J. *Polym. Sci.,* **1950**, 5, 249.

[9] T. Kelen and F. Tudos, *J. Macromol. Sci., Chem*., A9, **1975,** 1, 1.

[10] F. Tudos and T. Kelen, T. *J. Macromol. Sci., Part A,* **1981,** *16*, 1283.

[11] R. Mao and M. B. Huglin, *Polymer,* **1993**, 34, 1709.

[12] S. Igarashi, *J. Polym. Sci., Polym. Lett. Ed.,* **1963**, 1, 359.

[13] Y. S. Li, O. Sugita, Y. Sumii and O. Yasuhiko; *Jpn. Kokai Tokkyo Koho JP*, **2009**, 001773 A.

[14] J. Y. Jang, S. U. Cho and H. Y. Choi, Repub. Korean Kongkae Taeho Kongbo KR 2009132117 A 30 Dec **2009**.

[15] S. Hayashi, M. Fukuoka and Y. Sumii, Kokai Tokkyo Koho JP 2007238802 A, **2007**.

[16] Y. L. Huo, Y. Lin, K. Y. Yu and X. R. Zhu, *Intl. J. Poly. Mat.,* **2003**, 52, 61.

[17] Y. Liu and Z. Cheng, *Hecheng Xiangjiao Gongye*, **2001**, 24, 219.

[18] W. Zhong, Y. Xia, X. Lie and S. Jiao, *Hecheng Xiangjiao Gongye*, **1999**, 22, 163.

[19] K. Shikano and T. Saito, *Jpn. Kokai Tokkyo Koho JP* 2011225706 A **2011.**

[20] M. Yamagata, T. Amano and K. Kataoka, *PCT Int. Appl. WO* 2011108573 A1, **2011**.

[21] K. Tsunashima, Y. Daichi, K. Sato, K. Takami and T. Yamamoto, *Jpn. Kokai Tokkyo Koho JP* 2009155514 A, **2009.**

[22] S. Trenor, T. Long and B. Love, *J. Adhesion*, **2005**, 81, 213.

[23] T. Muraoka, H. Akami, K. Inosaka, H. Kawaguchi and S. Ohtsuka, *Jpn. Kokai Tokkyo Koho JP* 11079979 A2, **1999**.

[24] G. Yi, H. Huang, S. Zhang and W. K. Lin, *CN* 102167879 A **2011**.

[25] X. Cai, H. Zhang, W. B. Xu and Z. Zhou, *Feng-mei Baozhuang Gongcheng*, **2011**, 32, 65.

[26] D. Y. Chen, Y. G. Jiang, R. W. Fan, H. Peng and Y. Q. Xia, *Laser Physics*, **2009**, 19, 939.

[27] T. Tatebe and S. Oka, *Jpn. Kokai Tokkyo Koho JP* 2008163086 A **2008**.

[28] P. Xu, H. Wang, R. Tong, R. Lv, Y. Shen and Q. Du, *Poly. Degrad. Stab.,* **2006**, 91, 1522.

[29] L. M. Muratore, K. Steinhoff and T. P. Davis, *J. Mater. Chem.*, **1999**, 9, 1687.

[30] X. Li, X. Yin, P. Wu, Z. Han and Q. Zhu, *Chin. J. Polym. Sci.*, **1998**, 16, 25.

[31] M. Fryd and K. B. Visscher, *PCT Int. Appl. WO* 2000020520 A1 **2000**.

[32] K. Yamakawa, K. Mizutani and H. Sawada, *Jpn. Kokai Tokkyo Koho JP* 10045867 A2 **1998.**

[33] K. Mizutani, S. Yoshimatsu and K. Yamakawa, *Eur. Pat. Appl. EP* 796904 A2 **1997**.

[34] M. Midokawachi, T. Yamazaki, H. Okochi and K. Shirotani, *Jpn. Kokai Tokkyo Koho JP* 09324292 A2 **1997**.

[35] J. W. Burgman, G. M. Terrago and C. A. Verardi, *PCT Int. Appl. WO* 9726305 A1 **1997**.

[36] P. Liang and Z. Meng, *CN* 102093782 A **2011**.

[37] G. Liu, *CN* 102070984 A **2011.**

[38] D. R. Fung, S. H. Hsu, H. H. Wu and H. J. Juang, *CN* 102019737 A **2011**.

[39] D. Zhang, Z. Fang and L.Tang, *CN* 101962430 A **2011**.

[40] M. Kiguchi and R. Nakai, *PCT Int. Appl. WO* 2011013497 A1 **2011**.

[41] G. Zeng, N. Chen and T. Wang, *Zhongguo Tuliao*, **2009**, 24, 29.

[42] X. Chen, F. Shen and Y. Deng, *CN* 101818033 A **2010**.

[43] T. Kanazawa, *Jpn. Kokai Tokkyo Koho JP* 2009275170 A **2009**.

[44] F. Li, Z. K. Li, Z. Y. Yang, X. J. Zhang and L. Shi, *Gongneng Gaofenzi Xuebao,* **2009**, 22, 17.

[45] W. T. Grubbs and A. Ramirez, *PMSE Preprints*, **2007**, 96, 626.

[46] P. K. Dhal, A. Despande and G. N. Babu, *Polymer,* **1982**, 23, 937.

[47] M. A. Sherwin and J. V. Koleske, *US* 4711944, **1987**.

[48] W. Xu, Q. An, L. Hao and L. Huang, *J. Appl. Poly. Sci*., **2012**, 125, 2376.

[49] Y. Wu, C. Ge, J. Xu, J. Bi and Q. Chen, *Poly. Composites*, **2008**, 29, 1193.

[50] C. Inomae, Y. Morishima and S. Ishiwatari, *Jpn. Kokai Tokkyo Koho JP* 2011211130 A **2011**.

[51] T. Takeuchi, S. Yano, Y. Morishima and S. Ishiwatari, *Jpn. Kokai Tokkyo Koho JP* 2008031213 A **2008**.

[52] M. Gerst, G. Auchter and B. Schuler, *Ger. Offen. DE* 19920807 A1 **2000.**

[53] Y. Takamatsu and H. Sakamoto, *Jpn. Kokai Tokkyo Koho JP* 09316416 A2 **1997.**

[54] A. Burmeister, C. Harder, C. Nagel and W. Schacht, *Eur. Pat. Appl. EP* 752435 A2 **1997**.

[55] Y. Fu, Q. Q. Ni, K. Kurashiki and I. Masaharu, *Zairyo*, **2003**, 52, 992.

[56] K. Muramoto, H. Hori and K. Izumiya, *Jpn. Kokai Tokkyo Koho JP* 2003251263 A2 **2003**.

[57] H. Muramoto, S. Yokoi and S. Kodama, *Jpn. Kokai Tokkyo Koho JP* 2003221546 A2 **2003**.

[58] T. Shimizu, M. Watanabe and K. Kumagaya, *Jpn. Kokai Tokkyo Koho JP* 2002011563 A2 **2002**.

[59] H. He and Z. S. Faming, *CN* 102241795 A **2011**.

[60] Z. Xu, X. Wei and K. Liu, *CN* 102167929 A **2011**.

[61] F. Yan, G. Huang and W. Zhang, *CN* 102134296 A **2011**.

[62] H. Yamaguchi, S. Kamo, T. Shigemoto and Z. Komiya, *Jpn. Kokai Tokkyo Koho JP* 2005331873 A **2005**.

[63] A. S. Brar, S. Hooda and A. K. Goyal, *J. Mol. Structure*, **2007**, 828, 25.

[64] T. Siriwittayakom, N. Suebsanit, R. Molloy and M. Prasitsilp, *Chiang Mai J. Sci.,* **2001**, 28, 71.

[65] R. Xu, W. Zhang and G. Li, *Gaofenzi Xuebao*, **1988**, 4, 264.

[66] J. Hou, X. Zhou and X. Zhou, *Poly.-Plastics Tech. and Engi.,* **2011**, 50, 260.

[67] I. Kageishi, C. Kasuya and Y. Ando, *Jpn. Kokai Tokkyo Koho JP* 2009221297 A 1 **2009**.

[68] N. J. Trujillo, S. H. Baxamusa and K. K. Gleason, *Mat. Res. Soc. Symp. Proc.,* **2009,** 1134.

[69] M. C. Fernandez, G. Martinez, C. M. Sanchez and E. L. Madruga, *J. Poly. Sci., A: Poly. Chem.,* **2001**, 39, 2043.

[70] J. Lebduska, J. M. Snuparek, K. Kaspar and M. Mach, *Chem. Prum*., **1986**, 36, 648.

[71] J. Horsky, O. Quadrat, B. Porsch and L. S. Mrkvickova, *J. Coll. Surf., A: Physi.*

Engg. Aspects, **2001**, 180, 75.

[72] M. C. Fernandez, G. Martinez, C. M. Sanchez and E. L. Madruga, *Polymer*, **2000**, 41, 8155.

[73] G. Martinez, C. M. Sanchez, E. L. Madruga and M, C. Fernandez, *Polymer*, **2000**, 41, 6021.

[74] K. Bauerova, J. Rak, M. Chalabala, J. Heinrich and V. Tyrackova, *Drug Dev. Ind. Pharm*., **1988**, 14, 2477.

[75] Y. Ono and A. Yamamoto, *Jpn. Kokai Tokkyo Koho JP* 2011236269 A **2011.**

[76] H. Nakano, Y. Ono and H. Kano, *Jpn. Kokai Tokkyo Koho JP* 2011236267 A **2011**.

[77] A. Ueki, K. Fukuhara and S. Nakajima, *Jpn. Kokai Tokkyo Koho JP* 2011219511 A **2011.**

[78] A. V. Sushchenko, E. V. Vusataya, G. A. Gadebskii, L. N. Plotnikov, S. Y. Khavantsev and L. V. Rudakova, *RU* 2419411 C2 **2011**.

[79] Y. Nakagawa and M. Doi, *Jpn. Kokai Tokkyo Koho JP* 2009249573 A **2009.**

[80] B. Vazquez, J. S. Roman, C. Peniche and C. M. Eugenia, *Macromolecules,* **1997**, 30, 8440.

[81] K. Matsushige, *Jpn. Kokai Tokkyo Koho JP* 2011121869 A **2011**.

[82] G. S. Sailaja, P. Ramesh and H. K. Varma*, J. Mat. Sci., Mat. Medicine,* **2010**, 21, 1183.

[83] G. S. Sailaja, T. V. Kumari, Y. Yokogawa and H. K. Varma, *Key Engi. Materials*, **2006**, 309, 493.

[84] G. S. Sailaja, P. Ramesh and H. K. Varma, *MACRO* 2004, Intl. Conf. Poly. Adv. Tech., Thiruvananthapuram, India, Dec. 15-17, **2004**.

[85] P. D. Dalton, L. Flynn and M. S. Shoichet, *Biomaterials,* **2002**, 23, 3843.

[86] Y. Luo, P. D. Dalton and M. S.Shoichet, *Chem. Mat.,* **2001**, 13, 4087.

[87] M. Feng and M. V. Sefton, *J. Biomater. Sci., Polym. Ed*., **2000**, 11, 537.

[88] M. A. Abd El-Ghaffar, M. S. Hashem, N. M. Ahmed, O. A.Osman and Y. S. Mohammed, *Egyptian J. Textile and Poly. Sci. Tech.,* **2008**, 12, 61.

[89] H. Tumturk, S. Aksoy and N. Hasirci, *Starch/Staerke*, **1999**, 51, 211.

[90] T. Yan, B. Tan and N. Jian Ao, *Gaofenzi Tongbao*, **2010**, 7, 50.

[91] J. Prachayawarakorn and K. Boonsawat, *J. Appl. Poly. Sci.,* **2007**, 106, 1526.

[92] C. Migliaresi, L. Nicolais and R. Vinciguerra, *Adv. Biomater*. *Biomater Biomech*., **1984**, 5, 403.

[93] M. S. Choudhary and I. K. Varma, *Angew. Makromol. Chem*., **1980**, 87, 75.

[94] C. Migliaresi, L. Nicodemo, L. Nicolais and P. Passerini, *Chim. Ind*., **1985,** 67, 114.

[95] C. Migliaresi, L. Nicodemo, L. Nicolais and P. Passerini, *Polymer*, **1984**, 25, 686.

[96] C. Migliaresi, L. Nicodemo, L. Nicolais, P. Passerini, M. Stol, J. Hrouz and P.Cefelin, *J. Biomed. Mater. Res.,* **1984**, 18, 137.

[97] R. J. Barsotti and S. H. Ma, *U.S. Pat. Appl.* 2006100350 A1 **2006**.

[98] M. Hisashi, Y. Fujimura, M. Ohata, Y. Mihara and H. Hori *Jpn. Kokai Tokkyo Koho JP* 2005162916 A2 **2005.**

[99] H. Kitano, T. Inamiya, K. Murayama, H. Kotsubo and Y. Morimura, *PCT Int. Appl. WO* 2005035635 A1 **2005.**

[100] H. Kamiyama, *Jpn. Kokai Tokkyo Koho JP* 2005042001 A2 **2005**.

[101] H. Kitano, S. Kotsubo and T. Inamiya, *Jpn. Kokai Tokkyo Koho JP* 2003113355 A2 **2003**.

[102] W. Chen, J. Yang and L. Zhang, *CN* 101982494 A **2011**.

[103] Y. Fu and Y. Jin, *CN* 101921374 A **2010**.

[104] A. Despande, P. K. Dhal and D. D. Despande, G. N. Babu, *Org. Coat. Appl. Polym. Sci. Proc.,* **1981**, 46, 353-359.

[105] H. Nishizawa and M. Fujishima, *Jpn. Kokai Tokkyo Koho JP* 52081345 **1977.**

[106] A. Despande, P. K. Dhal and G. N. Babu, *Appl. Polym. Sci. Proc*., **1983,** 49, 336.

[107] N. Yoshikawa and H. Ito, *Jpn. Kokai Tokkyo Koho JP* 2000325872 A2 **2000.**

[108] M. Tagami and T. Sawada, *Jpn. Kokai Tokkyo Koho JP* 09292518 A2 **1997.**

[109] R. W. Fan, X. H. Li, S. S. Yue and Y. G. Jiang, *Chinese Physics Letters,* **2008**, 25, 700.

[110] S. K.Ooi, W. D. Cook, G. P. Simon and S. H. Christopher *Eur. Poly. J.*, **2002**, 38, 903.

[111] B. Pascual, I. Goni and M. Gurruchaga, *J. Biomed. Mater. Res*., **1999**, 48, 447.

[112] K. Ito, T. Yamashita and S. Kawagishi, *Jpn. Kokai Tokkyo Koho JP* 2007137939 A **2007**.

[113] S. Kawagishi and K. Itoh, *Eur. Pat. Appl. EP* 1452558 A1 **2004**.

[114] K. Ito, *Jpn. Kokai Tokkyo Koho JP* 2003096305 A2 **2003**.

[115] H. Doi, T. Umeki, Y. Tange and H. Matsuda, *Jpn. Kokai Tokkyo Koho JP* 2001342216 A2 **2001**.

[116] B. Bruchmann, G. Mohrhardt, H. Renz, U. Poth, H. Baumgart and S. Bitter, *Ger. Offen. DE* 19828935 A1 **1999**.

[117] W. Chen, J. Yang and L. Zhang, *CN* 101982494 A **2011**.

[118] Y. Fu and Y. Jin, *CN* 101921374 A **2010**.

[119] H. Liu, R. Xu and H. Qian, *CN* 102002129 A **2011**.

[120] W. Tu, Z. Zheng, J. Hu and F. Wang, *CN* 101928534 A **2010**.

[121] L. Xiong, *CN* 1418909 A **2003**.

[122] A. Kato, T. Ohkoshi and H. Takeda, *PCT Int. Appl. WO* 2004094545 A1 **2004.**

Part B: Adsorption /Desorption Isotherms (Swelling-Deswelling Studies)

4.28 Introduction

Hydrogels are polymeric materials with a large number of hydrophilic groups that are capable of absorbing and retaining water in their three dimensional networks.[1-3] They swell by absorbing water and shrink on drying but are prevented from dissolving due to their chemically or physically crosslinked network. They can retain large amounts of water even under pressure as well as fluid containing electrolytes. These properties of hydrogels find applications in industrial applications as well as in consumer items.[4-8] In addition to implantation technology, hydrogels also are also evaluated in controlled drug delivery systems,[9] soft contact lenses,[10] wound dressings,[11] artificial implants,[12] dialysis membrane,[13] surgical prostheses,[14] agrochemistry,[15] environmental monitoring,[16] etc. Their sensitive response to external stimuli such as pH,[17] temperature, ionic strength,[18] magnetic field,[19] and electric field,[20] enable them to be coined "intelligent polymers" or "smart materials." These materials are extremely useful in biomedical and pharmaceutical applications mainly due to their high water content and latex like nature which is similar to natural tissue, as well as their biocompatibility.[21]

The theory of swelling of crosslinked networks was proposed by Flory.[22] The structure of hydrogels that do not contain ionic moieties can be analysed by the Flory–Rehner theory.[23] This combination of thermodynamic and elasticity theories states that a crosslinked polymer gel immersed in a fluid and allowed to reach equilibrium with its surroundings is subject only to two opposing forces: the thermodynamic force of mixing and the retractive force of polymer chains. At equilibrium these two forces are equal.

The effect of salt types and their concentration on water swelling and deswelling mechanism, equilibrium water content (EWC) of interpenetrating hydrogel networks based on poly(vinyl alcohol) (PVA) and 2-hydroxyethyl methacrylate (HEMA) have been studied.

The swelling characteristics of hydrogels are found to be strongly dependent on the type and amount of monomers, crosslinking agents, and initiators. It also

depends upon the polymerisation parameters such as polymerisation technique, temperature, time, pH, presence of salt, and surfactant concentration.

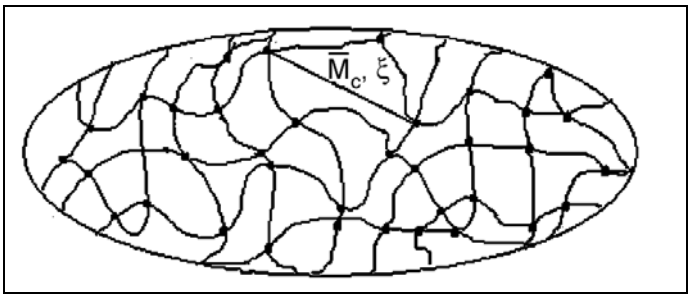

Figure 4.76: Schematic representation of cross-linked structure of a hydrogel

In the present work absorption and desorption study, equilibrium swelling behaviour of six hydrophilic-hydrophobic, hydrophilic-hydrophilic copolymers of azeotropic compositions but differing concentrations of cross-linking agent were evaluated.

4.29 Synthesis of Copolymers

Details regarding monomers used and their source are presented in Section 3.2.1. Ethanolamine from SD Fine Chemicals Ltd., India and cumene hydroperoxide (Aldrich Chemical Co.) was used as received. Sodium chloride (NaCl) extra-pure grade from Sigma-Aldrich was used. Deionised water obtained by using Millipore (Milli Q) system, was used for making solutions and for all swelling and deswelling experiments with isotonic solution of sodium chloride.

Bulk terpolymerisation of azeotropic copolymer compositions was carried out by using cumene hydroperoxide and ethanolamine redox pair initiator. The polymerisation was carried out in glass vials (internal diameter 2 cm and length 7–8 cm). The feed composition of crosslinker ethylene dimethacrylate (EGDMA) was varied as 2.5, 5, 7.5, 10 mol% with total monomer mole. The solutions of monomer and crosslinker were stirred, filled in glass vials (internal diameter 2 cm and length 7–8 cm), deoxygenated with oxygen free nitrogen gas for 10 minutes and sealed. Polymerisation was carried out by cumene hydroperoxide and ethanolamine (1:1) redox pair initiator at room temperature and kept overnight. To ensure that no unreacted monomer was left in the terpolymerisation system, final curing was performed for 10 hours at 80ºC. The glass vials were broken to obtain solid, crosslinked copolymer (of azeotropic composition) in cylindrical form. These samples were cut into desired thickness with a sharp-edged blade and left in double-distilled

water for 48 hours. so as to remove final traces of monomers, and then dried in an oven at 30 °C. Swelling–drying cycles were carried out 3 times and finally the disks were dried under vacuum to constant weight.

4.30 Swelling-Deswelling Study

The increase in mass of samples, immersed in distilled water at 28±1ºC was monitored gravimetrically. Preweighed samples were immersed in excess deionised water. The swollen samples were periodically removed, blotted free of surface water using tissue paper and weighed on Mettler Toledo AG 245 analytical balance (accuracy 0.0001 g), and returned to the swelling medium. Measurements were taken until the samples reached a constant weight. The swelling ratio and equilibrium water content (EWC) of the gels swollen to equilibrium were determined using equations 4.2 and 4.3:

$$\text{Swelling Ratio (S.R.)} = (Wt - Wd)/ Wd \qquad 4.2$$

Where, *Wt* is weight of polymer at time "*t*" and *Wd* is the dry weight of polymer sample.

$$\text{Equilibrium water content (EWC)} = (Meq - Mo) / Meq \qquad 4.3$$

Where, *Meq* is the mass of swollen gel at equilibrium and *Mo* is the mass of dry gel at time zero.

The deswelling behaviour of synthesised copolymers was studied in isotonic salt solution (0.9 wt.% solution of sodium chloride in deionised water). Many researchers have evaluated deswelling studies of polymeric materials by varying the salt concentration, type of salt, variation in the solvent etc. The main objective of this study was to determine the amount of water retained by these copolymers in the isotonic salt solution, which mimics that experienced by contact lens.

4.31 Characterisation of Copolymers

Differential scanning calorimetry (DSC) measurements were conducted using a TA 2920 analyser from TA Instruments DA 73085, a RCS DA cooler. All samples were run against an aluminium reference in crimped aluminium pans. A temperature range of -50 to 150°C was used to determine glass transition temperature (T_g) of copolymers. Scans were recorded at a heating rate of 20°C /min. A second scan was

required for the assessment of glass transition temperature (T_g), defined as the inflection point in the heat capacity jump.

The thermal stability of the copolymers was studied by thermogravimetric analysis (TGA) employing a TGA-7 model from Perkin Elmer instruments. The samples were heated at a rate of 20°C/min under nitrogen in the temperature range of 40 to 800°C.

4.32 Poly(hydroxyethyl acrylate-*co*-methyl methacrylate) at Azeotropic Composition

Bulk polymerisation of azeotropic compositions of poly(hydroxyethyl acrylate-*co*-methyl methacrylate) **[**poly(MMA-*co*-HEA)] with varying crosslinked density of ethylene dimethacrylate (EGDMA) were synthesised as described in Section 4.28.

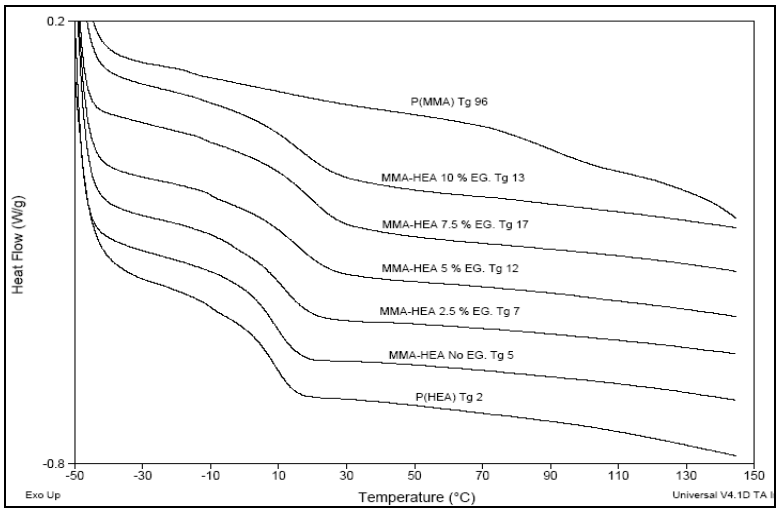

Figure 4.77: DSC thermograms of poly(MMA-*co*-HEA) with differing cross-link density, homopolymer of MMA and HEA.

The glass transition temperature (T_g) of synthesised poly(MMA-*co*-HEA) with variation in crosslink density are presented in Figure 4.77. As indicated in Section 4.4.2 and Figure 4.12 for varying copolymer composition, T_g values of copolymers at azeotropic, unique and specific, composition also is seen to change with increasing crosslinked density. TGA thermogram presented in Figure 4.78, shows that copolymers are thermally stable up to 350ºC and that thermal stability increases with increase in crosslinked density.

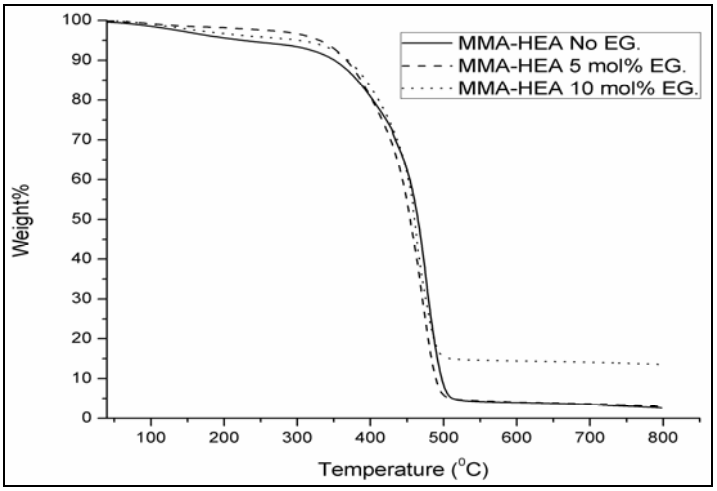

Figure 4.78: TGA thermograms of poly(MMA-*co*-HEA) with differing crosslink density.

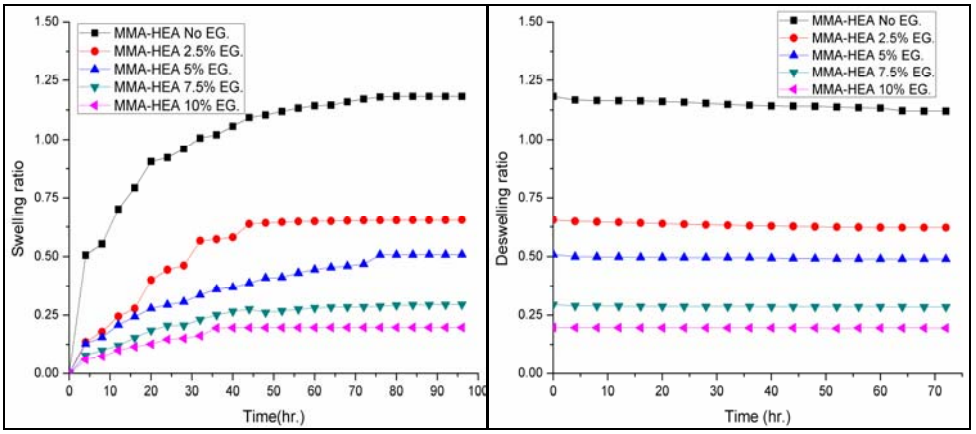

(a) **(b)**

Figure 4.79: Swelling (a) deswelling (b) graph of poly(MMA-*co*-HEA) with differing cross-link density.

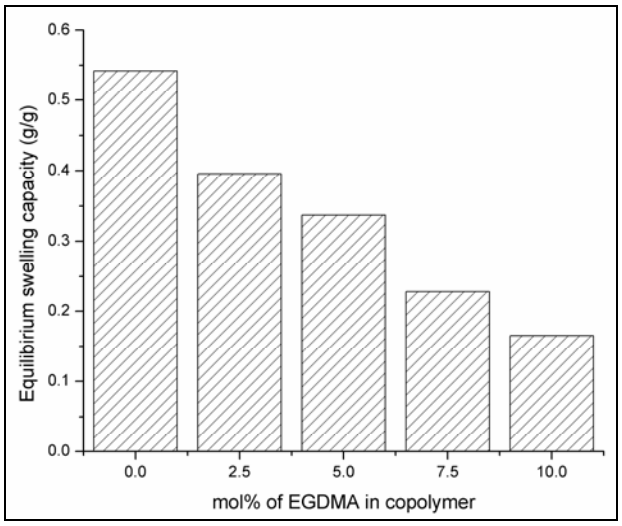

Figure 4.80: Equilibrium swelling of poly(MMA-*co*-HEA) with differing cross-link density.

4.33 Poly(2-hydroxyethyl methacrylate-*co*-2-hydroxyethyl acrylate) at Azeotropic Composition

Bulk terpolymerisation of azeotropic copolymer composition of HEMA-HEA with varying mole percent of ethylene dimethacrylate (EGDMA) were synthesised, as described in Section 4.28.

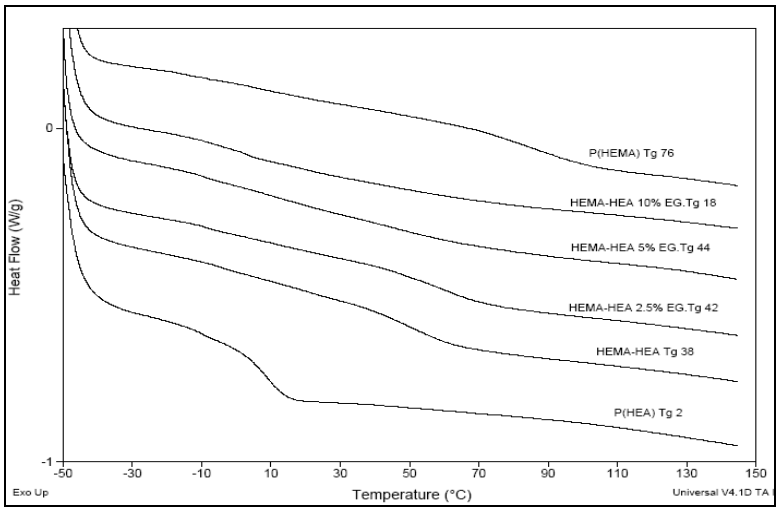

Figure 4.81: DSC thermograms of poly(HEMA-*co*-HEA) with differing cross-link density, homopolymer of HEMA and HEA.

The DSC data presented in Figure 4.81 for poly(HEMA-*co*-HEA) exactly mirrors that observed at azeotropic composition for poly(MMA-*co*-HEA). The T_g values depend on copolymer composition (Section 4.6) as well as cross-linked density at a particular (azeotropic) composition.

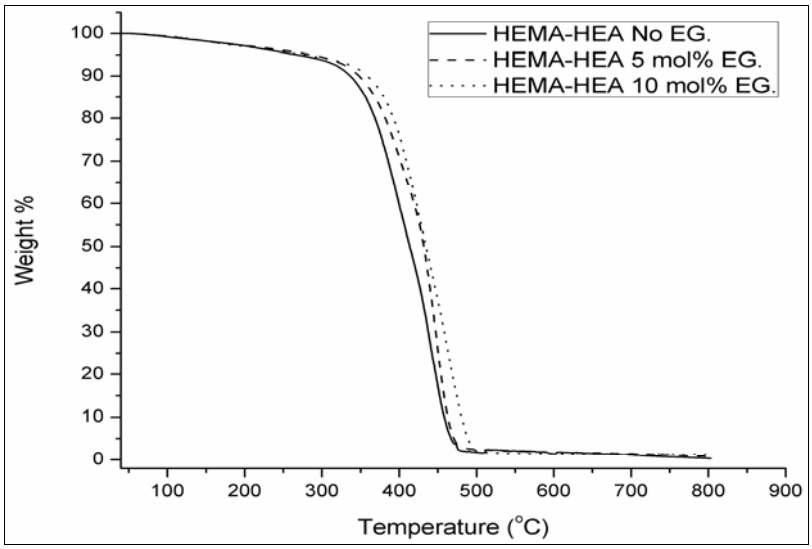

Figure 4.82: TGA thermograms of poly(HEMA-*co*-HEA) with differing cross-link density.

Thermal stability of copolymer was studied by TGA Figure 4.82. Thermogram shows that these copolymers similarly are thermally stable up to 350ºC, there is a slight increase in thermal stability with increase in crosslink density.

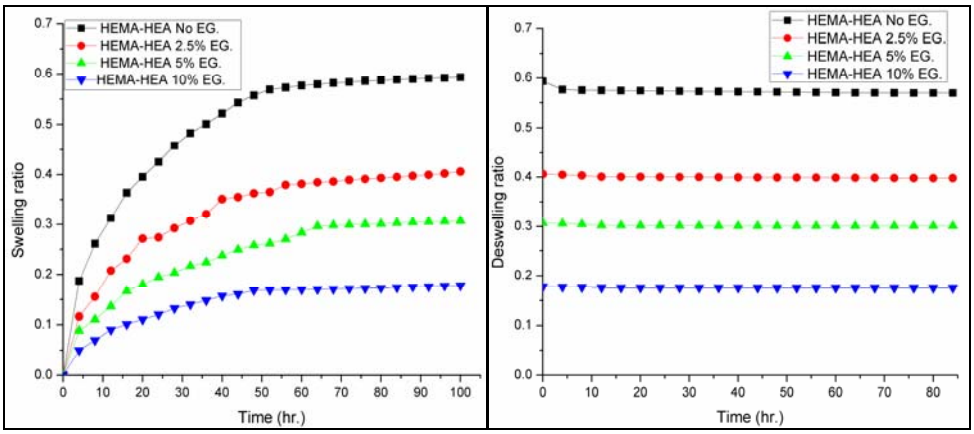

(a) **(b)**

Figure 4.83: Swelling (a) deswelling (b) graph of poly(HEMA-*co*-HEA) with differing cross-link density.

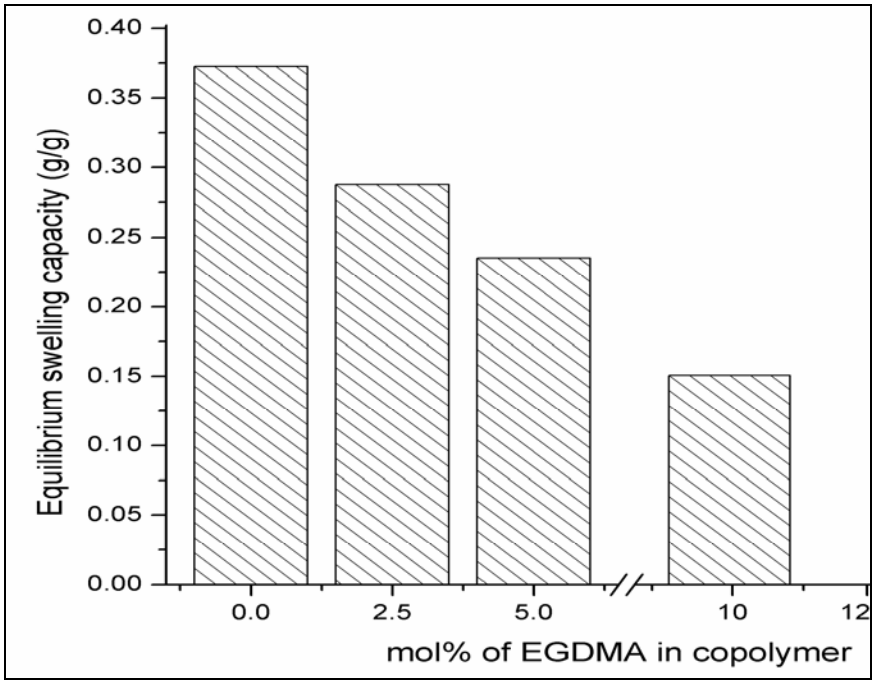

Figure 4.84: Equilibrium swelling capacity of azeotropic poly(HEMA-*co*-HEA) with differing cross-link density.

Swelling profiles shows that absorption of water by the hydrogel depends on the crosslinked density, in Figure 4.83. The equilibrium swelling capacity is matrix dependent. Deswelling profile shows that there is no change in the water content in isotonic salt solution. The maximum water absorption capacity of copolymers is shown as equilibrium water content (EWC) in Figure 4.84.

4.34 Poly(butyl acrylate-*co*-2-hydroxypropyl acrylate) at Azeotropic Composition

Azeotropic composition of poly(butyl acrylate-*co*-2-hydroxypropyl acrylate) [poly(BA-*co*-HPA)] was bulk polymerised with varying crosslink density of ethylene dimethacrylate (EGDMA) as described in Section 4.28.

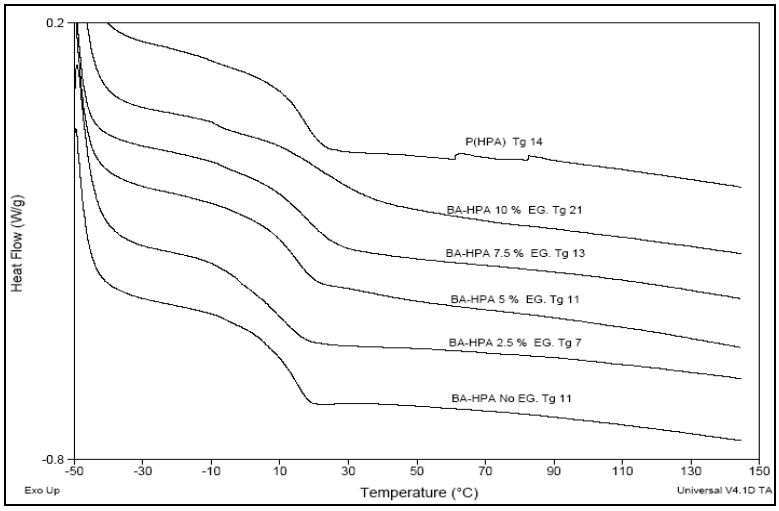

Figure 4.85: DSC thermograms of poly(BA-*co*-HPA) with differing cross-link density, homopolymer of BA and HPA.

The DSC data for poly(BA-*co*-HPA) presented in Figure 4.85, is similar to those obtained with the previous 2 systems. For foldable intraocular lens an important criteria is that T_g needs to be below the ambient temperature. This azeotropic copolymer shows T_g in the range of 7 to 21ºC which indicates that it is amenable to mechanical folding.

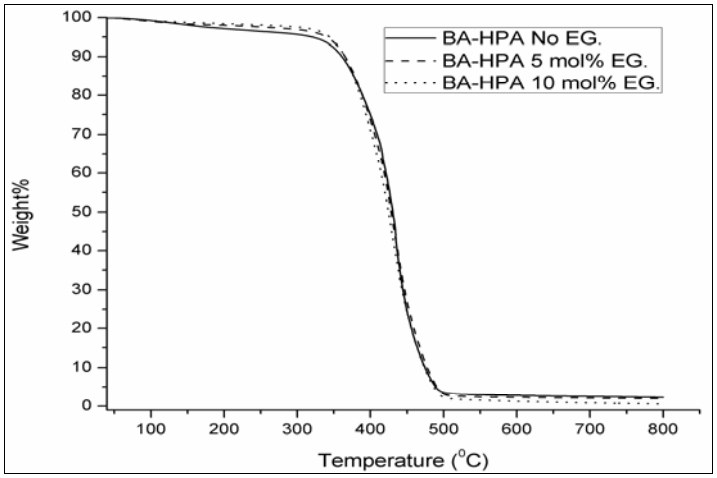

Figure 4.86: TGA thermograms of poly(BA-*co*-HPA) with differing cross-link density.

These polymers are thermally stable, as seen from TGA data presented in Figure 4.86.

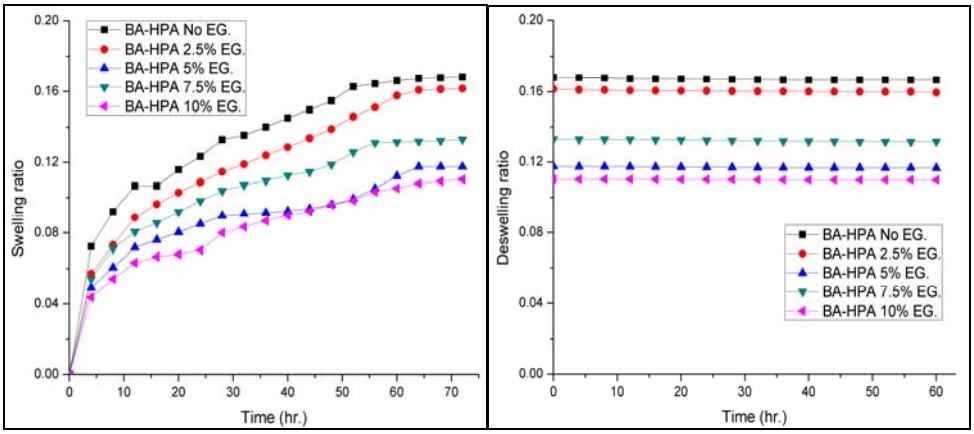

(a) **(b)**

Figure 4.87: Swelling (a) deswelling (b) graph of poly(BA-*co*-HPA) with differing cross-link density.

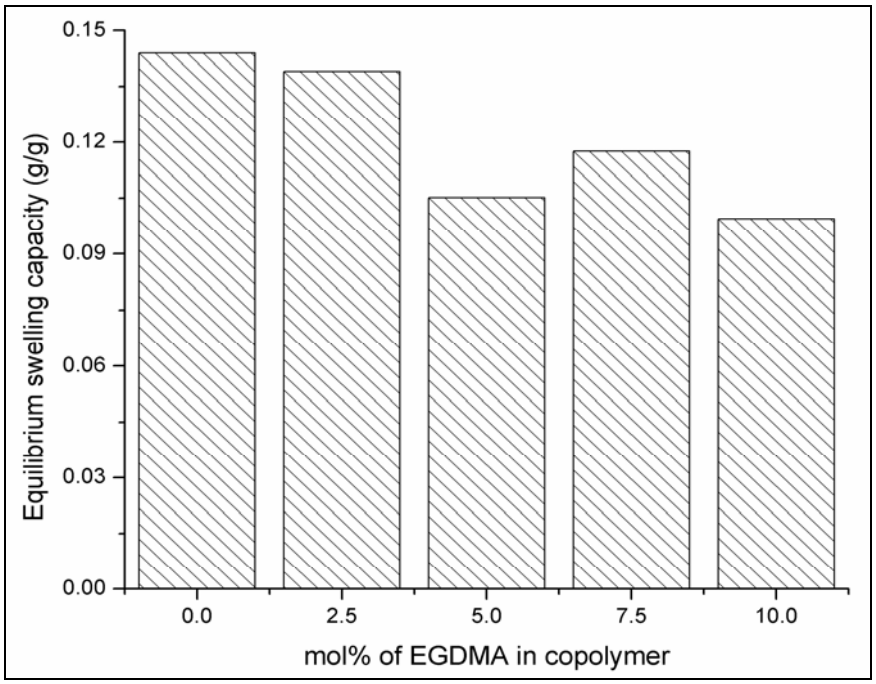

Figure 4.88: Equilibrium swelling capacity of poly(BA-*co*-HPA) with differing cross-link density.

Swelling profiles show a trend in water absorption. The maximum swelling is seen in the copolymer with no crosslinker and decreases with increase in crosslinked density as shown in Figure 4.87. Deswelling profile is steady for this copolymer which shows very little water loss. The water absorption capacity of copolymers is shown as equilibrium water content (EWC) in Figure 4.88.

4.35 Poly(2-ethylhexyl methacrylate-*co*-2-hydroxypropyl acrylate) at Azeotropic Composition

Bulk terpolymerisation of poly(EHMA-*co*-HPA) at azeotropic composition with varying mole-fractions of crosslinker, ethylene dimethacrylate, were conducted as described in Section 4.28.

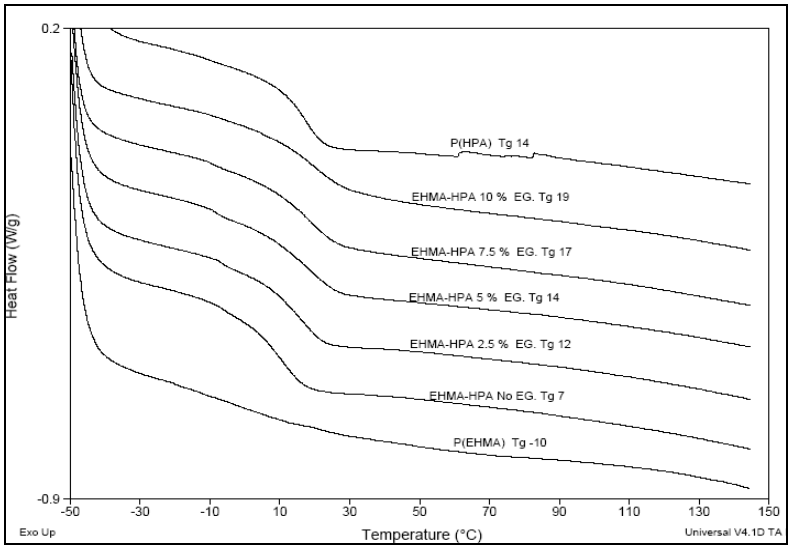

Figure 4.89: DSC thermogram of poly(EHMA-*co*-HPA) with differing cross-link density, homopolymer of EHMA and HPA.

The DSC thermogram of poly(EHMA-*co*-HPA) presented in Figure 4.89 and the TGA thermogram presented in Figure 4.90 mirror those observed with earlier systems at azeotropic composition in relation to crosslinked density. These azeotropic copolymers show T_g in the range of 7 to 19ºC.

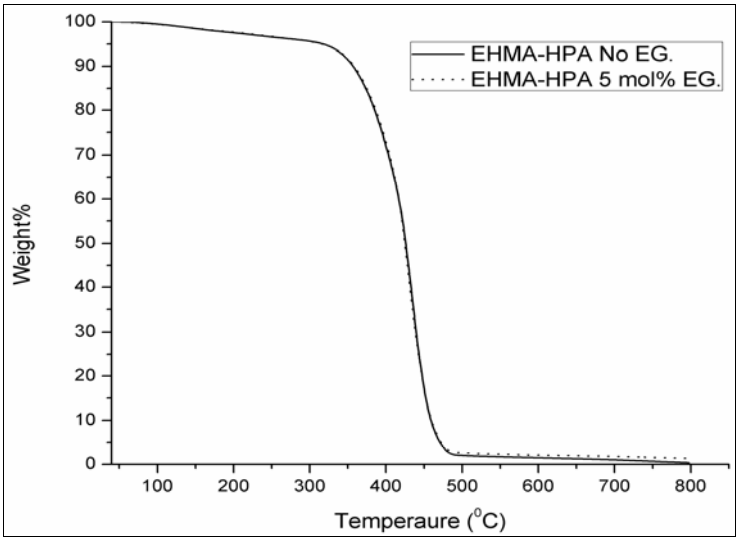

Figure 4.90: TGA thermograms of poly(EHMA-*co*-HPA) with differing cross-link density.

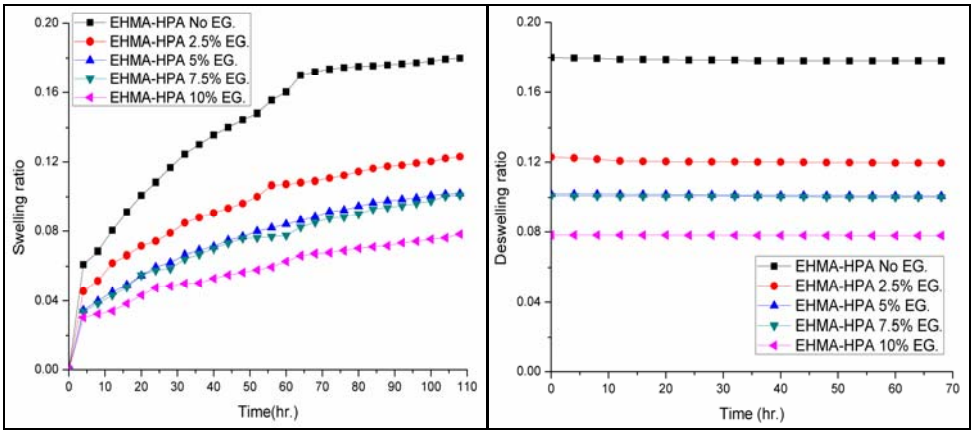

(a) **(b)**

Figure 4.91: Swelling (a) deswelling (b) graph of poly(EHMA-*co*-HPA) with differing cross-link density.

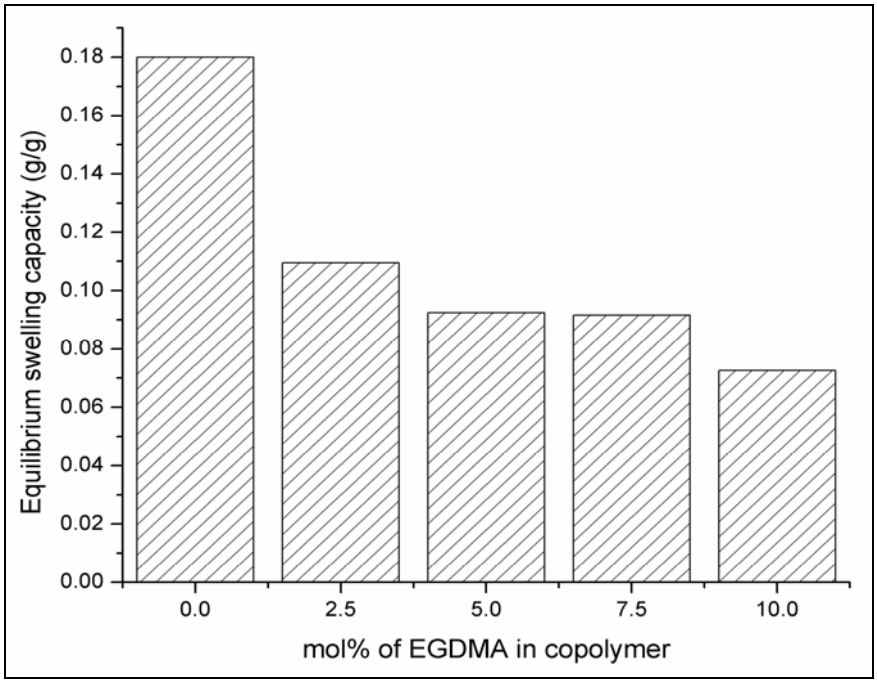

Figure 4.92: Equilibrium swelling capacity of poly(EHMA-*co*-HPA) with differing cross-link density.

Swelling of this copolymeric system show maximum swelling for polymer with no cross-linker and decreases as cross-linking goes on increasing as in Figure 4.91. The water absorption capacity of copolymer pair EHMA-HPA with 5 and 7.5 mol% EGDMA shows nearly equal equilibrium water content (EWC) as in Figure 4.92. Deswelling profile shows no weight loss retaining maximum amount of water in isotonic salt solution.

4.36 Poly(2-hydroxyethyl acrylate-*co*-2-hydroxypropyl acrylate) at Azeotropic Composition

Bulk terpolymerisation of azeotropic poly(HEA-*co*-HPA) with varying mole fraction of ethylene dimethacrylate were synthesised as described in Section 4.28.

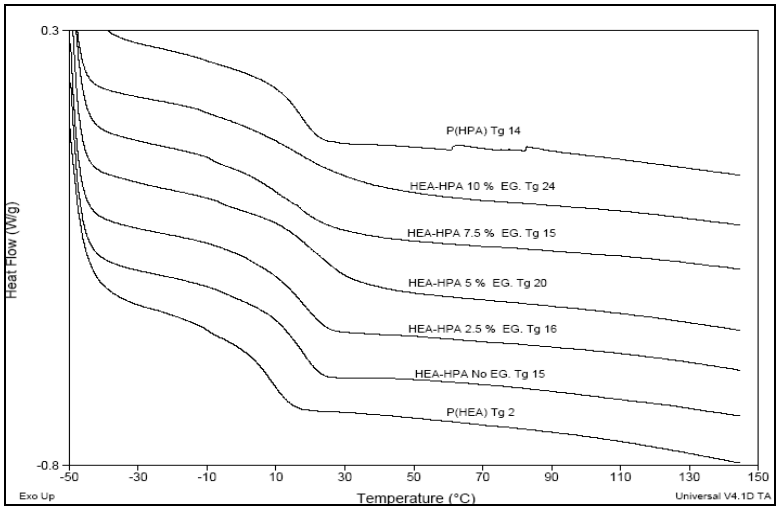

Figure 4.93: DSC thermograms of poly(HEA-*co*-HPA) with differing cross-link density, homopolymer of HEA and HPA.

T_g values presented in Figure 4.93 are in the range of 15 to 24ºC.

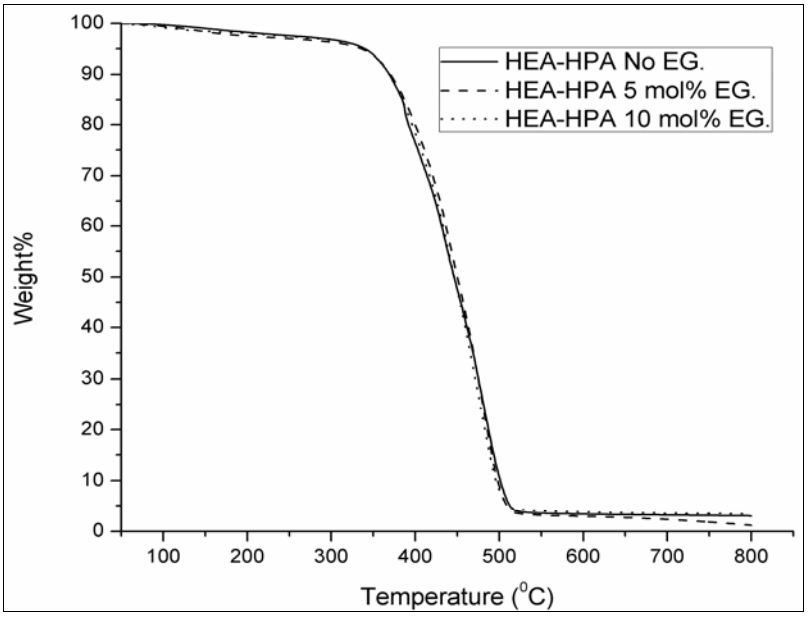

Figure 4.94: TGA thermograms of poly(HEA-*co*-HPA) with differing cross-link density.

TGA thermogram in Figure 4.94 shows that azeotropic copolymers are thermally stable to 350 ºC.

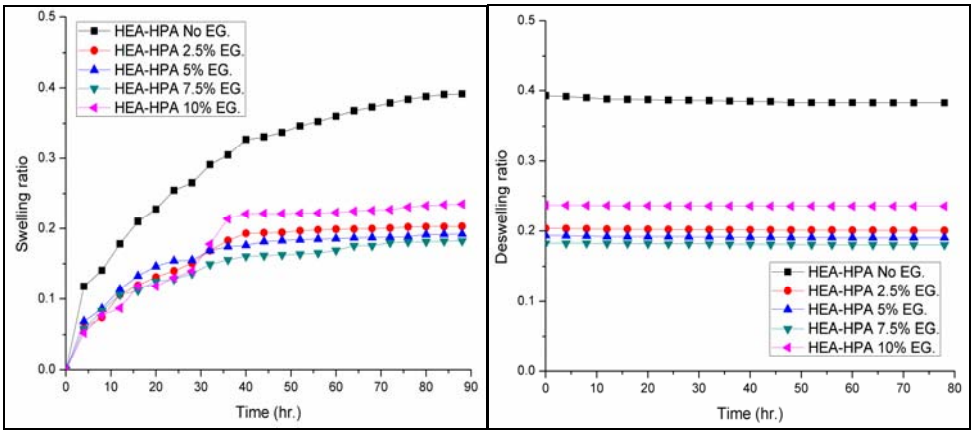

(a) **(b)**

Figure 4.95: Swelling (a) deswelling (b) graph of poly(HEA-*co*-HPA) with differing cross-link density.

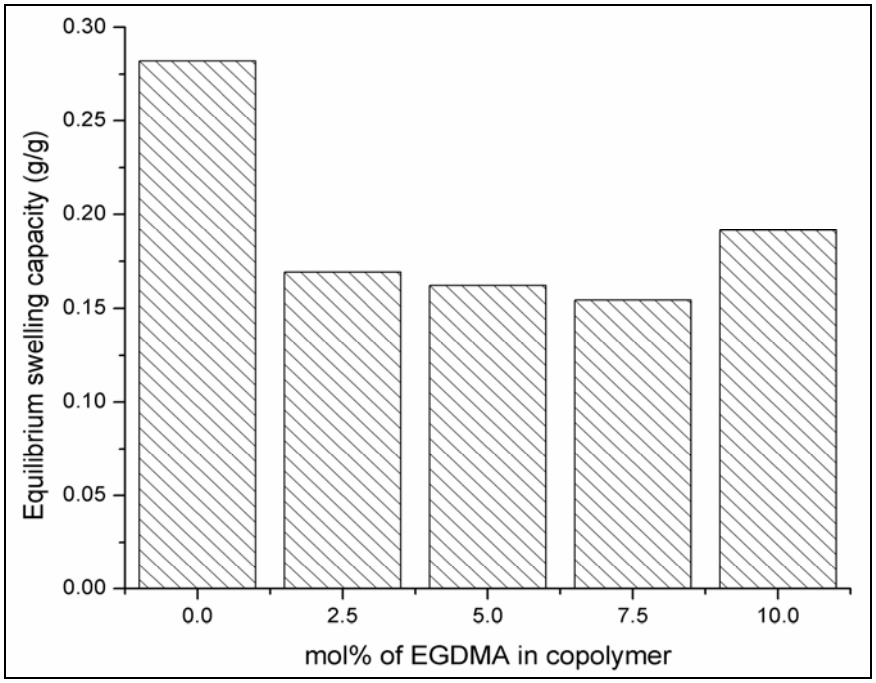

Figure 4.96: Equilibrium swelling capacity of poly(HEA-*co*-HPA) with differing cross-link density.

Swelling profiles show that absorption of water by hydrogel depends on the crosslinked density in Figure 4.95. The equilibrium swelling capacity is matrix dependent. Deswelling profile shows that there is no change in the water content in isotonic salt solution. The maximum water absorption capacity of copolymers is shown as equilibrium water content (EWC) in Figure 4.96.

4.37 Poly(2-hydroxyethyl acrylate-*co*-2-hydroxypropyl methacrylate) at Azeotropic Composition

Bulk terpolymerisation at azeotropic composition of poly(HEA-*co*-HPMA) with varying mole fraction of ethylene dimethacrylate were synthesised as presented in Section 4.28.

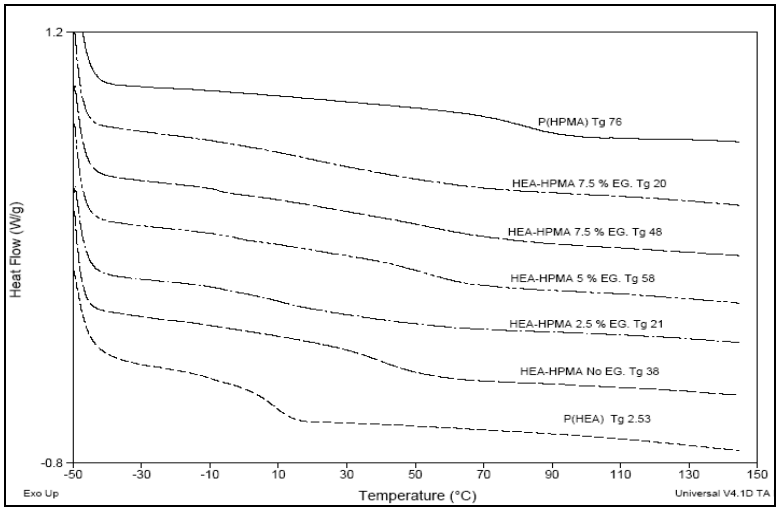

Figure 4.97: DSC thermograms of poly(HEA-*co*-HPMA) with differing cross-link density, homopolymer of HEA and HPMA.

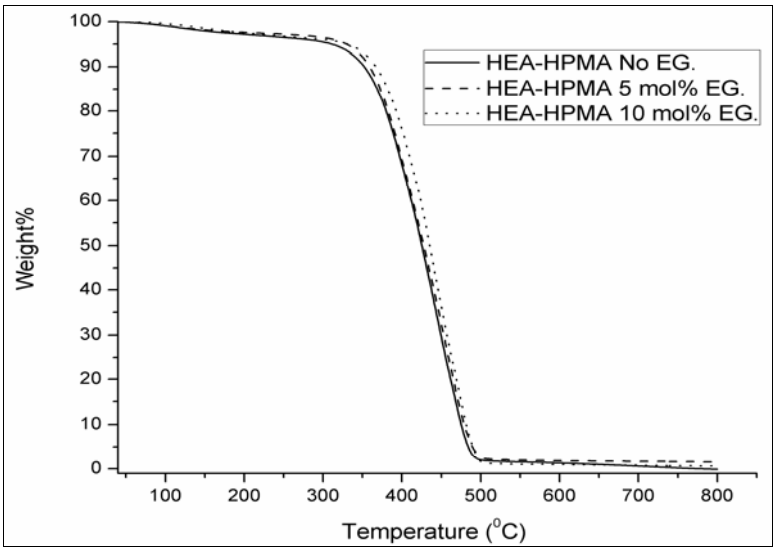

Figure 4.98: TGA thermograms of poly(HEA-*co*-HPMA) with differing cross-link density.

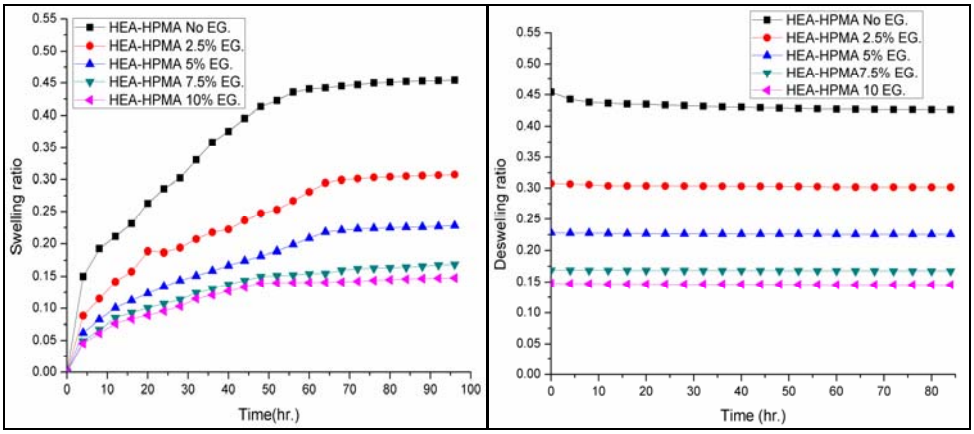

(a) **(b)**

Figure 4.99: Swelling (a) deswelling (b) graph of HEA-HPMA copolymers with differing cross-link density.

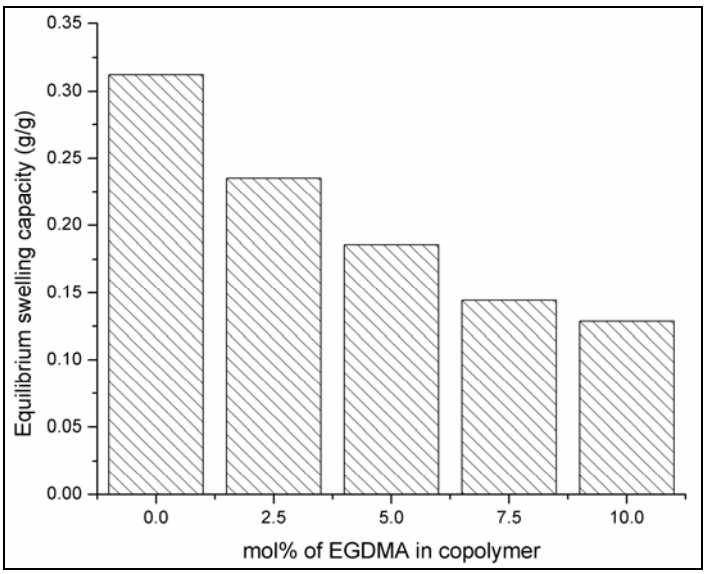

Figure 4.100: Equilibrium swelling capacity of poly(HEA-*co*-HPMA) with differing cross-link density.

The glass transition temperature (T_g) of synthesised copolymer with variation in crosslinked density were determined from differential scanning calorimetry (DSC) Figure 4.97. Data of T_g values shows that copolymers have different T_g than homopolymer, and that it increases with increasing crosslinked density because of increase in the rigidity of polymer matrix. Thermal stability of copolymer is studied by TGA Figure 4.98. Thermogram shows that copolymers are thermally stable upto 350ºC, and there is a slight increase in thermal stability of polymers with increase in crosslinked density.

Swelling profiles show that absorption of water by hydrogel depends on the crosslinked density in Figure 4.99. The equilibrium swelling capacity is matrix

dependent. Deswelling profile shows that there is no change in the water content in isotonic salt solution. The maximum water absorption capacity of copolymers is shown as equilibrium water content (EWC) in Figure 4.100.

4.38 Comparative Evaluation of Azeotropic Copolymers

The following six copolymers which form azeotropic and invariant compositions were evaluated at this very copolymer composition using ethylene dimethacrylate as crosslinker: Poly(2-hydroxyethyl acrylate-methyl methacrylate), poly(2-hydroxyethyl acrylate-2-hydroxyethyl methacrylate), poly(2-hydroxyethyl acrylate-2-hydroxypropyl acrylate), poly(2-hydroxyethyl acrylate-2-hydroxypropyl methacrylate), poly(2-hydroxypropyl acrylate-butyl acrylate) and poly(2-hydroxypropyl acrylate-ethylhexyl methacrylate). These are abbreviated as poly(HEA-MMA), poly(HEA-HEMA), poly(HEA-HPA), poly(HEA-HPMA), poly(HPA-BA) and poly(HPA-EHMA), respectively. The copolymers within each series had 0, 2.5, 5.0, 7.5 and 10 mol% ethylene dimethacrylate. As a general trend the T_g increased with mol% of ethylene dimethacrylate. All polymers swelled in deionised water and showed marginal deswelling in 0.9 wt.% sodium chloride solution, the isotonic optical solution. The polymers were evaluated with the singular purpose of determining whether these meet the most primary requirement for contact lens and intraocular lens application, namely swelling in water and retaining water at isotonic conditions. All polymers met the primary requirement. The trend lines relative hydrophilicity and hydrophobicity within these hydrogels are summarized in Table 4.106 below.

Table 4.106: Equilibrium swelling in water, deswelling in 0.9 wt.% sodium chloride solution and T_g of azeotropic copolymer composition at 2.5 wt.% CLD

Copolymer	Swelling Wt.%	Deswelling Wt.%	T_g °C
Poly(HEA$_{.95}$-MMA$_{.05}$)	39.55	5.03	7
Poly(HEA$_{.23}$-HEMA$_{.77}$)	28.75	2.18	42
Poly(HEA$_{.86}$-HPA$_{.14}$)	16.92	1.46	10
Poly(HEA$_{.84}$-HPMA$_{.16}$)	23.52	1.93	21
Poly(HPA$_{.37}$-BA$_{.63}$)	13.91	1.26	7
Poly(HPA$_{.44}$-EHMA$_{.56}$)	10.96	2.84	12

The data, when observed in isolation, gives a very unpredictable look. It must be added that the unique azeotropic copolymer composition within each system is different. Hence, hydrogel of higher equilibrium swelling may be obtained by a

combination of a hydrophilic monomer with a hydrophobic one rather than between two hydrophilic monomers, as would have been predicted *a priori*. The only two which still are unpredictable are poly(HEA$_{.86}$-HPA$_{.14}$) and poly(HEA$_{.84}$-HPMA$_{.16}$). The methacrylate comonomer HPMA leads to greater swelling relative to a lesser hydrophobic HPA. All copolymers other than poly(HEA$_{.23}$-HEMA$_{.77}$) (with T_g of 42^{o}C) are suitable for further evaluation as hydrogels for human lens applications.

To summarise, seven systems out of 25 copolymers consisting of monomer combinations of non-ionisable hydrophilic with hydrophobic or hydrophilic are capable of forming azeotropic compositions. Six of these combinations were examined under conditions these would encounter for human contact applications. Five systems show promise in this regard.

4.39 References

[1] K. N. Plunkett, J. S. Moore, *Langmuir*, **2004**, 20, 6535.

[2] M. D. Loos, B. L. Feringa, J. H. Esch, *Eur. J. Org. Chem.,* **2005**, 3615.

[3] I. Katime, E. D. de Apodaca, E. Rodriguez, *J Appl Polym Sci*., **2006**, 102, 4016.

[4] A. L. Buyanov, I. V. Gofman, L. G. Revel'skaya, A. K. Khripunov, A. Tkachenko, *J. Mech. Behav. Biomed. Mater.,* **2010**, 3, 102–111.

[5] S. Li, *Bioresource Technology,* **2010**, 101, 2197–2202.

[6] Y. Wu, H. Park, T. Kai, B. D. Freeman, D. S. Kalika, *J. Membr. Sci.,* **2010**, 347, 197–208.

[7] B. Chu, B. S. Hsiao, *J. Polym. Sci. Part B: Poly. Phy.,* **2009**, 47, 2431–2435.

[8] A. Martinez-Ruvalcaba, J. C. Sanchez-Diaz, F. Becerra, L. E. Cruz-Barba, *Express Polymer Letter.* **2009**, 3, 25–32.

[9] N. A. Peppas, *Curr. Opin. Colloid Interface Sci.,* **1997**, 2, 531.

[10] T. V. Chirila, I. J. Constable, G. J. Crawford, S. Vijayasekaran, D. E. Thompson, Y. C. Chen, W. A. Fletcher, B. J. Griffin, *Biomaterials*, **1993**, 14, 26.

[11] R. Jeyanthi, K. P. Rao, *Biomaterials*, **1990**, 11, 238.

[12] Y. Ikada, *Polymer Journal*, **1991**, 23, 551.

[13] D. F. Williams, *In Concise Encyclopedia of Medical and Dental Materials,* Pergamon Press: Oxford, England, **1990.**

[14] D. Saragdin, E. Karadag, O. Guven, *Polym Bull*., **1998**, 41, 577.

[15] B. L. Rivas, H. A. Maturana, E. Pereira, *Angew. Makromol.Chem.,* **1994**, 220, 61.

[16] M. J. Snowden, B. Z. Chowdhury, B. Vincent, G. E. Morris, *J. Chem. Soc. Faraday Trans.,* **1996**, 92(24), 5013.

[17] Y. H. Bae, T. Okano, S. W. Kim, *J. Polym. Sci. Polym. Phys.,* **1990**, 28, 923.

[18] R. A. Siegal, B. A. Firestone, *Macromolecules,* **1988**, 21, 3254.

[19] C. R. Mayer, V. Cabail, T. Lalot, R. Thouvenot, *Adv. Mater*., **2000**, 6, 12.

[20] S. Y. Kim, H. S. Shin, Y. M. Lee, C. N. Jeong, *J. Appl. Polym. Sci*., **1999**, 73, 1675.

[21] A. M. Lowman, and N. A. Peppas, *Hydrogels- Encyclopedia of Controlled Drug Delivery*, Wiley, New York, 397-418, **1999**.

[22] P. J. Flory, *Principles of Polymer Chemistry*, Cornell University Press, New York, **2006**, Chapter-13, 576-593.

[23] P. J. Flory, J. Rehner, *J. Chem. Phys.,* **1943**, 11, 521-526.

Chapter V

Summary, Conclusion and Future Directions

5.1 Summary and Conclusions

The overall goal of this research was to study and develop hydrogel materials for ophthalmic applications**.** Acrylic polymers have wide applications in day-to-day life, out of which an important one is clear and transparent substances used for preparation of optical materials such as contact and intraocular lens. Acrylic polymeric system is further broadly classified into two types, hydrophobic and hydrophilic. Hydrophobic (meth)acrylates are mainly used in intraocular lens synthesis as these materials have higher refractive index. Hydrophilic (meth)acrylates have hydroxyalkyl units as pendant hydroxy groups and these are used for swellable contact and intraocular lens application.

Early in the 1800s the technology of vision correction by using a lens in intimate contact with the cornea was well known and practiced in the form of a glass lens. After continuous evolution in the field of lens for over a century, in the 1930's contact lenses came into the market. In 1936, poly(methyl methacrylate), PMMA, a resin with greater clarity than glass, was introduced. Through lathing of this new resin, the first commercial contact lenses were developed and introduced. In 1970 poly(hydroxyethyl methacrylate), p(HEMA), hydrogel based lens were commercially introduced in the market. These new materials became very popular due to their hydrophilic property and eventually formed a part of hydrogels.

In hydrophilic lens water absorption makes the material flexible and hence there is no intrinsic need for high refractive index or flexibility, which are key criteria in hydrophobic lens. Hydrophilic adsorption and desorption profiles against isotonic aqueous fluids are important. These lens materials have additional hydrophilic groups which can be further modified into chemical structures that easily bind to anticoagulant agents such as heparin and thus prevent protein deposition, which otherwise would ultimately lead to opacification.

Cataract is the opacification of lens due to age or ocular trauma that decreases the transparency of the eye. The surgical procedure is replacement of natural crystalline lens by a hydrophilic/hydrophobic polymer (intraocular) lens. By several combinations of acrylic monomer**s** many researchers have improved stability, clarity and biocompatibility of the lens.

Co and terpolymerisations are the prime methods which are used to increase the amorphous character of polymeric materials which in turn results in increase in the transparency and flexibility of polymer chains. Copolymers have their own unique properties which are different from those of homopolymers. In copolymer composition the sequence distribution of different monomer units is very important to ensure homogeneity which again reveals the importance of copolymerisation kinetics.

In the present work a detailed investigation of several copolymerisation systems, which have very high potential value in intraocular lens application material, have been studied. For an industrially relevant system, azeotropic compositions are established by studying each copolymerisation for reactivity ratios.

Chapter I give an overall view of hydrogels which are a unique class of polymeric materials that play a vital role in numerous areas of biotechnology and medicine. The absorption of water and its retention within the polymer matrix is a key feature of these materials which further prepares it for wide applications in living systems such as separation media, soft contact lenses, artificial organs, dental materials, optical lens implants, artificial skin, carrier for controlled drug delivery, optical sensors, and dialysis media. Hydrogel based soft contact lenses have an advantage over hard contact lenses, in that these systems are relatively richer in water, making them more permeable to oxygen than the hard ones. Generations of IOLs which state the development of IOLs from the first day to the present day were elaborated. Also types of IOLs, manufacturing process and thorough literature survey about hydrophilic IOLs were summarised.

Chapter II deals with detailed information about methods to evaluate reactivity ratios developed early from 1940's to more sophisticated computational methods. The first comprehensive theory of copolymerisation with copolymer composition equation was established by Mayo and Lewis in 1944. They derived this equation by applying a steady state approximation to four propagating steps of free radical polymerisation by combining two monomers. The simple form of this equation is given below.

$$\frac{m_1}{m_2} = \frac{r_1[M_1]^2 + [M_1][M_2]}{r_2[M_2]^2 + [M_1][M_2]}$$

Where, the monomer reactivity ratios $r_1 = k_{11}/k_{12}$ and $r_2 = k_{22}/k_{21}$ are kinetic parameters which measure the relative rate of addition of a radical to its own monomer and the addition of the same radical to the comonomer. $[M_1]$ and $[M_2]$ are molar concentrations of monomers in the feed and $d[M_1]/d[M_2]$ is the relative rate of addition of the two monomers to the chain. The development of Mayo-Lewis equation for binary copolymerisation was based on the terminal kinetic model. The copolymerisation of two monomers, A and B, gives rise to the formation of a copolymer chain whose composition and sequence distribution, are dependent on the relative proportion of applied monomers as well as the monomer and radical reactivities.

Different types of monomers show different types of copolymerisation behaviour. Depending on the reactivity ratios of the monomers, the copolymer can incorporate the comonomers in different ways. The copolymer which results after the copolymerisation may have ideal, random, alternate or block type of copolymeric structure.

Methods to estimate reactivity ratios are classified as differential of integral depending on whether they started from the differential or integral form of the Mayo-Lewis equation. Many methods have been used to estimate reactivity ratios of a large number of comonomers. Tidwell and Mortimer distinguished four different procedures for the calculation of monomer reactivity ratios in copolymerisation, via. linearisation, approximation, intersection, and curve fitting. There are many methods which determine the compositional parameters such as reactivity ratios. Chapter II is a detailed compilation of a list of major methods which have evolved since 1940s to modern computational procedures.

The copolymerisation equation describes only the copolymer composition on a macroscopic scale, which is the overall composition of a copolymer sample produced from the comonomer feed. This does not explain the exact arrangement of the two monomers along the polymer chain and distribution of the monomer.

In present study copolymerisations of hydrophilic-hydrophobic and hydrophilic-hydrophilic acrylate/methacrylates were carried out by solution polymerisation technique using methyl isobutyl ketone, (MIBK), as solvent with 2, 2'-azobisisobutyronitrile (AIBN) as free radical initiator in oxygen free conditions at

70°C. The feed compositions of the monomers are varied from 10/90 to 90/10. The reaction time was selected so as to yield moderate copolymer conversions in order to be within the realm of applicability of differential copolymerisation equation. Cyclohexane was used as the non-solvent which contains butyl methacrylate (BMA) as internal standard (IS) for gas chromatography analysis.

Several chemical and physical methods have been cited in literature for the characterisation of copolymer microstructure. Copolymer composition has been determined by elemental analysis, infrared absorption spectroscopy, ultraviolet absorption spectrophotometry, proton (^{1}H) nuclear magnetic resonance and ^{13}C NMR spectroscopy, pyrolysis gas and mass spectroscopy. The solubility problem of hydrophilic-hydrophobic copolymer systems limits direct analysis of the solid polymer sample. To overcome the solubility problem of amphiphilic copolymers, we developed a more systematic gas chromatographic method to analyse for the unreacted monomers which was faster and more accurate, with minimum error and clear separation of the monomer peaks from each other.

From the monomer feed ratios with composition varying from 10/90 to 90/10, the reactivity ratios of copolymeric systems were determined by Finemann-Ross (FR), Kelen-Tudos (KT), extended Kelen-Tudos (Ext. KT) and Mao-Huglin (MH) methods. Results of reactivity ratios are given in Table 5.1.

This data of reactivity ratios shows that reactivity of hydrophilic monomer is greater than their hydrophobic counterpart. The reactivity of methacrylates is greater than that of acrylates. Out of these 25 monomer pair combinations we were able to find the exact azeotropic compositions for seven pairs of monomer combinations which are presented in the following Table 5.2.

Table 5.1: Reactivity ratio values by extended Kelen-Tudos method for monomer pair studied

Sr. No.	Monomer pair	r_1	r_2
1	Methyl acrylate(M_1)-*co*-2-hydroxyethyl acrylate(M_2)	1.467	1.855
2	Butyl acrylate(M_1)-*co*-2-hydroxyethyl acrylate(M_2)	0.638	2.033
3	2-Ethyl hexyl acrylate(M_1)-*co*-2-hydroxyethyl acrylate(M_2)	0.442	1.367
4	Methyl methacrylate(M_1)-*co*-2-hydroxyethyl acrylate(M_2)	0.154	0.968
5	2-Ethyl hexyl methacrylate(M_1)-*co*-2-hydroxyethyl acrylate(M_2)	0.749	1.030
6	2-Hydroxyethyl methacrylate(M_1)-*co*-2-hydroxyethyl acrylate(M_2)	0.860	0.549
7	Methyl acrylate(M_1)-*co*-2-hydroxypropyl acrylate(M_2)	1.514	0.856
8	Butyl acrylate(M_1)-*co*-2-hydroxypropyl acrylate(M_2)	0.103	0.861
9	2-Ethyl hexyl acrylate(M_1)-*co*-2-hydroxypropyl acrylate(M_2)	0.700	1.431
10	Methyl methacrylate(M_1)-*co*-2-hydroxypropyl acrylate(M_2)	0.902	0.819
11	2-Ethyl hexyl methacrylate(M_1)-*co*-2-hydroxypropyl acrylate(M_2)	0.724	0.936
12	2-Hydroxyethyl acrylate(M_1)-*co*-2-hydroxypropyl acrylate(M_2)	0.098	0.477
13	Methyl acrylate(M_1)-*co*-2-hydroxyethyl methacrylate(M_2)	0.469	3.618
14	Butyl acrylate(M_1)-*co*-2-hydroxyethyl methacrylate(M_2)	0.483	3.432
15	2-Ethyl hexyl acrylate(M_1)-*co*-2-hydroxyethyl methacrylate(M_2)	1.127	5.127
16	Methyl methacrylate(M_1)-*co*-2-hydroxyethyl methacrylate(M_2)	0.740	2.234
17	2-Ethyl hexyl methacrylate(M_1)-*co*-2-hydroxyethyl methacrylate(M_2)	0.775	2.252
18	2-Hydroxypropyl methacrylate(M_1)-*co*-2-hydroxyethyl methacrylate(M_2)	1.067	0.728
19	Methyl acrylate(M_1)-*co*-2-hydroxypropyl methacrylate(M_2)	2.089	2.034
20	Butyl acrylate(M_1)-*co*-2-hydroxypropyl methacrylate(M_2)	0.302	1.764
21	2-Ethyl hexyl acrylate(M_1)-co-2-hydroxypropyl methacrylate(M_2)	0.245	3.955
22	Methyl methacrylate(M_1)-*co*-2-hydroxypropyl methacrylate(M_2)	0.344	1.472
23	2-Ethyl hexyl methacrylate(M_1)-*co*-2-hydroxypropyl methacrylate(M_2)	0.813	1.563
24	2-Hydroxy ethyl acrylate(M_1)-*co*-2-hydroxypropyl methacrylate(M_2)	0.539	0.627
25	2-Hydroxypropyl acrylate(M_1)-*co*-2-hydroxy propyl methacrylate(M_2)	1.079	1.052

In human contact applications it is important to ensure that the level of residual monomers in synthesised polymer is extremely low. One way to ensure this is to follow polymerisation kinetics for a long time, so that after that certain time

interval all feed monomers have converted into the polymers. However, as both monomers in copolymerisation will have different relative rates of addition into the growing copolymeric chain, that leads to one which has more reactivity than the other and it will get depleted first. This leads to heterogeneity and homopolymerisation rather than copolymerisation. In such cases the copolymer and homopolymer get separated which leads to inhomogeneity in the polymer matrix, with subtle variances in refractive indices along the copolymer blocks.

Hence, it is of paramount importance that very careful studies of copolymerisation are carried out so as to establish kinetically a unique (azeotropic) composition for each, two component copolymer system wherein the copolymer has an exact identical composition as that of feed. Such copolymeric systems will have best possible chance for accomplishing complete homogeneity as well as containing very low levels of residual monomers in it.

Table 5.2: Azeotropic copolymer compositions

Sr. No.	Monomer pair	M_1	M_2
1	Methyl methacrylate(M_1)-*co*-2-hydroxy ethyl acrylate(M_2)	0.0498	0.9502
2	2-Hydroxyethyl methacrylate(M_1)-co-2-hydroxy ethyl acrylate(M_2)	0.7741	0.2259
3	Butyl acrylate(M_1)-*co*-2-hydroxypropyl acrylate(M_2)	0.1447	0.8553
4	2-Ethyl hexyl methacrylate(M_1)-*co*-2-hydroxypropyl acrylate(M_2)	0.1576	0.8424
5	2-Hydroxyethyl acrylate(M_1)- *co*-2-hydroxypropyl acrylate(M_2)	0.3684	0.6313
6	Methyl methacrylate(M_1)-*co*-2-hydroxypropyl acrylate(M_2)	0.8392	0.1608
7	2-Hydroxyethyl acrylate(M_1) -*co* -2-hydroxypropyl methacrylate(M_2)	0.4386	0.5614

Copolymer blocks of the azeotropic compositions listed above were prepared by bulk polymerisation using varying mole fraction (0, 2.5, 5.0, 7.5 and 10.0) of ethylene dimethacrylate (EGDMA). These hydrogels were used to study swelling with water and deswelling with 0.9 wt.% sodium chloride solution. These hydrogels show good thermal stability which was analysed by thermogravimetric analysis (TGA) method. The glass transition temperature (T_g) of copolymers are determined by differential scanning calorimetry (DSC) which shows that T_g of many copolymers are close to room temperature and increases linearly with crosslinked density. Low T_g is required for easy folding of lens.

Water absorption studies of these hydrogels were carried out using deionised water by the gravimetric method, with constant time interval till it reached equilibrium state. The deswelling study was done in isotonic salt solution. The results show that polymer absorbs water and retains this water even in isotonic salt solution.

The studies presented in this thesis will help to obtain a better understanding of current IOL polymers and to develop new and better polymers for IOLs.

5.2 Future Work

During the course of this research, many new opportunities for future experimentation became evident. The following are the some of important potential work plans.

- To study sewlling-deswelling behavior of these hydrogels in different ions with varying their concentration.
- Material characterisation such as refractive index, tensile testing, UV-absorption studies etc.
- DSC study for T_g determination of swelled and deswelled polymer.
- Surface modification of the hydrogels for heparin binding.
- Determination of kinetic parameters by advanced computational methods.
- *In vitro* biocompatibility study.
- *In vivo* studies of synthesised polymer networks.
- Synthesis of hydrogel with new monomers, and determination of kinetic parameters.
- Synthesis of these copolymeric systems with UV initiators and to determine their kinetic parameters.